CORRELATES OF RISK OF TB DISEASE IN INFANTS WITH DIFFERENTIAL RESPONSE TO BCG VACCINATION

By

Samuel Ayaba Njikan

A dissertation submitted in fulfillment of the requirements for the degree of Doctor of Philosophy (PhD) in the Faculty of Health Sciences, Department of Paediatrics and Child Health, School of Child and Adolescent Health, University of Cape Town

Supervisors: Prof. Willem A. Hanekom

Dr. Elisa Nemes

Assoc. Prof. Thomas J. Scriba

July 2014

DECLARATION

I, Samuel Ayaba Njikan, hereby declare that the work on which this thesis is based is my original work (except where acknowledgements indicate otherwise) and that neither the whole work nor any part of it has been, is being, or is to be submitted for another degree in this or any other university.

I empower the university to reproduce for the purpose of research either the whole or any portion of the contents in any manner whatsoever.

Signature:

Date:

SUMMARY

Studying prospective immune correlates of risk of TB disease following BCG vaccination is an important first step towards determining correlates of protection against TB, which can be identified only in a placebo-controlled randomized controlled trial (RCT) of an effective vaccine. To study correlates of risk of TB disease, we collected and stored blood from healthy 10-week old infants vaccinated with BCG at birth. During two years of follow up, infants who developed lung TB were defined as cases, while those who did not develop TB disease were defined as controls. We measured Th1/Th17 cytokine production by BCG-specific T cells, release of pro- and anti-inflammatory mediators, cytotoxic T cell potential and proliferation in response to BCG as potential correlates of risk of TB disease but none of these outcomes were different between cases and controls. However, transcriptional profiling of PBMC revealed two clusters of infants and interestingly, the gene expression profiles from cases and controls in the two clusters were in opposite directions. Based on this, we hypothesised that analysing the two clusters of infants separately will allow discovery of correlates of risk of TB, which were absent when clustering was not taken into account.

Analysing the two clusters separately, we found several T cell outcomes as well as gene expression profiles that were different between cases and controls within each cluster. In cluster 1, frequencies of BCG-specific CD4+ T cells producing granulysin, granzyme B and perforin in different combinations were higher in cases compared to controls while in cluster 2, frequencies of BCG-specific CD4+ T cells producing perforin only were higher in controls compared to cases. Frequencies of BCG-specific CD4+ T cells in producing IL-17 were higher in cases compared to controls in cluster 2. We also found that inflammatory and innate genes were up-regulated in cases compared to controls in cluster 2 with no differential gene expression in cluster 1. Pathway analyses by GSEA and IPA also showed up-regulation and down-regulation of inflammatory genes in cluster 2 and cluster cases respectively compared to

controls. Based on this, we concluded that too much or too little inflammation increases risk of developing TB disease.

We next compared the two clusters in an attempt to understand the biology. We found that cluster 2 infants had higher frequencies of BCG-specific total CD4+ T cells producing IFN-γ, TNF-α and IL-2 compared to cluster 1. In addition, polyfunctional CD4+ T and CD8+ T cells producing IFN-γ, TNF-α and IL-2 were also higher in cluster 2 compared to cluster 1. Several other T cell subsets as well as secreted mediators were higher in cluster 2 compared to cluster 1. Pathway analysis by IPA showed and IFN-γ dominated pathway with up-regulation of genes in this pathway in cluster 2 compared to cluster 1. We concluded that clustering of gene expression profiles was linked to differential response to BCG vaccination and this should be taken into account for discovery of host correlates of risk of TB disease.

To validate these findings in another cohort of cases and controls, we used two approaches to define differential response to BCG vaccination. The first approach was hypothesis-driven. Firstly, we used a logistic regression model to identify the best T cell marker for differential BCG response. A model that incorporated the frequencies of total BCG-specific CD4+ producing IFN-γ, TNF-α and IL-2 gave the best classification. We next used the expression of CXCL9 transcript as a marker of differential response to BCG. The second approach was unbiased where we used a gene expression signature to define differential response to BCG vaccination. Correlates of risk of TB disease previously identified could not be validated in differential BCG responders defined by these three markers.

The findings in this thesis will contribute significantly in the search for a biomarker of risk and/or protection against TB disease. This is the first study that has assessed risk of developing TB disease while taking response to BCG vaccination into account. Differential response to BCG vaccination was a pre-requisite for the identification of candidate correlates of risk of TB disease. Infants with either too strong or weak myeloid inflammatory responses to BCG

vaccination were more at risk of developing TB disease. This therefore suggests that heterogeneity in immune responses to BCG vaccination should be taken into account in future correlates of risk studies.

LIST OF ABBREVIATIONS

AIDS	Acquired Immuno Deficiency Syndrome
APCs	Antigen presenting cells
BCG	Bacillus Calmette-Guérin
cDNA	Complementary Deoxyribonucleic acid
CCR	Chemokine receptor
CD	Cluster of differentiation
CFP-10	Culture filtrate protein 10
CFUs	Colony forming units
CMA	Classification for Microarrays
CMV	Cytomegalovirus
Ct	Cycle threshold
CTB	Cholera toxin B
CTLA	Cytotoxic T-lymphocyte antigen
CV	Coefficient of variation
CXCL9	Chemokine ligand 9
DC	Dendritic cell
DC SIGN	Dendritic Cell-Specific Intercellular adhesion molecule-3-Grabbing Non-integrin
Δ	Delta
DMSO	Dimethyl sulfphoxide
DNA	Deoxyribonucleic acid
DOTS	Directly observed treatment strategy
EDTA	Ethylenediamine tetra-acetic acid
EGF	Epidermal growth factor
ELISA	Enzyme-linked immunosorbent assay
ELISPOT	Enzyme-linked immunosorbent spot
EPI	Expanded program on immunization
ES	Enrichment score

ESAT-6	6 kDa early secretory antigenic target
Et	Expression threshold
FC	Fold change
FCS	Fetal calf serum
FDR	False discovery rate
g	Gravity
G-CSF	Granulocyte-colony stimulating factor
GE	Gene expression
GM-CSF	Granulocyte-macrophage colony-stimulating factor
GSEA	Gene set enrichment analysis
HIV	Human immunodeficiency virus
HLA	Human leukocyte antigen
HPRT	Hypoxanthine-guanine phosphorisbosyltransferase
HPV	Human papilloma virus
ICS	Intracellular cytokine staining
IFN-α	Interferon alpha
IFN-γ	Interferon gamma
IL	Interleukin
IGRAs	Interferon gamma release assays
IPA	Integrated pathway analysis
iTreg	Induced regulatory T cells
LDA	Linear discriminant analysis
LIMMA	Linear models for microarray analysis
LTBI	Latent tuberculosis infection
LPS	Lipopolysaccharide
MAD	Median absolute deviation
MDR	Multidrug resistant
MHC-I	Major histocompatibility complex class I
MHC-II	Major histocompatibility complex class II

MIG	Monokine induced by gamma
Min	Minute
MIP	Macrophage inflammatory protein
mL	Milliliter
MOI	Multiplicity of infection
M.bovis	*Mycobacterium bovis*
M.tb	*Mycobacterium tuberculosis*
M.vaccae	*Mycobacterium vaccae*
NAAT	Nucleic acid amplification technology
NK	Natural killer
ng	Nanogram
NLR	Nod-like receptor
NO	Nitric oxide
NRAMP	Natural resistance associated macrophage protein
NTM	Non-tuberculous *mycobacteria*
OG	Oregon green
Pac	Pacific
PAM	Prediction analysis for microarrays
PAMPs	Pathogen associated molecular patterns
PBMC	Peripheral blood mononuclear cell
PBS	Phosphate buffered saline
PCR	Polymerase chain reaction
PHA	Phytohaemagglutinin
PLS	Partial least square
PMA	Phorbol 12-myristate 13-acetate
PPD	Purified protein derivative of *M.tb*
PRR	Pathogen recognition receptor
qRT-PCR	Quantitative real time polymerase chain reaction
RAG	Recombinase-activating genes

rBCG	Recombinant Bacillus Calmette-Guérin
RCT	Randomized controlled trial
RNA	Ribonucleic acid
RNA-Seq	Ribonucleic acid-sequencing
ROS	Reactive oxygen species
RPMI	Rosewell park memorial institute
SATVI	South African Tuberculosis Vaccine Initiative
SEB	*Staphylococcal enterotoxin B*
SNP	Single nucleotide polymorphism
TB	Tuberculosis
TCR	T cell receptor
TGF-α	Transforming growth factor α
Th	T helper
TLR	Toll-like receptor
TNF- α	Tumor Necrosis Factor-alpha
Treg	Regulatory T cells
TST	Tuberculin skin test
UNS	Unstimulated
WHO	World health organization
XDR	Extremely Drug Resistance
μL	Microliter

DEDICATION

This thesis is dedicated to my folks who have supported me in every way parents should throughout my academic career. Thank you so much mum and dad. You are the best.

ACKNOWLEDGEMENTS

I will like to start by thanking Prof. Willem Hanekom for giving me the opportunity to join SATVI four years back and served as my academic mentor throughout this period. Your supervision and mentorship has made me grow so much in science and I hope to apply all what I learnt through you in the fight against TB.

Many thanks to my co-supervisors, Dr Elisa Nemes and Assoc Prof. Thomas Scriba. You were always available and spent endless time in assisting me to design experiments, analyse data and interpret results. Thank you for your sacrifice most especially over the weekend and late at night.

I also wish to extend my appreciation to team SATVI. I learnt to work as a team with you guys, from the students right up to the director. Thanks for all the good interactions and memorable socials.

Special thanks to the mothers and babies who willingfully participated in this study. Thanks to the NIH for funding this project.

I also wish to extend my sincere appreciation to our collaborators Dr Rafick Sekaly, Dr Ali Filali and Dr Helen Fletcher for continuous scientific input throughout this study. Thanks for all the sacrifices by doing telephonic conferences very early in the morning or late at night.

My sincere gratitude to my beloved sisters, Solange and Wendy. You guys have always been there for me spiritually, financially, emotionally and socially. Special thanks to my nephews and niece (Ryan, Nathan and Adorabella) and uncle mike for always being there.

Special thanks to my friends Marcel, Rene and Fina, Dr Muki Shey and wife, Mr Ndutu Lawrence and wife who in their own special way helped me through this journey. To my cousins BI, Gwen and husband Pst Shaddrack and their son Prince senior, thank you all for your support.

Thanks to my PIFAM friends Linus, Oliver, So, George, Desiree, Jessy and Anjong.

Thanks to a special friend who supported and encouraged me at the beginning of this journey but unfortunately could not see the end. RIP Jennifer.

Last but not least, I want to thank God almighty for giving me the grace and strength I needed throughout this period. You alone are worthy lord to be praised and adored for you've been faithful from the ages past. That is why your name is forevermore.

LIST OF FIGURES

LIST OF TABLES

TABLE OF CONTENTS

RESEARCH PROBLEM

BCG is known to induce variable immune responses within a given population. However, it is still not known if this variability in immune response is associated with its poor efficacy. Understanding why certain individuals still develop disease despite having a detectable immune response to BCG as well as which functions or components of the immune response contributes to protective immunity would help in the design and assessment of better vaccines.

Chapter 2 of this thesis, which contains data produced by others, served as background for this study and aimed at identifying correlates of risk of TB in BCG vaccinated infants. No correlate could be identified in any of the work presented in chapter 2. However, upon further analysis of gene expression profiles, two distinct clusters of infants with opposite gene expression profiles were observed. The main aim and hypothesis for my thesis was based upon identification of these two clusters of infants.

AIM and HYPOTHESIS

To identify immune responses that correlate with risk of TB disease separately in two clusters of BCG vaccinated infants.

We hypothesised that immune responses that are either too strong or weak will associate with risk of developing TB disease in BCG vaccinated infants

SPECIFIC AIMS and HYPOTHESES

1. To identify immune correlates of risk of TB disease in two clusters of BCG vaccinated infants.

   We hypothesised that different immune correlates of risk will be identified separately in two clusters of BCG vaccinated infants.

2. To identify biomarkers of clustering in BCG vaccinated infants

   We hypothesised that clustering of gene expression profiles in BCG vaccinated infants will associate with differential response to BCG vaccination.

   We further hypothesised that several T cell functions as well as gene signatures will associate with this differential response to BCG vaccination.

3. To validate prospective immune correlates of risk of TB disease in an independent cohort of BCG vaccinated infants.

   We hypothesised that candidate correlates of risk of developing TB disease can be validated in another cohort of BCG vaccinated infants.

The work presented in this thesis was based on a collaborative study with scientists from the Jenner Institute in Oxford and Vaccine and Gene Therapy Institute in Florida.

CHAPTER 1: LITERATURE REVIEW

1.1) Epidemiology of Tuberculosis

1.1.1) Definition of Tuberculosis

Tuberculosis (TB) is a contagious airborne disease caused by infection with the bacterium *Mycobacterium tuberculosis (M.tb)*. Although TB can affect almost every organ of the body, *M.tb* primarily infects lungs [1] It is transmitted when an uninfected person inhales micro droplets of fluid containing the bacterium from an infected person's cough. Upon inhalation of these droplets containing the bacterium, a person may become infected. However, not every infected person tends to progress to TB disease. Up to 90% of individuals who become infected never progress to disease. Latently infected individuals are usually asymptomatic and cannot spread the germs. Only about 10% of infected people progress to disease, but this risk is increased up to 20 fold in those infected with HIV [2, 3]. These people are said to have active TB disease and they usually present with signs and symptoms such as continuous coughing, fever, night sweats and weight loss. Because infants and young children (less than 4 years old) have an immature immune system compared to older children and adults [4, 5], they tend to be more susceptible to TB disease [6]. The work in this thesis therefore focuses on infant TB immunology.

1.1.2) Burden of Disease

In 2012, WHO estimated the global TB incidence to be 8.6 million people and 13% of this population was co-infected with HIV. There was an estimated 1.3 million deaths from TB with just under 1 million being HIV-negative [7]. Africa accounts for 80% of TB cases living with HIV. The highest TB burden worldwide is found in Asia and Africa (Figure 1) and Africa alone has over 27% of the world's cases and the highest rates of cases and deaths [7]. The highest TB burden in Africa is found in South Africa, where TB is the first cause of death.

WHO estimates show that there were over 0.5 million cases and 74,000 deaths amongst children in 2012 worldwide [7].

Our studies are conducted in the Worcester region of the Western Cape, one of the highest TB burden areas in South Africa, recording an incidence of 1,000/100,000 TB cases per year in children less than 2 years of age [8].

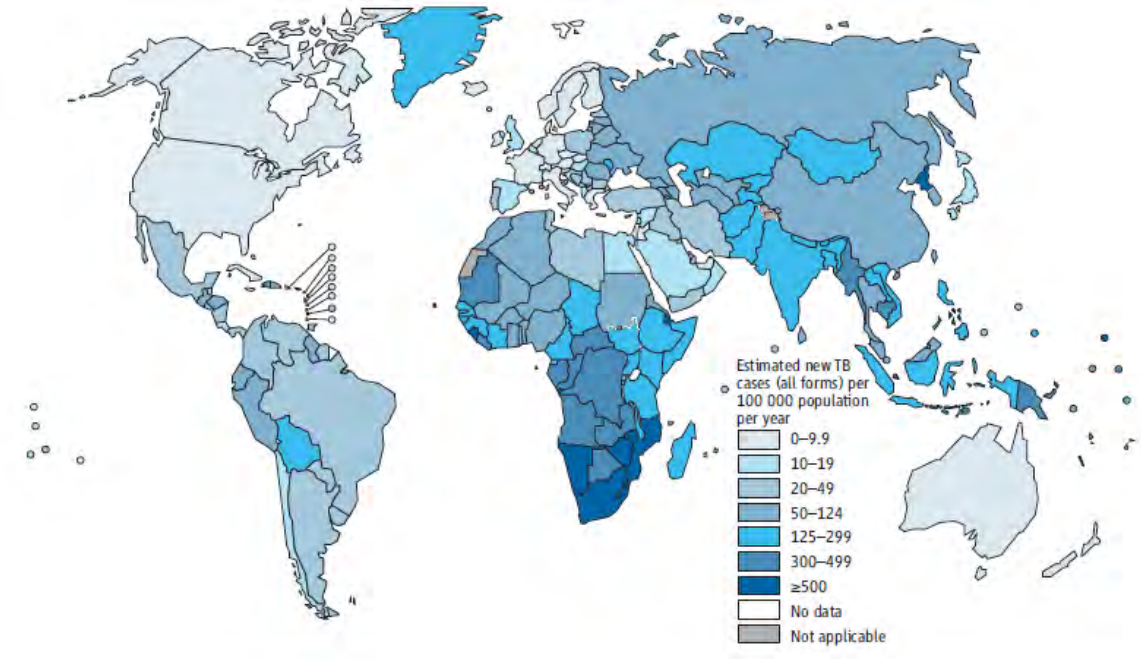

Figure 1:Developing countries had highest TB incidence rates in 2012
(Map Courtesy WHO Global Tuberculosis Report, TB publications, Maps, Global TB incidence 2013).

1.1.3) Prevention and Control

Control of the TB epidemic involves active detection of cases, treatment and vaccination [9].

1.1.3.1) Diagnosis

Rapid and accurate diagnosis of TB is fundamental to limit its spread. There are several diagnostic tools used worldwide to diagnose *M.tb* infection but the two

most widely used are the tuberculin skin test (TST) and, more recently, IFN-γ release assay (IGRA). Both tests rely on the detection of acquired immune responses towards mycobacterial antigens, suggestive of current or previous infection with *M.tb*. TST assesses delayed host reaction to *M.tb* proteins, purified protein derivative (PPD) but may also be positive in individuals previously exposed to environmental mycobacteria or vaccinated with BCG, as many antigens present in PPD are conserved across different mycobacteria. TST sensitivity can be reduced by HIV infection [10, 11]. IGRAs measure IFN-γ responses to *M.tb*-specific antigens, early-secreted antigenic target 6 (ESAT6) and culture filtrate protein 10 (CFP10). Since these antigens are not expressed by BCG and most environmental mycobacteria, this test is more specific than TST. IGRAs may also be influenced by HIV infection although they are more sensitive than TST [12, 13]. Reliability of IGRAs in diagnosing children less than five years old has not yet been determined [14, 15].

As earlier mentioned, TST and IGRAs are useful in diagnosing *M.tb* infection but not TB disease. For diagnosis of disease, a wide range of other tests or assays are used which include sputum microscopy, culture, X-ray, epidemiological scoring as well as nucleic acid amplification technology (NAAT) method (gene Xpert MTB/RIF assay) [9, 16, 17]. Bacteriological confirmation of *M.tb* presence in sputum by microscopy and/or culture is the most definitive way of diagnosing TB. However, there is a major limitation in using this method in infants because sputum samples are difficult to collect and they usually have very few bacilli after collection [18]. For this reason, sputum induction and gastric lavage may be used to collect sputum samples from young infants and children. Induced sputum is a simple and non invasive process which involves inhalation of a nebulised hypertonic solution, which then liquefies the airway secretion, thus promoting coughing up of sputum [19]. Gastric lavage on the other hand involves the insertion of a tube down through the nose or mouth into the stomach, followed by addition and removal of small volumes of normal saline. Although gastric lavage is mostly used for children under the age of two years, it is more invasive and takes more time than induced sputum [20] . In addition, it

is difficult to perform on out patients [20]. Chest X-rays are also commonly used as the first method to diagnose active TB disease. Misdiagnosis is common using this method in areas where there is lack of trained radiologists [17] and in people co-infected with HIV where there is an overlap with opportunistic infections [21]. The latest diagnostic test to be endorsed by WHO for TB diagnosis is the gene Xpert MTB/RIF assay [22]. This assay was endorsed at the end of 2010. It detects *M.tb* DNA in sputum samples, with a read out in less than 2 hours. This assay may be ideal in areas with high TB incidence but has major limitations as it is costly, requires annual servicing and calibration of each machine, stable electricity supply, restricted operating temperature and humidity as well as limited shelf-life of diagnostic cartridges [9, 21, 23, 24].

Despite all the diagnostic tools available for TB, diagnosis in children as well as sputum smear-negative pulmonary and extra-pulmonary TB in adults remain a challenge because of the paubacillary nature of the disease and difficulty in obtaining specimens [25, 26].

1.1.3.2) Treatment

The main aims of treating TB are to: cure the patient, prevent death from active disease, prevent relapse of TB, reduce transmission to others and prevent development and transmission of drug resistance [27]. There are more than 22 drugs available to treat TB and these drugs are used in different combinations based on the circumstance. Drugs used to treat TB can be combined into first line (used to treat most new TB cases or patients unexposed to prior TB treatment), second or third line regimens (used for treatment of drug resistant TB) [27]. TB treatment regimen is similar between children and adults [28] but different for latent infection and active disease. Latent TB infection can be treated with the first line drug Isoniazid for 6 months or a combination of Isoniazid and Rifampicin for 3 months [29]. However, treatment of LTBI in high burden settings is limited only to children under 5 years of age and HIV infected adults. Patients with active TB disease can be treated with a combination of multiple first line drugs for 6 months in two phases [30]. Non-compliance to the

treatment program may lead to emergence of resistant strains of TB [31]. Treatment of multi drug resistant (MDR) TB is more difficult compared to drug susceptible TB [30]. XDR *M.tb* is resistant to first line and second line drugs, therefore third line drugs are used to treat it and these drugs are often less effective, more toxic and expensive [32].

1.1.3.3) Vaccination

An effective vaccine against TB would be the most sustainable intervention to control the worldwide epidemic [33]. The only licensed vaccine against TB, Bacille Calmette-Guerin (BCG), is effective in preventing severe forms of TB in children [34], but has variable efficacy in protection against pulmonary disease across all age groups [35, 36]. Due to the variability in protection conferred by BCG, there is an urgent need for the development of new and better vaccines against TB.

1.2) Bacille Calmette-Guerin (BCG)

1.2.1) History

BCG is a live attenuated vaccine containing the non-virulent strain of the mycobacterium that causes TB in cows (*M. bovis*). This vaccine was developed early last century by Calmette and Guerin in France, by sub-culturing *M. bovis* for several years until it lost its virulence in animals such as cows and guinea pigs. This altered organism was then named Bacille Calmette-Guerin (BCG), after the scientists that developed it. This vaccine was used for the first time in humans to protect against TB in 1921.

At first, BCG cultures were only maintained in Paris, but were later sub cultured and distributed to several laboratories all over the world for continued sub culture. After several years, the strains grown in different laboratories worldwide were no longer identical. To limit these variations, the organism is now grown in many laboratories using “freeze-dried” (lyophilized) cells so that each batch starts with the same cells.

Since 1921 when this vaccine was first administered in humans (orally in infants), it has been the most widely administered vaccine and estimated to have been given over 4 billion times to 1 billion recipients [37]. BCG has been part of the expanded programme on immunisation (EPI) from the early 1970s and its safety has never been an issue until recently [37]. BCG has been shown to cause disseminated disease in infants with HIV, posing a risk in HIV+ individuals where TB is highly endemic [38]. For this reason, the WHO recommends that BCG should not be given to HIV infected children [37], but the reality is in South Africa, BCG is still administered to all infants at birth because it protects against severe forms of TB [38].

1.2.2) Efficacy

Meta-analyses have shown that BCG efficacy in protecting against lung TB is highly variable and ranges from no effect to 80% [35] [36]. Nevertheless, BCG has been shown to be consistently efficacious in protecting infants and children against disseminated or severe forms of TB (miliary TB and TB meningitis) [34]. For this reason, BCG is still commonly used in high TB burden countries and even in countries where protective efficacy is negligible, especially in babies.
Different possible reasons for the variable efficacy of BCG vaccine have been proposed but none seem to explain the lack of efficacy in both low and high TB burden countries. Some of the reasons include (i) Different BCG strains; (ii) Host genetic variation; (iii) Pre-exposure to non-tuberculous mycobacteria (NTM); (iv) Interference by parasitic infections.

i) Different BCG strains

BCG vaccine strains used all over the world display different properties, which may include genetic variants of the mycobacterial strains as well as the preparation of the vaccine. Several studies have thus been conducted to determine if these differences could be the reason for the variable efficacy in

protection of the vaccine. In a case-control study analysis by Comstock in Indonesia and Columbia, it was observed that there was a reduction in protection when Paris and Danish strains of BCG were used compared to Japan and Glaxo respectively [39]. Also, in another study done in South Africa, comparing the effect of the Danish strain to the Japanese strain on induced immune response in vaccinated infants, it was found out that different strains resulted in different levels of immune responses 10 weeks after vaccination [40]. Most recently, in a randomized trial done in Australia, comparing the Danish, Japanese and Russian strains of BCG in newborns, significant differences were observed in immunity conferred by the different strains [41]. However, the fact that certain BCG strains have been shown to be more effective in certain populations than others, suggests that efficacy in not only dependent on strain variation [42, 43]. To support this observation, a recent meta-analysis has shown that BCG efficacy in preventing pulmonary and disseminated TB was not affected by vaccine strain [44].

ii) Host Genetic Variation

Several studies have been conducted to investigate the relationship between susceptibility to TB and host genetic variation. Some of these studies showed that susceptibility to TB and other mycobacterial infections is influenced by several genes which control cellular immune mechanisms (including HLA-DR, HLA-DQ, vitamin D receptor, IFN-γ receptor polymorphisms, and NRAMP) [45-48]. Recently in our group variation in toll-like receptor 6 (TLR6) was shown to associate with altered innate immune responses and *M.tb* recognition [49]. In another study done by the Hawn Laboratory in collaboration with our group (SATVI) on South African infants, it was shown that single nucleotide polymorphisms (SNPs) in the innate immune genes, TLR1 and TLR6, were associated with altered adaptive immune responses following vaccination with BCG [50]. BCG efficacy may at least in part be explained by the difference in genetic make-up of different populations.

iii) Pre-exposure to non-tuberculous mycobacteria (NTM)

Most populations in the world are exposed to various NTM, which share similar antigens with BCG. This can induce cross-reactive immune responses and hence mask the effect of BCG. Pre-clinical studies have shown that BCG protection is reduced in mice that have been exposed to *M. avium* [51]. Consistent with this finding is the observation that BCG efficacy tends to be lower in populations living in warmer regions of the globe, particularly in rural areas [52], probably due to presence of NTM. This becomes a real concern in clinical settings where there is high prevalence of NTM. In these settings, pre-exposure to NTMs may mask the effects of BCG [44]. This hypothesis was supported in a BCG efficacy trial in South India, where a certain degree of efficacy (29%) was observed in participants that had no prior sensitisation with NTMs (*M .intracellulae*) or who had low tuberculin reactivity at baseline [44]. No efficacy was observed in those with tuberculin reactivity. In South Africa, BCG is given at birth and this reduces the potential exposure to NTM, therefore vaccine-induced responses may be independent of pre-exposure to NTMs.

iv) Interference by parasitic infections

Another hypothesis suggests that simultaneous infection with parasites reduces the efficacy of BCG [53, 54]. It has been shown that parasitic infections skew the immune system towards a response that does not favour effective control of *M.tb* [53, 54]. However, in the Western Cape, the prevalence of maternal helminth infection was found to be very low (<10%), probably suggesting that this might have little or no effect on vaccine efficacy [55].

Understanding determinants of variable immune response elicited by BCG remains a very important aspect in evaluating its efficacy. Although several factors have been shown to influence BCG efficacy such as co-infections with parasitic infections, pre-exposure to NTM and host genetic make-up, very few studies have investigated the effect of these factors on the variability in BCG-induced immune responses. Because the work in this thesis investigates

variability in immune responses elicited by BCG and correlates of risk of TB disease following BCG vaccination, it was very critical to assess the effect of these factors in this study in order to rule them out as possible reasons for this variability. Section 1.4 below discusses the effects some of these factors have on immune responses elicited by BCG vaccination. It was important to note that some these factors as well as route of BCG administration did not seem to have such an effect in the Western Cape [55, 56]. For these reasons, SATVI clinical setting in the Worcester region of the Western Cape is ideal to characterise immune responses induced by BCG vaccination and their possible role in preventing TB disease in infants. Understanding why BCG-induced immune response may protect some individuals but not others may inform rational vaccine design and it is the focus of this thesis. For example, our group completed a randomised controlled trial in 11, 680 BCG vaccinated infants to compare the efficacy of percutaneous versus intradermal BCG vaccination [56]. In this study, infants were vaccinated with BCG at birth (Japan strain) either percutaneously or intradermally and followed up for a period of two years. Within this period, infants who developed TB were identified as well as those who did not develop TB despite exposure to TB contacts. In order to assess the immune responses elicited by BCG, blood was collected from a subset of 5,674 infants at 10 weeks of age and stored. These samples form the basis for the work in this thesis.

1.3) New TB vaccines pipeline

As earlier mentioned, the only licensed vaccine against TB is BCG. However, its protection against pulmonary disease is variable [35]. There is therefore the need to develop better and more effective vaccines against this deadly pandemic. The development of new TB vaccines will be accelerated by knowledge of correlates of risk of TB disease which could later translate into correlates of protection. The work from this study therefore would directly be applied to the development of new TB vaccines in the pipeline. In the absence

of immunological correlates of risk, what we learn about the variability of immune responses induced by BCG may also inform better immunogenicity tests to assess new TB vaccines which are currently tested in clinical trials. In this light, there are 14 TB vaccine candidates currently in clinical trials (Table 1;[57]). Of these, 4 are in phase I for safety testing, 8 are in phase II for safety and immunogenicity testing and 2 in phase III [57]. MVA85A has recently been tested in the first phase IIb efficacy trial since BCG licensure. MVA85A is a modified vaccinia Ankara virus containing antigen 85A from *M.tb* [58]. This vaccine was designed to boost the immune responses induced by BCG but results showed that no additional protection was conferred by this vaccine, compared to BCG alone [59]. Two other vaccine candidates, *M. Vaccae* and *M. indicus pranii* which are whole cell mycobacteria vaccines have just recently completed phase III trials [57]. In addition to the 14 candidates currently tested in clinical trials, there are at least 35 vaccine candidates in preclinical development and 21 next generation vaccines in the discovery phase [57]. Next generation vaccines are vaccines that are in the research and development stage with some preclinical evidence of conferred protection.

Table 1: TB vaccine development pipeline in 2013

Agent	Strategy	Type	Sponsors	Status
M. indicus pranii	Immunotherapeutic	Whole-cell *M. indicus pranii*	Department of Biotechnology (Government of India), Cadila Pharmaceuticals	Phase III
M. vaccae	Immunotherapeutic	Whole-cell *M. vaccae*	AnHui Longcom	Phase III pending
MVA85A/ AERAS-485	Prime-boost	Viral vector	Oxford University, Aeras	Phase IIb
M72 + AS01	Prime-boost	Adjuvanted subunit	GSK, Aeras	Phase IIb
Crucell Ad35/ AERAS-402	Prime-boost	Viral vector	Crucell, Aeras	Phase II (formerly phase IIb)
VPM1002	Prime	Live recombinant rBCG	Vakzine Projekt Management GmbH, Max Planck Institute for Infection Biology, TuBerculosis Vaccine Initiative (TBVI), Serum Institute of India	Phase IIa
RUTI	Immunotherapeutic	Fragmented MTB	Archivel Farma	Phase IIa
Hybrid 1 + IC31	Prime-boost	Adjuvanted subunit	Statens Serum Institut (SSI), TBVI, Intercell, European & Developing Countries Clinical Trials Partnership	Phase IIa
Hybrid 56 + IC31	Prime-boost	Adjuvanted subunit	SSI, Aeras	Phase IIa
Hybrid 4 + IC31/ AERAS-404	Prime-boost	Adjuvanted subunit	Aeras, Sanofi Pasteur	Phase IIa
ID93 + GLA-SE	Prime-boost	Adjuvanted subunit	Infectious Disease Research Institute, Aeras	Phase I
Ad5Ag85A	Prime-boost	Viral vector	McMaster University, CanSino	Phase I
MTBVAC	Prime	Live genetically attenuated MTB	University of Zaragoza, Biofabri, TBVI	Phase I
Dar-901	Prime-boost	Whole-cell *M. vaccae*	Geisel School of Medicine at Dartmouth University	Phase I pending

Vaccination strategies have implored the use of different kinds of vaccines. Vaccine candidates in clinical trials to date are live attenuated or recombinant, viral vectored, whole cell or fragmented mycobacterium and adjuvanted subunit vaccines.

1.3.1) Live attenuated or recombinant vaccines

These vaccines are designed to replace BCG as prime vaccines. A live attenuated vaccine is a vaccine whose virulence has been weakened by

deletion of certain genes but can still induce a cellular immune response. An example of such a vaccine in clinical trials is MTBVAC, which is a live attenuated *M.tb* vaccine. MTBVAC was constructed by the deletion of two virulence genes, phoP and fadD26 and it is the first live attenuated *M.tb* vaccine to have entered clinical trials [60]. This vaccine has been shown to induce an immune response that is long lasting in mice compared to BCG [60]. On the other hand, another live recombinant vaccine comprises BCG that has been designed to over-express key *M.tb* antigens. VPM1002 is an example of such a vaccine and is the most advanced live recombinant vaccine in a clinical trial being presently in phase IIa. This vaccine was constructed by knocking out the urease gene in BCG and inserting listeriolysin gene from *Listeria monocytogenes,* thereby allowing the recombinant BCG to escape the phagosome [61, 62]. This vaccine has been shown to be safe, while inducing CD4+ and CD8+ T cell responses similar to BCG in BCG naive, HIV negative newborns [63]. Another live recombinant vaccine that reached phase I clinical testing in 2004 is rBCG30, but plans for further development have been put on hold [37].

1.3.2) Viral vectored vaccines

These vaccines are designed by modifying non replicating viruses which serve as transport of *M.tb* DNA into human cells. Upon entry into cells, the *M.tb* DNA is transcribed into proteins and these proteins can induce immune responses [58]. These vaccines have mainly been used in prime-boost strategies to boost the immune response induced by BCG. MVA85A, Crucell AD35 and Ad5Ag85A are examples of viral vectored vaccines. In a phase IIb trial MVA85A conferred no additional protection over BCG alone [59]. Aeras 402, which comprises the human adenovirus serotype 35 expressing the *M.tb* antigens TB10.4, Ag85A and Ag85B, had been shown to induce robust CD8+ T cell responses but moderate CD4+ responses in a phase I clinical trial [64]. But this vaccine was later reduced from a phase IIb to phase II trial (proof-of-concept to safety and immunogenicity respectively) after reviewing the preliminary data [57]. The last

of the three viral vectored vaccine to be presently in clinical trial is Ad5Ag85A, which is a recombinant, replication-deficient adenovirus serotype 5 expressing Ag85A. Greater immune responses have been shown with this vaccine in individuals who received BCG compared to BCG-naive persons [65].

1.3.3) Adjuvanted subunit vaccines

These vaccines are designed by fusing different *M.tb* proteins into immunogens, which are then formulated with specific adjuvants. In the field of vaccinology or immunology, adjuvants are agents that are added to vaccines to provoke the immune system to respond to a particular antigen but do not confer immunity themselves [66]. Subunit vaccines are also used in prime-boost strategies and there are presently five candidates in clinical trials. The most advanced of these vaccines is M72, which contains the *M.tb* proteins 32A and 39A in a fusion protein and formulated in the adjuvant AS01. This vaccine has been shown to induce good Th1 and Th17 responses in a population of *M.tb* infected individuals in South Africa [67]. In this same study, there was evidence suggestive of the fact that this vaccine may boost T cell populations primed by natural infection with *M.tb* [67]. Three other subunit vaccines currently tested in clinical trials are all formulated with the adjuvant IC31 [68, 69]. These are Hybrid 1 (contains Ag85B and ESAT6), Hybrid 56 (Ag85B, ESAT 6 and the latency antigen Rv2660) and Hybrid 4 (Ag85B and TB10.4) (Table 1). Although Hybrid 1 has been shown to induce a robust CD4 T cell response as measured by IFN-γ and there are still ongoing studies investigating it, its elimination by H56 is most likely as H56 contains antigens in both active disease and latent infection. The last of the adjuvanted subunit vaccine in clinical trials is ID93, which contains the antigens Rv2608, Rv3619, Rv3620 (active disease antigens) and Rv1813 (latency antigen) formulated in the adjuvant GLA-SE.

1.3.4) Whole cell or fragmented mycobacterium vaccines

These vaccines are made up of replication-deficient, inactivated whole cell or fragmented mycobacteria. In combination with chemotherapy, these vaccines

may be therapeutic as they work to improve the treatment of either active disease or LTBI. Examples of such vaccines are RUTI, Dar 901, *M. Vaccae*, *M. indicus pranii.*

New vaccines are designed to: i) prime the immune system prior to *M.tb* infection or environmental NTM exposure ii) boost the already existing immunity conferred by BCG iii) prevent transmission or clear the infection.

i) Prime vaccines

These vaccines are meant to be used in infants and newborns before they become exposed to *M.tb* or environmental mycobacteria. BCG is still mostly used as a prime vaccine but several vaccine candidates have been designed to replace BCG. The aim is to use recombinant BCG (rBCG) or attenuated *M.tb* strains as a replacement for conventional BCG [70]. Most prime vaccines are live attenuated because they have the ability to replicate and can therefore induce immune responses similar to the virulent form.

ii) Boost vaccines

These are vaccines designed to enhance the already existing immunity conferred by BCG (prime vaccine). Typically, these vaccines consist of mycobacteria specific antigens that are coded in viral vectors (viral vaccines) or delivered with Th-1-inducing adjuvants (subunit vaccines). There is much debate in the field of TB vaccinology with regards to the optimal time to administer a boost vaccine. Nevertheless, TB incidence peaks in very young children less than 4 years [71] and in adolescence [72], suggesting that these populations should be primarily targeted by preventive vaccines. However, more recently there is a general consensus that prevention of transmission will make the greatest impact on the global epidemic. Since *M.tb* is most likely transmitted by adolescents and adults, the primary targets for vaccination would be adolescents just before they get infected [73].

iii) Post Infection/therapeutic vaccines

These can either be vaccines given to latently infected individuals to prevent reactivation or to individuals with active disease together with chemotherapy to prevent transmission and shortening the treatment regimen [70]. Inactivated mycobacteria and the subunit vaccines H56, H1, ID93 and M72 are proposed candidates for this kind of approach [70].

Of the 14 new vaccine candidates in clinical trials, SATVI has conducted clinical trials on 7 candidates [74].

1.4) Heterogeneity in immune responses induced by vaccinations

A major limitation in the design and development of new vaccines is the inter-individual variation in vaccine-induced immune responses. Variability in immune responses may be due to host factors such as genetic factors, environmental factors such as demographic distribution, co-infections, pre-exposure to vaccine antigens as well as vaccine delivery routes.

Polymorphisms in key immune response genes have been associated with heterogeneity of vaccine-induced responses [75, 76]. For example, HLA genes play a pivotal role in determining immune responses to T cell antigens and are consequently the most analysed in gene association studies of infectious diseases [77]. HLA loci are highly polymorphic, to ensure efficient presentation and recognition of a broad range of foreign antigens. Nevertheless, it has been hypothesised that individual variability of immune responses induced by vaccines may be associated with HLA polymorphism [78, 79]. For example, following BCG vaccination in a group of 86 caucasian leprosy patients, lack of HLA-D3 was associated with no or low responses measured by skin test responsiveness [80]. In another study where BCG was administered to healthy caucasians, high or normal responders to BCG were associated with HLA-DR4 [81].

Pre-exposure to vaccine antigens and/or vectors is another co-factor for heterogeneity in vaccine induced responses and this has been shown in various vector-based vaccines [82-84]. An example of such is the STEP trial in which high risk HIV individuals were administered with an HIV vaccine made up of an adenovirus (Ad5), synthetically modified to contain the nef, gag and pol proteins from HIV. The results showed that placebo recipients had lower rates of HIV acquisition compared to vaccinees that were seropositive for adenovirus 5 (Ad5) [85, 86].

Age as well as gender have also been shown to have an effect on vaccine-induced immunogenicity or efficacy [87, 88]. BCG has been shown to induce variable response in infants vaccinated at birth compared to later time points [89-91] . For example, Kagina *et al* showed higher frequencies of BCG-specific Th1 cytokines when BCG vaccine was delayed from birth to 10 weeks of age in South African infants [89]. However, the opposite of this was seen by Lutwama *et al*, in Ugandan infants whereby the birth vaccinated group had increased frequencies of CD4+ T cells producing IFN-γ compared to those who received BCG at 6 weeks [91]. The discrepancy in these results could be accounted for by the difference in socio economic status, geographic location as well as study design. These data however point to the fact that BCG response may be affected by age of administration.

Co-infection with bacteria, viruses as well as parasites has effects on the human immune system and this could consequently affect the immunogenicity of several vaccines [92, 93]. For example Elias *et al* evaluated whether anti-helminthic therapy prior to BCG vaccination could increase the immunogenicity of BCG vaccination in a helminth-infected population. They found that BCG-induced Th1 immune responses (number of cells producing IFN-γ and IL-12 after *in vitro* stimulation with PPD) were impaired in individuals who received the placebo compared to those who received the treatment (dewormed) [53].

1.5) Immunopathogenesis of Tuberculosis

1.5.1) Immunological life cycle of Tuberculosis

Immune responses against *M.tb* infection have been shown to control its growth. However these responses do not completely clear the bacterium in most situations. Understanding these responses has been a major scientific challenge and incomplete understanding has been a major limitation in the rational design of TB vaccines better than BCG. Despite extensive studies of human immune responses to *M.tb*, there has been no clear understanding of correlate of effective immunity against *M.tb* [94]. A proposed framework for understanding and studying TB immunity in both humans and animals is based on the assumption that there are multiple stages in human responses to *M.tb* [95]. Understanding these responses at the different stages of the life cycle of *M.tb* may provide a better understanding of the mechanisms involved in protection [95].

1.5.1.1) Stage 1: Infection stage

Primary infection occurs when *M.tb* is transmitted by aerosol and is internalized by professional phagocytic cells including macrophages, neutrophils and dendritic cells (DCs) recruited in the lungs [96, 97]. This stage is characterized by recognition of *M.tb* components by various pathogen recognition receptors (PRRs), such as Toll-like receptors (TLRs) and NOD-like receptors (NLRs) [98]. TLRs are believed to be an important recognition system for *M.tb* mainly through TLR2, TLR9 and TLR4 [99]. Polymorphism in TLR genes have been shown to increase susceptibility to TB in humans. For example, Chen *et al* reported an association between TB susceptibility and TLR2 genetic polymorphism (haplotype A-G-T) [100]. Also, Caws *et al* have shown an association between TLR 2 polymorphism and disseminated TB [101]. Despite numerous *in vitro* data regarding the recognition of mycobacteria by TLR2 and TLR4, knock-out mice deficient for these receptors have shown very little enhanced susceptibility to infection with *M.tb* [102]. For example, $TLR4^{-/-}$ mice showed variable responses to the challenge with *M. tuberculosis,* with either

normal resistance to infection [103] or chronic pneumonia and increased mortality ([104-106]. Also, following low dose infection with *M.tb* *TLR2*$^{-/-}$ mice showed a decrease in clearance of the bacteria and developed chronic pneumonia [107], whereas in other studies only minor effects have been found [103, 108]. Studies conducted in MyD88-deficient and TLR2, 4 and 9-deficient mice suggest that these mice had increased susceptibility to *M.tb* and TLR2,4 and 9 were important in the initial host response but not for the initiation of an adaptive response [109]. C-lectin receptors such as mincle, dendritic cell-specific intercellular adhesion molecule-3-grabbing non-integrin (DC-SIGN) and mannose receptors (MRs) can also recognise *M.tb* and initiate pathogen internalisation. Recognition through some of these receptors leads to activation of macrophages while others allow quiescent entry of *M.tb* into the cells [110]. Recruited and infected cells aggregate leading to formation of early granulomas. Granuloma formation is the hallmark of *M.tb* infection. A granuloma is a well-organized structured collection of innate and adaptive immune cells that is formed to contain the pathogen [94]. Cells that form the granuloma might include macrophages, DCs, neutrophils, T and B cells [94, 111, 112]. *M.tb* can persist in hypoxic conditions within the granuloma by altering gene transcription patterns and adopting a dormant lifestyle and may continue to replicate when host immunity wanes [113, 114]. Resident lung DCs take up *M.tb* or infected apoptotic cells and migrate to the local draining lymph node where naive T cells are primed through antigen presentation. The primed T cells migrate back to the lung and secrete IFN-γ, which activates infected macrophages to kill *M.tb* through the production of nitric oxide (NO). TNF-α is important in activating macrophages and maintaining the granuloma structure. Macrophages containing *M.tb* may undergo apoptosis or necrosis releasing viable *M.tb* [115]. However, other macrophage mechanisms aimed at killing *M.tb* in humans are mediated by TLR-induced vitamin D-dependent induction of the antimicrobial peptides cathelicidin and β-defensin 2 (DEFB4) [116-120]. When *M.tb* is not effectively killed or controlled within the granuloma, *M.tb* can eventually be transmitted. Transmission of *M.tb* occurs when the caseous granuloma breaks

and the caseum with viable bacilli is deposited into the airways. The bacilli are then coughed up into the air and are inhaled by another host either uninfected or with an existing infection [121]. However, the formation of caseum and eventual calcification of the granuloma may also be an indication of successful containment of the bacilli.

During the early stages of the infection, the recruitment of phagocytic cells to the site of infection may be of benefit to the pathogen as it provides additional cellular targets to infect [122, 123]. *M.tb* has evolved multiple mechanisms to survive and multiply inside specialized phagocytes, which include: a) Prevention of phagosomal trafficking and maturation, to allow escape from lysosomal-mediated mechanisms of restriction, killing and degradation [124-126]; b) Expression of several virulence factors, to enable cell to cell spread [122]; c) Inhibition of host cell apoptosis, which would enhance antigen presentation to T cells, in favour of necrosis, an inflammatory process that supports mycobacterial spread [115, 127, 128].

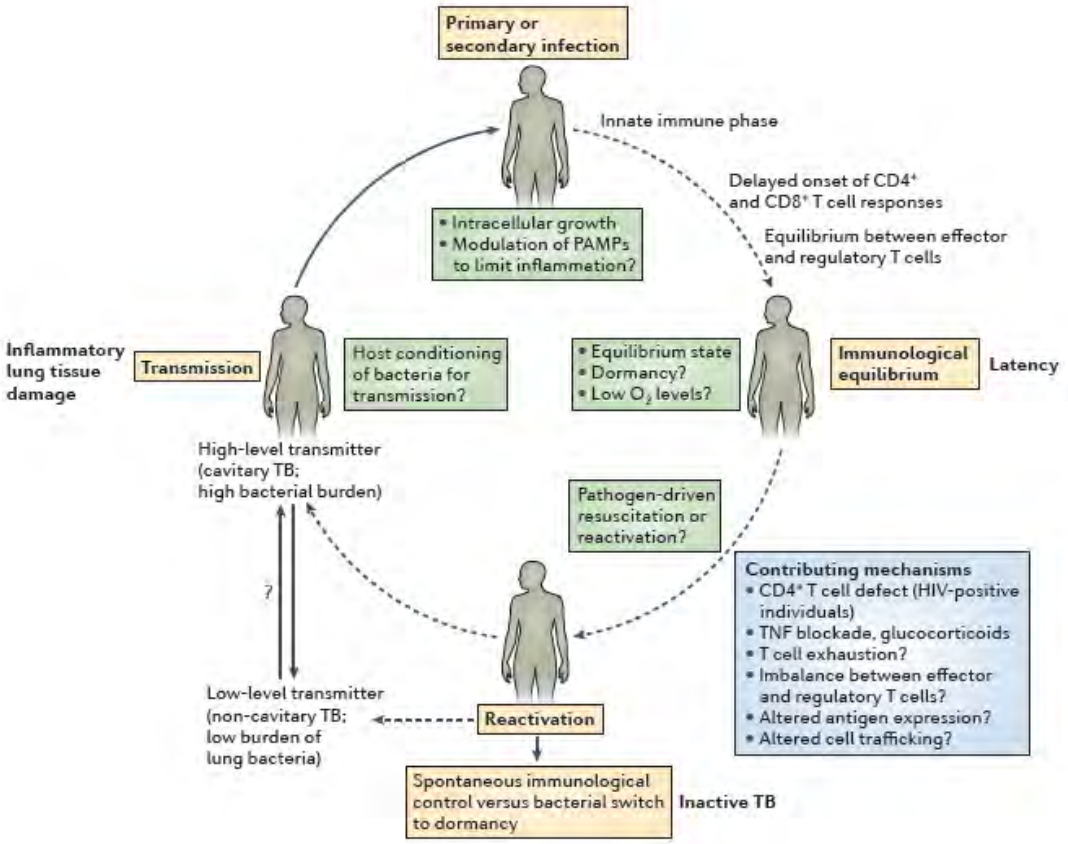

Figure 2: Stages in the immunological life cycle of tuberculosis.
The framework for the life cycle is based on clinical, epidemiological and immunological studies in humans. Included are examples of some of the immunological mechanisms and functions that characterize each stage, in cases where they are known. PAMP, pathogen-associated molecular pattern; TB, tuberculosis; TNF, tumour necrosis factor. (Ernst, 2012).

1.5.1.2) Stage 2: Immunological Balance

The adaptive immune response to *M.tb* is characterized by a delay in onset compared to other pathogens in humans. Studies that have evaluated immune responses following *M.tb* exposure of naive individuals to an active case of pulmonary TB have shown that measurable immune responses (measured as skin test reactivity using Pirquet or TST) in humans appear approximately after 42 days following *M.tb* exposure [129, 130]. A similar delay in onset of activation of antigen-specific T cells has been reported in mice following aerosol infection with *M.tb* [110, 111, 117, 118]. Lin *et al* showed a 1.5 fold decrease in bacterial

burden in lung granulomas including sterilisation of lung granulomas in macaques infected with *M.tb* from 4 to 11 weeks, which suggests killing at the onset of the adaptive immune response [131]. Studies in mice and non-human primate models have demonstrated that these responses occur earliest in the lymph node that drains the lungs [124, 132-134]. This has been attributed to a delay in transport of the bacterium by myeloid DCs from the lungs to the draining lymph nodes [125, 133]. After the onset of the adaptive response, about 90% of humans control bacterial growth and never progress from this latent, asymptomatic infection to active TB disease [95]. In mice, accumulation of effector CD4+ and CD8+ T cells in the lungs upon *M.tb* challenge is essential for long-term survival, but only marginally decreased bacterial load in the lungs [135]. Other studies in mice and non-human primates have shown continuous bacterial replication despite overall control of bacterial growth [136, 137]. This therefore suggests that latent TB is a state of bacterial and immunological equilibrium rather than a state of bacterial stasis.

Adaptive immune responses to *M.tb* largely depend on CD4+ T cells in humans, mice, cattle and non-human primates [138-140]. MHC class II deficient mice were more susceptible to disease due to lack of control of bacterial growth [141]. In humans, HIV-infected individuals with low CD4+ T cell counts are more susceptible to TB disease [142]. CD8+ T cells secrete IFN-γ, which activates macrophages to kill the bacteria [143]. Although CD8+ T are involved in fighting against *M.tb*, they cannot compensate for the lack of CD4+ T cells [143, 144].

1.5.1.3) Stage 3: Postprimary TB

In low endemic settings, most cases of TB in adults are due to reactivation of latent *M.tb* probably due to very little transmission and must be distinguished from a secondary infection, which can occur even in immunocompetent individuals. However, in high endemic countries, where there is ongoing transmission of the bacteria, most cases of TB are due to repeated infection [145]. Reactivation TB is characterized by bacteria shedding in cough and it usually reflects progression to active, symptomatic disease [146]. Reactivation

of TB can occur decades after infection [147] and this reactivation can be attributed to a weakened immunity [95].

Two main mechanisms have been described in humans as potential reasons for reactivation of TB. The first mechanism relies on quantitative and qualitative defects in CD4+ T cells driven by HIV infection [138]. Studies in humans have suggested that before CD4 counts reach a very low level following HIV infection, there is faster depletion of *M.tb* specific CD4+ T cells compared to CD4+ T cells specific for other infections [148]. In addition, depletion of CD4+ T cells by SIV in non-human primates has been shown to cause reactivation and progression of TB [139]. However, the exact mechanism used by CD4+ T cells to maintain and control *M.tb* in the latent state is unknown. The second mechanism is the therapeutic neutralization of TNF [149], especially by monoclonal antibodies [150]. Although the effect of blocking TNF has not been fully characterized, it has been linked to a) Decreased in macrophage-mediated antimicrobial activity [151] b) Induction of higher frequency of Treg cells [152] c) Depletion of a subset of CD45RA+ effector memory CD8+ T cells that secrete granulysin and have been shown to kill *M.tb* in vitro [153]. Diabetes mellitus [154] and treatment with glucocorticoids [155] have also been linked with an increased risk of TB reactivation. Other conditions such as silicosis, haematological malignancies, cancer chemotherapy, gastrectomy, uraemia as well as age have all been linked to increased reactivation of *M.tb* [156] though the underlying mechanisms have not been fully elucidated. These two mechanisms are somehow "modern" mechanisms of reactivation. However, the main risk factor for TB reactivation, which also happens to be common between the mechanisms described above, is relative immunocompromise.

1.6) Role of T cells in immune mediated control of TB

The role of T cells in the protective immunity against TB has been well established. Within granulomas, the effective control of *M.tb* has been

associated with recruitment of mycobacteria-specific T cells and activation of macrophages. Different T cell subsets including cytotoxic T lymphocytes (CD8+) and CD4+ T cells (Th1, Th17, Th22, Th2, and regulatory T cells (Tregs) have been reported to play roles in protecting against TB [125, 143, 144, 157, 158].

1.6.1) Th1 cells

CD4+ T cells likely play a more important role in TB immunity compared to CD8+ T cells. This is because CD4+ T cells have been shown in animal as well as human studies to control *M.tb* infection and progression to active TB disease [94, 144]. In murine models, it has been shown that protective immunity against TB is achieved in RAG mice (deficient in B and T cells) that received adoptively transferred CD4+ T cells [159]. In humans, individuals infected with HIV are more likely to progress to TB disease compared to HIV negative [142].

CD4+ T cells can be further divided into multiple lineages with significantly different immune responses to *M.tb* infection [160]. Protective immunity by CD4+ T cells is mediated by Th1 cells that secrete cytokines, mainly IFN-γ [144]. This protective immunity has been shown to be dependent on IL-12_p40 in mice [125, 141, 144, 161]. In humans, polymorphisms in the IL-12/IFN-γ pathway genes have been linked to susceptibility to pulmonary TB and mycobacterial disease [162] and the function responsible for these associations is IFN-γ. Treating rheumatoid arthritis patients with anti-TNF therapy increased their risk of developing TB disease [163]. In humans, IFN-γ has been shown to induce autophagy [164] while *M.tb* induced TNF-α production leads to apoptosis of infected alveolar macrophages [165]. These two mechanisms function to reduce bacterial burden.

IL-2 has been shown to be pivotal in enhancing immune responses by driving proliferation of antigen-specific T cells, which is required for these cells to carry out their effector functions as well generation of memory T cells [166].

CD4+ T cells co-expressing IFN-γ, TNF-α and IL-2 together (polyfunctional cells) have been shown to be more protective against TB in mice [167]. These polyfunctional cells have also been shown to correlate with vaccine-induced protection against *L. major* in a mouse model [168]. In humans, increased frequencies of these cells have been observed in latently infected individuals compared to TB patients [169, 170] supporting the supposedly protective role of these cells postulated in animal models. However, the opposite has been reported by Caccamo *et al*., where they found increased frequencies of these cells in TB disease patients compared to LTBI [171].

1.6.2) Th17 cells

Th17 cells, which produce the pro-inflammatory cytokines IL-17 [172] and IL-22 [173], have also been studied in immunity against TB. Two SNPs in the IL-17F gene have been associated with susceptibility to both pulmonary and extra pulmonary TB disease [174]. Kagina *et al* showed that BCG vaccination induces low levels of IL-17 in children [175] whereas Scriba *et al* reported higher levels of BCG-specific IL-17 and IL-22 producing CD4+ T cells in adults [176]. Scriba *et al* also showed lower frequencies of mycobacteria-specific Th17 cells in individuals with active TB compared to healthy controls [176]. Compared to active TB disease patients, latently infected individuals have been associated with increased frequency of IL-17+ T cells [177]. At the site of disease, higher levels of IL-22 have been reported compared to IL-17 [178]. The role of IL-17 in TB has been extensively described in mice [179-183]. This cytokine has been shown to be induced in both *M.tb* infection and challenge models [182, 183]. Gopal *et al* showed that vaccine-induced protection is diminished in mice deficient of IL-17 but not IFN-γ [179]. In addition, mice receiving early IL-17 cytokine therapy have been shown to have an enhanced vaccine-induced protection against TB in *M.tb* mice challenge models [179]. Recently, Gopal *et al* showed that wild type mice controlled infection compared to IL-17$^{-/-}$ mice following infection with the virulent *M.tb* strain HN878, suggesting a protective role of IL-17 [184]. All these show that Th17 cells may contribute to immunity

against TB. However, the function of IL-17 is not fully understood and further studies are required.

1.6.3) Regulatory T cells (Tregs)

Evidence of the role of Tregs in immunity against TB has been reported in mice, whereby there was a decrease in protection conferred by BCG with the appearance of Tregs [185]. Tregs have also been shown to impair Th1 responses [186]. IL-10 and TGF-β are produced mainly by Tregs and these have been shown to inhibit proliferation and production of cytokines by other T cells [187]. In humans, higher frequencies of Tregs have been reported in patients with TB disease compared to healthy uninfected individuals [188]. Whether Tregs are induced to counter balance excessive inflammation during disease or their pre-existing enrichment may affect protective immune responses, predisposing to disease, has not been established.

1.6.4) Cytotoxic T lymphocytes

Intracellular control of mycobacteria and intracellular infections has been linked with cytotoxic T lymphocytes (CTLs). One of the ways that CTLs carry out this effector function is through the secretion of cytolytic molecules such as granzymes, granulysin and perforin [189]. In *M.tb* infection, cytotoxic CD4+ [189] and CD8+ [190] have been shown to play key roles in TB immunity. More recently, it has been shown that some of these cytotoxic proteins such as granzyme B, granulysin and perforin are expressed by BCG-specific memory T cells following newborn vaccination with BCG [191]. However, these cytolytic molecules may have different roles in mediating immunity against *M.tb*. For example, perforin has been shown to perforate the cell membrane of *M.tb* infected cells, allowing entry of granzymes that either kill the *M.tb* directly or kill the infected cell [192]. *M.tb* target cell death by granulysin is through disruption of the cell membrane which leads to release of cytochrome c and the apoptosis inducing factor (AIF) as well as influx of extracellular calcium [193, 194]. However, the effector function of granulysin is dependent on perforin [195].

Similar to granulysin, granzymes depend on perforin for their cytotoxic activity. Granzyme B induces apoptosis of target cell by activating caspases 3 and 7 [196]. T cell cytotoxic potential may be critical in controlling *M.tb* and therefore was assessed in our study of immune correlates of risk of TB disease.

1.6.5) CD8+ T cells

CD8+ T cells recognise *M.tb* antigens presented on MHC I molecules by infected cells. Mice deficient in β2-microglobulin (no MHC I) have been shown to be more susceptible to *M.tb* [197]. Also, depletion of CD8+ T cells in non-human primates is associated with impaired BCG induced immunity against TB [198]. Although the main function of CD8+ T cells is to eliminate infected cells through cytotoxicity, they also produce TNF-α and IFN-γ [199, 200]. Soares *et al* showed that following routine BCG vaccination of newborns, CD8+ T cell responses measured at 10 weeks of age were characterized by IFN-γ and IL-2 production [201]. Also, IFN-γ production by *M.tb* specific CD8+ T cells in young children has been associated with an immunologic signature of primary *M.tb* infection resulting in disease [202].

1.7) Spectrum of Human Tuberculosis

From a clinical point of view, diagnosis and treatment of TB are based on the fact that following infection with *M.tb*, an individual may develop either active disease or may become latently infected. However, recent understanding and interpretation acknowledges that *M.tb* infection does not result in this binary outcome but rather in a heterogeneous spectrum of clinical states [113, 203] (Figure 3A).

Following initial infection with *M.tb*, some individuals develop active disease, referred to as primary or primary progressive disease with distinct clinical presentation and possibly different host genetic susceptibility [204, 205]. The clinical presentation can range from systemic responses which include fever, weight loss, night sweats to local responses such as cough, lymphadenopathy and lung cavities [206]. These symptoms may represent the host response to

the pathogen which has been suggested to be inadequate, hence development of disease. The imbalance between pro and anti-inflammatory responses has been suggested to be one of the causes for progression to active TB disease (Figure 3B) [207].

Latent TB on the other hand represents a diverse response to *M.tb* infection with different clinical outcomes (Figure 3A). As earlier mentioned, diagnosis of latent infection is made based on the presence of recall immune responses against *M.tb* antigens. This suggests that latent TB reflects a heterogeneous group of individuals which include: i) those who have subclinical disease, ii) progress to active disease, iii) those who at first suppress infection but later go on to develop disease, iv) those who maintain life-long infection, v) those who effectively clear the infection [113, 208] (Figure 3A). Heterogeneity in lung lesions following *M.tb* infections has been demonstrated in both humans and nonhuman primates [113, 209, 210], but the lack of data hampers accurate interpretation of the immunological responses needed for the establishment of latency [207]. However, a balance between pro and anti-inflammatory responses has been suggested to be important in the establishment of latency [207] (Figure 3B).

The need for better diagnostic tools that differentiate the complete spectrum of immune responses to *M.tb* [113, 203, 211] has been brought to light by the heterogeneity within the latent TB population which is now recognised globally [113].

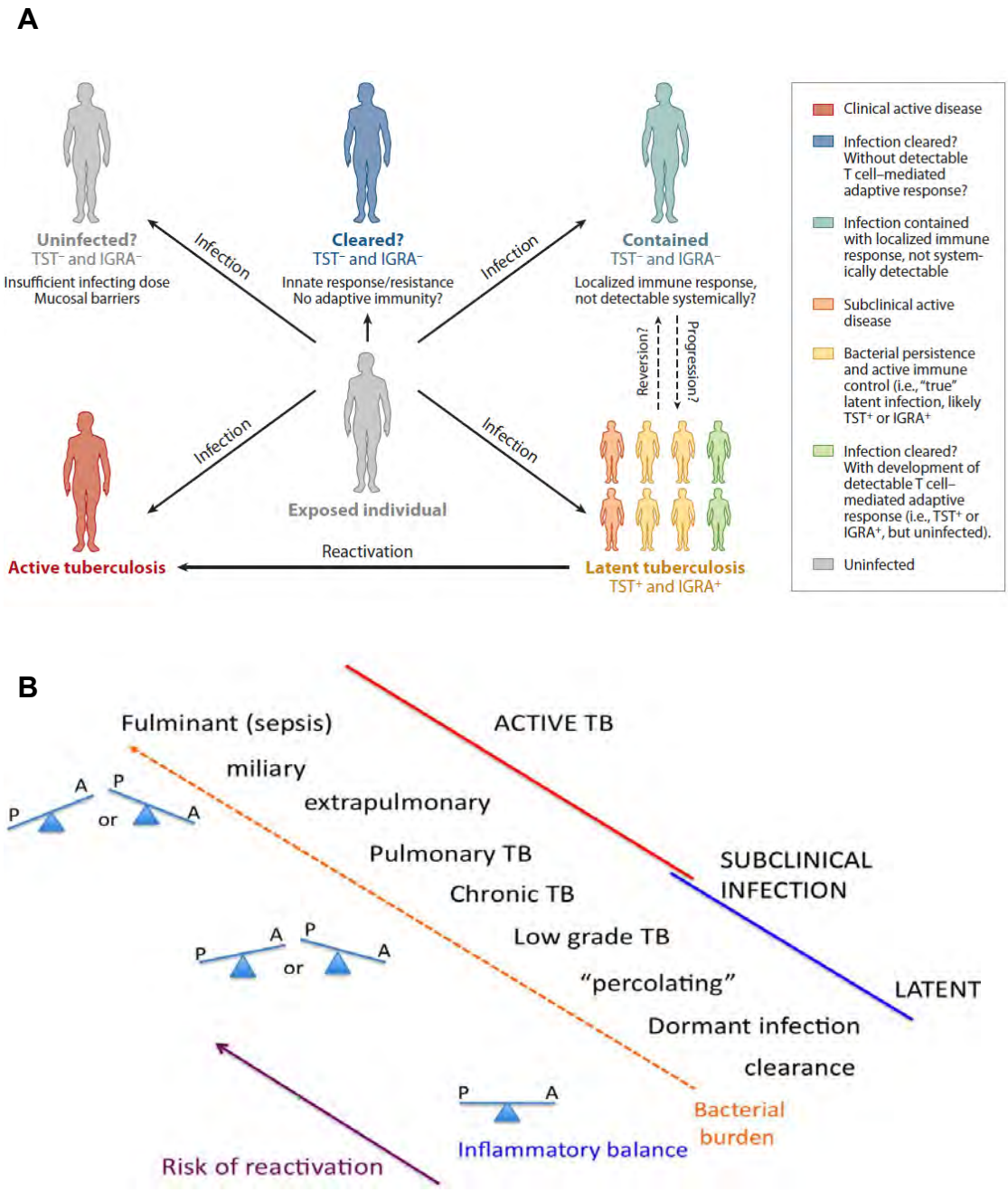

Figure 3: Heterogeneous outcomes following *M.tb* infection. (O'Garra *et al*., 2013; Lin *et al*., 2010)

A) Infection status based on tuberculin skin test (TST) and IFN-γ release assay (IGRA). Positive TST and/or IGRA results are shared by individuals who have subclinical infection, cleared the infection but have detectable T cell responses and those who have an immune response but still remain infected. Negative TST and/or IGRA shared by those individuals who have cleared the infection with no detectable T cell responses, those who remain uninfected and those who have cleared the infection with also no detectable immune responses. **B)** The clinical outcomes of active (red line) and latent (blue line) infection. Bacteria burden shown by the dashed orange line. The seesaws reflect the pro- (P) and anti-inflammatory (A) mediators and the purple line reflects the risk of reactivation in latency.

1.8) Immunological correlates of Risk of TB disease

An immune correlate of protection is a measureable response to a vaccine that indicates a person is protected from being infected or developing a disease [212]. The ability to assess the protective efficacy of a vaccine by measuring the proportion of vaccinees who generate a particular immune response without having to measure clinical outcomes provides significant advantages and is important for vaccine development, monitoring of effectiveness and licensure. A better understanding of the interrelationship between vaccination, immune response, protection and clinical outcomes is of great interest not only to immunologists or vaccinologists but also to regulatory authorities. Without a clear knowledge of protective immunity, vaccine effectiveness can only be determined in large phase III clinical trials.

Correlates of protection have been of significant advantage in facilitating clinical trials of new vaccines against several infectious diseases. For example, following vaccination against Hepatitis B, antibody titres ≥10 mIU/ml have been shown to correlate with the induction of the T helper cell responses that mediate memory B cell responses such that there is an anamnestic response that prevents disease and/or infection in the vaccinee after exposure to the Hepatitis B virus [213, 214]. This antibody titre is used as the cut-off for vaccine induced response in hepatitis B vaccine clinical trials [215]. In influenza, the haemagglutination- inhibition (HAI) antibody titre is the universally accepted correlate of protection[216]. However, a number of novel approaches to the design of new influenza vaccines are under consideration and the development of these new vaccines have focused on HAI as a correlate of protection [216-218]. In Europe, post vaccination HAI titres are used as the basis for the approval of the annual updated influenza vaccine and also for the licensure of new haemagglutinin based vaccines [219].

An effective vaccine that prevents pulmonary TB disease would be an ideal tool to impact the global epidemic [37]. One of the main reasons that hamper the development of efficacious vaccines is the lack of or limited knowledge on

correlates of protection after vaccination. Without a clear correlate of protective immunity against TB, potential vaccine candidates have to undergo large and expensive phase III efficacy trials [220]. Vaccine-induced correlates of protection can only be identified in randomised controlled trials of an effective vaccine but, as earlier mentioned, the only licensed vaccine against TB, BCG, is only partially effective. In alternative, we are studying prospective correlates of risk of TB disease upon BCG vaccination, to inform future studies of correlates of protection [221]. Correlates of risk are immunological markers that correlate with the rate or level of clinical end point used to measure vaccine efficacy in a given population [221].

Optimal cohort selection, appropriate definition of TB cases as well as delineation of adequate follow up period are all critical aspects in designing studies aimed at investigating correlates of risk of TB disease. By definition, correlates of risk may be addressed only before disease occurs, therefore a prospective study, involving thousands of high-risk healthy participants, and at least two years of follow-up are required. Cross sectional comparisons of immunological markers in participants with latent/asymptomatic *M.tb* infection and active TB disease have been performed in many relevant studies [94, 222-226], and generated useful knowledge about immune responses occurring during different stages of the infection and disease. These responses are not necessarily predictive of vaccine efficacy or protection from disease upon natural infection.

Design of immune correlate studies should also take into account the collection of appropriate biological samples to measure host parameters (biomarkers), and try to foresee which technologies may be used at the time of analyses. Biomarkers generally are measurable characteristics, which may be used as an indicator of a biological state or condition. They can be applied in many scientific fields, but in relation to our study, this may be a gene expression signature that identifies individuals more likely to develop disease. Biomarker discovery can

rely on both hypothesis-driven approaches, which rely on assumptions based on current knowledge, or be unbiased and hypothesis generating.

Based on our knowledge of TB immunobiology, we have previously assessed biomarkers that are thought to play a role in fighting against TB, but were not able to identify potential correlates of risk of TB disease [175]; Scriba and Keyser *et al*., In prep). In this thesis, we also applied unbiased approaches, in the form of gene expression profiling, to discover biomarkers of risk of TB disease.

Biomarkers associated with protection against primary *M.tb* infection and development of TB disease could serve as surrogate endpoints in efficacy trials of new TB vaccines. This would allow more rational selection of vaccine candidates in the preclinical and early stages of clinical development as well as shortening of clinical trials [57]. Complexity of the dynamic interaction between *M.tb* and the immune system suggests that a single biomarker of efficacy may never exist (Figure 4). Different biomarkers will have to be identified for different stages of infection and disease. Ideally, an effective vaccine against TB should confer protection across all populations and stages of TB; that is prevent infection of healthy individuals, clearance of *M.tb* in infected individuals and prevent progression to disease [227].

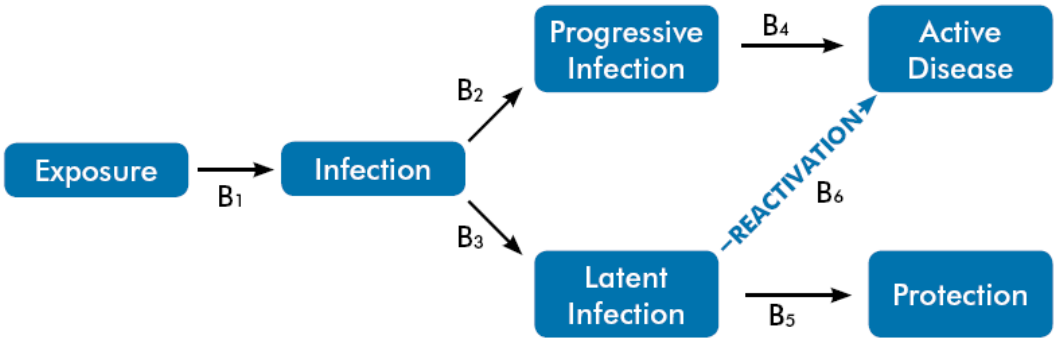

Figure 4: Biomarkers for different stages of *M.tb*'s immunological life cycle. (Image courtesy of TB vaccine pipeline report, July 2013).
B=Biomarker. B_1= Biomarker for exposure to infection, B_2 and B_4= Biomarkers for progression to active disease, B_3 and B_5= Biomarkers for latent infection, B_6= Biomarker for reactivation

Continuous performance of efficacy trials without a clearer knowledge of what is a protective immunity against TB may lead to research fatigue among donors, policy makers, host countries and even TB affected communities. Validated biomarkers are urgently needed to avoid this, as well as reducing cost and time for vaccine candidates to get into large phase III trials.

1.9) Systems Biology

1.9.1) Approaches

Systems biology is an emerging research strategy that focuses on complex interactions within biological systems using a holistic approach, rather than a reductionist approach. The overall aim of systems biology is to understand the dynamic aspects of networks [228]. To understand complex biological systems, integration of experimental as well as computational research is necessary [229]. Systems biology is often studied by monitoring relevant pathways after perturbation of biological systems [230]. This is followed by integration of large data sets to formulate mathematical models that describe the system's structure and its response to perturbations [230].

Systems biology has been applied in different areas of study and, for each of these, different technology platforms have been used. Some of these areas include:

- Genomics – Sequencing of deoxyribonucleic acid (DNA), including intra-organism cell specific variations *e.g.* Telomere variation.

- Epigenomics – Identification of cell specific gene expression regulating factors not empirically coded in the genomic sequence *e.g.* DNA methylation.

- Transcriptomics – Gene expression profiling.

- Proteomics – Measurement of proteins and peptides.

- Metaboloics – Organismal, tissue or cell level measurements of small molecules known as metabolites.

- Phenomics – Variation in phenotypes as they change in disease progression and over lifespan.

1.9.2) Gene Expression Profiling

The role of T cells in immunity against TB has been the main reason why they are studied as potential correlates of risk against TB. Nevertheless, unbiased approaches, which do not limit what may comprise protective immunity against TB have been used to identify potential correlates of risk of TB disease. Genome-wide transcriptional profiling is one of such approaches, which has been used to identify these correlates as well as to depict novel molecular mechanisms involved in host control of pathogens [221, 223, 231]. For these reasons, genome-wide transcriptional profiling was used to identify potential biomarkers of risk of TB disease in this study.

The measurement of the activity (expression) of thousands of genes at once to create a global picture of cellular functions is known as gene expression profiling [232, 233]. It examines the expression level of mRNAs in a given cell

population and, while knowledge of the proteins a cell expresses (proteomics) may be more functionally relevant than knowing how much mRNA is made from each gene, gene expression profiling provides the most global picture possible in a single experiment.. This approach assumes that genes that share a common pattern of expression under certain conditions are functionally related and that change in these gene expression pathways reflects the physiological changes in a cell. This therefore makes it possible to define physiological states and infer phenotypes based on these gene expression patterns [234].

Gene expression profiling usually involves the use of high-throughput techniques and several methods have been used to measure thousands of transcripts simultaneously. Some of these methods include: serial analysis of gene expression (SAGE), massively parallel signature sequencing (MPSS), oligonucleotide arrays, cDNA microarrays and most recently RNA sequencing (RNA-Seq) [234, 235]. Microarrays are currently the most widely used technique.

Microarray analysis is regarded as a hypothesis generating approach: it allows identification of relevant genes and expression pathways that can be further investigated in future studies. For this reason, microarrays have been used in:

- Description of genes involved in developmental, pathological and physiological processes (gene discovery) [236, 237].
- Description of regulatory networks (gene regulation) [238, 239]
- Identification of gene expression patterns that represent prognostic indicators and define disease states (diagnosis) [240] .
- Drug discovery and toxicology [241] .
- Identification of a whole blood gene expression signatures of active TB disease [223].

The workflow of microarray analysis is quite simple (Figure 5). This involves the generation of messenger RNA (mRNA) from two samples/conditions under investigation. Each mRNA molecule is then transcribed to a complementary DNA (cDNA) with a reverse transcriptase enzyme. This process allows incorporation of fluorescent nucleotides to the cDNA, as both samples are labelled with different dyes. The labelled cDNA generated from the mRNA is loaded onto a DNA microarray plate where it hybridises or binds to its synthetic cDNA attached on the microarray plate. The fluorescent intensity of the hybridisation is then measured on a scanner and downstream analysis to identify differential gene expression is performed by a bioinformatician. However, the over simplicity of this concept tends to hide the potential problems as each step in the experiment is a potential source of error.

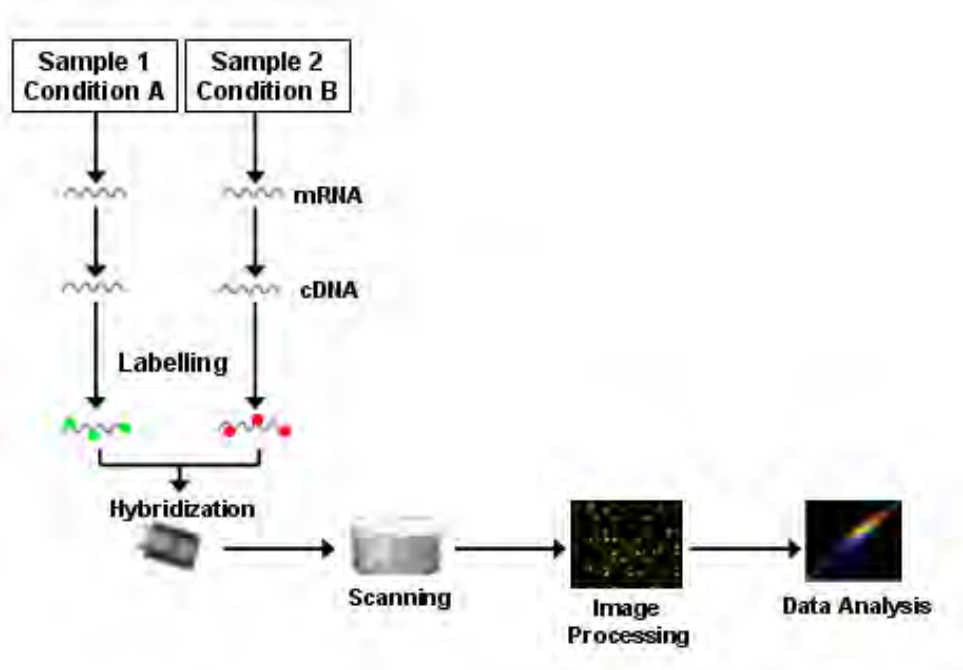

Figure 5: Course of typical microarray experiment (Murphy, 2002).

Microarray experiments usually produce large amounts of data making it critical to analyse. There is no standardised statistical approach to analyse microarray data, despite continuous effort to define optimal procedures for data analysis

and presentation [242]. Following data processing and normalisation, different analysis strategies are used to analyse microarray data (Figure 6).

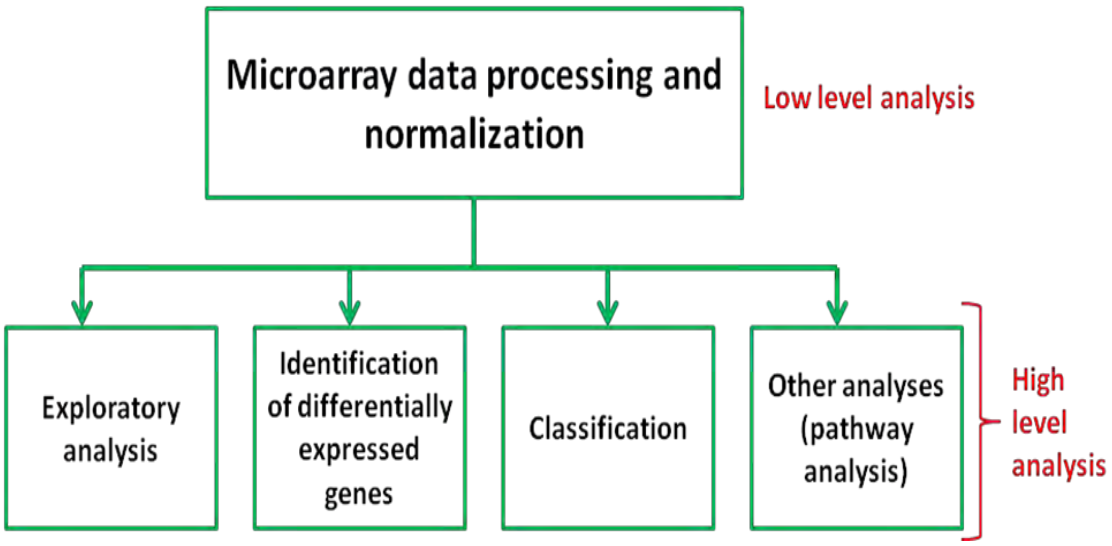

Figure 6: Different approaches used for microarray data analysis

Some of the commonly used methods of analyses include:

i) Low level analysis

Before any downstream analysis on microarray data, a low level analysis is performed which involves the exclusion of poor quality spots and normalisation to remove systematic errors [243].

To bring up-regulated and down-regulated values to the same scale for easy comparison, the fluorescent intensities of the spots are firstly log transformed. A Spot is excluded from analysis if its intensity is lower than the background plus two standard deviations [244].

The process of normalisation involves balancing the fluorescent intensities of the two labelling dyes to remove systematic errors. Some of the common methods of normalisation are [244]:

- Global normalisation, which uses all the genes on the array.

- Housekeeping genes normalisation, which uses those that are constantly expressed.

- Internal controls normalisation, which uses exogenous controls added during the hybridization step.

Despite the use of all these methods, they have been proven to be inadequate for data normalisation of microarrays. Reasons for this are that housekeeping genes are not constantly expressed as previously thought and dye fluorescence can be influenced by spot intensity and spatial location on the array [245]. Recently, different methods have been used to normalize array data. One of such methods thought to be more superior to other methods uses non-linear normalisation on the basis of gene intensity and spatial location [244, 246]. The most common and widely used non-linear normalisation method is the quantile normalisation [247]. This method was derived from quantile-quantile plots and it adjusts the distribution of gene expression pooled from each array to be the same [248]. This method is the default normalisation method in Bioconductor [249], which is the most widely used and open source platform for analysing microarray data in R (R core team, 2006).

ii) High level analysis

Following low level analysis, a high level analysis is performed which involves the application of several statistical methods as well as data mining techniques to uncover patterns of gene expression. The commonly used high level analyses are (Figure 6):

a) Exploratory analysis: This involves understanding the similarities and/or dissimilarities of the gene expression levels among all samples. The aim of this analysis is to find genes with similar gene expression profiles using a clustering technique [247]. There are two types of clustering analyses: Supervised and unsupervised. While unsupervised classification requires no pre-defined test,

supervised analysis on the other hand requires known biological information about the gene sets to guide the clustering algorithm. There are two categories of unsupervised clustering which are hierarchical and non-hierarchical analyses with the former being commonly used [250]. The K-means clustering (centroid) [251] and self-organisation maps (SOM) [252] are other types of clustering analyses used.

b) Identifying differentially expressed genes: A two-fold increase or decrease in expression is usually used to identify differentially expressed genes using a fixed threshold cut-off. Systemic and biological variation in microarray experiments makes this method statistically inefficient [247] and might increase the risk of getting false positives or negatives. To complement this analysis, statistical methods are applied which rank genes according to their probability of differential expression [247]. Examples of such statistical methods include: student *t* test, Analysis of variance (ANOVA), Bayesian method and the Mann-Whitney test [253-255]. To control for type I errors such as false discovery rate (FDR) and family wise error rate (FWER), which may arise when comparing thousands of outcomes, the resulting *p*-values generated from the statistical analysis are adjusted for multiple comparison [256] .

c) Class prediction analysis: This involves using genes expression profiles to classify samples. A classifier algorithm is trained using gene expression profiles in a given set of samples and used to assign groups in a new set of samples [247]. This kind of analysis is also called supervised analysis, and includes linear discriminant analysis (LDA) [257] and k-nearest neighbour [258]. However, generalising the classifier for all situations and over-training on the same data set resulting in "over-fitting" are the major challenges when using this model. Validation of the trained classifier is essential to create a balance between accuracy and generalisation. Cross-validation is often used for this and the most common method used is called the leave-one-out in which one sample is taken from the training set to be a validation sample for each round of analysis [259].

d) Pathway analysis: Analysing microarray data in pathways could lead to better understanding of the system as genes never act alone in biological systems, but rather as a cascade of networks [247]. There are three approaches to performing pathway analyses:

The first is further exploratory analysis of the cluster analysis to see if genes that cluster together might be involved in the same pathway [260].

The second is to reverse engineer the global genetic pathways followed by the identification of global regulatory networks [261]. This method assumes that by perturbing the system there will be a change in expression of other proteins in the network and this change in expression is an image of the underlying network. Examples are Boolean and Bayesian networks [262, 263] .

The last approach is studying the expression from a pathway perspective itself. Expression data can be linked to metabolic pathways and evaluated to identify which metabolic pathways are affected by transcriptional changes. Examples include gene set enrichment analysis (GSEA) and integrated pathway analysis (IPA).

1.9.3 Statistical and biological validation of microarray results

Validation of microarray results is necessary because of the statistical issues that come with analysing the data [264, 265]. Microarrays are often used as a first step to identify genes that associate with an outcome under investigation. However, the amount of false positives that can be generated during the analyses process can be very high especially with small sample sizes and the small differences in gene expression between the conditions [266]. Validation is therefore usually performed on independent groups of samples from which the original transcriptomic profiles were identified to overcome these false positive rates [267]. The group of samples on which microarrays are performed for gene identification are usually referred to as the discovery or training set while the group of samples on which the validation of these genes are performed are referred to as the validation or test set. After identification of a smaller subset of

differentially expressed genes by microarray in the training set, validation can be performed using quantitative real time polymerase chain reaction (qRT-PCR) in the validation set. This technique has been shown to be very sensitive and very rapid to accurately quantify results generated by microarray [266].

The qPCR method, however, can be an expensive and relatively low throughput technique. For these reasons, the Fluidigm Dynamic Array Integrated Fluidic Circuits (IFC) and the Biomark HD system offers more throughput and is ideal for validation of microarray results [268, 269]. This technique can be used to measure expression of up to 96 transcripts from 96 different samples, allowing for a total of 9216 reactions to be performed in a single experiment. The IFC has tens of thousands of microfluidic controlled valves and interconnected channels to move both the reagents and samples in several patterns [268]. The elastometric material that makes up these valves deflects under pressure, creating a tight seal, which controls the flow of fluids in the IFC. The samples (DNA) are partitioned and randomly distributed in small volumes into the different chambers followed by PCR amplification in the presence of a fluorophore-containing probe. A positive fluorescence is indicative of DNA in the chamber while no fluorescence or blank is indicative of no DNA in the chamber [270]. This new qPCR technology makes it possible to perform high throughput gene expression analyses with very small amounts of both reagents and sample volumes because the IFCs reduce the 10-20ul volume used in a normal qPCR down to 10 nanolitres [268, 269].

For the validation analysis performed in this thesis, we first selected the most differentially expressed genes by microarray in the training set. Using a multiplex quantitative real time PCR (Fluidigm) we then measured the expression of these genes in the training set. This was to validate gene expression profiles between microarray and the Fluidigm. For validation, the expression of these genes was measured by Fluidigm in the validation set (Figure 7).

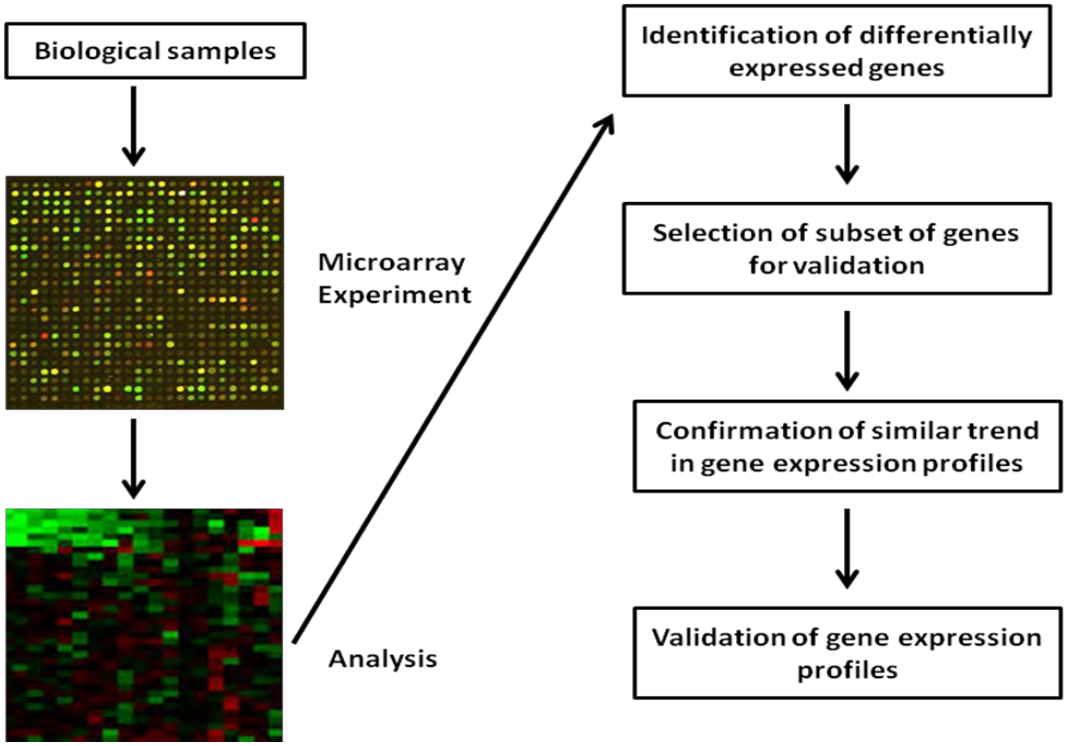

Figure 7: Schematic representation of validation procedure

1.10 Assays used to measure vaccine immunogenicity

In most TB vaccine clinical trials, immunological assays are designed to measure vaccine-specific T cell immunity. In humans, the majority of these assays evaluate the magnitude and/or quality of vaccine-specific memory T cells in the peripheral blood because it is easier and less invasive to obtain compared to lymph nodes, lung tissue or bronchial alveolar lavage. Typically, peripheral whole blood or peripheral blood mononuclear cells (PBMC) are re-stimulated with vaccine antigens *in vitro* [271] and the responding cytokine-producing cells can be measured by Elisa, Elispot or by flow cytometry [272]. The choice of method to use largely depends on the selected outcomes of interest and the resources available.

Samples used for these assays may be fresh (just after collection), cryopreserved or both. The assay duration is very critical and this usually varies depending on the questions being addressed and the feasibility of the

performance. The assay durations usually include; (i) short-term assay (less than 24 hours) (ii) medium-term assay (one to three days), or (iii) long-term assay (four or more days) [271].

In this thesis, we used all three assays depending on the T cell function we were investigating. We used the short term whole blood intracellular cytokine staining assay (12 hrs) to investigate the magnitude and cytokine profile of BCG-specific T cells by flow cytometry; as well as levels of secreted mediators in the plasma (7hrs) by luminex technology. Long term re-stimulation assays were used to assess the cytotoxic potential (3 days) and proliferative capacity (6 days) of BCG-specific T cells respectively by flow cytometry.

CHAPTER 2: CORRELATES OF RISK OF TB DISEASE IN BCG VACCINATED INFANTS

All studies reported in this chapter, partially published, were performed by other members of SATVI (Benjamin Kagina, Alana Keyser, Brian Abel, Thomas Scriba). The results generated from the studies in this chapter led to the primary work presented in this thesis. In order to convey a clear understanding of this thesis work, it was necessary to present a brief report on these studies. This chapter therefore serves as the background for this thesis work.

2.1) Rationale and approach

As previously mentioned, the most effective intervention against TB would be the widespread use of an efficacious vaccine [273]. Unfortunately, the only licensed vaccine against TB, BCG, has variable efficacy in protection against pulmonary TB [36], and this accounts for high TB rates worldwide. Therefore, there is urgent need to develop a new effective vaccine against TB, but this has proven difficult to achieve, partially because of lack of immunological correlates of protection. Identification of immunological determinants of protection against TB may be guided by studies of correlates of risk of developing TB disease [221]. As children are particularly susceptible to TB, we aimed to identify immunological correlates of risk of TB disease following newborn BCG vaccination. Blood was collected from 10 week old infants following BCG vaccination at birth, processed and cryopreserved. After a two year follow-up period, infants who developed TB disease (at risk of TB, defined cases) and those who did not develop disease (not at risk of TB, defined controls) were identified (see materials and methods). Blood stored at 10 weeks of age was

thawed and different immunological parameters investigated to identify potential correlates of risk of developing TB disease in these infants.

We hypothesised that frequencies of BCG-specific T cells producing Th1/Th17 cytokines as well as cytotoxic and proliferative capacity of T cells will correlate with risk of developing TB disease. Using this hypothesis-driven approach, we evaluated immune responses thought to be important for protection against TB. We focused on Th1/Th17 cytokine production by BCG-specific T cells, their proliferative and cytotoxic potential, and release of pro-inflammatory mediators in response to BCG.

We complemented these studies with an unbiased, hypothesis generating approach, by measuring PBMC gene expression profiles in response to BCG stimulation.

2.2) Materials and Methods

2.2.1) Participants

Ten-week old infants vaccinated with BCG at birth were enrolled at the SATVI field site in the Worcester area, near Cape Town, South Africa into a randomized controlled trial (RCT) [56] which aimed to determine whether percutaneous or intradermal delivery of Japanese BCG resulted in similar protection against TB. 5,724 from 11,680 infants enrolled for this RCT study were then recruited into our correlates of risk study. Exclusion criteria at 10 weeks of age were: BCG not received within 24 hours of birth, HIV-infected mother, any acute or chronic disease at the time of enrolment, significant perinatal complications in the infant, clinically anaemic, and household contact with any person with TB disease, or any person who was coughing. The protocol for this study was approved by the University of Cape Town Research Ethics Committee (271/2000) and written informed consent was obtained from parents or legal guardian. The study was conducted according to the US Department of Health and Human Services and Good Clinical Practice guidelines.

2.2.2) Participant follow up and TB case definition

Blood was collected from infants at 10 weeks of age and participants were followed up for a period of 2 years. Community-wide passive surveillance systems identified children with possible TB disease, those with symptoms suggestive of TB disease, or from households where an adult had TB disease [56]. These infants were admitted to a dedicated research ward for clinical examination, chest radiography, tuberculin skin testing, two early morning gastric aspirations and two sputum inductions for *M.tb* smear and culture [56]. All infants admitted to the research ward were also tested for HIV infection: a positive antibody test resulted in exclusion. The median time from vaccination to TB diagnosis was 12.3 months with minimum and maximum times being 1.1 and 23.9 months respectively.

For TB case definition, only pulmonary TB patients were included in this study. The reason for this was because this was the primary endpoint for TB diagnosis to assess correlates of risk of TB and in addition other forms of TB are relatively more difficult to diagnose. However, Hawkridge *et al* reported a total of 5 out of the 11,680 recruited in the study to have other forms of TB but the sample size was too small to perform any statistical comparisons [56]. Cases included were culture positive for *M.tb* after investigation (definite TB) or culture negative for *M.tb* but either had strong positive chest x-ray and clinical and/or epidemiological evidence of TB (probable TB). We included 2 groups of controls: infants who were living in the same TB endemic area but didn't meet criteria for TB investigation (community controls) or those who were exposed to patients with active TB in the household but found not to have TB after investigation (household controls).

2.2.3) Whole blood assay and intracellular cytokine staining

For logistic reasons, the Danish BCG strain was used for all experiments as opposed to the Japanese strain used for vaccination. The main reasons being that at the time when experiments were done, there was a shift in the country to the use of the Danish strain and almost all immunological assays implored the use of this strain. Heparinised blood was collected from all infants at 10 weeks of age and 1mL was incubated with BCG (Danish strain, Statens Serum Institute (SSI), used at 1.2 x 10^6 organisms/mL), as previously described [271]. Briefly, 1ml of blood was incubated with BCG and the co-stimulatory antibodies anti-CD28 and anti-CD49d (BD Biosciences, 1µg/mL each) for 7hrs at 37^{o}C. Blood was also incubated with co-stimulatory antibodies alone as negative control or with Staphylococcal Enterotoxin B (SEB, Sigma-Aldrich, 10µg/mL) as a positive control. After this incubation time, plasma was collected and cryopreserved (to measure release of soluble molecules) and Brefeldin-A (Sigma, 10µg/mL) was then added to the blood for intracellular cytokine capture, followed by incubation for an additional 5 hours at 37°C. After incubation, 2mM of EDTA (Sigma) was added, followed by vortexing for 10s and incubating at room temperature for

15mins. This was followed by addition of FACS lysing solution (BD Biosciences) to lyse red cells and fix white cells for 10mins at room temperature. Cells were then cryopreserved by pelleting and re-suspending in 10% DMSO in foetal calf serum (FCS) followed by step wise freezing to -70°C in a "Mr Frosty" (Nalgene) and transferred to liquid nitrogen the following day. Multiple vials of each sample were cryopreserved to avoid repeated freeze-thaw cycles. Cryopreserved cells were later thawed, washed and permeabilised using Perm/Wash solution (BD Biosciences). Cells were incubated for 1 hour with fluorescence-conjugated antibodies against surface antigens as well as intracellular cytokines at 4°C in the dark. Antibodies used were: anti-CD3 Pacific Blue (clone UCHT1), anti-CD4 QDot605 (S3.5, Invitrogen), anti-CD8 PerCP-Cy5.5 (SK-1), anti-γδ-TCR APC (B1), anti-IFN-γ Alexa 700 (B27), anti-TNF-α PE-Cy7 (Mab11), anti-IL-2 FITC (5344.111, all from BD Biosciences) and anti-IL-17 PE (eBio64CAP17, eBioscience). An LSRII flow cytometer (BD Biosciences) configured with 3 lasers and 12 fluorescence detectors, using FACS Diva 6.1 software, was used to acquire cells. Optimal photomultiplier tube (PMT) settings were established prior to sample analysis. Cytometer Setting and Tracking (CST) beads (BD Biosciences) were used to record the target MFI values for the baseline settings each day prior to sample acquisition. Compensation settings were set using anti-mouse kappa-beads (BD Biosciences) labelled with the individual fluorochrome-conjugated antibodies.

2.2.4) PBMC isolation and cryopreservation

PBMC were isolated from peripheral blood of 10-week old infants by ficoll density gradient centrifugation (Sigma), and cryopreserved in RPMI 1640 (Biowhittaker). Briefly, 10mL of blood was diluted with 20mL RPMI in a 50mL tube, capped and inverted to mix. 15mL of ficoll was placed in another 50mL tube and 30mL of the diluted blood was slowly layered on top of the ficoll. The blood was then centrifuged at 400g for 30mins at room temperature without brake and PBMC from the buffy coat carefully aspirated at the ficoll interface with a pipette and transferred into another tube. PBS was added to 50mL and

then centrifuged at 350g for 10mins at 22°C. Supernatant was decanted and cells resuspended in 1mL of 1X PBS by pipetting up and down. 1X PBS was added to 50mL, tube inverted 2-3 times and centrifuged at 350g for 10mins at 22°C. Supernatant was decanted and cells resuspended in 1mL RPMI and kept on ice. For cryopreservation, cells were pelleted and resuspended in RPMI containing 10% DMSO in FCS followed by step wise freezing to -70°C in a "Mr Frosty" (Nalgene) and transferred to the vapour phase in liquid nitrogen the following day. Because repeated freeze-thaw cycles can have serious effects on immunological as well as genetic findings, multiple vials of PBMCs were cryopreserved so as to avoid repeated freeze-thaw cycles and each vial was thawed only once.

2.2.5) Lymphoproliferation assay

Cryopreserved PBMC were thawed in culture medium (12.5% v/v AB+ serum in RPMI) containing 10μg/mL DNase (Sigma-Aldrich). After 2 washes, cells were stained with 1μg/mL Oregon Green (Molecular Probes) and rested in 5% CO_2 at 37°C overnight. PBMC were then incubated at 2 x 10^5 cells/well in 200μL culture medium with BCG at a multiplicity of infection (MOI) of 0.01 or 0.5μg/mL of SEB (positive control) in 5% CO_2 at 37°C for 6 days. Medium alone served as negative control. Four hours before the end of the incubation period, cells were re-stimulated with phorbol 12-myristate 13-acetate (PMA, Sigma-Aldrich 20ng/mL) and ionomycin (Sigma-Aldrich, 10μg/mL) to induce cytokine expression and Brefeldin-A (Sigma-Aldrich, 2μg/mL) added for intracellular cytokine capture. After incubation, cells were harvested with 2mM EDTA (Sigma-Aldrich) in PBS, followed by staining with 1μg/mL LIVE/DEAD® Fixable Violet Dead Cell Stain (Invitrogen). Cells were then fixed with FACS Lysing Solution (BD Biosciences) before cryopreservation. Cells were later thawed, washed and stained for 1 hour at 4°C with anti-CD3 Qdot605 (clone UCHT1) and anti-CD8 PerCP-Cy5.5 (Sk1) and acquired as described above. Re-stimulation with PMA and Ionomycin down regulates CD4 expression so CD4+ T cells were identified as CD3+CD8- cells [274, 275]

2.2.6) Cytotoxic marker assay

PBMC were thawed, washed and plated at 2 x 10^5 cells/well in 200μL RPMI containing 10% AB serum and incubated with either BCG at MOI of 0.1 or 0.05μg/ml SEB (positive control) in 5% CO_2 at 37°C for 72 hours. Medium alone served as negative control. Cells were then harvested, stained for viability with 1μg/mL LIVE/DEAD® Fixable Violet Dead Cell Stain (Invitrogen), fixed and cryopreserved as described above. Cryopreserved fixed cells were later thawed, washed and permeabilized with Perm/Wash solution (BD Bioscences). After permeabilization, cells were stained with the following antibodies for 1h at 4°C: anti-CD3 Qdot605 (clone UCHT1), anti-CD8 Cy5.5PerCP (SK1), anti-granzyme B Alexa 700 (GB11), anti-perforin FITC (δG9; all from BD Biosciences) and anti-granulysin PE (eBioDH2, eBioscience). Cells were acquired as described above.

2.2.7) Secreted mediators measurement

Supernatant collected from whole blood assays (plasma) was thawed once and levels of 29 cytokines/chemokines were determined with the human cytokine LINCO*plex* 29-bead array assay kit (LINCO Research, Millipore). Cytokines/chemokines measured were: interleukin-1α (IL-1α), IL-1β, IL-1RA, IL-2, IL-4, IL-5, IL-6, IL-7, IL-8, IL-10, IL-12p40, IL-12p70, IL-13, IL-15, IL-17, soluble CD40-ligand (sCD40L), epidermal growth factor (EGF), eotaxin, fractalkine, granulocyte-colony stimulating factor (G-CSF), granulocyte-macrophage colony-stimulating factor (GM-CSF), interferon-γ (IFN-γ), interferon-gamma-induced protein (IP-10), monocyte chemotactic protein-1 (MCP-1), macrophage inflammatory protein- (MIP-1-α, MIP-1β), transforming growth factor-α (TGF-α), tumor necrosis factor-α (TNF-α), and vascular endothelial growth factor (VEGF) according to manufacturer"s instructions. The Luminex 100 IS instrument with Luminex software (xMAP technology, Luminex Corporation) was used to detect fluorescence.

2.2.8) Gene expression profiling

Cryopreserved PBMC were thawed, washed in RPMI and rested for 6 hours at $1X10^6$ cells/ml in RPMI 1640 containing 10% human AB serum and 1% L-glutamine in 5% CO_2 at 37°C. After resting, PBMC were incubated in culture with BCG (Danish strain, SSI, reconstituted as previously described) at an MOI of 0.18 in 5% CO_2 at 37°C for either 4 or 12 hours. Medium alone served as negative control. Cells were then harvested and QIAmp RNA Blood Mini kit (Qiagen) was used to isolate RNA according to the manufacturer's instructions. Isolated RNA was stored at -80°C, later thawed and amplified using the Illumina RNA Amplification Kit (Ambion) as previously described [276].

Amplified RNA (750ng per array) was hybridized to the Illumina HumanRefSeq-8 BeadChip (version 2) according to the manufacturer's instructions. An Illumina bead array reader confocal scanner was used to scan the arrays.

2.2.9) Data analysis

FlowJo (Treestar) was used to compensate and to analyze the flow cytometric data. Boolean gates were generated to assess combinations of markers.

For whole blood intracellular cytokine staining assays, frequencies of cytokines from the negative control were subtracted from BCG-specific responses. Median absolute deviations (MADs) were calculated as follows: for each sample, the absolute deviation from the median was obtained by subtracting the frequencies of cytokine expressing cells of each sample from the median expression in the negative control for all unstimulated samples. The MAD was then calculated as the median of the absolute deviations of each sample from the median. Participants were included in the analysis if they meet the following criteria: (1) a positive control (SEB) CD4 T cell response higher than the median plus 3 MADs of the CD4 T cell response in the negative control, (2) number of CD3+ T cell events counted > 75,000.

For the proliferation assay, frequencies of proliferating cells from the negative control were subtracted from the BCG stimulated frequencies and infants were included in the analyses only if frequencies of Oregon Green^{low} CD4+ T cells in the positive control were greater than the median frequency plus 3 MAD of the negative control.

For the cytotoxic marker assay, frequencies of cytotoxic molecule^{+} T cells in the negative control were subtracted from frequencies of BCG stimulated responses and infants were included in the analyses only if frequencies of cytotoxic molecule-expressing CD4+ or CD8+ T cells in the positive control were greater than the median frequency plus 3 MAD of the negative control.

For the Luminex assay, cytokine data were imported directly into Microsoft Excel from the Luminex software. For analysis, standards were used to generate standard curves in duplicate for each cytokine; these curves were used to calculate cytokine levels. Cytokine levels from medium alone were subtracted from BCG stimulated levels to obtain final BCG-specific cytokine levels. Negative values and values below limit of detection were assigned a zero value.

For assessment of differences between cases and controls, a Mann-Whitney U test was performed, using Prism 4.0 (GraphPad Software Inc.).

For Microarray data analysis, raw Illumina probe data was first exported from Beadstudio followed by screening for quality. Probe set intensities were pre-processed, quantile-normalized and expression values transformed to log2 using Bioconductor (www.r-project.org). Genes with low expression and insufficient variation in expression across all samples were excluded using Bioconductor's gene filter package. Following gene filtering, only expression values with intensities greater than 200 units in at least 2 samples and an interquartile range of 0.2 (log 2 scale) across all samples were included for analysis. Unsupervised hierarchical clustering was used to obtain unbiased clusters of infants independent of clinical outcome.

2.3) Results

2.3.1) Participants

A total of 13,338 pregnant women were approached for the initial RCT study and 11,860 infants were vaccinated and recruited into the study. Reasons for exclusion were: still birth, prematurity, perinatal infection as well as withdrawal from study. 1578 mothers were therefore excluded from the study and from this number, only 11 withdrew consent [56]. From the 11,680 infants vaccinated with BCG at birth in the randomized controlled trial [56], we enrolled a total of 5,724 infants for this study. Different groups of babies were used for different assays reported in this chapter. Figure 8A below shows a summary of the enrolment into the various arms of the study. Firstly, the infants were divided into a training and validation set (Figure 8B). All infants included into this part of the study were from the training set, except for studies involving the cytotoxic potential of T cells that had infants from both training and validation sets. For infants in the training set, a total of 29 infants were identified as definite TB (microbiological confirmation) and were included as cases. For gene expression studies, a total of 26 definite TB cases were included for analysis. Controls in the training set, were divided into two: 55 community controls and 55 household controls (see section 2.2.2 for definitions) and both groups were used for all assays. However because not all samples from the various control groups were always available to perform the different assays, only community controls and household controls were used for release of secreted mediators and transcriptional profiling respectively. For infants in the validation set (cytotoxic potential), a total of 29 infants were identified as probable TB (see section 2.2.2 for definition) because there were not enough culture positive infants to form a validation set. Controls in the validation set were community controls that were never investigated for TB (n=55).

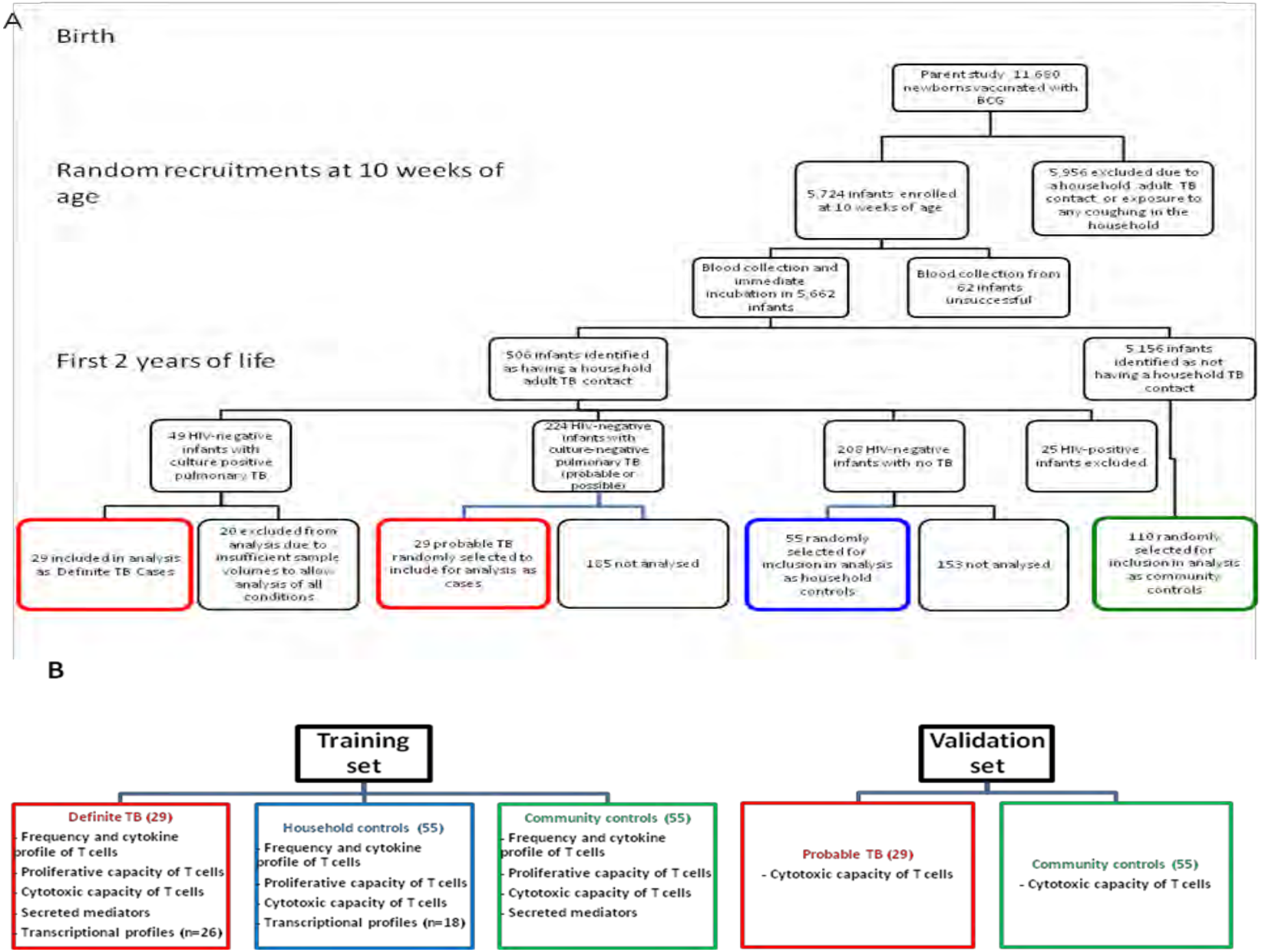
A
Birth
Random recruitments at 10 weeks of age
First 2 years of life
Parent study: 11,690 newborns vaccinated with BCG
5,724 infants enrolled at 10 weeks of age
5,956 excluded due to a household adult TB contact or exposure to any coughing in the household
Blood collection and immediate incubation in 5,662 infants
Blood collection from 62 infants unsuccessful
506 infants identified as having a household adult TB contact
5,156 infants identified as not having a household TB contact
49 HIV-negative infants with culture positive pulmonary TB
224 HIV-negative infants with culture-negative pulmonary TB (probable or possible)
208 HIV-negative infants with no TB
25 HIV-positive infants excluded
29 included in analysis as Definite TB Cases
20 excluded from analysis due to insufficient sample volumes to allow analysis of all conditions
29 probable TB randomly selected to include for analysis as cases
185 not analysed
55 randomly selected for inclusion in analysis as household controls
153 not analysed
110 randomly selected for inclusion in analysis as community controls
B
Training set
Definite TB (29)
- Frequency and cytokine profile of T cells
- Proliferative capacity of T cells
- Cytotoxic capacity of T cells
- Secreted mediators
- Transcriptional profiles (n=26)
Household controls (55)
- Frequency and cytokine profile of T cells
- Proliferative capacity of T cells
- Cytotoxic capacity of T cells
- Transcriptional profiles (n=18)
Community controls (55)
- Frequency and cytokine profile of T cells
- Proliferative capacity of T cells
- Cytotoxic capacity of T cells
- Secreted mediators
Validation set
Probable TB (29)
- Cytotoxic capacity of T cells
Community controls (55)
- Cytotoxic capacity of T cells

Figure 8: Participant enrolment into the different groups and cohorts of the study (Modified from Kagina et al., 2010).
A) Study design and participant enrolment into case/control groups. Controls were randomly selected using a random selection program on STATA. 185 probable/possible TB cases as well as 153 TB-negative cases were not analysed in order to make sample size more feasible and practical. **B)** Cases and controls included in the different assays and different cohorts of the study. Highlighted in red are cases while blue and green are household and community controls respectively. For transcriptional profile analysis in the training cohort, 26 cases and 18 household controls were used.

2.3.2) Frequency and cytokine profile of BCG-specific CD4+ and CD8+ T cells

As earlier mentioned, cytokines produced by T cells are measured as vaccine endpoints in clinical trials [253] and are also thought to be important in TB immunity [121, 144]. We therefore investigated these cytokines as potential correlates of risk of childhood TB disease development, following BCG vaccination at birth. An intracellular cytokine assay was used to evaluate frequencies and cytokine expression profiles of these T cells and these outcomes were compared between cases and controls. Figure 10 shows a representative flow cytometry plot of cytokine co-expression in CD4+ T cells in whole blood stimulated with BCG, SEB or left unstimulated.

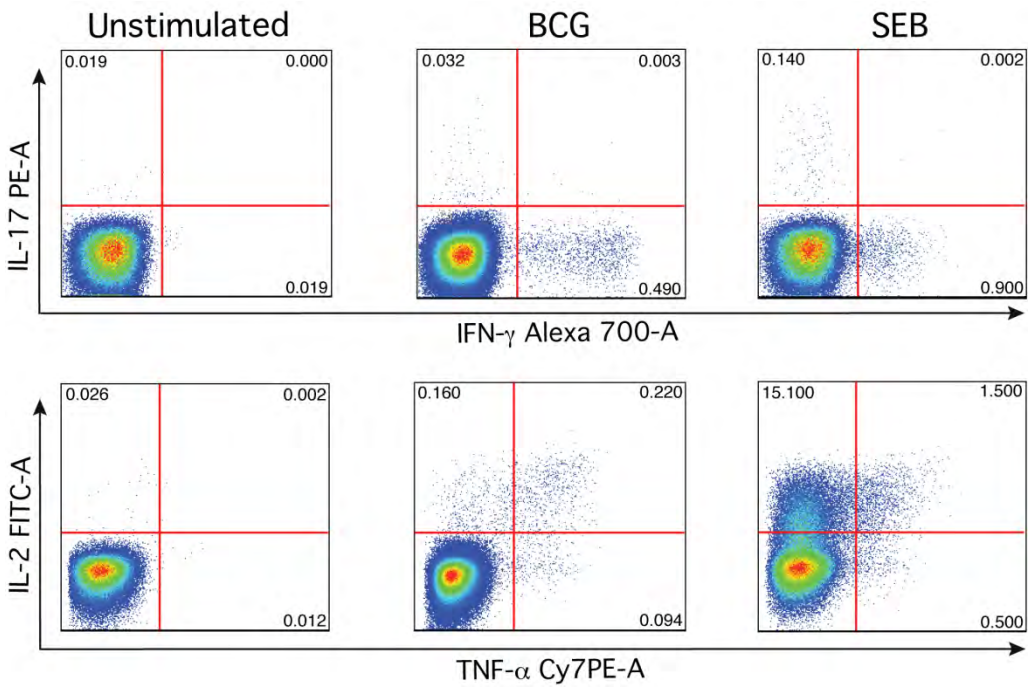

Figure 9: Representative flow cytometry plots of cytokine co-expression (Kagina *et al*., 2010).
Whole blood was incubated with BCG, SEB or left unstimulated for 12 hours and cytokine detected using an intracellular cytokine assay and flow cytometry.

There were no differences between the 3 groups in the frequencies of BCG-specific CD4+ T cells expressing any of the 4 cytokines (Figure 10A). Frequencies of CD4 T cells expressing different combinations of IFN-γ, TNF-α, IL-2 or IL17 were also similar in cases and controls (Figure 10B).

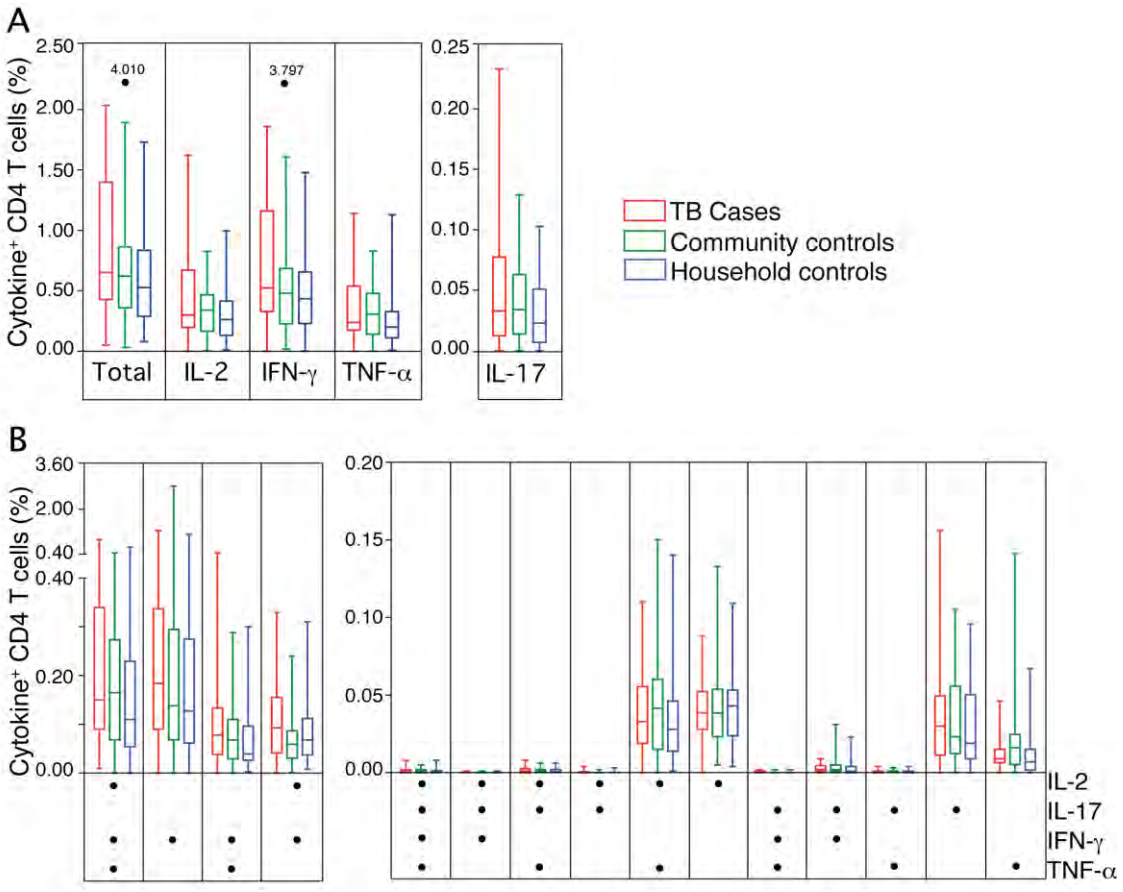

Figure 10: Frequency and cytokine expression profile of BCG-specific CD4+ T cells (Kagina *et al*., 2010).
Whole blood was incubated with BCG for 12 hours and cytokine detected using an intracellular cytokine assay and flow cytometry. (**A**) Frequencies total CD4+ T cells expressing IL-2, IFN-γ, TNF-α and IL-17 upon BCG stimulation. **(B)** Frequencies of BCG-specific CD4+ T cell-expressing different combinations of cytokines. Boolean gating was used to generate 15 distinct cytokine expressing subsets following selection of CD4+ T cells. Results are shown in box and whiskers plots with whiskers representing the maximum and minimum value; the box representing the interquartile range and the horizontal line in the box representing the median. No significant differences between the groups (all p>0.05) were observed using the Kruskal-Wallis test. Red boxes represent TB cases (n=29), green boxes represent community controls (n=55) and blue boxes represent household controls (n=55).

Similarly to CD4+ T cells, cases and controls did not differ in terms of frequencies of total cytokine-expressing BCG-specific CD8+ T cells (data not shown), nor cytokine combinations thereof (data not shown). Of note, CD8+ T cell responses to BCG were lower than those observed in CD4+ T cells, and mainly restricted to IFN-γ production.

2.3.3) Proliferative capacity of BCG-specific T cells

We have recently shown that newborn BCG vaccination induces mycobacteria-specific T cells endowed with proliferative capacity [191]. Proliferation capacity of BCG-specific T cells was assessed as potential correlate of risk of developing TB disease in BCG vaccinated infants. The *in vitro* lymphoproliferative capacity of these cells was measured as dilution of the intracellular dye Oregon Green upon cell division in response to BCG. Although BCG-specific proliferating T cells were detected in most of the infants, there were no differences in the proliferative responses between cases and the 2 control groups (Figure 11).

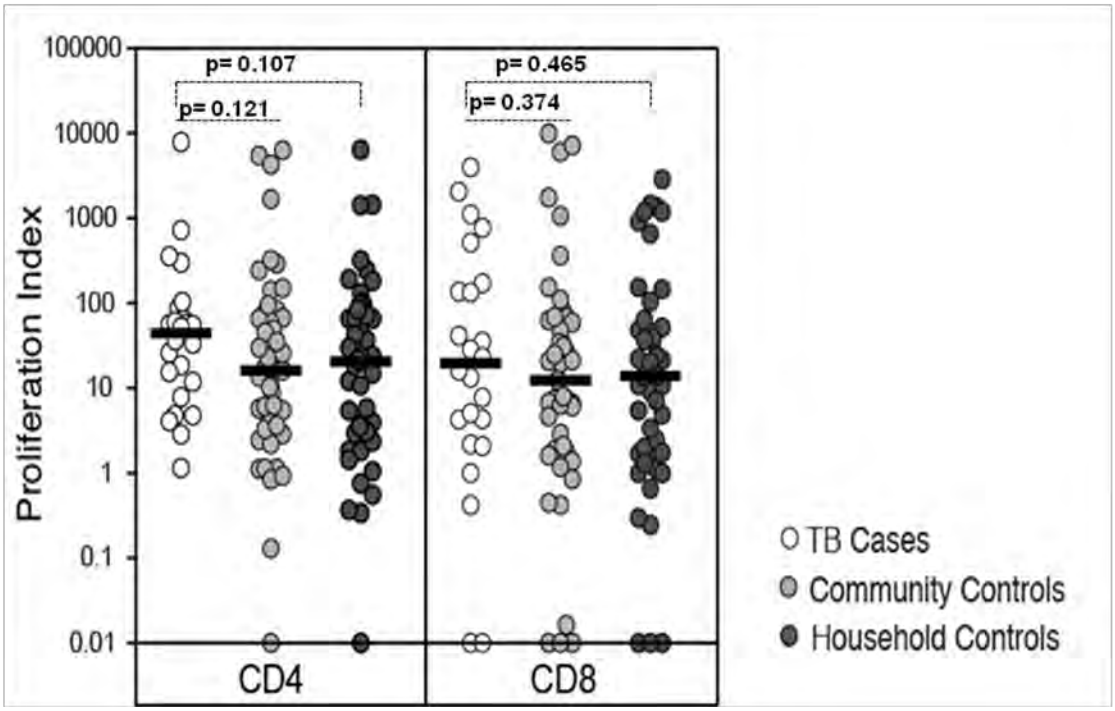

Figure 11: Proliferative capacity of BCG-specific T cells (Scriba and Keyser *et al*, manuscript in preparation).
PBMCs were stained with Oregon Green (OG) and stimulated for 6 days with BCG or left unstimulated. Proliferating cells were identified as OG^{low} CD8+ or CD8- (mainly CD4+) T cells. Proliferation index was calculated as the frequency of proliferating cells upon BCG stimulation, divided by the frequency of proliferating cells in unstimulated cells. Lines in the middle denote medians. Differences between the three groups were assessed using the Kruskal-Wallis test followed by Mann-Whitney test between any two groups. No significant differences were observed. TB cases (n=29), community controls (n=55) and household controls (n=55).

2.3.4) Cytotoxic potential of BCG-specific T cells

The cytotoxic markers granzyme B, granulysin and perforin are expressed by mycobacteria-specific memory T cells in newborns vaccinated with BCG [191]. The importance of these cytotoxic T cells in control of *M.tb* has been demonstrated in several studies through their cytolytic activity [189] or cytotoxic protein-mediated anti-mycobacterial activity [153]. We therefore sought to determine if proportions of BCG-specific T cells expressing the cytotoxic markers granzyme B, granulysin and perforin were associated with risk of TB. Following *in vitro* stimulation of PBMCs with BCG, expression of these markers by BCG-specific T cells was measured by flow cytometry. BCG-specific T cells were identified as CD8+ or CD8- (mainly CD4+) T cells expressing these cytotoxic molecules upon *in vitro* stimulation with BCG. This is because cells were restimulated with PMA and Ionomycin which has been shown to down-regulate CD4 T cells. Proportions of BCG-specific CD4+ T cells expressing granulysin were higher in cases, compared to household controls only (Figure 12A). In particular, proportions of CD4+ T cells co-expressing granulysin and granzyme B, or granzyme B and perforin, were higher in cases, compared to both controls (Figure 12B).

Among BCG-specific CD8+ T cells, cases showed higher proportions of granzyme B-expressing cells, compared to both control groups (Figure 12C). Proportions of CD8+ cells co-expressing granzyme B and granulysin were also increased in cases, compared to community controls only (Figure 12D).

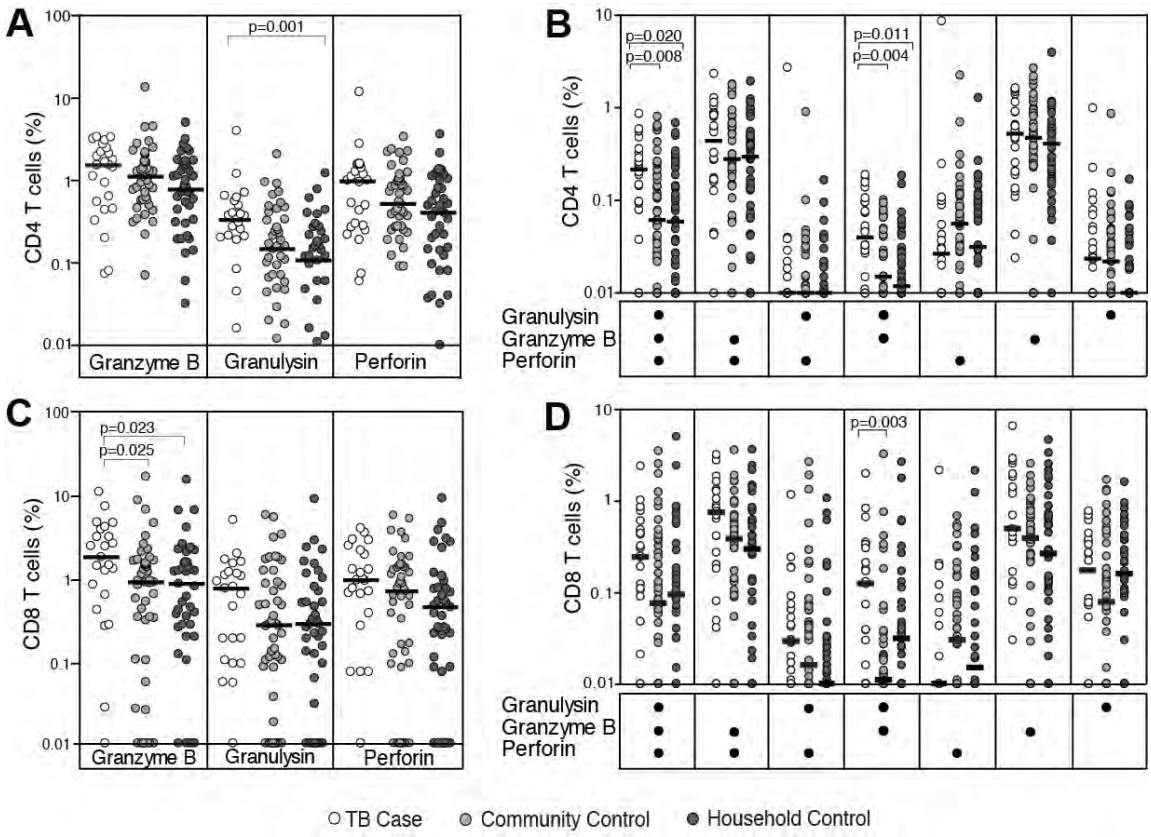

Figure 12: Cytotoxic potential of BCG-specific CD4+ and CD8+ T cells (Scriba and Keyser *et al*, manuscript in preparation).
PBMCs were stimulated with BCG or left unstimulated for 3 days and T cells expressing cytotoxic molecules were defined as BCG-specific T cells. Flow cytometry was used to detect BCG-specific CD4+ and CD8+ T cells expressing granzyme B, granulysin and/or perforin. Proportions of total BCG-specific CD4+ (**A**) or CD8+ (**C**) T cells expressing granzyme B, granulysin or perforin in cases and controls. Frequencies of BCG-specific CD4+ (**B**) or CD8+ (**D**) T cell subsets co-expressing combinations of the 3 cytotoxic molecules. Horizontal lines denote medians. The Kruskal Walis test was used to compare differences between the three groups and the Mann-Whitney test was used to compare the two groups. Only p-values below 0.05 are shown. TB cases (n=29), community controls (n=55) and household controls (n=55).

A major limitation in studies in which outcomes are determined by measuring multiple parameters is the increased likelihood of false positive results. Nevertheless, these false positives can be overcome by validating the findings on another set of participants. To validate the findings described above, these outcomes were measured in another set of 29 TB cases and 55 Community controls. Proportions of BCG-specific CD4+ and CD8+ T cells expressing the different cytotoxic markers that were candidate correlates of risk of developing TB disease in infants in the training set were not significantly different in the

validation set (data not shown). We therefore could not validate our initial results that frequencies of cytotoxic CD4+ or CD8+ T cells were associated with risk of developing TB disease.

2.3.5) Secreted mediators measurement

Levels of pro-inflammatory mediators measured in supernatant of BCG stimulated whole blood were also compared between cases and controls. Apart from the Th-1 promoting cytokine intereukin-12-p40 (IL12p40), which was higher in cases compared to household controls, no other lymphokines were significantly different between the two groups (Figure 13). However, after adjusting for multiple comparison using Bonferroni, this significant difference was lost.

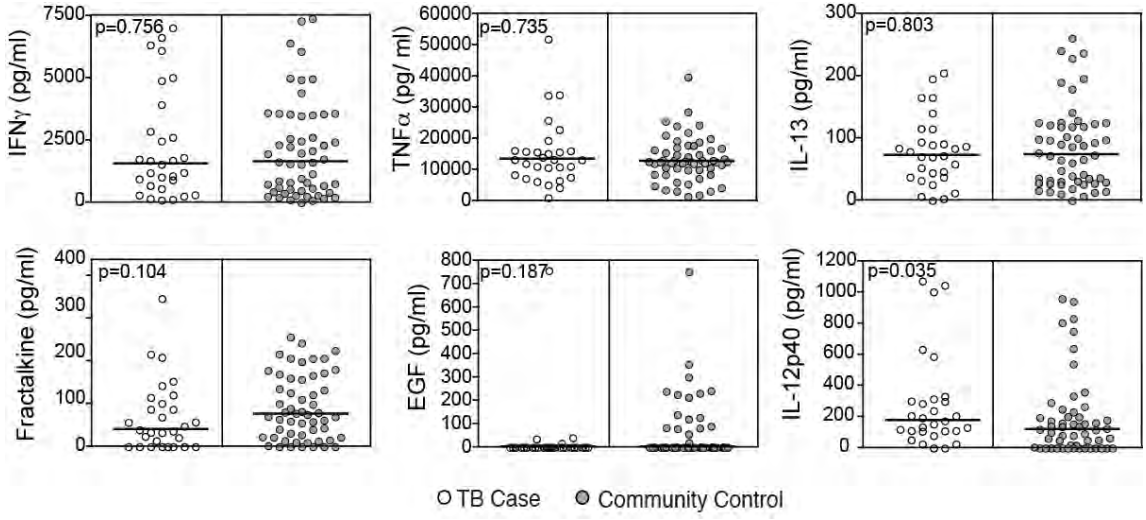

Figure 13: Soluble levels of secreted mediators (Scriba and Keyser *et al.*, manuscript in preparation).
Levels of 29 chemokines/cytokines were measured in plasma by multiplex bead array after incubation of whole blood with BCG or medium alone for 7 hours. The following selected cytokines are shown: IFN-γ, TNF-α, IL-13, Fractalkine, EGF and IL-12p40. BCG-specific levels were determined by subtraction of levels in plasma from whole blood incubated with medium alone, from those in BCG-stimulated blood. Horizontal lines denote medians. The Mann-Whitney U test was used to compare the two groups and p-values shown. Only IL-12p40 levels were different between cases and controls of all secreted mediators measured. TB cases (n=29) and community controls (n=55)

2.3.6) Gene signature of risk of developing TB disease

For over ten years now, transcriptional profiling has been applied in several human diseases to provide surrogate markers for clinical phenotyping [277] and to accurately predict prognosis [278]. It has been used to identify potential therapeutic targets as well as diagnostic and prognostic biomarkers in patients with autoimmune diseases [279]. Recently, Berry *et al* identified a blood signature of active TB disease using genome wide transcription profiling of whole blood [223]. To determine if a gene expression signature correlates with prospective risk of developing TB disease, we used genome-wide transcription profiling of PBMCs stimulated with BCG. RNA was extracted from PBMCs stimulated with BCG or left unstimulated, hybridized to Illumina HumanRefSeq-8 BeadChip (version 2) and gene expression measured using an Illumina bead array reader confocal scanner. We observed greater differential response in PBMC stimulated for 12 hours compared to 4 hours stimulation in our preliminary analysis. We therefore focused our downstream analysis on the 12 hour stimulation time point. Following unsupervised hierarchical clustering analysis in the BCG stimulation condition only, 25 genes were differentially expressed between cases and controls with a fold change > 1.3 and a nominal p value of 0.05 (Figure 14). However, after adjusting for multiple comparisons and setting the false discovery rate (FDR) p-value at 0.05, there was no differential gene expression between cases and controls.

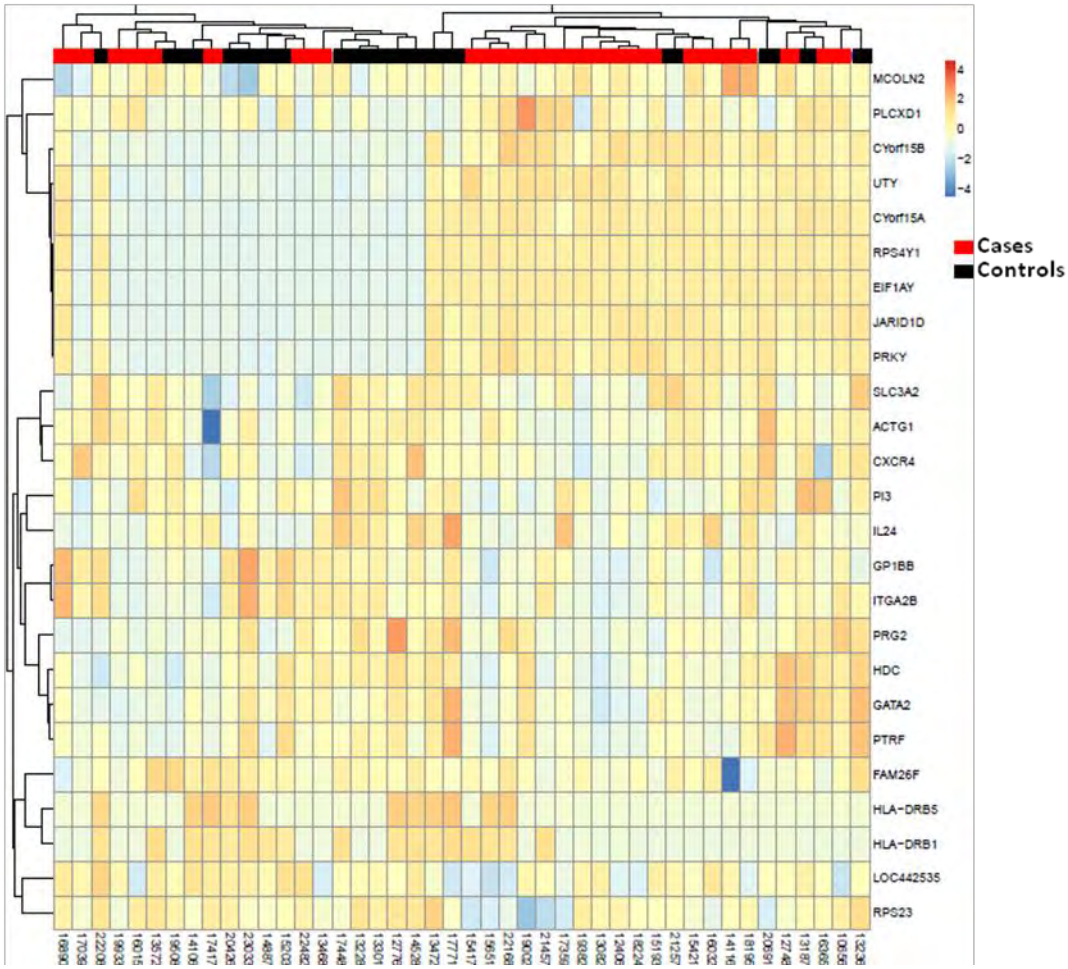

Figure 14: Heatmap showing differential gene expression between cases and controls. PBMC stimulated with BCG for 12 hours and gene expression analysis performed by microarray. Unsupervised hierarchical analysis was performed and 25 genes were differentially expressed between cases (red, n=26) and controls (black, n=18) with FC>1.3 and nominal p-value of 0.05. These differences did not hold after correction for multiple comparisons (FDR=0.05).

2.4) Discussion

We aimed to identify correlates of risk of TB disease in infants vaccinated with BCG at birth. Two approaches were used: hypothesis-driven and unbiased or hypothesis-generating approaches. We were not able to identify correlates of risk of TB disease using either of the approaches.

Frequencies of Th1/Th17 BCG-specific CD4+ and CD8+ T cell did not correlate with risk of developing TB disease in infants, following BCG vaccination at birth [175], nor did the frequencies of polyfunctional T cells. Several studies have shown that Th1 cytokines play key roles in TB immunity [280-283]. Darrah *et al* showed that polyfunctional CD4+ T cells correlated with vaccine-induced protection against Leishmaniasis in mice [168]. IL-17 expression by CD4+ T cells has also been shown to play a role in protection against TB; this is why we also investigated this cytokine as a correlate of risk of TB disease [181]. Experimental and clinical studies have all demonstrated roles of CD8+ T cells in TB immunity. For example Bruns *et al* showed that patients undergoing anti-TNF therapy, had decreased numbers of antigen-specific effector memory CD8+ T cells, which led to a decrease in antimicrobial activity against *M.tb,* which was associated with an increase in incidence of TB disease [153]. No differences between cases and controls were observed when these markers where measured as potential correlates of risk of TB disease.

Because T cell responses to mycobacteria are very complex [284, 285], we sought to investigate other T cell outcomes as potential correlates of risk of TB disease. We investigated the cytotoxic and lymphoproliferative capacity of BCG-specific T cells. Our results showed that these markers do not correlate with risk of developing TB disease in infants. Silva *et al* suggested a key role in protection against TB by granule mediated cytotoxicity of CD4+ and CD8+ T cells [286]. We also investigated plasma levels of 29 chemokines/cytokines after stimulation with BCG, which also did not correlate with risk of developing TB disease. These results however do not mean that T cells are not essential in TB

immunity. On the other hand, our data suggest that T cell function by itself might not be sufficient to prevent TB disease. As earlier mentioned, the immune system is very complex and so is the immune response following *M.tb* infection which involves different cell types. Recently, Kozakiewicz *et al* showed that in a mouse model, B cells can regulate neutrophilia following *M.tb* infection and vaccination with BCG by modulating IL-17 responses [287]. Studies such as these suggest that measuring other immunological outcomes should be considered in future correlates of risk of TB disease studies.

T cell outcomes investigated as potential correlates of risk of TB disease in this study were based on our current knowledge of what we think is important in immunity against *M.tb*. However, we also used genome wide transcriptional profiling, an unbiased approach which does not rely on previous knowledge. We observed similar PBMC gene expression between cases and controls. Transcriptional profiling has been used in several human diseases to understand the molecular mechanisms which lead to pathogenesis and identify markers that correlate with clinical phenotypes. For example in cancers, transcriptional profiling has been used to accurately predict prognosis leading to effective and directed treatment [277]. In this study, transcriptional profiling was used to differentiate between acute myeloid leukaemia (AML) and acute lymphoid leukaemia (ALL) as well as between B-cell ALL and T-cell ALL, which could all have similar clinical presentations. The application of gene expression profiling in TB has been widely used recently [222-226]. Berry *et al*., compared gene expression profiles between persons with latent TB and those with active disease and identified a blood signature of active disease [223]. In another study carried out in South African and Malawian HIV-infected and uninfected individuals, a 27 and 44 gene signature could distinguish TB from LTBI and other diseases, respectively [222]. The aim of this study was to identify gene transcripts that could be used to diagnose TB in HIV-infected individuals [222]. However, in all these studies reported above, gene expression was compared between TB disease and latently infected individuals. In our study, all analyses

were performed when infants were healthy and most likely not infected with *M.tb*. The phenotype of healthy BCG vaccinated infants who ultimately progress to TB or remain healthy is a very challenging phenotype to analyse.

We observed high heterogeneity in the response to BCG vaccination within this study population. In our study, known factors that could influence BCG immunogenicity, such as helminth infection or route of BCG administration, were unlikely to account for such heterogeneity, according to previous studies conducted by our group [55, 56]. For example, Hatherill *et al* found that maternal infection with helminths in the Western Cape was less than 10%, suggesting it has negligible effect on BCG variability [55].

Post immunization variability in immune responses has been used as marker of disease susceptibility [75]. For example, in measles vaccine trials, vaccine recipients have been categorised into "low" or "non responders" and "high" or "responders", respectively based on the level of antibody responses [288, 289]. Chen *et al* showed that low responders to measles vaccine post immunization were not protected from measles when exposed to the virus compared to high responders [288]. Similarly, Mathias *et al* also showed that non responders to a single dose of measles vaccine in whom a measurable response was detected only after a second dose were six times more likely to develop measles after exposure compared to responders [289]. These two examples show an association between vaccine response and development of disease in that individuals with a weak vaccine-induced response are more likely to develop disease compared to those with a strong response. However, there are several pathogens and/or vaccines that can cause diseases at the extremes of both weak and strong immune responses such, as *Aspergillus spp* and *Vaccinia virus* (used as vaccine against small pox) [290]. Casadevall *et al* proposed that host damage can be depicted by the nature of the immune response and that both the host and the pathogen can contribute to virulence (Figure 15). Host-pathogen interaction can confer a certain degree of benefit to the host. In as

much as the pathogen can lead to host damage, host responses could also contribute to host damage. The "U" shape on the graph shows that host damage can be maximal if host immune responses are either too weak or strong (Figure 15). This model fits well with the known importance of CD4 T cells in TB, whereby too low CD4 T cell count, observed in progressive HIV infection is associated with increased risk of TB, while on the other hand, cavitation is mainly observed in the presence of normal CD4 count [138]. We did not consider such complex host responses in the analyses performed in this chapter. In the next chapters, our further investigations considered non-linear associations between immunity and clinical outcome, under this hypothesis that marked heterogeneity in immune responses within a given population could mask potential correlates of risk of TB disease.

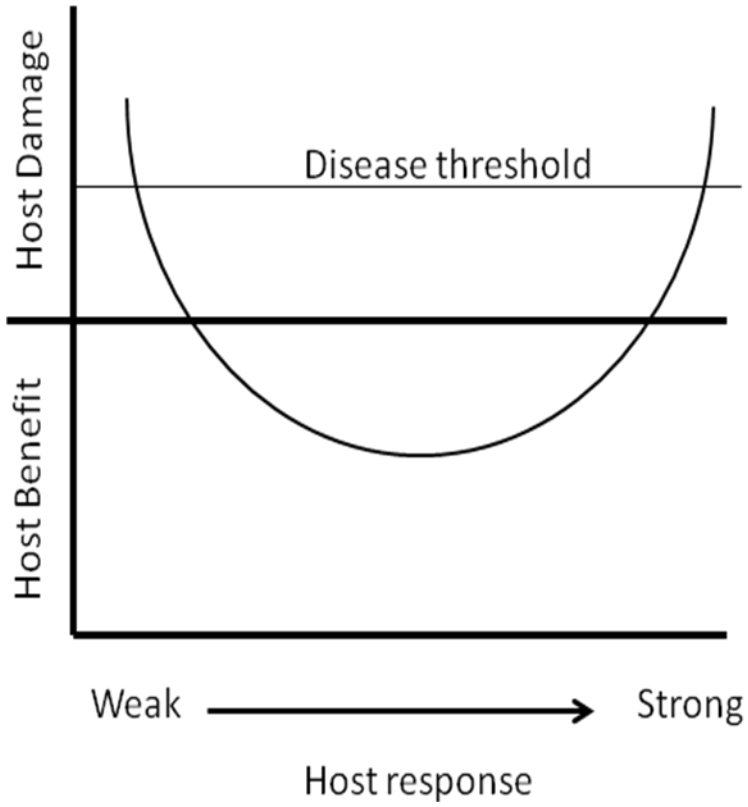

Figure 15: Damage-Response framework (Adapted from Casadevall *et al*., 2003).

2.5) Conclusion

Our results suggests that BCG-induced T cell functions as well as PBMC gene expression profiles in healthy 10-week-old infants do not correlate with risk of developing TB disease during the first 2 years of life. Further analysis and investigation of other T cell outcomes may be considered for identification of these correlates.

CHAPTER 3: CORRELATES OF RISK OF TB DISEASE ACCORDING TO CLUSTERING OF GENE EXPRESSION PROFILES

In this chapter, re-analyses of microarray data was by our collaborators in VGTI and Jenner Institute while all other re- analyses were done by Samuel Njikan.

3.1) Introduction

In the previous chapter, we reported that no correlate of risk of TB disease could be identified among BCG-specific T cells functions as well as gene expression profiles investigated following routine BCG vaccination in infants. However, the analyses did not take into account the complex nature of host responses proposed in a damage-response framework which suggests that very strong and weak host immune responses to infections can predispose to disease [290]. We therefore hypothesised that heterogeneity in immune responses may mask correlates of risk of TB disease. In this chapter, we sought to acknowledge this heterogeneity in immune responses and further identify potential correlates of risk of TB disease

To address our aims, further analyses were performed on gene expression profiles as well as BCG-specific T cell outcomes measured in the previous chapter. Different analysis strategies are frequently used to mine data generated from microarray experiments. Some of these analyses include unsupervised clustering, identification of differentially expressed genes, class prediction analysis and pathway analysis. These kinds of analyses are useful in generating new hypotheses and the validity of such analyses is based on both biological knowledge and statistical significance [291].

Hierarchical clustering analysis is one method used to explore microarray data. It can be performed with either supervised or unsupervised methods. In supervised analysis, prior knowledge on biological/clinical outcomes is

considered during the process while no prior knowledge is needed for unsupervised clustering. This analysis strategy has been used to uncover gene expression patterns in acute myeloid leukaemia [292]. Following clustering analysis, different analysis strategies can be performed to identify differentially expressed genes between the conditions under study to uncover potential biomarkers. Linear models for microarray analysis (LIMMA) and prediction analysis for microarrays (PAM) are methods used to identify differentially expressed genes and subsequent biomarkers. These two analysis platforms are found in Bioconductor's R analysis software.

Understanding the biology of biomarkers or gene expression-based classifiers is an important step in fully appreciating their significance. Pathway analyses are usually performed to understand the biological significance of the gene expression in the classifier. Gene set enrichment analysis (GSEA) as well as integrated pathway analysis (IPA) are commonly used to identify the most differentially expressed biological pathways across the conditions under study. These methods have been used in several studies [293-295] and have been shown to be promising in clinical diagnostics.

.

3.2) Materials and Methods

This chapter mainly focuses on further analysis of the results generated in the previous chapter.

3.2.1) Whole blood assay and intracellular cytokine staining

See section 2.2.3

3.2.2) Lymphoproliferation assay

See section 2.2.5

3.2.3) Cytotoxic marker measurement

See section 2.2.6

3.2.4) Secreted mediators measurement

See section 2.2.7

3.2.5) Gene expression profiling

See section 2.2.8

3.2.6) Data analysis

See section 2.2.9

Bioinformatic data analysis (Figure 17) was performed in collaboration with Helen Fletcher (University of Oxford, UK), Rafick Sekaly and Ali Filali (Vaccine and Gene Therapy Institute, FL, USA).

3.2.6.1) Hierarchical clustering analysis

Firstly, the probe intensities were normalised across all samples. Following this normalisation, probe intensities from unstimulated samples were subtracted from probe intensities in BCG stimulated. Background subtracted probe intensities were used to perform clustering analysis. This analysis was

performed using R's cluster package [249], which makes use of the hierarchical clustering algorithm. Unsupervised hierarchical clustering followed by semi-supervised hierarchical clustering analyses were used to identify clusters of infants and following identification of clusters, their stability and validation were determined by altering pre-clustering conditions to include different numbers of genes (5000 to 20000 genes).The Euclidean distance as well as Pearson's and Spearman's correlations were also used to assess stability of the different clusters.

3.2.6.2) Identification of differentially expressed genes

Differentially expressed genes were identified using Bioconductor's limma package [296]. Briefly, the fold change in gene expression between cases and controls was determined (up or down-regulated in cases compared to controls). An empirical Bayes method was used to moderate the standard error of the log fold change for expression values from each gene. This was followed by adjusting for multiple comparisons using the Benjamini and Hochberg method, which also controls the false discovery rate (FDR). The FDR was set at 0.05.

3.2.6.3) Class prediction analysis

A nearest-neighbour centroid method in Bioconductor's pamr package [297] was used for class prediction as well as selection of biomarkers. Briefly, the optimal shrinkage threshold used to build the centroid was determined by using an internal k-fold cross validation. After estimating the cross-validation error for each threshold, the optimal threshold that gave the lowest cross-validation error rate was chosen.

3.2.6.4) Pathway analysis

Analysis of pathways of gene expression was performed using Gene Set Enrichment Analysis (GSEA) [298], which is a non-parametric statistical method. This analysis makes use of a list of ranked genes to determine if a particular phenotype is associated with a known biological pathway or sets of genes. An

enrichment score (ES) is used to evaluate this association and an empirical phenotype-based permutation method is used to assess the statistical significance of each gene set's ES. The GSEA accounts for multiple comparisons by normalising the ES for each gene and calculates a false discovery rate (FDR) for each normalised ES.

We systematically tested gene sets from the Molecular signature Database (MsigDB, http://www.broad.mit.edu/gsea/msigdb) canonical pathways (cp) version c2.cp.v3.0. within the C2 collection which contains 913 gene sets to which we added a collection of 28 immune related gene sets described in Chaussabel *et al* [299]. A total of 220 gene sets were filtered out because they were either very small (less than 15 genes) or very high (more than 500 gene sets). Briefly, genes found to be differentially expressed between cases and controls (up or down-regulated in cases compared to controls) were ranked according to fold change in expression. The GSEA was then used to compare this list of ranked genes to known datasets of genes housed in the GSEA C2:cp molecular signature database (739 data set). Gene expression in cases and controls were ranked with specific pathways in the GSEA and FDR was set at 0.05.

In addition to GSEA, integrated pathway analysis (IPA) was used to identify genes that have been shown to correlate with several diseases from the ingenuity biological database (www.ingenuity.com). Briefly, genes were inserted into ingenuity's IPA and a search was performed to identify defined molecular interactions between genes. This was then used to generate a network of genes. For network analysis, IPA computed a score (p-score=-$\log_{10}$(p-value)) according to a list of focus genes stored in the ingenuity database and the set of input genes. This score is derived from a p-value and takes into account the size and number of genes in the network to approximate how relevant this network is to the original list of genes. A score of 1 indicates there is a 1 in 10 ($p<0.1$) and 2 indicates a 1 in 100 ($p<0.01$) chance that the genes in a network

are together by chance. Therefore the higher the score, the more likely that genes found in a network are together not by chance. The network identified is presented as a graph indicating the molecular relationships between genes/gene products.

3.3) Results

3.3.1) Clustering of gene expression profiles

Following quantile normalisation, background gene expression values (UNS) were subtracted from BCG stimulated values (BCG-UNS). Figure 16 shows a summary of the different analysis performed. Using unsupervised hierarchical clustering analysis after background subtraction, we observed two distinct clusters of infants according to gene expression profiles induced by *in vitro* BCG stimulation (Cluster 1, n=20; Cluster 2, n=24; Figure 17A). Differential gene expression between cluster 1 and cluster 2 identified 461 genes in opposite directions with an FDR p value <0.05 and a FC>1.3. Within the two different clusters, there was equal distribution of cases and controls (Figure 17B). In cluster 1, there were 11 cases and 9 controls, while cluster 2 had 15 cases and 9 controls (Figure 17B).

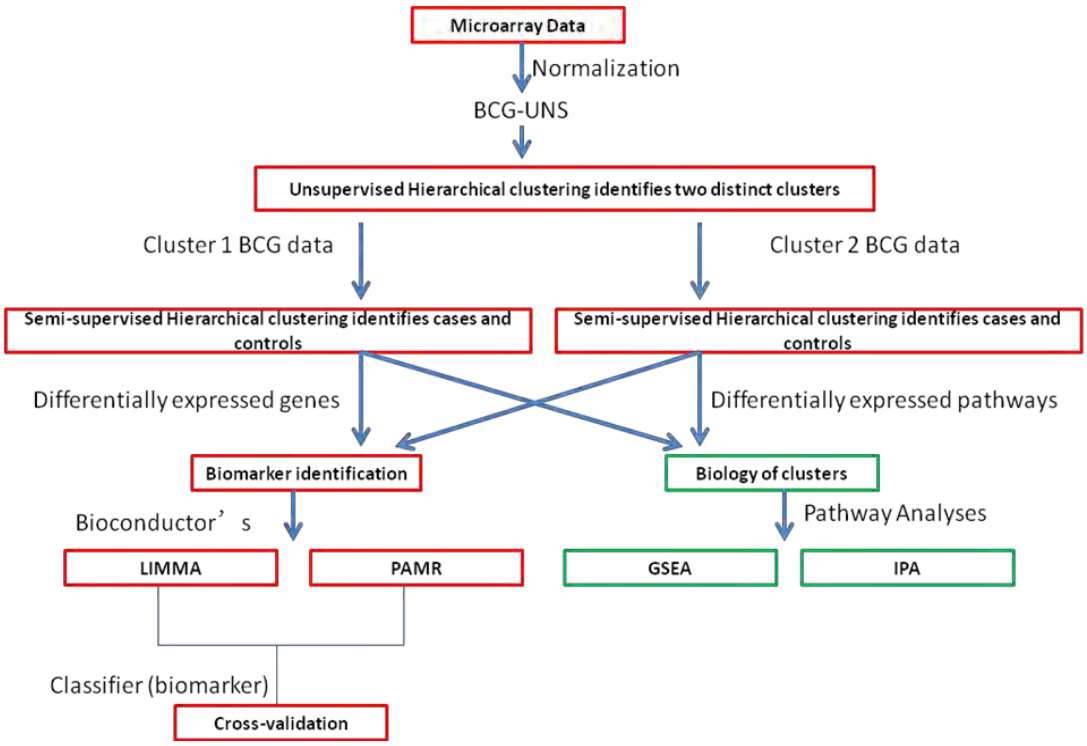

Figure 16: Flow chart of different bioinformatics analysis performed.

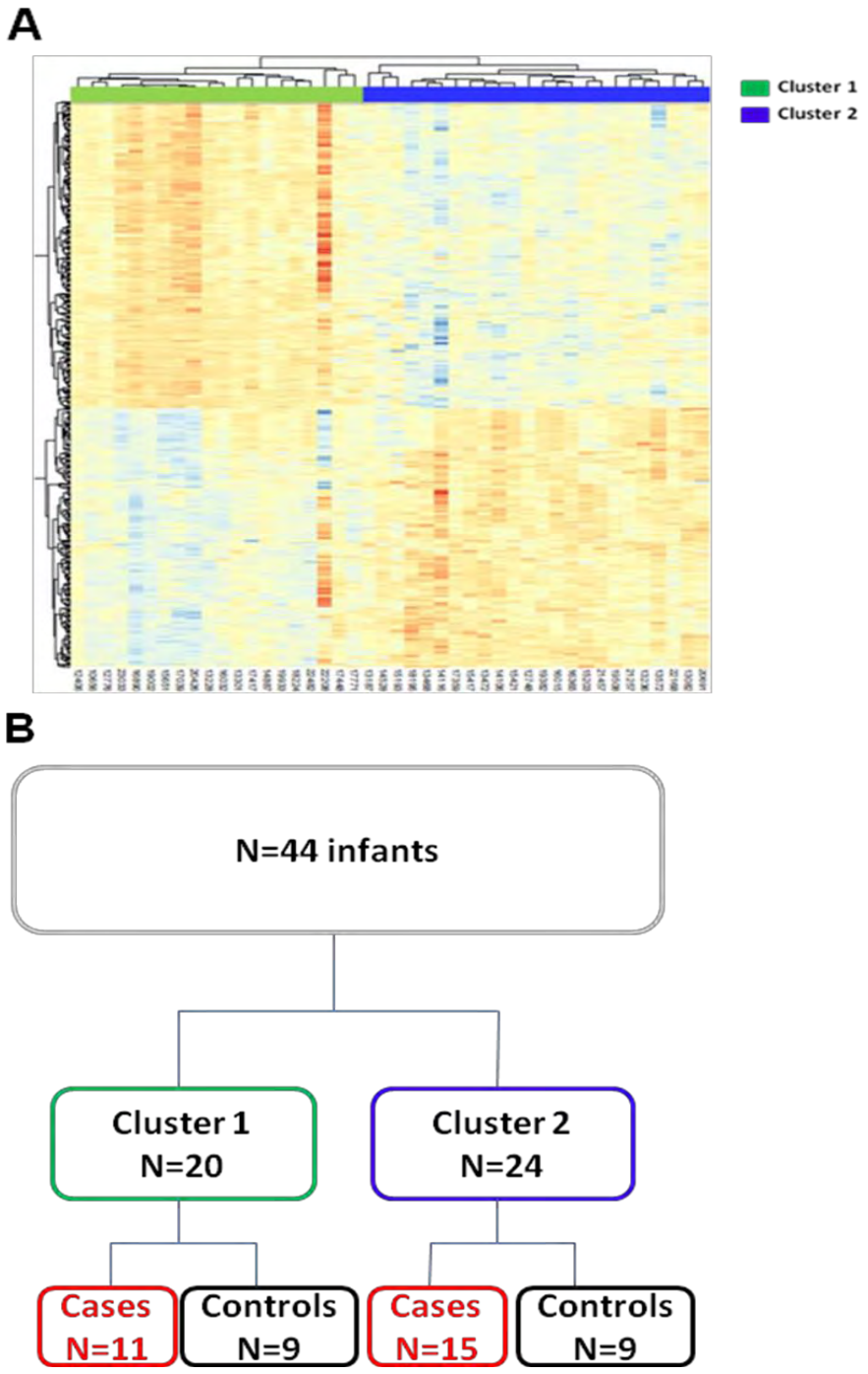

Figure 17: Clustering of gene expression profiles.
Normalized probe intensity from PBMC stimulated with media only (UNS) was subtracted from the normalized probe intensity from PBMC stimulated with BCG. Unsupervised hierarchical clustering was performed (Pearson correlation with 20,000 probes) resulting in two distinct clusters of infants (cluster 1 and cluster 2). **A)** Heat map showing 461 differentially expressed genes between the two clusters with a FC> 1.3 and FDR <0.05. Up-regulated and down-regulated genes denoted by orange and blue respectively. **B)** Distribution of cases (red, n=26) and controls (black, n=16) within clusters 1 (green) and 2 (blue).

3.3.2) Correlates of risk of TB disease

We observed two distinct clusters of infants with opposite gene expression profiles in response to *in vitro* BCG stimulation with each cluster including both cases and controls. This observation could be explained by the damage-response framework proposed by Casadevall *et al* [290]. We hypothesised that cases and controls may also display different transcriptional profiles in different clusters of infants. We therefore separately compared cases and controls in the two clusters of infants, to uncover potential correlates of risk of TB disease in each cluster.

3.3.2.1) Gene signature of risk of TB disease

Further analysis of both clusters separately showed groups of cases and controls in each. However, case and control groups in cluster 2 were more pronounced and clear than cluster 1.

To identify a gene signature of risk of TB disease, analysis was performed in BCG stimulated and unstimulated conditions separately. Differential gene expression was already present in the unstimulated samples (data not shown) but it was not strong enough to attain statistical significance. However, it seems like stimulation with BCG enhanced these differences, which attained significance when cases and controls were compared. Subtracting the background lead to loss in differential gene expression. For this reason, correlates were identified only in the BCG stimulation condition. Semi-supervised analysis of both clusters separately revealed two clusters of cases and controls in each. In cluster 1, 341 genes were differentially expressed between cases (11 infants) and controls (9 infants) (Figure 18A). However, this differential gene expression was not seen after adjusting the p-value for multiple comparisons (FDR <0.05) when linear models for microarray analysis (LIMMA) was performed. Cases (15 infants) and controls (9 infants) from cluster 2 showed differential expression of 206 genes, determined by LIMMA analysis (Figure 18B), where a fold change (FC) >1.5 was used to identify differentially

expressed genes at a false discovery rate (FDR) <0.05. A total of 5 infants were misclassified with these criteria (3/15 cases and 2/9 controls) (Figure 18B). Of these 206 transcripts, 74 were able to predict cases and controls determined by prediction analysis for microarray (PAM) upon cross-validation. Among these genes, S100A8 (S100 calcium binding protein A8) and CD14 were the most up-regulated in cases compared to controls with a fold change> 3.5.

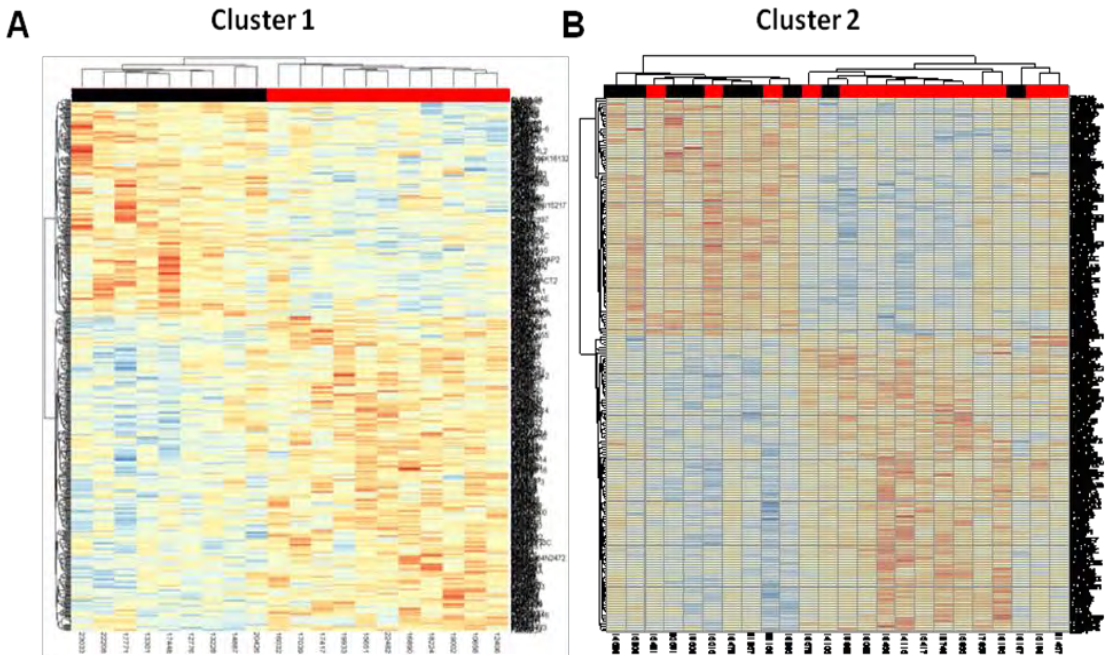

Figure 18: Differentially expressed genes between cases and controls.
Gene expression profiles of PBMCs stimulated with BCG for 12hrs. Semi-supervised clustering followed by LIMMA analysis was performed in BCG stimulated samples only to identify differential gene expression between cases and controls. **A)** Semi-supervised clustering analysis showing 341 genes differentially expressed between cases (n=11) and controls (n=9) in cluster 1. **B)** LIMMA analysis with an FDR of 0.05 following semi-supervised clustering analysis showing 206 genes differentially expressed between cases (n=15) and controls (n=9). Cases are shown in red and controls in black. Orange colour on heat maps denote genes up-regulated in cases compared to controls while blue colour denotes genes down-regulated in cases compared to controls.

3.3.2.2) T cell correlates of risk of TB disease

We next assessed the T cell outcomes measured in the previous chapter between cases and controls in the two clusters of infants separately. We hypothesised that analysing the two clusters separately will uncover differences in BCG-specific T cells between cases and controls that were absent when the data was analysed together.

Firstly we assessed if frequencies and cytokine profiles of BCG-specific CD4+ and CD8+ T cells were different between cases and controls in the two clusters of infants. No differences were observed in frequencies and cytokine profiles between cases and controls in cluster 1. However, cases in cluster 2 were associated with higher frequency of IL-17-producing CD4+ T cells compared to controls (Figure 19). However, after adjusting for multiple comparison using Bonferroni, this significant difference was lost. No other differences were observed between cases and controls in CD4+ T cells and CD8+ T cells (Table 2).

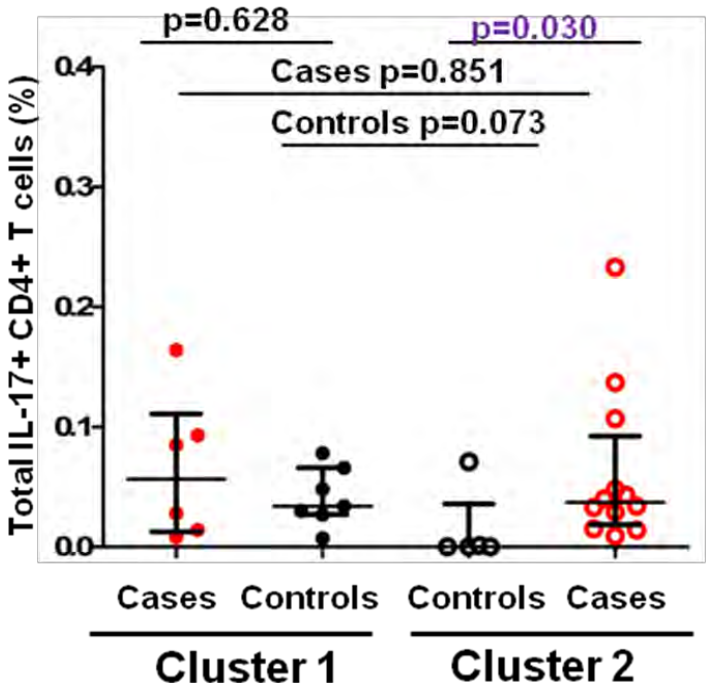

Figure 19: Frequencies of BCG-specific IL-17-expressing CD4+ T cells between cases and controls.
Whole blood was incubated with BCG for 12 hours and cytokine detected using an intracellular cytokine assay and flow cytometry. Frequencies of total CD4+ T cells expressing IL-17 upon BCG stimulation. Mann-Whitney U test was used to compare differences between groups. Cases (red) and controls (black). Horizontal lines denote median and whiskers denote interquartile range. A p value < 0.05 was considered significant (purple). Cluster 1 (cases, n=6 and controls, n=7). Cluster 2 (cases, n=12 and controls n=5).

We next assessed the cytotoxic capacity of CD4+ and CD8+ T cells between cases and controls in the two clusters. In cluster 1, cases had higher CD4+ T cells co-expressing granulysin, granzyme B and perforin (Figure 20A), or co-expresing granulysin and granzyme B (Figure 20B) as well as granzyme B and perforin (Figure 20C) compared to controls. In cluster 2, cases were associated with lower expression of CD4+ T cells producing perforin only (Figure 20D).

When we compared cases and controls between the two clusters, we observed that cluster 2 controls had higher CD4+ T cells co-expressing granulysin and granzyme B (Figure 20B) as well as granzyme B and perforin (Figure 20C) compared to cluster 1 controls. However, after adjusting for multiple comparison using Bonferroni, this significant difference was lost. There were no other

differences observed in both CD4+ and CD8+ T cells between cases and controls in cluster 1 and cluster 2 (Table 2).

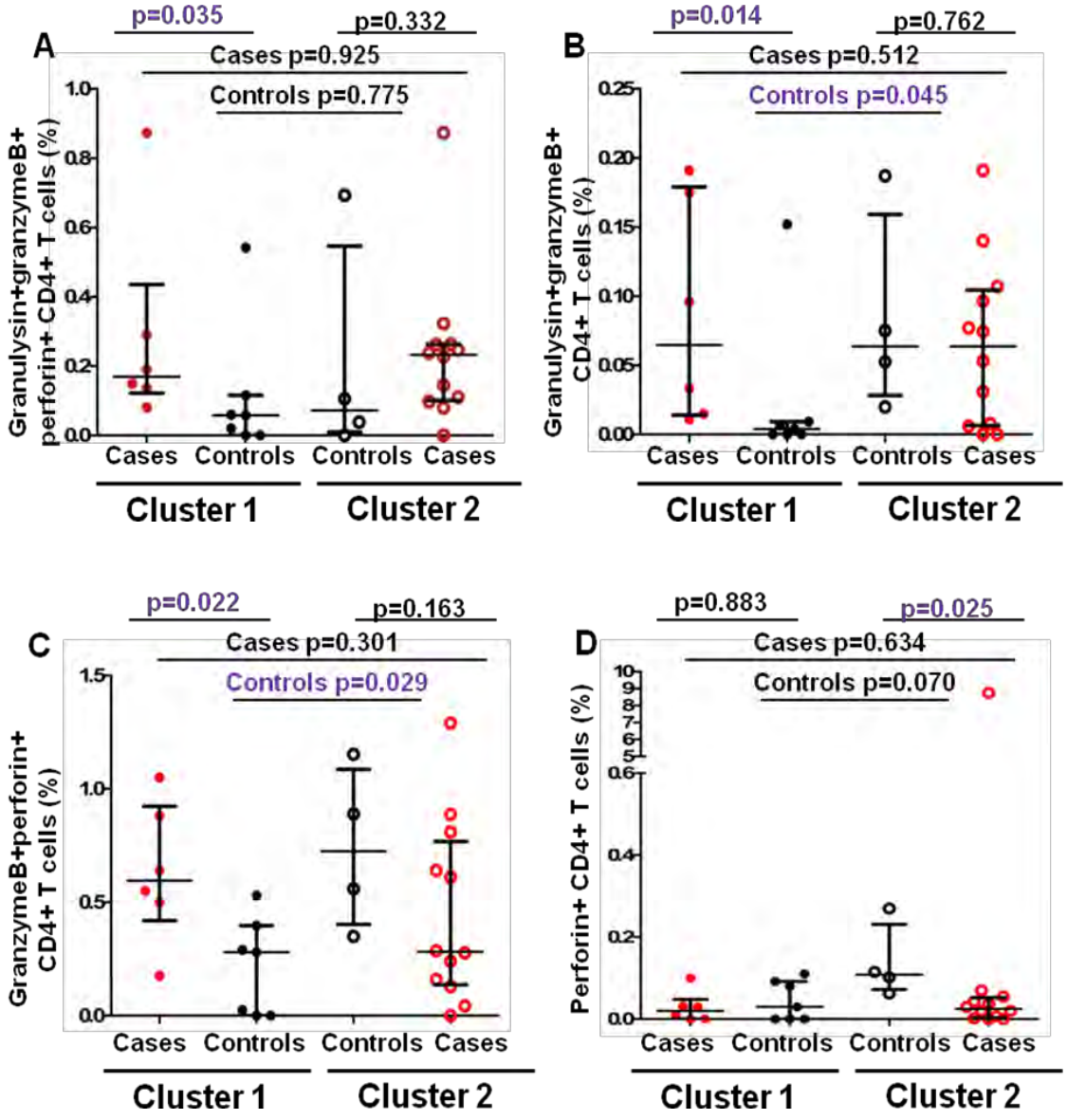

Figure 20: Cytotoxic potential of BCG-specific CD4+T cells in the two clusters.
PBMCs were stimulated with BCG or left unstimulated for 3 days and flow cytometry was used to detect BCG-specific CD4+ T cells expressing granzyme B, granulysing and/or perforin. BCG-specific T cells were defined by subtracting the unstimulated value from the BCG stimulated value. Frequencies of CD4+ T cells co-expressing **(A)** granulysin, granzyme B and perforin **(B)** granulysin and granzyme B **(C)** granzyme B and perforin or **(D)** perforin only. The Kruskal Wallis test was used to assess differences in any of the groups. Mann-Whitney test was used to compare any two groups (cases in red and controls in black). Horizontal lines on graphs represent median and whiskers represent interquartile ranges. P-values < 0.05 were significant (purple). Cluster 1 (cases n=6 and controls n=7). Cluster 2 (cases n=12 and controls n=4).

We next compared levels of secreted mediators between cases and controls within the two clusters separately. Cases were associated with lower levels of IL-8 in cluster 1 (Figure 21A) and TGF-α in cluster 2 (Figure 21B) compared to controls. Comparing cases and controls between the two clusters, we observed that cluster 2 controls had increased levels of TGF-α compared to cluster 1 controls (Figure 21B). There was also increased levels of IL-1β in cluster 2 cases compared to cluster 1 cases (Figure 21C). No other differences in secreted mediators were observed (Table 2).

There were no differences observed in the proliferative capacity of either CD4+ or CD8+ T cells (Table 2).

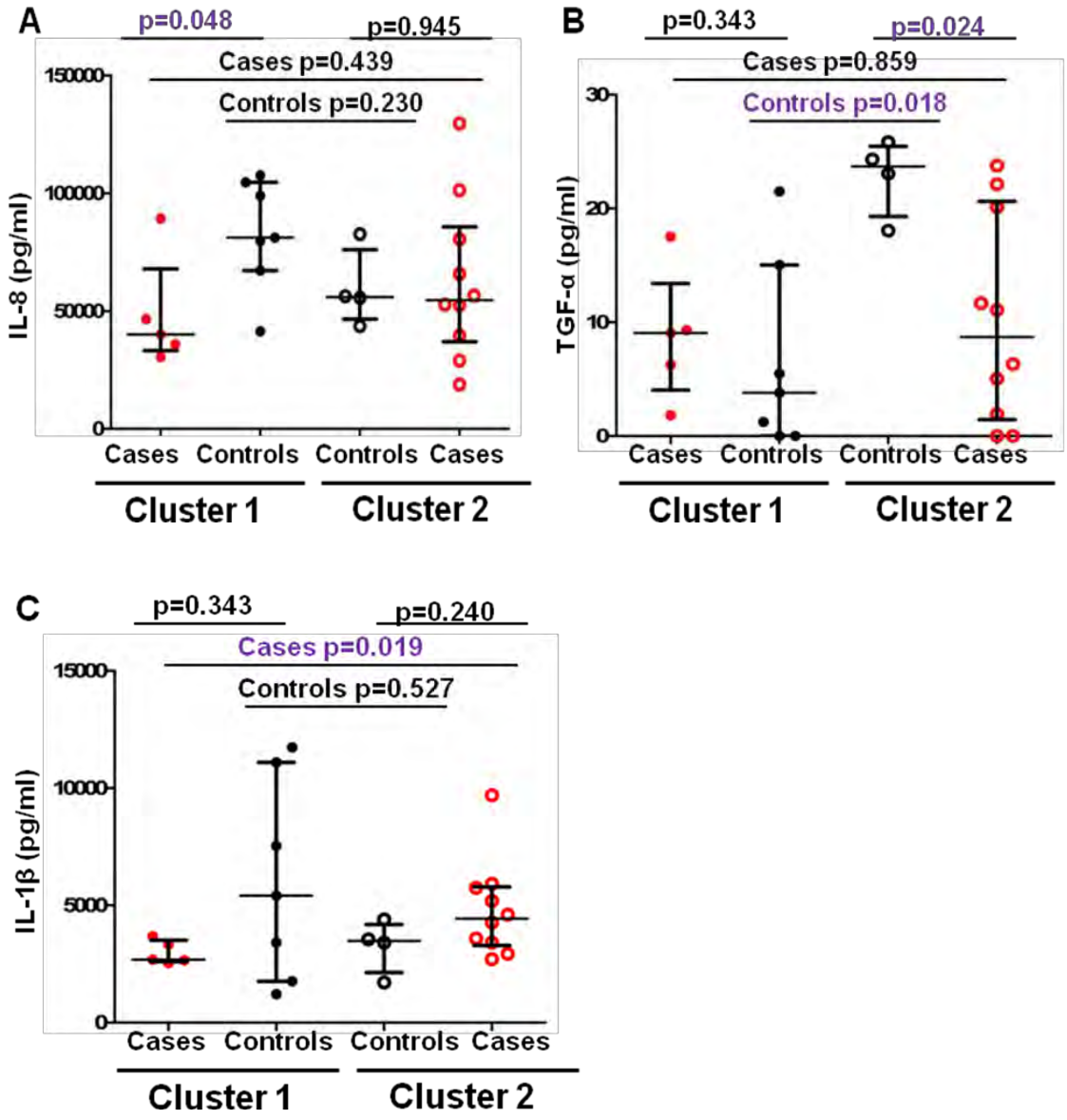

Figure 21: Levels of secreted mediators in cases and controls from clusters 1 and 2. Whole blood was incubated with BCG or no antigen for 7 hrs and secreted molecules were measured by luminex bead array. Values measured in unstimulated controls were subtracted from BCG-stimulated samples and are shown. Levels of **(A)** IL-8 **(B)** TGF-α **(C)** IL-1β. Horizontal lines and whiskers on graphs denote median and interquartile range respectively. The Kruskal Wallis test was used to assess differences in any of the groups and the Mann-Whitney test was used to compare any two groups (cases in red and controls in black). Only p-values below 0.05 were considered significant (purple). Cluster 1 (cases, n=5 and controls, n=7). Cluster 2 (cases, n=10 and controls n=4).

Table 2: BCG-specific T cell outcomes not significantly different between cases and controls in both cluster 1 and cluster 2 infants

Frequency and cytokine profiles of CD4+ T cells	Frequency and cytokine profiles of CD8+ T cells	Cytotoxic and proliferation capacity of CD4+ T cells	Cytotoxic and proliferation capacity of CD8+ T cells	Secreted mediators
Total IFN-γ (p=0.268)	Total IFN-γ (p=0.307)	Total granulysin (p=0.102)	Total granulysin (p=0.312)	EGF (p=0.643)
Total TNF-α (p=0.187)	Total TNF-α (p=0.458)	Total granzyme B (p=0.792)	Total granzyme B (p=0.874)	IL-2 (p=0.733)
Total IL-2 (p=0.268)	Total IL-2 (p=0.267)	Total perforin (p=0.082)	Total perforin (p=0.714)	IL-4 (p=0.136)
IL-2+IL-17+IFN-γ+α+ (p=0.686)	Total IL-17 (p=0.245)	Granulysin+Perforin+ (p=0.163)	Granulysin+Granzyme B+Perforin+ (p=0.370)	IL-5 (p=0.355)
IL-2+IL-17+IFN-γ+ (p=0.062)	IFN-γ+ (p=0.561)	Granulysin+ (p=0.585)	Granulysin+Granzyme B+ (p=0.168)	IL-6 (p=0.106)
IL-2+IL-17+TNF-α+ (p=0.196)	TNF-α+ (p=0.168)	Granzyme B+ (p=0.361)	Granulysin+Perforin+ (p=0.562)	IL-7 (p=0.733)
IL-2+IL-17+ (p-=0.389)	IL-2+ (p=0.288)	Total proliferation (p=0.874)	Granzyme B+Perforin+ (p=0.313)	IL-10 (p=0.304)
IL-2+IFN-γ+TNF-α+ (p=0.154)	IL-17+ (p=0.316)		Granulysin+ (p=0.792)	IL-12_p70 (p=0.374)
IL-2+IFN-γ+ (p=0.958)	IL-2+IL-17+IFN-γ+TNF-α+ (p=0.086)		Granzyme B+ (p=0.516)	IL-13 (p=0.945)
IL-2+TNF-α+ (p=0.398)	IL-2+IL-17+IFN-γ+ p(=0.099)		Perforin+ (p=0.775)	IL-15 (p=0.373)
IL-2+ (p=0.915)	IL-2+IL-17+TNF-α+ (p=0.379)		Total proliferation (p=0.958)	IL-17 (p=0.839)
IL-17+IFN-γ+TNF-α+ (p=0.082)	IL-2+IL-17+ (p=0.843)			IFN-γ (p=0.839)
IL-17+IFN-γ+ (p=0.161)	IL-2+IFN-γ+TNF-α+ (p=0.186)			IP-10 (p=0.436)
IL-17+TNF-α+ (p=0.254)	IL-2+TNF-α+ (p=0.156)			GM-CSF (p=0.839)
IFN-γ+TNF-α+ (p=0.205)	IL-2+IFN-γ+ (p=0.313)			TNF-α (p=0.239)
IFN-γ+ (p=0.492)	IL-17+IFN-γ+TNF-α+ (p=0.631)			Eotaxin (p=0.942)
TNF-α+ (p=0.835)	IL-17+IFN-γ+ (p=0.541)			Fractackline (p=0.373)
Total subsets (p=0.268)	IFN-γ+TNF-α+ (p=0.874)			IL-12_p 40 (p=0.539)
	Total subsets (p=0.370)			MIP-1α (p=0.197)

3.3.3) Biological processes associated with risk of TB disease

Differential gene expression between cases and controls was observed when cluster 1 and 2 were analysed separately. We now want to investigate if unique biological pathways will associate with cases and controls in each cluster when the two clusters are analysed separately. We hypothesised that cases and controls within the two clusters will have differential expression of biological pathways. Using Gene Set Enrichment Analysis (GSEA), we observed different biological pathways associated with cases and controls in the two clusters separately. In cluster 1, the majority of the pathways associated with cases where pathways involved in protein synthesis (green) and glucose metabolism (grey) (Table 3). There were a few pathways associated with T (pink) and B cells (blue) as well as mitogen activated protein kinase (MAPK) (orange) signalling in cases (Table 3). Cluster 1 controls were associated with myeloid cells (purple), inflammation (red) and MAPK signalling pathways (orange) (Table 4). The majority of genes up-regulated in controls compared to cases were myeloid cell and inflammatory genes suggesting that diminished immune activation might increase risk of developing TB disease.

In cluster 2, pathways associated with controls and not cases were pathways involved in protein synthesis (green), glucose metabolism (grey) and CD4 T cell signalling (pink) (Table 5). MAPK signalling (orange), inflammatory (red) and myeloid cell activation pathways (purple) were the main pathways identified and the majority of these pathways were over represented in cases compared to controls (Table 6). These pathways were therefore associated with risk of TB disease in this group of infants. B cell signalling pathways (blue) as well as glucose metabolism (grey) were also identified and found to associate with risk of TB disease (Table 6). The majority of genes up-regulated in cases compared controls were myeloid and inflammatory genes. This data suggests that excessive immune activation increases risk of developing TB disease.

Table 3: GSEA pathways associated with cluster 1 cases

Cluster 1 cases	FDR
Protein synthesis (Reactome_ Viral_ MRNA_ Translation)	0.0000
Protein synthesis (Reactome_ Translation)	0.0000
Protein synthesis (Reactome_ Peptide_ Chain_ Elongation)	0.0000
Protein synthesis (Reactome_ GTP_ Hydrolysis_ And_ Joining_ Of_ The_ 60s_ Ribosomal_ Subunit)	0.0000
Protein synthesis (Reactome_ Gene_ Expression)	0.0000
Protein synthesis (Kegg_ Base_ Excision_ Repair)	0.0000
Protein synthesis (Kegg_ Aminoacyl_ tRNA_ Biosynthesis)	0.0000
Protein synthesis (Reactome_ tRNA_ Aminoacylation)	0.0000
Protein synthesis (Reactome_ Cytosolic_tRNA_Aminoacylation)	0.0000
Protein synthesis (M_ 3.7_ Spliceosome_ Methylation_ Ubiquitin)	0.0000
Protein synthesis (M_204_ Ribosomal proteins)	0.0000
Protein synthesis (Reactome_ Formation_ of_ a_ Pool_ of_ Free_ 40s_ Subunits)	0.0014
Protein synthesis (Reactome_ Influenza_ Viral_RNA_ Transcription_ And_ Replication)	0.0042
Protein synthesis (Kegg_ Ribosome)	0.0056
Protein synthesis (M_ 1.7_ MHC_ Ribosomal_ Proteins)	0.0058
Protein synthesis (Kegg_ Cytosolic_ DNA_ Sensing_ Pathway)	0.0075
Protein synthesis (ABC_ Transporters)	0.0078
Protein synthesis (Reactome_ Influenza_ Life_ Cycle)	0.0078
Glucose Metabolism (Reactome_ Integration_ Of_ Energy_ Metabolism)	0.0000
Glucose Metabolism (Reactome_ Glucose_ Regulation_ Of_ Insulin_ Secretion)	0.0000
Glucose Metabolism (Reactome_ Regulation_ Of_ Beta_ Cell_ Development)	0.0014
Glucose Metabolism (Reactome_ Regulation_ Of_ Gene_ Expression_ In_ Beta_ Cells)	0.0014
Glucose Metabolism (Kegg_ Pentose_ Phosphate_ Pathway)	0.0048
Glucose Metabolism (Reactome_ Regulation_ Of_ Insulin_ Secretion)	0.0049
Glucose Metabolism (Kegg_ One_ Carbon_ Pool_ By_ Polate)	0.0098
T Cell (M_ 3.8_ CDC_ TCR_ Creb_ Glycosylase)	0.0000
B Cell (M_ 1.3_ B cells)	0.0000
MAP Kinase Signalling (Kegg_ Parkinsons_ Disease)	0.0056
MAP Kinase Signalling (Biocarta_ ATRBRCA_ Pathway)	0.0082

Table 4: GSEA pathways associated with cluster 1 controls

Cluster 1 controls	FDR
Myeloid cells (M_ 2.6_ Myeloid Lineage)	0.0000
Myeloid cells (M_ 1.5_ Myeloid Lineage)	0.0000
Myeloid cells (M_ 1.2_ Platelets)	0.0000
Myeloid cells (Kegg_ Haematopoietic_ Cell_ Lineage)	0.0000
Inflammation (M_ 3.3_ Inflammation II)	0.0000
Inflammation (M_ 3.2_ Inflammation I)	0.0000
Inflammation (Kegg_ Systematic_ Lupus_ Erythematosis)	0.0000
Inflammation (Kegg_ Sphingolipid_ Metabolism)	0.0028
MAP kinase signalling (Reactome_ Metal_ Ion_ Transporter)	0.0000
MAP kinase signalling (Reactome_ JAak_ STAT_ Signalling_ Pathway)	0.0000
MAP kinase signalling (Reactome_ RNA_ Polymerase_I_ Promotion)	0.0032
MAP kinase signalling (Reactome_ FRS2_ Mediated_ Cascade)	0.0057

Table 5: GSEA pathways associated with cluster 2 controls

Cluster 2 controls	FDR
Protein synthesis (Reactome_ Peptide_ Chain_ Elongation)	0.0000
Protein synthesis (Reactome_ Translation) Protein synthesis (Reactome_ Formation_ of_ a_ Pool_ of_ Free_ 40s_ Subunits)	0.0003
Protein synthesis (Reactome_ Translation)	0.0005
Protein synthesis (Kegg_ Ribosome)	0.0007
Protein synthesis (Reactome_ GTP_ Hydrolysis_ And_ Joining_ Of_ The_ 60s_ Ribosomal_ Subunit)	0.0008
Protein synthesis (Reactome_ Viral_ MRNA_ Translation)	0.0020
Protein synthesis (Reactome_ Formation_ Of _ The_Ternary_ Complex_ And_ Subsequently_ The_ 43S_ Complex)	0.0093
Protein synthesis (Reactome_ Translocation_ Of_ Zap70_ To_ Immunological_ Synapse)	0.0207
Protein synthesis (M_ 1.7_ MHC_ Ribosomal_ Proteins)	0.0243
Protein synthesis (Reactome_ Metabolism_ of_ Proteins)	0.0271
Protein synthesis (Reactome_ Influenza_ Viral_RNA_ Transcription_ And_ Replication)	0.0307
Protein synthesis (Reactome_ Transloation_ Initiation_ Complex_ Formation)	0.0387
Glucose Metabolism (Reactome_ Regulation_ Of_ Beta_ Cell_ Development)	0.0009
Glucose Metabolism (Reactome_ Regulation_ Of_ Gene_ Expression_ In_ Beta_ Cells)	0.0022
T Cell (Reactome_ Phosphorylation_ Of_ CD3_ And_ TCR_ Zeta_ Chains)	0.0090
T Cell (M_ 3.8_ CDC_ TCR_ Creb_ Glycosylase)	0.0155
MAP Kinase Signalling (M_ 2.9_ ERK_ Transactivation_ Cytoskeletal_ MAPK_ JNK)	0.0056

Table 6: GSEA pathways associated with cluster 2 cases

Cluster 2 cases	FDR
Myeloid cells (M_ 2.6_ Myeloid Lineage)	0.0000
Myeloid cells (M_ 1.5_ Myeloid Lineage)	0.0000
Myeloid cells (Kegg_ Lysosome)	0.0031
Myeloid cells (Kegg_ FC_ Gamma_ R_ Mediated_ Phagocytosis)	0.0032
Myeloid cells (Kegg_ Glycosaminoglycan_ degradation)	0.0059
Myeloid cells (M_ 2.3_ Erythrocytes)	0.0130
Myeloid cells (Reactome_ Platelet_ Activation_ Triggers)	0.0150
Myeloid cells (Kegg_ Other_ Glycan_ Degradation)	0.0180
Myeloid cells (Kegg_ Acute_ Myeloid_ Leukaemia)	0.0182
Myeloid cells (Biocarta_ NK_ Cell_ Pathway)	0.0210
MAP kinase signalling (Biocarta_ RAS_ Pathway)	0.0000
MAP kinase signalling (Biocarta_ ECM_ Pathway)	0.0026
MAP kinase signalling (Biocarta_ SPP_ Pathway)	0.0027
MAP kinase signalling (Reactome_ FRS2_ Mediated_ Cascade)	0.0028
MAP kinase signalling (Reactome_ Semaphorin_ Interactions)	0.0030
MAP kinase signalling (Reactome_Nuclear_Events_Kinase_And_Transcription_ Factor_ Activation)	0.0030
MAP kinase signalling (Biocarta_ ERK_ Pathway)	0.0031
MAP kinase signalling (Reactome_ ERK_ MAPK_ Targets)	0.0034
MAP kinase signalling (Reactome_ MAPK_ Activation_ In_ TLR_ Cascade)	0.0035
MAP kinase signalling (Reactome_ SEMA4D_ In_ Semaphorin_ Signalling)	0.0063
MAP kinase signalling (Reactome_ Signalling_ To_ ERKS)	0.0083
MAP kinase signalling (Biocarta_ CDC42RAC_ Signalling)	0.0091
MAP kinase signalling (Reactome_MAPK_Targets_Events_Mediated_ By_ MAPK)	0.0104
MAP kinase signalling (Reactome_ Signalling_ To_ RAS)	0.0116
MAP kinase signalling (Biocarta_ HER2_ Signalling)	0.0116
MAP kinase signalling (Reactome_ GSK3_ Pathway)	0.0257
MAP kinase signalling (Reactome_ Signalling_ By_ NGF)	0.0363
Inflammation (M_ 3.3_ Inflammation II)	0.0191
Inflammation (M_ 3.2_ Inflammation I)	0.0027
Inflammation (Biocarta_ Il-12_ Pathway)	0.0114
Inflammation (Kegg_ Chemokine_ Signalling_ Pathway)	0.0180
Inflammation (Reactome_ Toll_ Receptor_ Cascades)	0.0000
Inflammation (Reactome_ Toll_ Like_ Receptor_ 3_ Cascade)	0.0253
Inflammation (Biocarta_ IL-17_ Pathway)	0.0378
Inflammation (Reactome_ Innate_ immunity_ Signalling)	0.0448
Inflammation (Kegg_ Sphingolipid_ Metabolism)	0.0469
B Cell (SA_ B_ Cell_ Receptor_ Complexes)	0.0000
B Cell (Biocarta_ BCR_ Pathway)	0.0187
B Cell (ST_ B_ Cell_ Antigen_ Receptor)	0.0283
Glucose Metabolism (Kegg_ Amino_ Sugar_ And_Nucleotide_Sugar_ Metabolism)	0.0441
Glucose Metabolism (Kegg_ Glyoxylate_ And_ Dicarboxylate_ Metabolism)	0.0450

We next evaluated whether functional gene networks were associated with differential gene expression between cases and controls in the two clusters separately using IPA with all 20,000 genes. IPA is a web- based software that constructs networks based on known interactions and/or associations from literature. Similar to what we observed with the GSEA, we found that cases in cluster 2 were associated with gene networks that were involved in Inflammatory Response, and Post-Translational Modification (Figure 22). This network generated a score of 44 and comprised of 35 genes. This score is calculated from the p-value and gives the probability that the genes in this network are together by chance. A score of 2 and above represents a 99% probability ($p<0.001$) that gene co-regulation is not by chance and the higher the score the higher this probability. Of these 35 genes, 17 were up-regulated (red) and 7 were down-regulated (green) in cases compared to controls while 11 transcript had no differential expression between cases and controls. Most importantly, transcripts up-regulated in cases compared to controls (red) were associated with inflammatory responses.

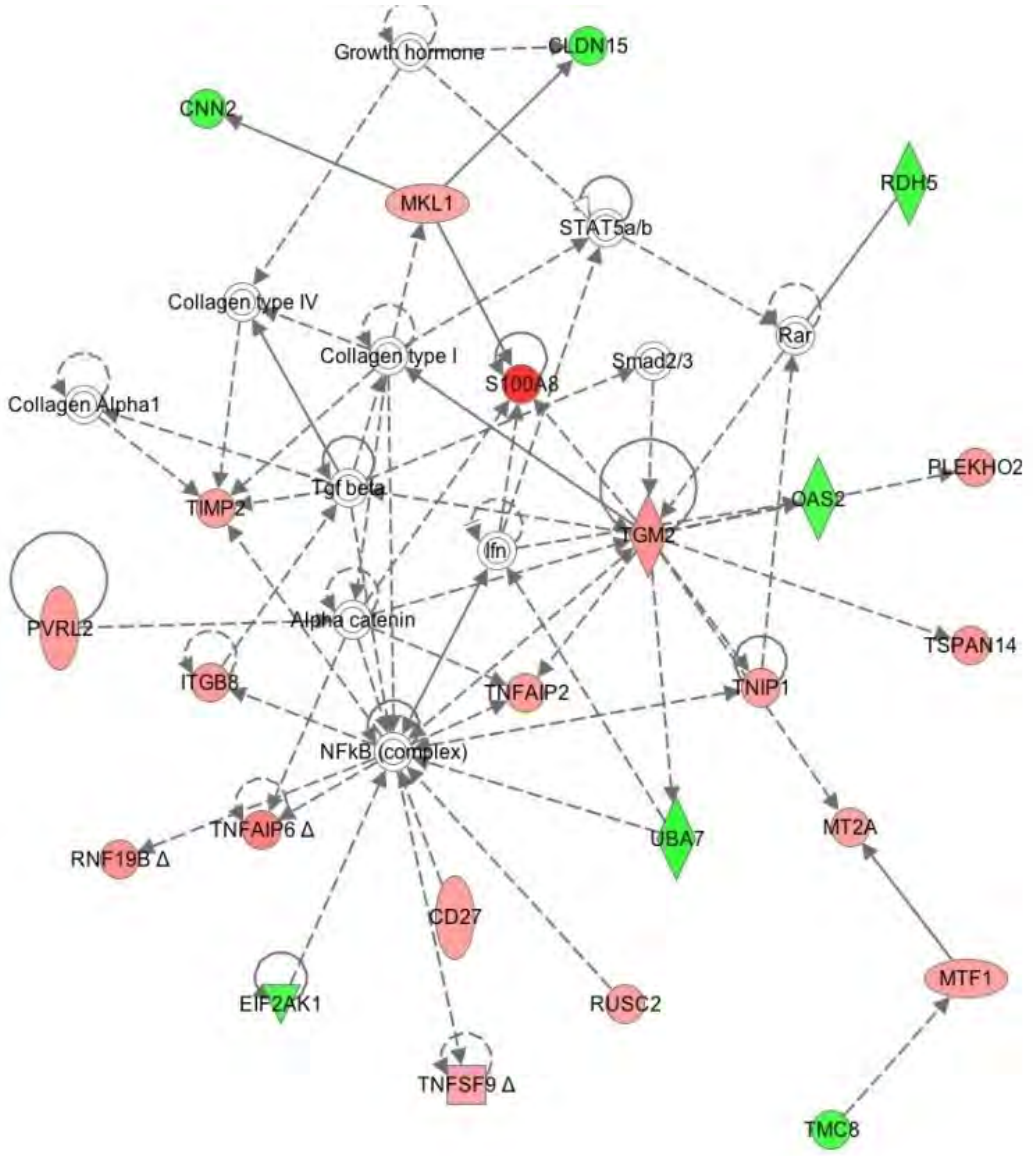

Figure 22: Gene network identified by IPA between cases and controls in cluster 2.
Visual representation of principal network generated using 20,000 genes. Network shows 35 genes involved in Inflammatory Response, Ophthalmic Disease and Post-Translational Modification. Genes highlighted in red are up-regulated and in green are down-regulated in cases compared to controls. Solid lines denote direct interactions while dashed lines represent indirect interactions.

Following the observation that cases in cluster 2 infants were associated with myeloid cell pathways as well as higher expression of CD14 gene, we sought to confirm this finding by flow cytometry. We observed trends of higher frequencies of CD14+ cells (Figure 23A) and lower frequencies of CD3+ cells (Figure 23B) in cases compared to controls in cluster 2 (unpublished data). When we compared myeloid to lymphoid ratio between cases and controls in cluster 2, we also found a trend suggesting that cases had higher myeloid to lymphoid ratios compared to controls (Figure 23C, unpublished data). However, there was no statistical significant difference between cases and controls.

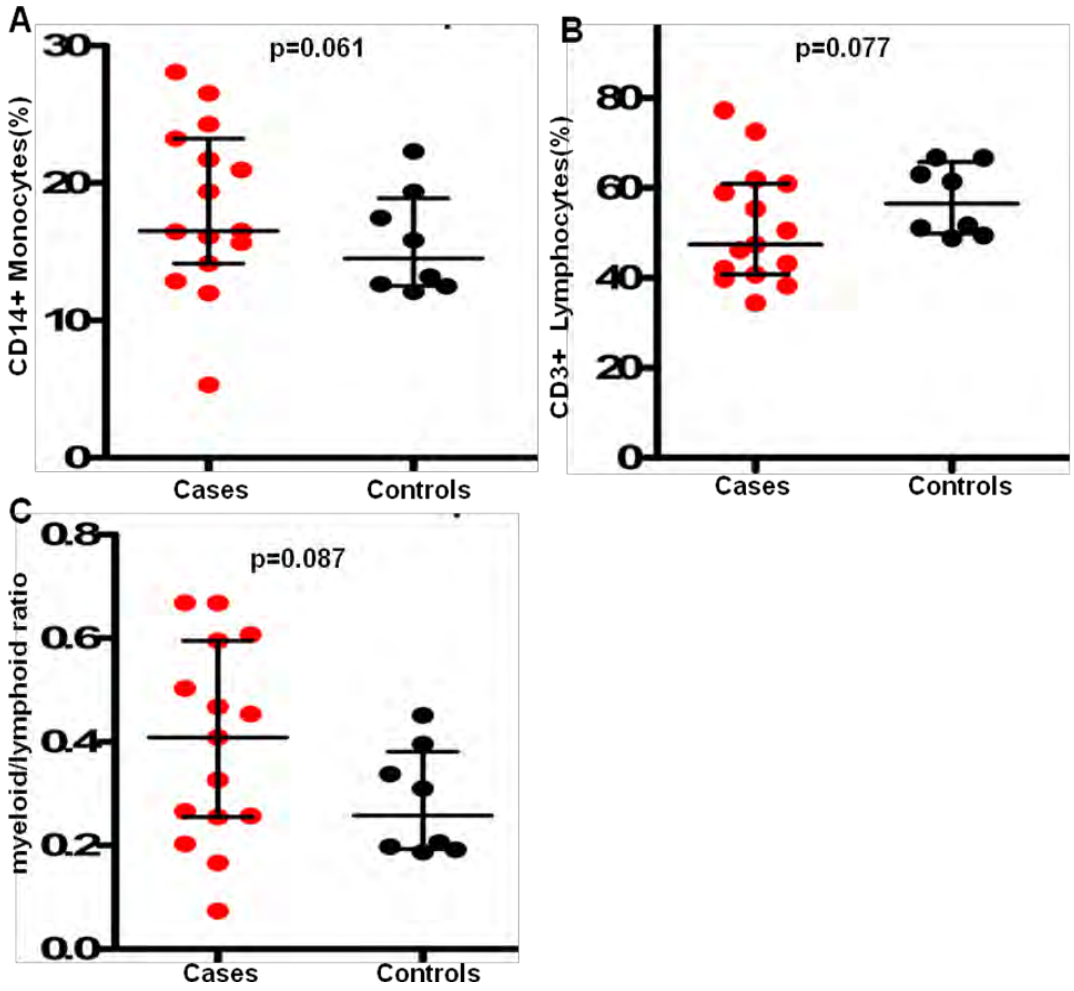

Figure 23: Frequencies of myeloid and lymphoid cells in cluster 2 cases and controls. Cryopreserved PBMC were thawed, washed, and immediately stained for myeloid and lymphoid markers. The frequencies of **(A)** CD14+ monocytes and **(B)** CD3+ lymphocytes were expressed as relative proportions of live CD45+ leukocytes. Percentage of myeloid cells was calculated by adding together % CD14+ cells and % myeloid DC. Percentage of lymphoid cells was calculated by adding together % CD3+ and % CD19+ cells. **(C)** The ratio between myeloid and lymphoid cells was calculated by dividing total myeloid by total lymphoid cell populations. Cases (n=15) are shown in red while controls (n=8) are shown in black. Horizontal lines depict median and p values were calculated by Mann-Whitney test.

3.4) Discussion

In the previous chapter, we reported that no correlate of risk of TB disease could be identified according to the outcomes we measured in healthy 10-week-old infants. Using unsupervised hierarchical clustering analysis, we identified two clusters of infants based on their gene expression profiles after *in vitro* stimulation of PBMC with BCG. Unsupervised hierarchical clustering analysis has been used in several studies to mine microarray data [300-302]. It is one of the most widely used methods to analyse this kind of data by generating clusters based on highly differentially expressed genes whose pattern of expression are similar [303]. Gene expression profiles in the two clusters of infants was in opposite direction. Following this observation, we hypothesised that analysing the clusters separately would allow identification of correlates of risk of TB. Analysing the two clusters of infants separately, allowed identification of differential gene expression signatures and T cell functions in infants who ultimately developed TB disease or remained healthy in each cluster. This finding was very important in that, for the first time, we were able to identify markers that were different between 10-week old BCG vaccinated infants who later on developed disease and those who remained healthy. However, this was only possible after the observation of two different clusters of infants by gene expression profiles as these correlates were absent when the infants were analysed together. An explanation for this can be that given the analysis approach we applied which rely on analyses of group averaging differences, the opposite gene expression in the two clusters cancel out distinct patterns when the infants are analysed together, hence no differential expression were apparent between cases and controls.

A 74-gene expression signature for risk of TB disease was identified in infants who clustered in the second group (cluster 2). This signature mainly comprised myeloid, innate and inflammatory genes. Among these genes, S100A8 (S100 calcium binding protein A8) and CD14 were the most up-regulated in cases compared to controls with a fold change> 3.5. S100A8 is a calcium and zinc

binding protein that has been shown to play a key role in innate immunity to infections [304, 305]. Recently, this protein has been shown to play a major pathologic role in TB by mediating accumulation of neutrophils in the lungs and inflammation in humans, non human primates and mice [306]. In humans and non human primates, increased levels of S100A8-producing neutrophils were found in inflammatory lung lesions of active TB individuals compared to those latently infected [306]. Interestingly, in humans increased levels of this protein were found in serum of active TB patients compared to serum obtained from latently infected individuals and healthy controls [306]. Following *M.tb* infection in mice, S100A8-producing monocytes were found in mice that had increased inflammation [306]. CD14 is a monocyte differentiation antigen and forms an important component of the innate immune system [307]. It is required for the TLR-4 mediated recognition of *M.tb* and has been shown to elicit lung inflammation in *M.tb* infected mice [308]. Soluble levels of CD14 have been shown to be a specific marker of monocyte/macrophage activity [309]. Although the role of CD14 in TB has not been fully investigated in humans, elevated levels of this protein have been found in BAL and serum of active TB patients [310]. Our data suggests that there is enrichment of myeloid cells (monocytes) in cases compared to controls in cluster 2 infants. This finding was confirmed by showing a trend in higher frequencies CD14+ cells and lower frequencies of CD3+ cells in cases compared to controls in cluster 2 infants. Although there was no statistical significance between the two groups, the trends in the frequencies of these cells reflected what we observed at the gene expression level. The association between risk of TB disease and myeloid/lymphoid cell ratio has also been described recently by Naranbhai *et al* in HIV-positive adults before and after starting anti-retroviral therapy [311]. In this study, it was observed that there was a higher risk of HIV-infected individuals to develop TB disease over time if they had either too high or low myeloid to lymphoid cell ratio [311]. In our study however, all infants were HIV-uninfected at time of enrolment.

IL-17 and IFN-γ are pro-inflammatory cytokines that are induced during primary TB. Among other functions, they act as chemotactic mediators, recruiting cells to site of infection and thus help in stabilisation of the granuloma. However, a balance of both Th1 and Th17 cells during infection is essential to avoid immunopathology. A shift towards IL-17 may cause too much influx of neutrophils, which might lead to tissue damage [158]. In an *M.tb* infection model in IFN-$\gamma^{-/-}$ mice, there was increased expression of IL-17 in the lungs, which induced S100A8, which in turn mediated influx of neutrophils leading to exacerbated lung inflammation [306]. In our study, IL-17 producing cells were higher in cases compared to controls in cluster 2, with no difference in IFN-γ producing cells. However, cases and controls were compared at 10 weeks of age when they were all healthy and had no exposure to *M.tb*.

Cytotoxic molecules produced by CD4+ T cells in cases and controls was found to be opposite in the two clusters of infants. In cluster 1, cases were associated with higher frequencies of BCG-specific CD4+ T cells producing granulysin, perforin and granzyme B, while in cluster 2 cases showed similar or lower frequencies of these cells compared to controls. Pitabut *et al* showed that TB patients have increased granulysin and perforin in circulation compared to healthy controls [312]. This suggests that infant response to BCG stimulation in the two clusters might be different, confirming our hypothesis of identifying correlates of risk of TB disease separately. We hypothesised that because we observe these two clusters of infants with opposite gene expression profiles, analysing them separately would allow for identification of correlates of risk of TB disease in each cluster.

In cluster 1 infants, plasma levels of IL-8 was higher in controls compared to cases. IL-8 is a chemokine that plays a role in regulating leucocyte influx in TB disease [313]. Elevated levels of this protein have been found in BAL [314-316], pleural fluid [317] and plasma [318] of TB patients. This is however opposite to what we see in our study. In the studies reported above, IL-8 levels were

assessed in patients with TB disease but in our study, IL-8 was measured when infants were all healthy (10 weeks of age) hence the possible reason for the disparity in results. Transforming growth factor-alpha (TGF-α) is known to stimulate neural cell proliferation in the human adult brain [319]. However, its role in TB has not yet been established. Nevertheless, the fact that this chemokine as well as IL-1β were different between clusters 1 and 2 controls as well as cluster 1 and 2 cases respectively, further supports our hypothesis of identifying correlates of risk of TB disease in the two clusters separately.

GSEA showed that enriched (cluster 2) or decreased (cluster 1) expression of inflammatory as well as myeloid gene pathways were associated with risk of developing TB disease. In cluster 2 infants, cases had increased expression of pathways associated with myeloid cells, inflammation as well as type I/II interferons while there was decreased expression of T cell pathways compared to controls. These transcriptomic patterns have been reported in several other studies [223, 226, 320]. For example, Berry *et al* showed up-regulation of inflammatory, myeloid cells and type I/II interferon gene pathways and down-regulation of T cell pathways in TB disease compared to latent infection [223]. This finding was also supported by a study performed by other members of our laboratory aimed at identifying correlates of risk of TB disease in adolescents (Penn-Nicholson, Hanekom, Scriba *et al*., unpublished data). In this study, these patterns associated with risk of TB disease in *M.tb* infected adolescents as far as 18 months before they developed disease. Nevertheless, the fact that we see a similar pattern of gene expression may indicate innate responses to mycobacteria, suggesting that this may be due to persistence of BCG. It has been suggested that myeloid genes specifically up-regulated in TB disease are expressed by macrophages and dendritic cells and this may reflect innate cells trafficking to the inflammed lungs [320]

Casadevall *et al* have proposed that host immune responses to pathogens that are too strong or weak can lead to host tissue damage [290]. Following BCG

vaccination, there can be several factors that account for this dichotomy in inflammatory responses which can be environmental, genetic or even persistence of the BCG itself. To address these hypotheses, other members of our laboratory are currently studying the effects of delaying BCG from birth to 10 weeks. In this study, a group of infants will be vaccinated with BCG at birth and in another group, BCG vaccination will be delayed to 10 weeks of age. Blood will be collected from both groups of infants at 10 weeks of age just before the delayed group receive BCG. Gene expression profiles will be compared between the two BCG vaccinated groups of infants. If BCG persistence is the reason for this dichotomy in inflammatory response, then the signatures previously identified should be found only in the BCG birth vaccinated arm and not the delayed group. However, if this dichotomy is genetic and not dependent on BCG persistence, then this signature should be present in both groups of BCG vaccinated infants.

Up- or down-regulation of MAPK signalling was also associated with risk of developing TB in both clusters. Immunohistochemical analysis of lung biopsies of TB patients has shown phosphorylation of p38MAPK in macrophages surrounding the granulomas and *in vitro* studies have shown that p38 activity regulates matrix degradation by macrophages [321]. Yang *et al* also showed that this pathway is essential for inflammatory responses in TB through toll-like receptors [322]. These also support our findings suggesting that too much or too little inflammation might increase the risk of developing TB disease. Gene network analysis using IPA also showed up-regulation of inflammatory genes in cases compared to controls confirming what was observed with the gene signature of risk of TB disease as well as GSEA.

3.5) Conclusion

Taken together, we showed that cases and controls are associated with different patterns of immune response to BCG in the 2 clusters of infants, but a consistent pattern could not be identified. Our data suggest that excessive or inadequate inflammation in response to BCG, possibly driven by myeloid cells, is associated with prospective risk of developing TB disease in different groups of infants. However, taking into account differential gene expression in response to BCG stimulation (clustering) was a key factor in identifying correlates of risk of TB disease. Indeed, we saw opposite gene expression profiles between cases and controls in the two clusters. We also observed different T cell correlates of risk, at times in opposite directions, in the two clusters. The next chapter focuses on understanding the biology of this clustering.

Our findings are limited by the small sample sizes, especially considering the variability in some of the groups. For this reason, this finding requires further validation in an independent cohort of infants.

CHAPTER 4: ASSOCIATION BETWEEN CLUSTERING OF GENE EXPRESSION AND DIFFERENTIAL RESPONSE TO BCG VACCINATION

In this chapter, re-analyses of microarray data was by our collaborators in VGTI and Jenner Institute while all other re-analyses were done by Samuel Njikan.

4.1) Introduction

In the previous chapter, we observed complex models of immunity as proposed by the damage-response framework whereby either too much or too little inflammatory responses associated with increased risk of developing TB disease in BCG vaccinated infants. However, clustering of infants into two groups based on their gene expression profiles was a pre-requisite for discovering potential biology-related correlates of risk of TB. Since accounting for this clustering allowed identification of biological correlates of risk of TB disease, it is important to understand the biological processes that underlie it.

The work in this chapter aimed to investigate the association between clustering of gene expression profiles and differential response to BCG vaccination. Since the two clusters of infants had differential gene expression profiles, we hypothesised they will also have differential response to BCG vaccination measured as frequency of BCG-specific T cells. For this, we re-analysed and compared BCG-specific T cell responses between the two clusters of infants.

Following this analysis, we performed several mechanistic investigations to further understand the biology of this clustering. Using GSEA and IPA, we investigated weather transcriptional profiles associated with biological pathways known to be important in immune responses were also associated with clustering of gene expression profiles.

4.2) Materials and Methods

4.2.1) Whole blood assay and intracellular cytokine staining

See section 2.2.3

4.2.2) Lymphoproliferation assay

See section 2.2.5

4.2.3) Cytotoxic marker measurement

See section 2.2.6

4.2.4) Secreted mediators measurement

See section 2.2.7

4.2.5) Gene expression profiling

See section 2.2.8

4.2.6) Data analysis

T cell outcomes measured in chapter 2 where compared between clusters 1 and 2. A Mann Whitney test was used to compare the two clusters and a significant difference was determined by a p-value of <0.05.

Biological pathways differentially expressed in the two clusters was assessed as described in section 3.2.6.4.

4.3) Results

To understand what underlies the clustering of infants into two groups based on their gene expression profiles, we sought to look for differences between clusters 1 and 2. For this, we first assessed whether technical parameters, demographic, epidemiological or biological conditions of either the mother or the child associated with the observed clustering. The parameters collected at time of enrolment and sample processing that were assessed included: birth weight, weeks of gestation, age at first bleed (day of sample procession), RNA quality, gender, ethnicity and vaccination route (Figure 24A-G). None of these parameters collected at enrolment were co-variates of clustering as there was no significant difference between the two clusters ($p>0.05$).

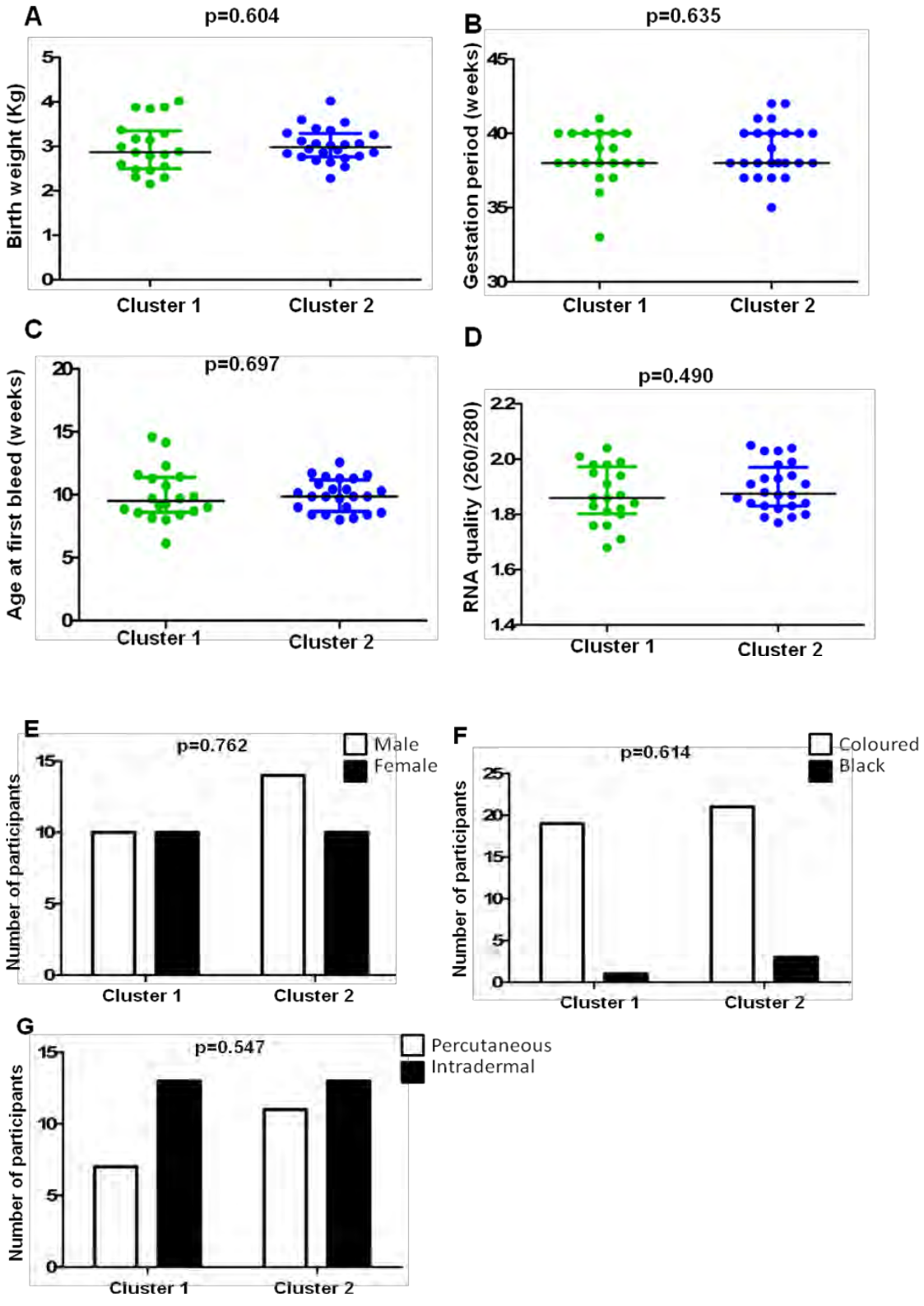
A
p=0.604
Birth weight (Kg)
Cluster 1
Cluster 2
B
p=0.635
Gestation period (weeks)
Cluster 1
Cluster 2
C
p=0.697
Age at first bleed (weeks)
Cluster 1
Cluster 2
D
p=0.490
RNA quality (260/280)
Cluster 1
Cluster 2
E
p=0.762
Male
Female
Number of participants
Cluster 1
Cluster 2
F
p=0.614
Coloured
Black
Number of participants
Cluster 1
Cluster 2
G
p=0.547
Percutaneous
Intradermal
Number of participants
Cluster 1
Cluster 2

Figure 24 (previous page): Co-variates of clustering
Demographic and technical parameters investigated as co-variates of clustering of infants. Mann Whitney test was used to compare A) birth weight, B) gestation period, C) age at first bleed and D) RNA quality between cluster 1 (green, n=20) and cluster 2 (blue, n=24). Fischer's exact test used to compare E) gender (clear bars=males and shaded bars=females), F) ethnicity (clear bars=coloureds and shaded bars=blacks) and G) route of BCG administration (clear bars=percutaneous and shaded bars=intradermal) between cluster 1 and 2. Horizontal lines and whiskers in graphs A-D denote median and interquartile range respectively. All p values were >0.05.

4.3.1) Association between clustering and BCG-specific T cell responses

Following the observation that certain infants clustered together by gene expression profiles after *in vitro* stimulation of PBMC with BCG, we sought to investigate underlying biological processes. Results of all T cell assays described in the previous chapter we re-analysed and compared between the two clusters. Among the 44 infant samples on which the microarray was performed, there were only 30 or less samples that had both microarray and T cell data. Analyses in this chapter are therefore on the 30 infants that had data from all analyses.

Firstly, we compared frequencies of Th-1 cytokine-expressing CD4+ and CD8+ T cells upon *in vitro* re-stimulation with BCG between the two clusters. Frequencies of BCG- specific CD4+ T cells expressing each IFN-γ, TNF-α and IL-2 (total cytokine+ CD4+ T cells) were higher in cluster 2 compared to cluster 1 (Figure 25A). In addition to this, polyfunctional CD4+ T cells co-expressing IFN-γ, TNF-α and IL-2, was more frequent in cluster 2 compared to cluster 1 (Figure 25B).

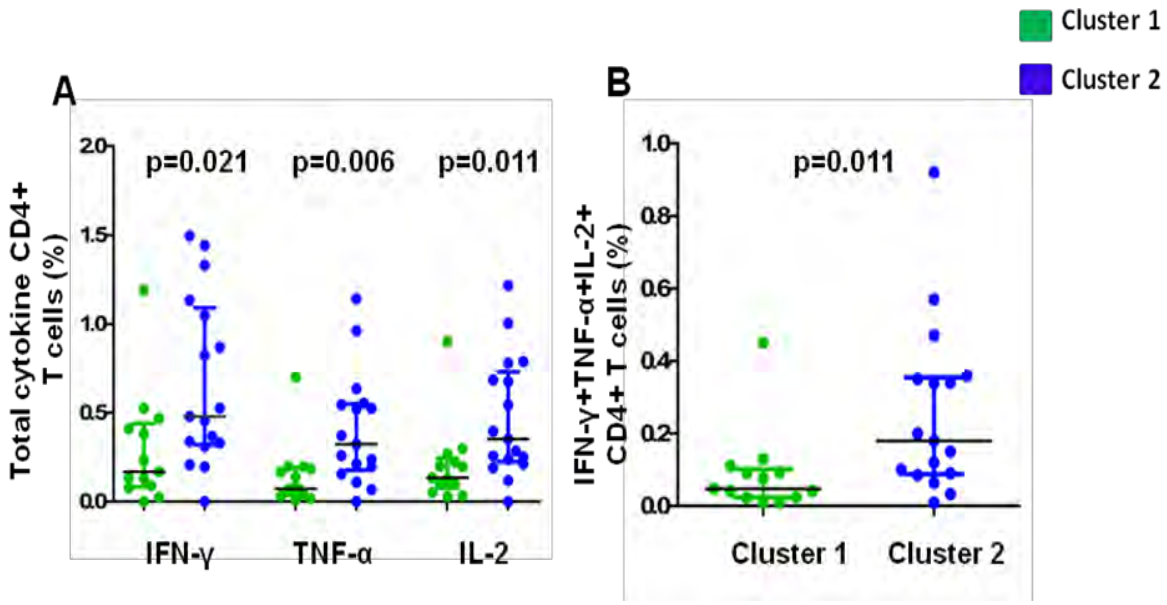

Figure 25: Frequencies of BCG-specific CD4+ T cells.
Whole blood was incubated with BCG for 12 hours and cytokine-expressing CD4+ T cells detected using an intracellular cytokine staining assay and flow cytometry. (**A**) Frequencies of total CD4+ T cells expressing IFN-γ, TNF-α and IL-2 upon BCG stimulation. **(B)** Frequencies of BCG-specific CD4+ T cells co-expressing IFN-γ, TNF-α and IL-2. Mann-Whitney U test was used to compare differences between clusters 1 (green, n=13) and 2 (blue, n=17). Horizontal lines represent median while whiskers represent the interquartile range. A p value of < 0.05 was considered significant.

Infants from cluster 2 also had higher frequencies of BCG-specific CD4+ T cells expressing: IFN-γ only (Figure 26A), IFN-γ and TNF-α (Figure 26B), TNF-α and IL-2 (Figure 26C) as well as TNF-α, IL-2 and IL-17 (Figure 26D), when compared to infants from cluster 1. No other T cell subsets were different between the two clusters (Table 7).

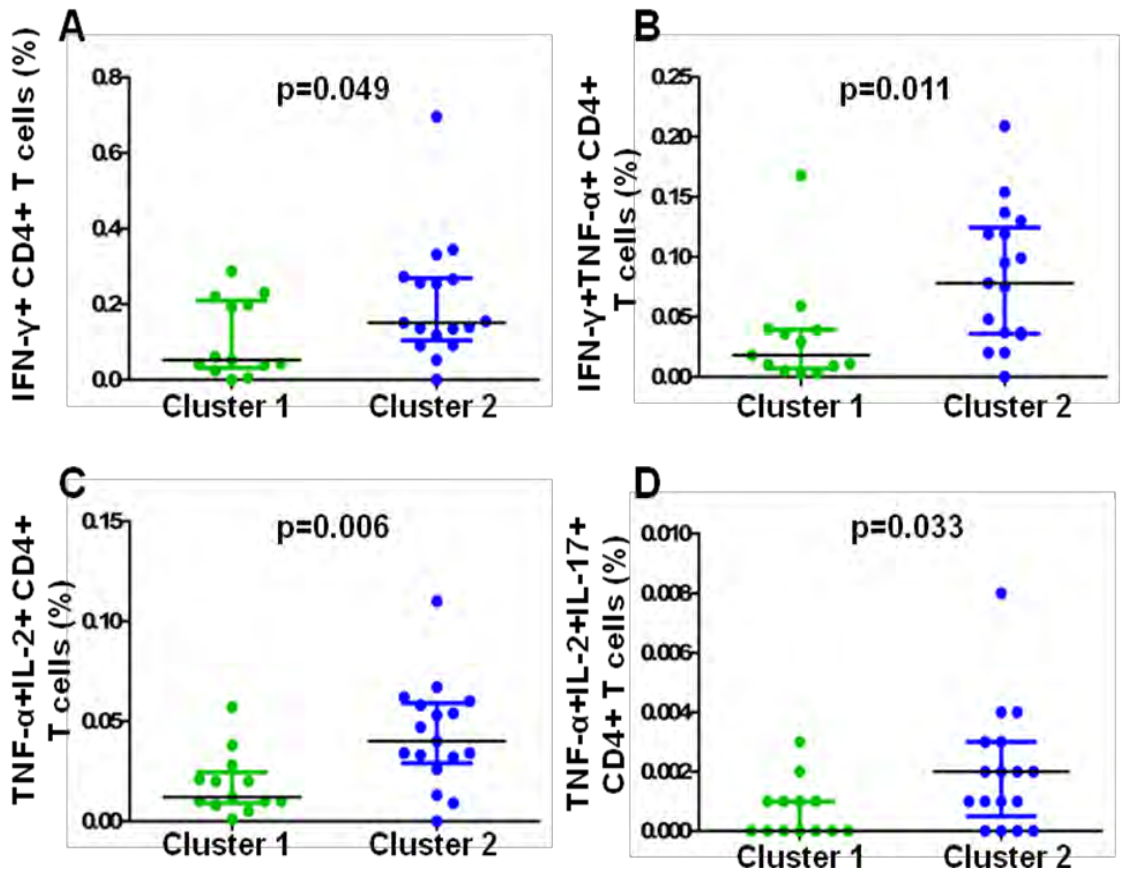

Figure 26: Cytokine profile of BCG-specific CD4+ T cells.
Whole blood was incubated with BCG for 12 hours and cytokine-expressing CD4+ T cells detected using an intracellular cytokine staining assay and flow cytometry. Frequencies of BCG-specific CD4+ T cells expressing (**A**) IFN-γ only. **(B)** IFN-γ, and TNF-α together, **(C)** IL-2 and TNF-α together **(D),** IL-2, IL-17 and TNF-α together. Mann-Whitney U test was used to compare differences between clusters 1 (green, n=13) and 2 (blue, n=17). Median and interquartile range are denoted by horizontal line and whiskers respectively. A p value of < 0.05 was considered significant.

As described before, CD8+ T cells predominantly expressed IFN-γ , while IL-2, TNF-α and IL-17 expressing CD8+ T cells were relatively infrequent. Also, BCG-specific CD8+ T cell responses were generally lower than CD4+ T cell responses. Similarly to CD4+ T cells, frequencies of BCG-specific CD8+ T cells expressing IL-2 and those co-expressing IFN-γ, TNF-α and IL-2 together were higher in infants from cluster 2 compared to cluster 1 (Figure 27A and B). No

other BCG-specific CD8+ T cell cytokine or subset was different between the two clusters of infants (Table 7).

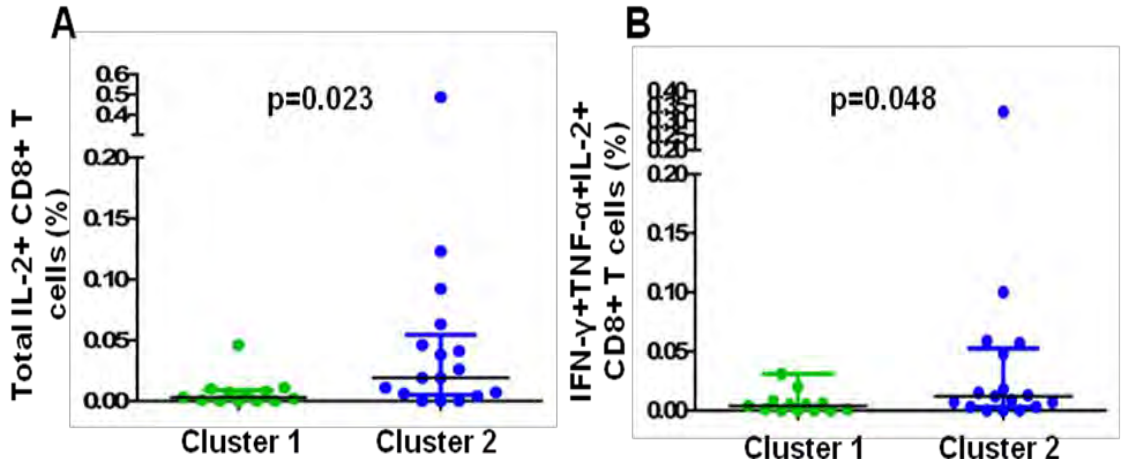

Figure 27: Frequencies of BCG-specific CD8+ T cells.
Whole blood was incubated with BCG for 12 hours and cytokine-esxpressing CD8+ T cells detected using an intracellular cytokine staining assay and flow cytometry. Frequencies of total CD8+ T cells expressing (**A**) IL-2, **(B)** IFN-γ, TNF-α and IL-2. Mann-Whitney U test was used to compare differences between clusters 1 (green, n=13) and 2 (blue, n=17). Horizontal lines and whiskers denote median and interquartile range respectively. A p value of < 0.05 was considered significant.

Analysis of levels of secreted mediators released in the supernatant of whole blood stimulated with BCG for 7 hours showed some differences between the two clusters. The Th-1 promoting cytokine, IL-12p70 (Figure 28A) as well as T cell homeostatic cytokine IL-15 (Figure 28B) were higher in cluster 2 compared to cluster 1. There were no other differences observed between the two clusters (Table 7).

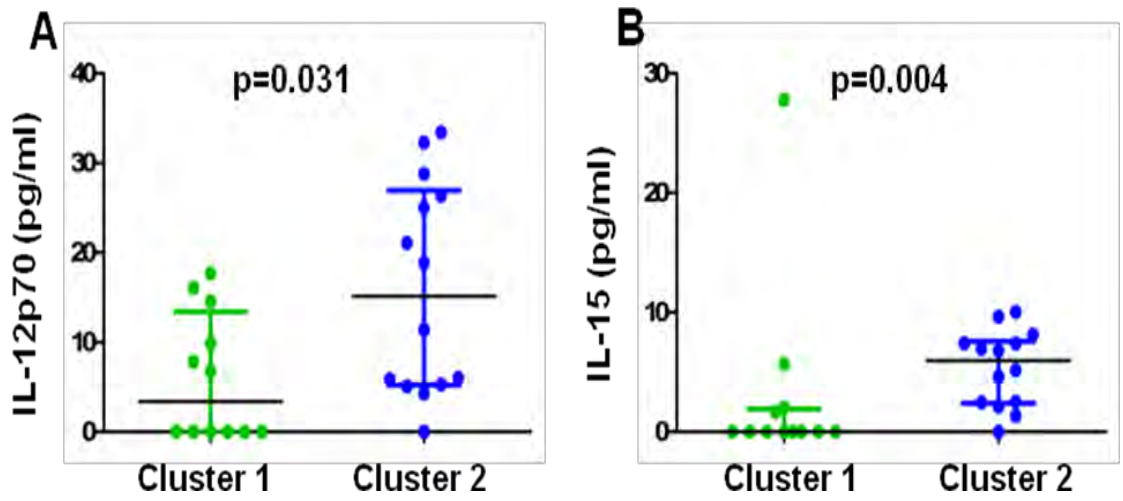

Figure 28: Secreted mediators.
Whole blood was incubated with BCG or no antigen for 7 hrs and soluble molecules were measured by luminex bead array. Values measured in unstimulated samples were subtracted from BCG-stimulated samples. Levels of IL12-p70 **(A)** and IL-15 **(B)** differed between cluster 1 (green, n=12) and cluster 2 (blue, n=13). Horizontal lines show medians while whiskers show interquartile range. The Mann-Whitney U test was used to compare the two groups.

Analysis of the proliferative capacity (figure 29) and up-regulation of the cytotoxic molecules granzyme B, granulysin and perforin by BCG-specific CD4+ and CD8+ T cells showed no differences between the two clusters (Figure 30).

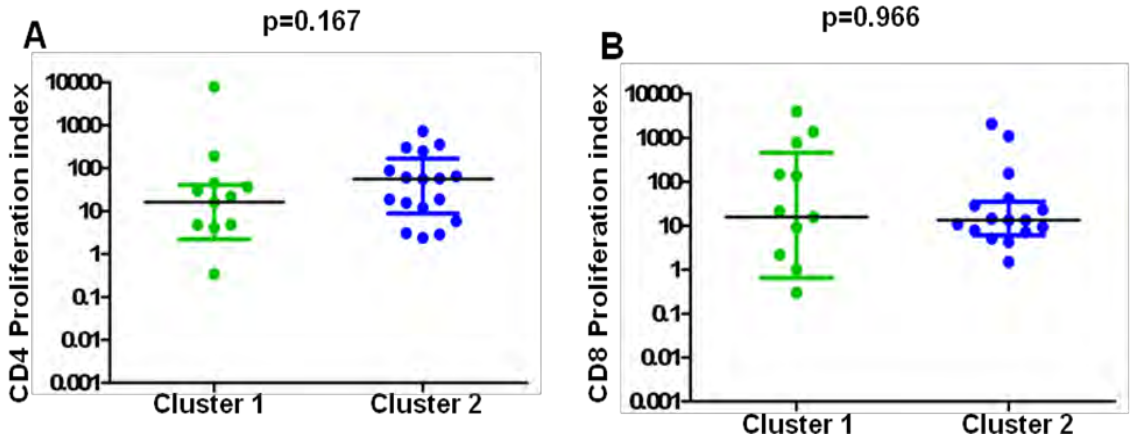

Figure 29: BCG-specific T cell proliferative capacity.
PBMCs were stained with Oregon Green (OG) and stimulated for 6 days with BCG or left unstimulated. Proliferating cells were identified as OG^{low} CD8+ or CD8- (mainly CD4+) T cells. Proliferation index was calculated as the frequency of proliferating cells upon BCG stimulation, divided by the frequency of proliferating cells in unstimulated cells. Differences in proliferative capacity of **(A)** CD4+ and **(B)** CD4+ T cells between cluster 1 (green, n=11) and cluster 2 (blue, n=17) were assessed using the Mann-Whitney test. Horizontal line on graphs denotes the median while whiskers denote interquartile range. No significant differences were observed.

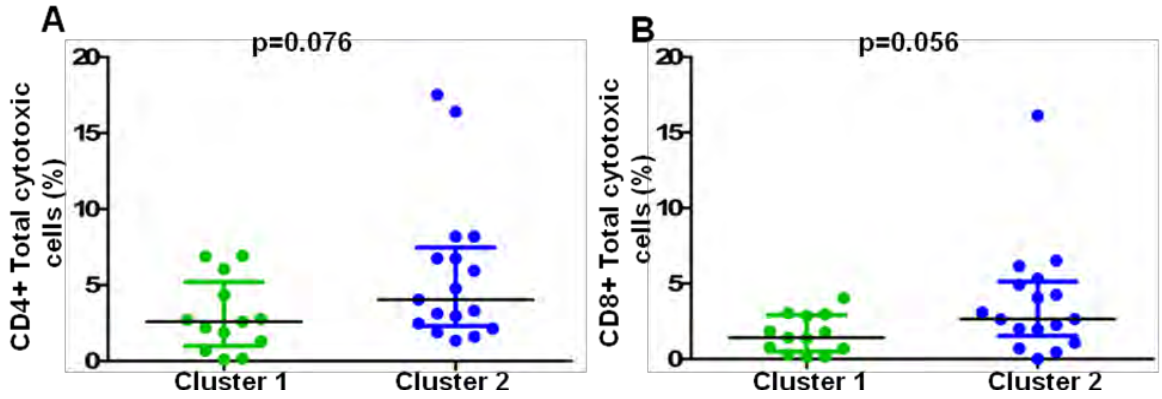

Figure 30: Cytotoxic capacity of BCG specific T cells.
PBMCs were stimulated with BCG or left unstimulated for 3 days and flow cytometry was used to detect BCG-specific CD4+ T cells expressing granzyme B, granulysing and/or perforin. BCG-specific T cells were defined by subtracting the unstimulated value from the BCG stimulated value. Frequencies of **(A)** CD4+ T and **(B)** CD8+ cells expressing total cytototxic molecules. Mann-Whitney test was used to compare cluster 1 (green, n=13) and cluster 2 (blue, n=17). Horizontal lines on graphs represent median and whiskers represent interquartile range.

Taken together, these data show that the clusters identified by unbiased analysis of global gene expression associated with the magnitude of BCG-specific Th1 responses.

Table 7: BCG-specific T cell outcomes not significantly different between cluster 1 and cluster 2

Frequency and cytokine profiles of CD4+ T cells	Frequency and cytokine profiles of CD8+ T cells	Cytotoxic and proliferation capacity of CD4+ T cells	Cytotoxic and proliferation capacity of CD8+ T cells	Secreted mediators
Total IL-17 (p=0.464)	Total IFN-γ (p=0.132)	Total granulysin (p=0.111)	Total granulysin (p=0.132)	TGF-α (p=0.084)
IL-2+IL-17+IFN-γ+α+ (p=0.063)	Total TNF-α (p=0.053)	Total granzyme B (p=0.379)	Total granzyme B (p=0.155)	IL-2 (p=0.425)
IL-2+IL-17+IFN-γ+ (p=0.189)	Total IL-17 (p=0.376)	Total perforin (p=0.217)	Total perforin (p=0.217)	IL-4 (p=0.363)
IL-2+IL-17+ (p-=0.120)	IFN-γ+ (p=0.130)	Granulysin+Granzyme B+Perforin+ (p=0.455)	Granulysin+Granzyme B+Perforin+ (p=0.278)	IL-5 (p=0.437)
IL-2+IFN-γ+ (p=0.072)	TNF-α+ (p=0.320)	Granulysin+Granzyme B+ (p=0.312)	Granulysin+Granzyme B+ (p=0.674)	IL-6 (p=0.897)
IL-2+ (p=0.131)	IL-2+ (p=0.424)	Granulysin+Perforin+ (p=0.483)	Granulysin+Perforin+ (p=0.754)	IL-7 (p=0.192)
IL-17+IFN-γ+TNF-α+ (p=0.265)	IL-17+ (p=0.354)	Granzyme B+Perforin+ (p=0.417)	Granzyme B+Perforin+ (p=0.219)	IL-10 (p=0.662)
IL-17+IFN-γ+ (p=0.898)	IL-2+IL-17+IFN-γ+TNF-α+ (p=0.054)	Granulysin+ (p=0.056)	Granulysin+ (p=0.572)	IL-8 (p=0.589)
IL-17+TNF-α+ (p=0.255)	IL-2+IL-17+IFN-γ+ p(=0.149)	Granzyme B+ (p=0.188)	Granzyme B+ (p=0.285)	IL-13 (p=0.789)
IFN-γ+TNF-α+ (p=0.205)	IL-2+IL-17+TNF-α+ (p=0.265)	Perforin+ (p=0.260)	Perforin+ (p=0.677)	IL-1β (p=0.446)
IL-17+ (p=0.315)	IL-2+IL-17+ (p=0.444)	Total proliferation (p=0.167)	Total proliferation (p=0.966)	IL-17 (p=0.237)
TNF-α+ (p=0.835)	IL-2+TNF-α+ (p=0.897)			IFN-γ (p=0.227)
	IL-2+IFN-γ+ (p=0.122)			EGF (p=0.280)
	IL-17+IFN-γ+TNF-α+ (p=0.923)			GM-CSF (p=0.341)
	IL-17+IFN-γ+ (p=0.101)			TNF-α (p=0.396)
	IFN-γ+TNF-α+ (p=0.872)			Eotaxin (p=0.626)
				Fractackline (p=0.083)
				MIP-1β (p=0.316)
				MIP-1α (p=0.463)

4.3.2) Gene expression pathways associated with clustering

We next assessed which gene expression pathways were differentially expressed in the two clusters by GSEA and IPA.

For GSEA analysis, a rank metric score for each gene was obtained within the two clusters. A rank metric score is the signal to noise ratio (BCG-UNS) used to position the gene in the ranked list. This ranked list was then compared to known datasets of genes housed in the GSEA C2:cp molecular signature database (MsigDB, http://www.broad.mit.edu/gsea/msigdb). Differentially expressed gene pathways included those associated with myeloid cells (mostly monocytes and dendritic cells in PBMCs), with IFN-γ, IFN-α and proinflammatory cytokine activity, lysosomal and cytototoxic T cell activities. In cluster 1, gene sets associated with myeloid cells, lysosomal activity and inflammation II (molecules inducing or inducible by inflammation and lysosomal enzymes) [299] had an increased expression compared to cluster 2 (Figure 31). Gene sets enriched in cluster 2 compared to cluster 1 were associated with inflammation (genes encoding molecules involved in inflammatory processes and regulation of apoptosis) [299], cytokine activity, interferon response (type I and II) and cytotoxic T cells (Figure 31). FDR was set at 0.05.

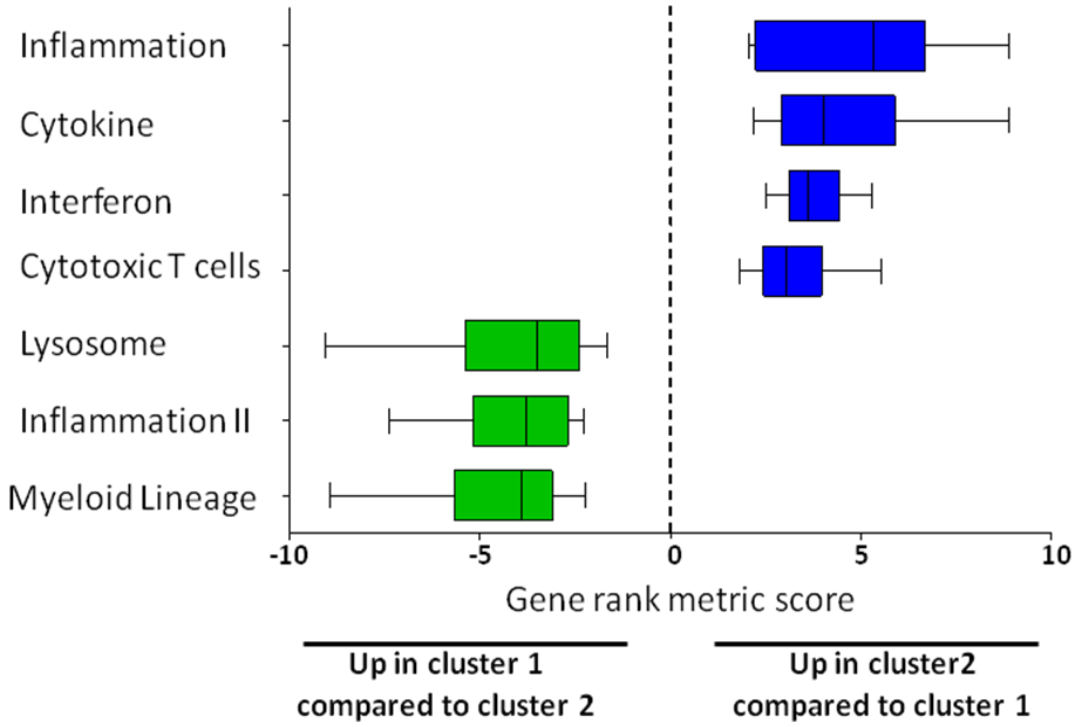

Figure 31: GSEA of differentially expressed pathways between clusters 1 and 2.
The most differentially expressed genes between cluster 1 (green) and cluster 2 (blue) in representative immune pathways. Gene rank metric score is signal to noise ratio for each gene (BCG-UNS). Inflammation included genes encoding molecules involved in inflammatory processes and regulation of apoptosis and inflammation II included molecules inducing or inducible by inflammation and lysosomal enzymes (Chaussabel *et al*., 2008).

When we evaluated the functional gene networks associated with differential gene expression between the two clusters using IPA with all 20,000 genes, a network of 35 genes with a score of 39 was generated (Figure 32). This network comprised genes that are co-expressed to regulate cellular growth and proliferation, haematological system development and function as well as tissue development (Figure 32). Of this 35 genes, 15 were down-regulated in cluster 1 compared to cluster 2 (red,) 15 were up-regulated in cluster 1 compared to cluster 2 (green) and 5 genes had no differential expression between the two clusters. 25 of these transcripts were found in our list of 461 genes differentially expressed between the two clusters identified by LIMMA analysis. Most

importantly, this pathway seems to be largely dominated by IFN-γ, as all the other focus molecules are directly or indirectly connected to it.

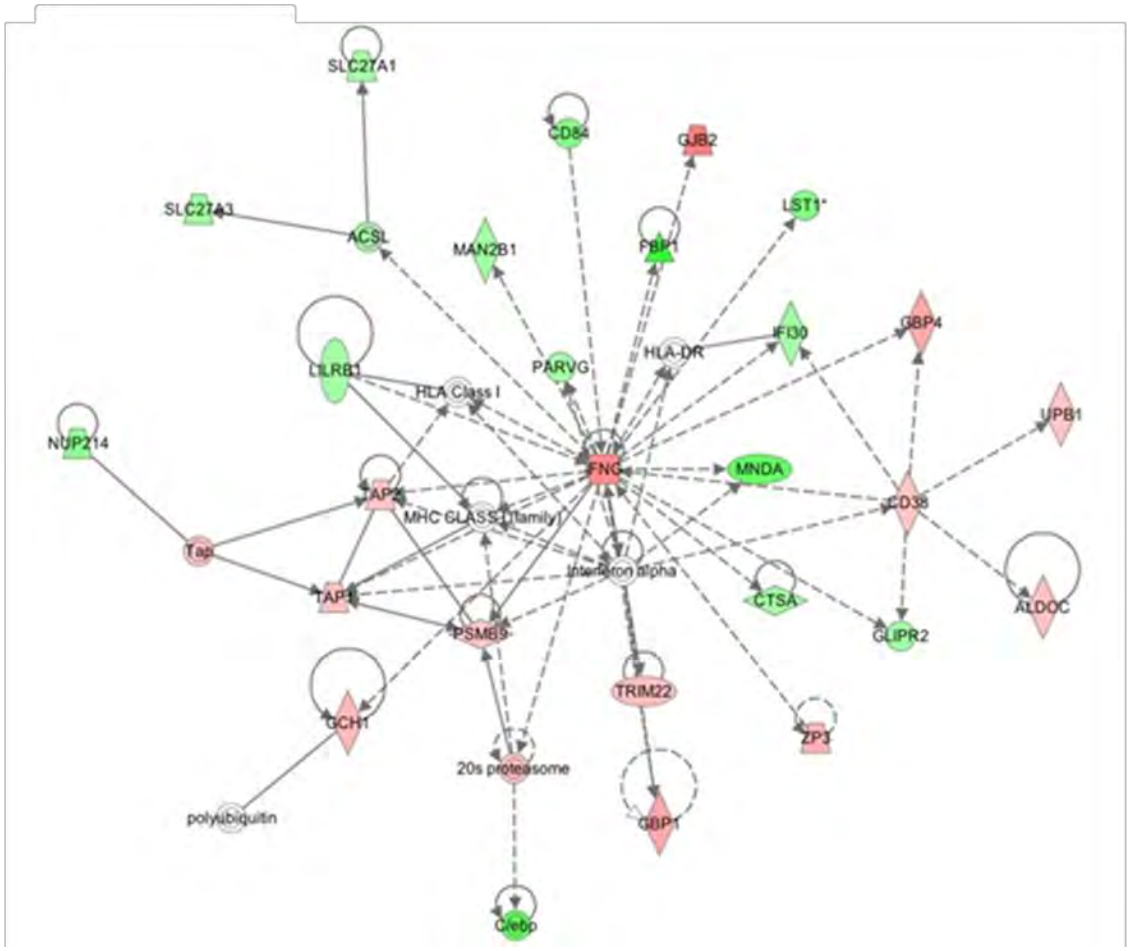

Figure 32: Gene network identified by IPA between cluster 1 and cluster 2.
Visual representation of principal network generated using 20,000 genes (BCG-UNS). Network shows 35 genes that work together for cell growth and proliferation, haematological system development and function as well as tissue development. Genes highlighted in green are up-regulated in cluster 1 compared to cluster 2, while those highlighted in red are down-regulated in cluster 1 compared to cluster 2. Solid lines denote direct interactions while dashed lines represent indirect interactions.

As seen from the IPA analysis, IFN-γ mRNA was upregulated in stronger responders compared to weaker responders. Interestingly, IFN-γ produced by CD4+ T cells was also higher in stronger responders compared to weaker responders. In order to back up this finding, a correlation analysis on IFN-γ mRNA expression and frequencies of IFN-γ-expressing CD4+ T cells was performed, and a significant positive correlation between the two was found (r=0.605, p=0.0002) (Figure 33A). To further support this finding, when we correlated CXCL9 mRNA expression (CXCL9 is a monokine induced by IFN-γ) to IFN-γ-expressing CD4+ T cells, this strong positive correlation was also observed (r=0.626, p=0.0001) (Figure 33B).

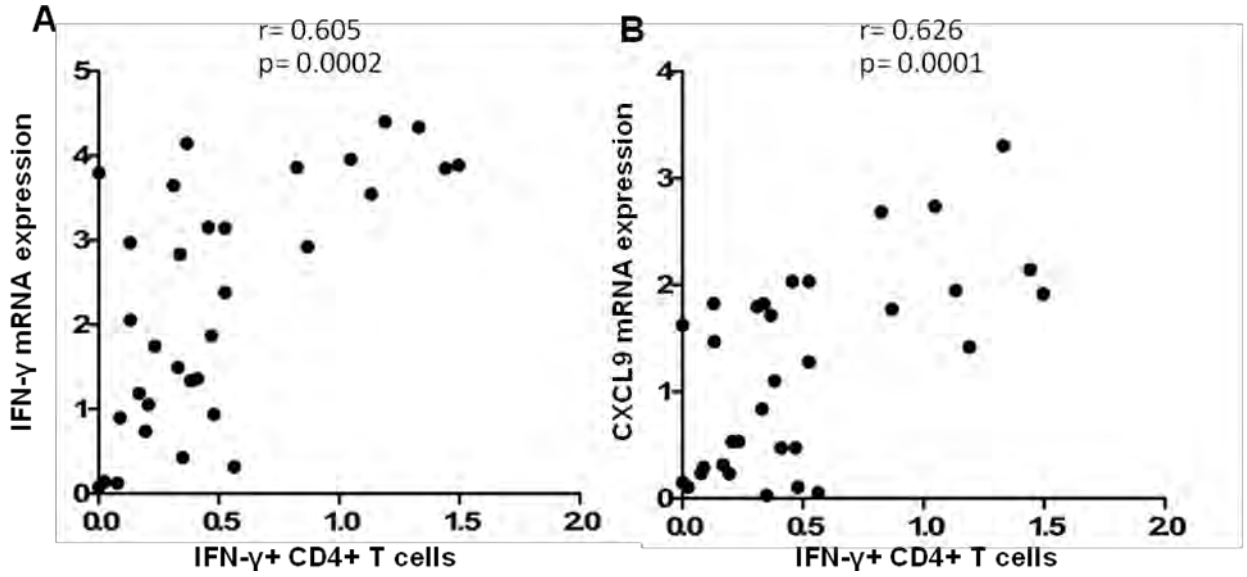

Figure 33: Correlation of IFN-γ and CXCL9 mRNA expression and IFN-γ-expressing CD4+ T cells.
PBMCs were stimulated with BCG or left unstimulated for 12 hrs. RNA was extracted, transcribed to cDNA and IFN-γ and CXCL9 expression were measured by microarray. Whole blood was incubated with BCG or left unstimulated for 12 hours and frequencies of IFN-γ-expressing CD4+ T cells measured by intracellular cytokine staining assay and flow cytometry. Following background subtraction, correlation between **A)** IFN-γ mRNA expression and frequencies of IFN-γ+CD4+ T cells and **B)** CXCL9 mRNA expression and frequencies of IFN-γ+CD4+ T cells were determined using spearman rank correlation.

4.4) Discussion

Following the observation of clustering of infant gene expression profiles upon *in vitro* BCG re-stimulation, we aimed to understand the biology associated with this phenomenon. After exclusion of demographic and sample processing factors that could have influenced our results, we compared BCG-specific T cell responses as well as expression of gene pathways between these two clusters. We consistently observed higher frequencies of BCG-specific T cells, mainly Th1, in cluster 2 compared to the cluster 1. Frequencies of CD4+ T cells expressing total IFN-γ, TNF-α, IL-2 and CD8 + T cells expressing total IL-2 were higher in cluster 2 compared to cluster 1. Th1 cytokines, especially IFN-γ, produced by CD4+ T cells are often measured as vaccine endpoints in clinical trials [323]. The magnitude of these responses is usually used to assess the immunogenicity of a vaccine. Importantly, frequencies of CD4+ and CD8+ T cell co-expressing IFN-γ, TNF-α and IL-2 (polyfunctional cells) were also higher in cluster 2 compared to cluster 1. Darrah *et al* showed that polyfunctional cells could be an additional measure of the quality of a T cell response, which correlated with Leishmania vaccine efficacy in a mouse model [168]. In addition to vaccine efficacy, these polyfunctional cells are also measured as immunogenicity end points in new TB vaccine trials [64, 324]. Despite this, no differences in frequencies of polyfunctional T cells were observed between cases and controls within cluster 2 (see chapter 3).

In our study, all participants received BCG at birth. Though all infants had detectable T cell responses measured at 10 weeks of age, the frequencies of BCG-specific T cells were higher in some infants compared to others. Our data show that infants from cluster 2 had a stronger antigen-specific T cell response to BCG than infants in cluster 1. Based on this data, we linked clustering of gene expression profiles in these infants to differential response to BCG vaccination where infants in cluster 2 are “stronger BCG responders” and those in cluster 1 are “weaker BCG responders”. This association between innate gene signature and magnitude of adaptive immune responses has been

described in several other vaccines. For example, Zak *et al* have reported a similar association between innate gene signature and magnitude of adaptive responses to MRKAd5/HIV vaccine [325]. In this study, 35 healthy HIV-uninfected adults were vaccinated with MRKAd5 Vaccine. Blood was collected immediately pre-vaccination and at 4-6, 24, 72 and 168 hours post-vaccination. Transcriptional profiling was used to identify differentially expressed genes between pre-vaccination and post vaccination time points. Using systems analysis, they found innate immune signatures that associated with immunogenicity of MRKAd5/HIV vaccine [325]. Immunogenicity was defined by the magnitude of gag-specific CD8+ T cell responses and participants were stratified as high or low responders based on this parameter. In yellow fever vaccine, Querec *et al* have shown that early innate gene signatures correlate with the magnitude of both CD8+ T cell and neutralising antibody responses [326]. Blood was collected at 0, 1, 3, 7 and 21 days post vaccination from 15 healthy volunteers. Differential gene expression between days 0 and 3 as well as days 0 and 7 was identified. Post vaccination (3 and 7 days) innate gene signatures were found to correlate with the magnitude of vaccine-induced CD8+ T cell and antibody responses measured at 60 days post vaccination [326]. This approach was also used by Tan *et al* whereby they showed that enrichment of signatures corresponding to proliferating B cells accurately defined antibody responses to influenza vaccine [327].

There could be several reasons underlying differential BCG immunogenicity and efficacy within a population. In our group, several factors that may play a role in BCG-induced immunity in our community have been studied. Davids *et al* compared the effect of Danish and Japanese BCG strains on the immune responses in infants vaccinated at birth and showed that infants who received the Japanese strain of BCG had significantly higher Th1 responses compared to those who received the Danish strain [40]. However, all 5,724 infants enrolled into our study received the Japanese BCG strain. Hawkridge *et al* reported no effect on BCG immunogenicity and efficacy when BCG is administered using

two different vaccination routes (percutaneous vs intradermal) [56]. Also, in South Africa, BCG is widely given to all infants at birth, before any exposure to non-tuberculous mycobacteria, suggesting that this in an unlikely cause of differential responsiveness to the vaccine [44]. Shey *et al* also reported that single nucleotide polymorphism (SNP) of TLR6 gene (G1083C and C746T) in South African adults who had received BCG at birth was associated with impaired mycobacteria specific responses [49]. This therefore suggests that polymorphisms in certain immune related genes within our community might influence response to BCG. However, when we investigated the association between SNP of TLR1 and TLR6 genes and response to BCG vaccination in these infants, no conclusion could be reached, as there were not enough individuals with this polymorphism to analyse (Shey, Hawn, Hanekom *et al*., unpublished observation). Overall, the frequency of these SNPs reported by Shey *et al* was very rare in our study population, and therefore these genetic polymorphisms are unlikely to underlie the differential response to BCG vaccination we observed. However, we cannot rule out that SNPs in other genes or regions of the genome may underlie this differential response.

Analysis of gene expression profiles of these infants showed that several pathways were differentially expressed between stronger and weaker BCG responders. Pathways involved in lysosomal activity, myeloid lineage and "inflammation II" were enriched in weaker responders compared to stronger responders while pathways up-regulated in stronger responders were associated with "inflammation I", cytokine, cytotoxic T cells and interferon pathways (type I and II). Our results are at odds with published literature. For example, Teles *et al* showed that type I interferons suppress type II interferons in infected lesions of *M.leprae* infected individuals [328]. In this study, transcriptional profiling performed on skin lesions showed that a score that reflected the expression of several genes associated with both type I and II interferons was always in opposite direction [328]. In our study, we found that several genes associated with both type I and II interferons were up-regulated in

stronger responders. Also, Zak *et al* showed that MRKAd5/HIV vaccine response was associated with increased expression of inflammatory, myeloid and interferon pathways and suppression of pathways associated with lymphoid lineage, cytotoxicity and T cells [325]. Other members of our laboratory found that upregulation of inflammatory pathways was also associated with upregulation of myeloid as well as interferon pathways in *M.tb* infected adolescents at prospective risk of developing TB disease (Penn-Nicholson, Hanekom, Scriba *et al*., unpublished data). However in our study, we had two groups of BCG vaccinated infants both made up of healthy *M.tb* uninfected infants at prospective risk of developing TB disease and those not at risk. "Inflammation II" gene set included molecules inducing or inducible by inflammation, such as IL-18, SERPINB1, ALOX5, ANPEP and AOAH while "inflammation I" included genes encoding molecules involved in inflammatory processes such as IL-8, ICAM1, C5R1, IL1A, and CD44 [299]. The observation of differential mechanism of inflammation in the two groups of infants might be a confirmation of the differential response to BCG vaccination. In the previous chapter, we found that inflammatory pathways in weaker responders were down-regulated in cases, while in stronger responders they were up-regulated in cases compared to controls. This might imply that the inflammation signature we observed in weaker responders is mainly driven by control samples, while in stronger responders is due to the cases. This supports our findings in the previous chapter suggestive of too little inflammation, as seen in cases in weaker responders, or too much inflammation, as seen in cases in stronger responders, increases the risk of developing TB disease. Pathways associated with myeloid lineages were also higher in weaker responders compared to stronger responders. However this was observed only when the background expression values were subtracted. Separate analysis of unstimulated PBMC showed that stronger responders had increased myeloid signatures, which were down-regulated upon stimulation with BCG (data not shown). This supports our hypothesis that the degree of inflammation seen in the two groups of infants is driven by myeloid cells, as discussed in chapter 3.

Cytokine as well as cytotoxic T cell gene sets were also up-regulated in cluster 2 compared to cluster 1. This is in agreement with what we observed at the protein level where BCG-specific T cells were higher in cluster 2 compared to cluster 1. This might suggest that inflammation observed in cluster 2 is driven by BCG-specific T cells while in cluster 1 it is driven by myeloid, cells hence two different modules of inflammation in both clusters.

IPA analysis showed enrichment of a network of genes involved in enhancement of cell growth and proliferation. Interestingly, this pathway was central to IFN-γ, which was up-regulated in stronger responders compared to weaker responders. This further supports the observation made at the protein level, whereby higher frequencies of IFN-γ-producing CD4+ T cells were detected in stronger BCG responders compared to weaker responders. To support this finding, there was a strong significant positive correlation between IFN-γ mRNA expression and IFN-γ-producing CD4+ T cells as well as between CXCL9 mRNA expression (a protein specifically induced by IFN-γ) and IFN-γ-producing CD4+ T.

Further mechanistic investigations were performed to better understand the biology of this clustering. However, we could not find any other significant differentially expressed pathway that was relevant to this study. Nevertheless, the fact that we identified a pathway largely dominated by IFN-γ in cluster 2 infants compared to cluster 1 backs up the CD4+ T cell data. In addition, the strong correlation between IFN-γ mRNA expression and CD4+ T cells making IFN-γ also adds more weight to this finding.

4.5) Conclusion

Together, our data suggests that immune responses elicited by BCG vaccination are heterogeneous and that this differential responsiveness to BCG should be taken into account in the discovery of potential correlates of protection and/or risk of TB disease. We therefore sought to validate these findings in an independent cohort of BCG vaccinated infants.

CHAPTER 5: VALIDATION OF CORRELATES OF RISK OF TB DISEASE IN DIFFERENTIAL BCG RESPONDERS

In this chapter, all Fluidigm, flow cytometry and quantitative real-time PCR experiments and analyses were done by Samuel Njikan. Fluidigm analyses for gene signatures were done by our collaborators in VGTI and Jenner Institute.

5.1) Introduction

In the previous chapters, we report that gene expression patterns of BCG-stimulated PBMCs in BCG-vaccinated infants separated them into 2 groups, which associated with differential response to BCG vaccination in 10-week old infants. Accounting for this differential response was a prerequisite for identification of host correlates of risk of TB disease following BCG vaccination. For the first time, we identified candidate correlates of prospective risk of TB disease in healthy infants, which could later translate into correlates of risk. However, several exploratory analyses, involving bioinformatics and systems biology approaches where used to mine our high dimensional data set. There is always a high chance of false positive discoveries in these analysis steps, especially considering the small sample size and the small changes in gene expression profiles between the conditions under study [266]. A validation of the results identified in the training set (samples on which results were generated) is therefore important to negate the likelihood of false positive discoveries.

Validation involves measuring the outcomes identified in the training set on an independent set of samples (validation set). Quantitative real time PCR (qRT-PCR) can be used to validate microarray results, since it allows measurement of only the most differentially expressed genes identified by microarray. Because this method is a relatively low throughput, we used a multiplex microfluidic qRT-PCR (Fluidigm) platform for validation. This technique allows simultaneous performance of up to 9216 qPCR reactions from 96 different samples and 96 different transcripts in a single experiment.

We aimed to identify biomarkers of clustering and validate prospective correlates of risk of TB disease in a second cohort of BCG vaccinated infants. For the application of validated correlates of risk of TB disease in clinical trials, performing global gene expression by microarray may be intensive and expensive. Therefore, measuring a few genes by real time PCR or routine immunological assays will be very practical in such trials. For the identification of these markers, we used two different approaches. The first approach was hypothesis driven, where we applied frequencies of BCG-specific CD4+ T cells and the expression of CXCL9 (MIG) mRNA as markers of differential BCG response in the validation set. This was based on the fact that: i) stronger BCG responders in the training set had higher frequencies of BCG-specific T cells compared to weaker BCG responders, ii) stronger BCG responders had higher expression of the IFN-γ-inducible gene pathway which correlated with the magnitude of IFN-γ-expressing CD4+ T cells compared to weaker responders.

The second approach was unbiased, where we applied a gene expression signature identified by microarray as a classifier for differential BCG response in the validation set, with minor attention to underlying biological meaning. We then sought to validate the correlates of risk of TB disease in stronger and weaker BCG responders identified by the expression of these markers.

5.2) Materials and Methods

5.2.1) Study participants

Another group of 10-week old infants vaccinated with BCG at birth enrolled into the RCT study at the SATVI field site in the Worcester area, near Cape Town, were included as study participants for this experiment (see section 2.2.1) [56]. Exclusion and inclusion criteria were identical to the previous group (section 2.2.1) with the exception of the factors below.

5.2.2) Participant follow up and TB case definition

As for the training cohort, blood was collected from healthy infants at 10 weeks of age, who were followed up for a period of 2 years to identify those who developed TB disease. Community-wide passive surveillance systems identified patients with possible TB disease and children with symptoms suggestive of TB disease, or from households where an adult had TB disease [56]. These infants were admitted to a dedicated research ward for clinical examination, chest radiography, tuberculin skin testing, two early morning gastric aspirations and two sputum inductions for *M.tb* smear and culture [56]. All infants admitted to the research ward were also tested for HIV infection: a positive antibody test resulted in exclusion.

Cases for the validation study were culture negative for *M.tb* but had a strong positive chest x-ray and clinical and/or epidemiological evidence of TB (probable TB, n=29). Controls included infants who were living in the same endemic community but did not meet criteria for TB investigation (community controls, n=55).

5.2.3) Whole blood assay and intracellular cytokine staining

See section 2.2.3

5.2.4) Lymphoproliferation assay

Cryopreserved PBMC (see section 2.2.4) were thawed in 12.5% v/v AB serum in RPMI containing 10μg/mL DNase (Sigma-Aldrich). Lymphoproliferation assay was performed as described in section 2.2.5. as described above.

5.2.5) Cytotoxic marker assay

See section 2.2.6

5.2.6) PBMC isolation and stimulation for primer/probe qualification and optimisation of Fluidigm gene expression panel

For optimisation experiments, fresh PBMCs from healthy donors were isolated as described in section 2.2.4. Cells ($1X10^6$ cells/ml) were then cultured with BCG at an MOI of 0.18 (5 vials) or left unstimulated (5 vials) for 12hrs at 37°C. Following incubation, 3 vials each unstimulated cells were combined with BCG stimulated cells and used for primer qualification, to ensure uniform representation of transcripts present in both unstimulated and stimulated cells. The remaining 2 vials each of BCG stimulated and unstimulated cells were separately used for optimising the fluidigm gene expression panel.

For infant samples used for validation, cryopreserved PBMCs were thawed, washed in RPMI 1640 and rested for 6 hours at 10^6 cells in RPMI 1640 containing 10% AB serum and 1% L-glutamine at 37°C and 5% CO_2. After resting, PBMC were then incubated in culture with BCG at an MOI of 0.18 for 12 hours at 37°C and 5% CO_2. Phorbol 12-myristate-13 acetate (PMA, 1μg/mL) and Ionomycin (5μg/mL) were used as positive control while medium alone served as negative control.

5.2.7) RNA Extraction for optimisation experiments and validation samples

Following the incubation period, cells were harvested and RNA extracted from combined and non combined cells (optimisation experiments), using the QIAamp RNA Blood Mini Kit (Qiagen) according to the manufacturer's instructions.

5.2.8) cDNA synthesis and Quantitative real-time PCR (qPCR) for CXCL9 expression

Complementary DNA (cDNA) was synthesised from the extracted RNA using Omniscript RT Kit (Qiagen), according to the manufacturer's instructions with Oligo dT_{12-18} primers (Invitrogen).

Quantitative real time PCR (qPCR) was performed using SensiMix^{TM}SYBR No-ROX (Bioline; USA) containing 2X SensiMix^{TM}SYBR No-ROX solution and 50mM $MgCl_2$ solution on a Rotor-Gene^{TM}6000 (Corbett) with the following primers:

CXCL9-F: 5'-TCCCATGAAGAAAGGGAACGGTGA-3'

CXCL9-R: 5'-AGAGGCTAACTGGGCACCAATCAT-3'

HPRT-F: 5'-TGGAGTCCTATTGACATCGCCAGT-3'

HPRT-R: 5'-AACAACAATCCGCCCAAAGGGAAC-3'

The thermal cycling conditions used for the qPCR were as follows:

Activation step of 95°C for 15mins

Denaturation step 94°C for 15sec

Annealing 60°C for 20sec

Elongation 72°C for 15sec

The house keeping gene HPRT was used to control for variation in cDNA quantity between samples and all reactions were performed in triplicate.

5.2.9) Generation of standard curve

A standard curve for each primer pair was generated by quantifying and purifying each transcript with a gel purification kit (Qiagen) and diluting the PCR products. Briefly, a conventional PCR was performed for each gene and the

PCR product run on a 2% agarose gel in 1XTAE buffer. The resulting PCR bands were excised and purified with a gel purification kit (Qiagen) according to the manufacturer's instructions. The product was then quantified using a nanodrop and several aliquots of six 10-fold serial dilutions (six standards) were made and stored at -20°C. A standard curve and amplification efficiency were determined by performing a qPCR on 1 aliquot each of the six standards and saved. All six standards could not be run for every single experiment to determine the standard curve due to limited space on the Rotor-Gene^{TM}6000 (Corbett). To overcome this, 2 of the 6 standards were run for each experiment and the saved standard curve for each gene was imported for downstream analyses.

5.2.10) Selection of differentially expressed genes

To identify gene classifiers of differential response to BCG vaccination and risk of TB disease, selection of genes differentially expressed between stronger and weaker BCG responders and between cases and controls in stronger responders respectively was performed. Two methods were used to identify genes differentially expressed between the various groups of infants. Firstly, k-means cluster analysis (centroid-based clustering) which uses an optimal shrinkage threshold to build a centroid was used to identify differentially expressed genes. The optimal threshold that gave the lowest error rate after cross-validation was chosen. Secondly, LIMMA analysis and an empirical Bayes method were used to identify genes differentially expressed between groups of infants as in section 3.2.1b. The genes were then sorted and ranked firstly by adjusted p value with 0.00001 and 0.05 used as a cut-off value for response to BCG vaccination and risk of TB disease, respectively. Genes were then sorted and ranked by log fold change (FC) in gene expression with FC>2 and 1.4 used as cut-off for response to BCG vaccination and risk of TB disease, respectively. Priority was given to the top most differentially expressed genes ranked by p-value and fold change using LIMMA analysis and centroid analysis.

5.2.11) TaqMan Gene Expression (GE) assay qualification and optimisation of a multiplex gene expression system (Fluidigm)

5.2.11.1) TaqMan GE assay selection

Primer/probes (TaqMan GE assays) for Fluidigm (Fluidigm Corporation, USA) were selected online from the list of TaqMan primer/probes that have been qualified for qPCR (Life Technologies, www.lifetechnologies.com). Criteria in order of priority for primer/probe selection included: 1) Probe sequence for Fluidigm must span the same region and/or be located on the same reference gene sequence as probes used for microarray to confirm similar expression profiles between microarray and Fluidigm. 2) Primer/probe sequence must span exon junctions to ensure amplification of mRNA and not genomic DNA. 3) Recommended primer/probe by Life Technologies. 4) An amplicon length of not more than 140bp. 5) Readily available assays (inventoried). However, not all 4 criteria could be met for all assays at all times so selection was prioritised on all assays that met the first criterion and any of the other 3.

5.2.11.2) cDNA synthesis for optimisation and Fluidigm experiments

RNA was reverse transcribed into cDNA using the superscript II reverse transcriptase kit according to the manufacturer's instructions with Oligo dT_{12-18} primers. Briefly, up to 100ng of RNA was mixed with Oligo dT_{15} primers and dNTP mix. Where necessary, low TE buffer was added to have a volume of 12µl. The mixture was heated for 5mins at 65°C. This was followed by quick chilling on ice and the addition of 4µl of 5X first strand buffer, 2µl of 0.1M DTT, 0.5µl RNase out and 0.5µl distilled water. The reaction was gently mixed and incubated for 2mins at 42°C. Following this incubation period, 1µl of superscript II RT was added and the reaction incubated for another 50mins at 42°C. Finally, the reaction was deactivated by heating at 70°C for 15mins and reaction volume made up to 100µl with low TE buffer.

5.2.11.3) Quality control of cDNA

After cDNA synthesis, a conventional PCR was performed using TaqMan universal PCR master mix to ensure that the cDNA synthesis step was successful. This was done on one cDNA sample from each batch of samples reverse transcribed at the same time. The B2M transcript was amplified as a housekeeping gene. Table 8 below gives a summary of PCR set up, modified from an ABI biosystems protocol.

Table 8: PCR set up for quality control of cDNA

Reaction component	Volume/ well	Final concentration (1X)
TaqMan Universal PCR Master mix	10 µl	1X
TaqMan GE assay	1 µl	1X
cDNA	4 µl	
Low TE buffer	5 µl	
Total volume	20 µl	

Following set up, PCR was performed using a Rotor-Gene^{TM}6000 (Corbett). Table 9 below shows the thermal cycling condition used for amplification, recommended by ABI biosystems.

Table 9: Thermal cycling conditions for quality control of cDNA

Initial setup		40 cycles each	
		Denature	Annealing/Extension
Hold 1	Hold 2	Cycle	
UNG activation 2 mins at 50°C	10 mins at 95°C	15 sec at 95°C	1 min at 60°C

5.2.11.4) Preamplification of cDNA

To overcome issues of low template numbers when distributing cDNA into the 96 wells in the microfluidic chambers so that amplification of all 96 TaqMan GE assays is possible, a preamplification (preamp) of the cDNA was usually done prior to running the samples on the Biomark HD system [329]. The preamp was performed using Fermentas PCR and TaqMan assay master mixes. Firstly, 0.2X TaqMan assay master mix was prepared by combining all TaqMan GE assays and doing a 1:100 dilution with nuclease free water. The preamp setup and thermal cycling conditions are shown in Tables 10 and 11, respectively. Number of optimal preamp cycles was pre-determined as described in section 5.2.11.6. Preamp cDNA was diluted 1:5 in low TE buffer.

Table 10: PCR set up for preamp of cDNA

Reaction component	Volume/ well	Final concentration
Fermentas PCR Master Mix	5 µl	2X
TaqMan assay mix	2.5 µl	0.2X
cDNA	2.5 µl	
Total volume	10 µl	

Table 11: Thermal cycling conditions for preamp of cDNA

	16 cycles each		
	Denature	Annealing/Extension	
Activation	Cycle		Hold
10 mins at 95°C	15 sec at 95°C	4 mins at 60°C	Indefinite at 4°C

5.2.11.5) Assay qualification

A piecewise assay qualification method [329] (Figure 34) was used for qualification of TaqMan GE assays for final analysis. Briefly, a 12-point, two-fold serial dilution of bulk RNA generated from combination of BCG stimulated and unstimulated cells (section 5.2.7) was performed. Each RNA dilution was replicated eight times, reverse transcribed, preamplified and run on the Biomark HD system. Expression threshold (Et =40-Ct) values were plotted against amount of RNA (expressed as a log scale). Parameters assessed were 1)

Linearity of RNA (input RNA is proportional to final signal), 2) Efficiency of TaqMan GE assays (signal doubles with every PCR cycle).

As shown in Figure 34, a step-wise evaluation of ≥5 consecutive RNA dilutions starting from the highest dilution in each replicate was done. The linear least-squares correlation (r^2) for each segment was calculated between the amplification cycles (Et) and the log of the RNA amount. To determine if the relationship between the signal and the amount of RNA was linear, the slope was calculated. A slope of 3.32 ($1/Log_2 10$) indicates a linear relationship and 100% efficient amplification. The efficiency (E) was calculated using the formula: $E=10^{1/slope} - 1$. For assays to qualify, at least one of the segments in any replicate must have an $r^2 \geq 0.97$ and slope between 3.1 - 3.6 (90% - 110% efficiency) [329].

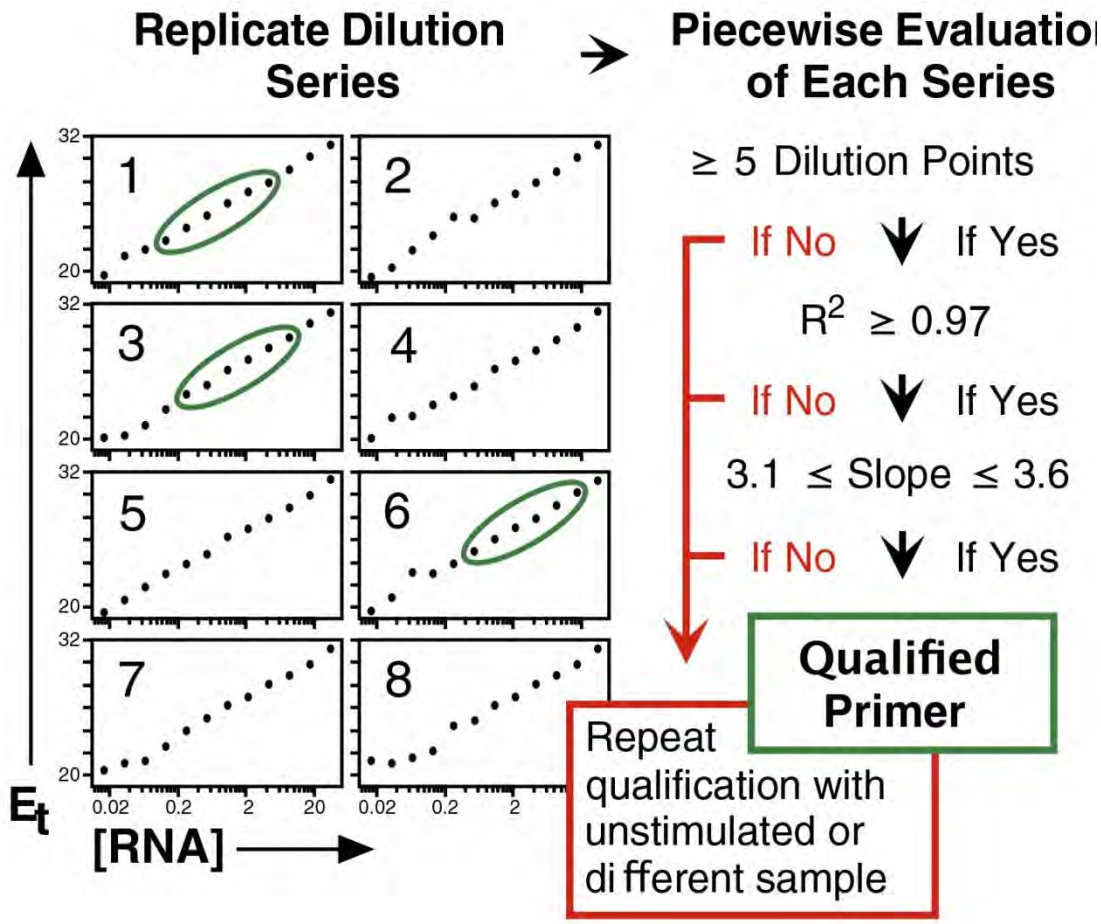

Figure 34: Piecewise assay qualification (Adapted from Dominguez *et al*., 2013).
Assay qualification using 12 serial dilutions of RNA replicated 8 times, searching for segments (≥5 consecutive serial dilutions) with efficient amplification (slope between 3.1 - 3.6) and linearity (r^2≥0.97). Assay was qualified if these criteria were met in at least 1 segment.

The piecewise assay qualification method was used to qualify only TaqMan GE assays for differential BCG responsiveness. Prior to the publication of this method, we had developed an in house assay qualification method, which we used to qualify TaqMan GE assays for risk of TB disease. Briefly, cryopreserved PBMCs generated from blood bank samples were thawed, washed in RPMI 1640 and rested for 6 hours at 10^6 cells in RPMI 1640 containing 10% AB serum and 1% L-glutamine at 37°C and 5% CO_2. After resting, PBMC were then incubated in culture with BCG at an MOI of 0.18 for 12 hours at 37°C and 5% CO_2. Phorbol 12-myristate-13 acetate (PMA, 1µg/mL) and Ionomycin (5µg/mL)

or Lipopolysaccharide (LPS 0.15µg/mL) were used as positive controls while medium alone served as negative control. RNA was extracted as described above and cDNA transcribed as described in section 5.2.11.2. Firstly, a conventional qPCR was performed on each transcript individually on the light cycler using the experimental set up in Table 8 and amplification cycle in Table 9. This was followed by performing a multiplex qPCR on the Fluidigm using the experimental set up in Tables 12 and 13 and amplification cycle in Table 14. Parameters assessed in both conventional and multiplex qPCR were: 1) Difference in ΔCt values between any two or more conditions (to confirm differential expression across stimulation conditions), 2) Log fold change of ΔΔCt > 2 or <0.5 between BCG and/or positive controls over the unstimulated condition. For assays to qualify, they had to meet at least 1 of the above criteria.

5.2.11.6) Optimal experimental conditions for Fluidigm

Bulk RNA generated from combined and non combined cells (section 5.2.7) was reverse transcribed, preamplified and run on the Fluidigm system. The optimal conditions tested were 1) number of preamp cycles (14, 16 and 18 cycles) and 2) preamp cDNA dilution (five 2 fold serial dilutions, no dilution - 1:16 dilution). Optimal experimental conditions were defined by the minimum number of preamp cycles and the maximum dilution of preamp cDNA that resulted in the following outcomes: (1) Optimal Ct values should reflect a wide dynamic range, preferably clustered with a median of all assays at 20-30 cycles, and with as few failed assays as possible; (2) ΔCt calculated using the geometric mean of the housekeeping genes should fluctuate as little as possible across cDNA dilutions.

5.2.12) Fluidigm 96.96 qPCR profiling

After determination of optimal experimental conditions, qPCR was performed using the Fluidigm system according to the manufacturer's instructions. Firstly, the chip was primed by injecting the control line fluid in each of the accumulators and running the prime script (136x) in the integrated fluidic circuit (IFC). This was followed by preparing both assay and sample mixes as shown

in Tables 12 and 13 respectively. 5µl each of both assay and sample mixes were loaded into the various inlets on the primed chip and mixed by running the load mix script (136X) on the IFC controller to mix samples and assays together on the chip. After mixing of samples and assays, the chip was placed in the Biomark instrument and amplification was performed using the standard GE 96X96 thermal cycling conditions recommended by the manufacturer shown in Table 14. Data was captured and analysed using the Fluidigm Real-Time PCR analysis software according to the manufacturer's guidelines.

Table 12: Assay mix

Reagent	Volume/well	Concentration
20X TaqMan GE Assay	3 µl	1X
Assay Loading Reagent (Fluidigm, PN85000736)	3 µl	1X
Total volume	6 µl	10X

Table 13: Sample Mix

Reagent	Volume/well	Concentration
TaqMan Universal Master Mix (ABI, PN 4304437)	3 µl	1X
Sample Loading Reagent (Fluidigm, PN85000735)	0.3 µl	1X
Pre-amplified cDNA	2.7 µl	
Total volume	6 µl	

Table 14: Thermal cycling conditions for 96.96 GE profiling

Thermal Mix			UNG and Hot start		PCR (40 cycles)	
50°C	70°C	25°C	50°C	95°C	95°C	60°C
120 sec	1800 sec	600	120 sec	600 sec	15 sec	60 sec

5.2.13) Data Analysis

5.2.13.1) Flow cytometry analyses

See section 2.2.9

For assessment of differences between cases and controls in stronger and weaker responders separately, a Mann-Whitney U test was performed, using Prism 4.0 (GraphPad Software Inc.).

5.2.13.2) Logistic regression analysis to determine response to BCG vaccination

This analysis was performed in collaboration with William Msemburi (MRC, South Africa) and later with Nkosilesisa Mpofu (University of Cape Town, South Africa). STATA was used for all logistic regression analyses. Firstly, data were tested for normality using the Shapiro Wilk test for normal distribution. For use of parametric test to compare differences between response groups, all data were log transformed. Baseline distributions and summary statistics of individual variables (univariate data exploration) with respect to the two response groups were conducted through the use of histograms, means and confidence intervals. Histograms as well as box and whiskers were used for graphical illustrations of the data distribution.

Following this analysis, univariate and multivariate model building using all T cell outcomes was performed and the model with the best overall correct

classification when benchmarked to the classification by clustering analysis was chosen.

5.2.13.3) qPCR analysis

Real time PCR analysis software on the Rotor-gene 6000 and light cycler machines were used for data analysis. The average Ct of three replicates was used for each sample. For the sample to be included for analysis, the % variation of each replicate from the known standard and the replicate Ct standard deviation must be ≤10% and 0.5 respectively. Quantification was calculated using the Pfaffl relative quantification method [330] and the cut-off for response was considered a fold increase of ≥1.

5.2.13.4) Fluidigm analysis

The Real-Time PCR analysis software on the Fluidigm instrument was used to generate amplification curves, heat maps and Ct values for each reaction according to the recommendations from the manufacturers. The quality threshold was set at 0.65 while Linear Derivative method was used for baseline correction. The Auto Global method was used to determine the Ct threshold. All failed assays (no amplification or quality threshold below 0.65) were excluded from analysis. Data was exported directly from the software into an excel spreadsheet for further analyses.

Raw expression values were pre-processed and quantile normalised as earlier described. The Partial Least Square-Discriminant Analysis (PLS-DA) from Bioconductor's Classification for Microarrays (CMA) package was used to classify stronger and weaker BCG responders as well as cases and controls in stronger BCG responders. This is a two-step procedure which involves dimension reduction and classifier fitting. In the dimension reduction step, a latent component (K) is constructed using PLS by treating the categorical variable (stronger and weaker BCG responders / cases and controls) as a continuous variable by assigning a dummy code (0, 1). Construction of K

component is followed by prediction of response classes (stronger and weaker BCG responders / cases and controls) using LDA.

5.3) Results

5.3.1) Participants

Enrolment of infants was performed as described in Figure 8A from section 2.3.1. Similar to the training set, different groups and numbers of participants were used for different assays reported in this chapter. Infants included into this part of the study were from both training and validation sets. For infants in the training set, on which microarray analyses were performed, a total of 26 were identified as definite TB (microbiological confirmation) and were included as cases and 18 were identified as household controls (see section 2.2.2 for definitions). Because there were not enough culture positive infants to be included in the validation set, a total of 29 identified as probable TB, were assigned as TB cases (see section 2.2.2 for definition). Controls in the validation set were community controls that were never investigated for TB (n=55). However, because not all infant samples were always available for the different analyses, slightly different numbers of participants were included in different analyses in the validation set. Figure 35 below shows the summary of the different participants included for different analyses.

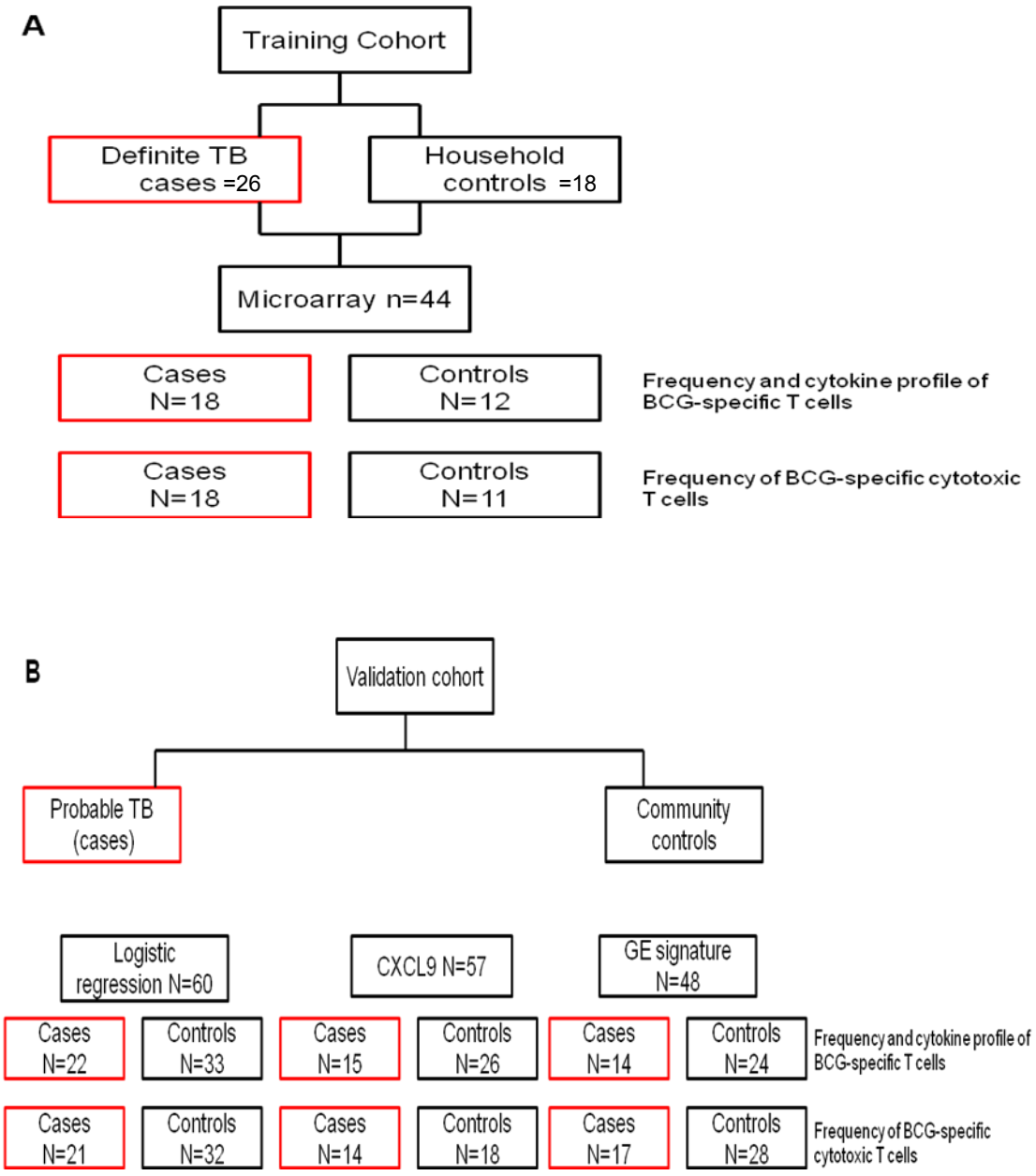

Figure 35: Participant enrolment into the different groups and cohorts of the study. Cases and controls included in the different assays and different cohorts of the study. **A)** Samples on which microarray analysis was performed in the training cohort (n=44). Among these 44 samples, there were 26 cases and 18 household controls. All 18 controls had gene expression data however due to sample availability, not all 18 controls were from the initial 55 controls. **B)** Samples on which logistic regression, CXCL9 and gene expression analyses were performed in the validation cohort. Highlighted in red are cases and black are controls in each of the analyses. Number of samples available for analyses of frequencies of cytokine and cytotoxic BCG-specific T cells in both cohorts.

5.3.2) T cell markers of differential response to BCG

5.3.2.1) Logistic regression model to define differential response to BCG vaccination

We showed in the previous chapter that frequencies of CD4+ T cells expressing the cytokines IL-2, IFN-γ and TNF-α were different between the two clusters in the training set. In addition to this, other T cell functions as well as secreted mediators were associated with clustering in the training set. Clustering in the training set was therefore linked to differential response to BCG vaccination. We sought to investigate if these markers could be used to define differential response to BCG vaccination whenever global gene expression profiles are not available. For this, we developed a logistic regression model to identify the best functional markers for differential response to BCG vaccination in the training that would then be validated in a test set.

Logistic regression will predict the odds of an infant to be a stronger or weaker responder to BCG vaccination, as defined by PBMC gene expression clustering profiles, based on one or more of the functional outcomes measured using other assays.

Firstly, we tested the whole data set for normal distribution. This was to determine which statistical test to use for comparing the two groups of responders to BCG vaccination. Data were not normally distributed, necessitating the use of a non-parametric test for analysis. The Shapiro Wilk test was used to assess normality of the different outcomes (Table 15). This test calculates the probability that the outcomes measured are normally distributed. It is based on the null hypothesis that sample data are not significantly different from the normal population. P-values < 0.05 indicate that data are not normally distributed while p-values >0.05 indicate normally distributed data. The Shapiro Wilk tests statistic and departure from normality are represented by W and V parameters, respectively. For normally distributed data the median value of V should be between 1.2 and 2.4. The Z score is represented by z while

probability for accepting or rejecting the null hypothesis is represented by p>z. Table 11 shows p values of <0.05 (last column).

Table 15: Shaprio Wilk test for normality of numerical values

Variable	Obs	W	V	z	p>z
CD4+ Total IL-2	32	0.83447	5.261	3.433	0.00030
CD4+ Total IFN-γ	32	0.87020	4.126	2.930	0.00169
CD4+ Total TNF-α	32	0.82753	5.482	3.518	0.00022

However, data was log transformed and a normality test performed again. The results showed that all log transformed data were normally distributed (Table 16). We therefore decided to use the log transformed data and parametric analyses for comparison between the two groups of infants. Table 11 shows normality of log transformed values using Shapiro Wilk test (p>0.05).

Table 16: Shapiro Wilk test for normality of log transformed values

Variable	Obs	W	V	z	p>z
Log CD4+ Total IL-2	32	0.96275	1.284	0.349	0.36337
Log CD4+ Total IFN-γ	32	0.95053	1.572	0.936	0.17471
Log CD4+ Total TNF-α	32	0.97744	1.717	-0.687	0.75406

To identify the best T cell markers for differential response to BCG vaccination in the training set, we applied both univariate and multivariate logistic regression model building. We first looked at the performance of each outcome individually and then used combinations of significant outcomes.

Our results showed that the univariate analysis yielded models were statistically significant in correctly classifying differential response to BCG vaccination (Table 17). However, the sensitivity and specificity of these models as well as the overall correct classification when benchmarked to global gene expression profiles, were variable (Table 17). Outcomes significantly different between stronger and weaker responders included frequencies of CD4+ T cells expressing total IFN-γ, total TNF-α and total IL-2, as well as plasma levels of IL-2 and TGF-α.

We went forward to perform multivariate analyses on these outcomes, which showed better sensitivities, specificities as well as overall correct classification (Table 17). However, the probability to correctly classify BCG response using multivariate analyses was not statistically significant ($p>0.05$). Since we needed to accurately classify our infants into the different response groups, we used the model that gave us the best overall classification irrespective of statistical significance. Looking at the overall correct classification into stronger and weaker responders, a model that included CD4+ T cells expressing total IFN-γ, TNF-α and IL-2 gave the best classification (90.63 %) (Table 18). The sensitivity and specificity of this model were 97.74% and 84.62% respectively. Multivariate analysis of analysis of soluble IL-2 and TGF-α did not yield better classification than the univariate models.

Table 17: Univariate logistic regression model for marker of differential response to BCG vaccination in the training cohort

Variable	P-value	Specificity	Sensitivity	Overall Classification	Number of participants
CD4 Total TNF-α	0.024	100.00%	68.4%	81.2%	73
CD4 Total IFN-γ	0.035	53.9%	79.0%	68.8%	73
CD4 Total IL-2	0.035	69.2%	73.9%	71.9%	73
Soluble IL-2	0.029	92.3%	57.9%	71.9%	42
Soluble TGF-α	0.066	97.4%	53.8%	78.1%	42

Table 18: Multivariate logistic regression model for marker of differential response to BCG vaccination in the training cohort

Variable	P-value	Specificity	Sensitivity	Overall Classification	Number of participants
CD4 Total TNF-α, IFN-γ, IL-2	0.558	84.62%	97.74%	90.63%	72
Soluble IL- 2, TGF-α	0.633	84.6%	68.4%	75.0%	43

Using this model, 3 out of the 32 infants used to build the model were misclassified (Table 19). Two out of 13 weaker responders and 1 out of 19 stronger responders were misclassified (Table 19) when benchmarked to the clustering analysis. We therefore used this model to define differential response to BCG vaccination in the validation cohort.

Table 19: Multivariate logistic regression model for marker of differential response to BCG vaccination in the training cohort

		Logistic regression		
		Weaker responders	**Stronger responders**	**Total**
Microarray	**Weaker responders**	**11**	**2**	**13**
	Stronger responders	**1**	**18**	**19**
	Total	**12**	**20**	**32**

5.3.1.2) Validation of T cell correlates of risk of TB in infants with differential response to BCG defined by logistic regression model

To validate correlates of risk of TB disease identified in the training set in an independent cohort of infants, we had to first identify differential responders to BCG vaccination. Using the logistic model, which incorporates the frequencies of CD4+ T cells expressing total IFN-γ, TNF-α and IL-2, we classified infants from the validation cohort into stronger and weaker BCG responders (Figure 36). Our result shows that stronger responders had a significantly higher frequency of total CD4 T cells expressing any combination of IFN-γ, TNF-α and IL-2 compared to weaker responders. Validation of correlates of risk was then undertaken in the two groups of infants separately.

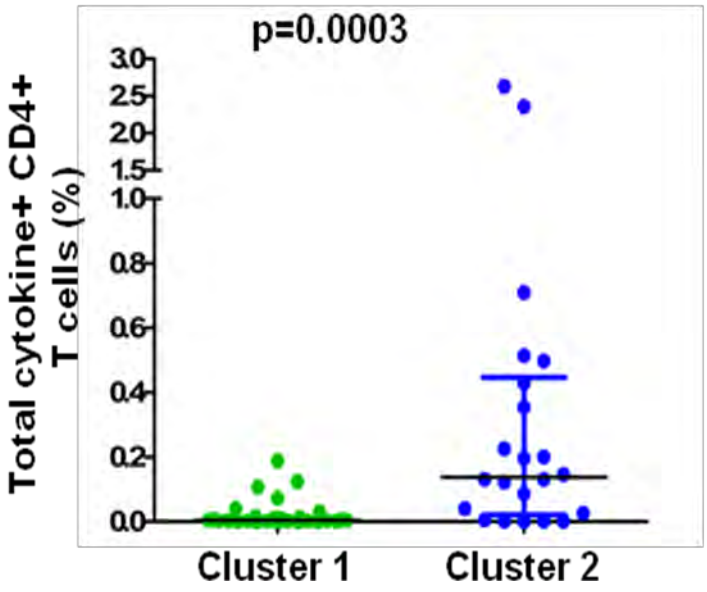

Figure 36: Logistic regression model for differential response to BCG stimulation in validation set.
Whole blood was incubated with BCG for 12 hours and cytokine detected using an intracellular cytokine assay and flow cytometry. Infants were classified into stronger or weaker responders using a logistic regression model incorporating the frequencies of CD4+ T cells expressing total IFN-γ, TNF-α and IL-2. Higher frequencies of CD4+ T cells producing total IFN-γ, TNF-α and IL-2 were observed in stronger (blue, n=22) compared to weaker responders (green, n=33). Mann Whitney U-test was used to assess differences between the two groups. Horizontal line and whiskers on graph denote median and interquartile range, respectively.

To validate T cell correlates of prospective risk of TB disease identified in the training set, we assessed frequencies of BCG-specific CD4+ T cells producing IL-17. These cells were found to be more abundant in cases compared to controls in stronger responders in the training set. We found no differences between cases and controls in stronger responders in the validation set (Figure 37).

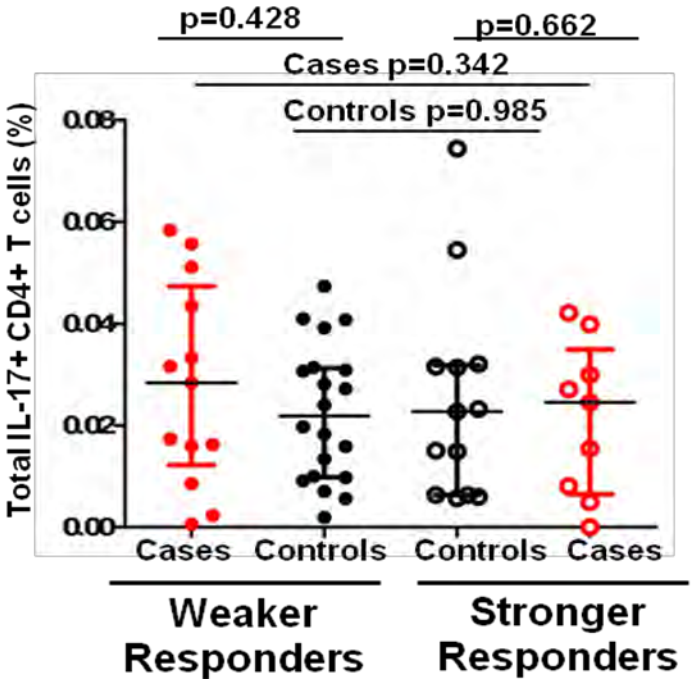

Figure 37: Frequency of BCG-specific CD4+ T cells producing IL-17.
Whole blood was incubated with BCG for 12 hours and cytokine detected using an intracellular cytokine assay and flow cytometry. Logistic regression model incorporating the frequencies of total CD4+ T cells producing IFN-γ, TNF-α and IL-2 was used to define differential response to BCG vaccination. In stronger responders, frequencies of CD4+ cells expressing IL-17 were not different between cases (red) and controls (black). The Mann Whitney test was used to asses differences between two groups. All p values were >0.05. Horizontal line and whiskers on graph denotes median and interquartile range, respectively. Weaker responders, cases n= 13 and controls n=20. Stronger responders, cases n=9 and controls n=13.

Next we sought to validate differences in BCG-specific CD4+ T cell cytotoxic potential observed between cases and controls in differential BCG responders in the training set. In the training set, cases in weaker responders had higher frequencies of BCG-specific CD4+ T cells producing granulysin, granzyme B and perforin together, granulysin and granzyme B together as well as granzyme B and perforin together compared to controls. However, we found the opposite in the validation set. In weaker responders, controls were associated with higher frequencies of BCG specific CD4+ T cells producing granulysin, granzyme B and perforin together (Figure 38A) as well as granzyme B and perforin together (Figure 38C). There was no difference in CD4+ T cells producing granulysin and granzyme B together between cases and controls (Figure 38B).

In stronger responders in the training set, controls showed higher frequencies of CD4+ T cells producing perforin only. There was no difference between cases and controls when this marker was assessed in stronger responders in the validation set (Figure 38D).

In the training set, controls in stronger responders had higher frequencies of BCG-specific CD4+T cells producing granulysin and granzyme B as well as granzymeB and perforin when compared to controls in weaker responders. However, this could not be validated since no difference was observed in the validation between controls in weaker and stronger responders (Figure 38C and D).

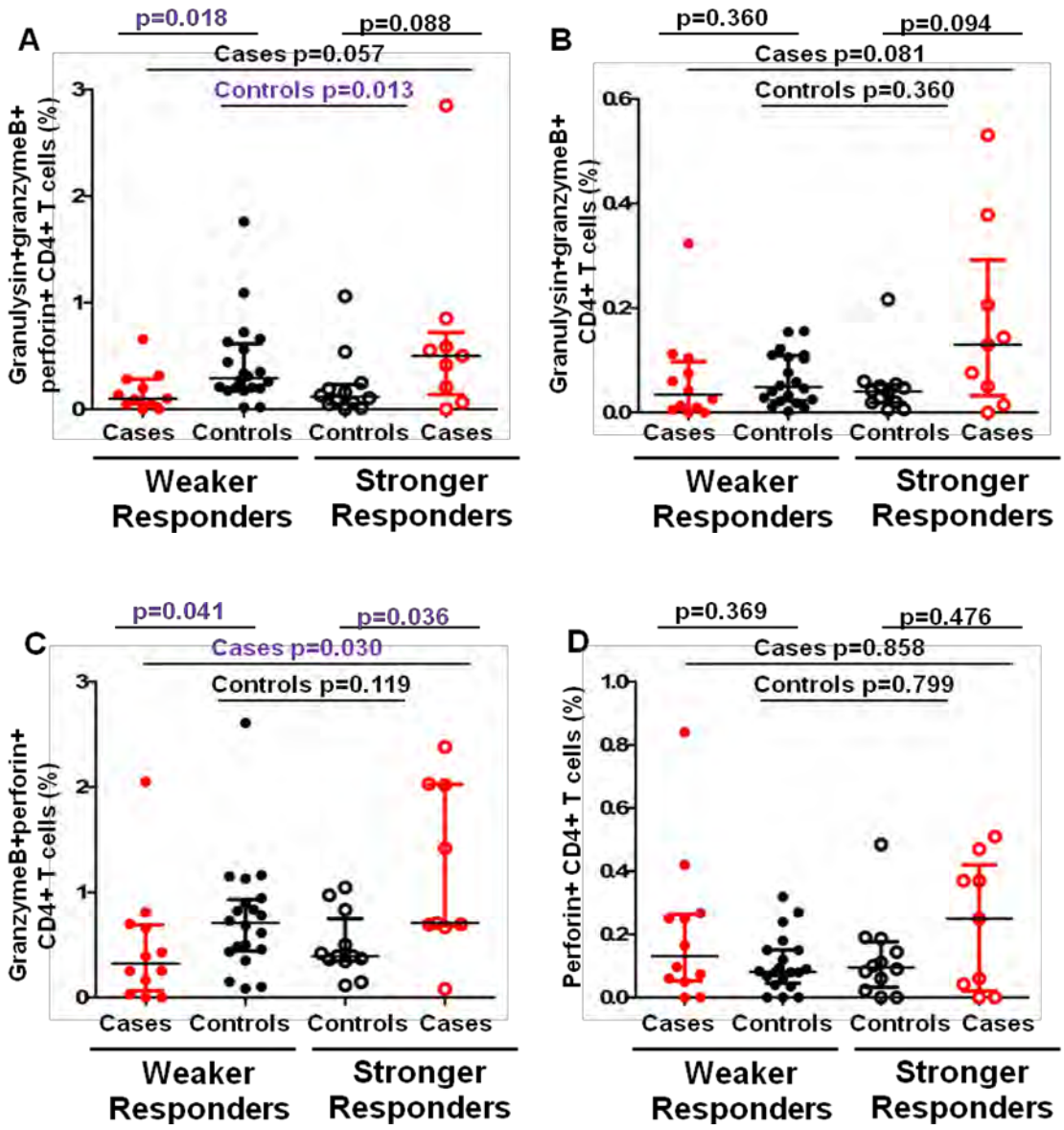

Figure 38: Cytotoxic capacity of BCG-specific CD4+ T cells.
PBMCs were stimulated with BCG or left unstimulated for 3 days and flow cytometry was used to detect BCG-specific CD4+ T cells expressing granzyme B, granulysing and/or perforin. BCG-specific T cells were defined by subtracting the unstimulated values from the BCG stimulated values. Logistic regression model incorporating the frequencies of total CD4+ T cells expressing total IFN-γ, TNF-α and IL-2 was used to define differential response to BCG vaccination. Frequencies of BCG-specific CD4+ T cells expressing **A)** granulysin, granzyme B and perforin together; **B)** granulysin and granzyme B together; **C)** granzyme B and perforin together; **D)** perforin only are shown. The Mann Whitney test was used to assess differences between two groups. Horizontal line and whiskers on graphs denote median and interquartile range, respectively. Only p values <0.05 were considered significant (highlighted in purple). Weaker responders, cases n= 12 and controls n=20. Stronger responders, cases n=9 and controls n=13

Using a logistic regression model, we were able to define differential response to BCG vaccination. However, correlates of risk of TB disease in differential BCG responders identified in the training set could not be validated in the test set using this model. We therefore decided to assess differential response to BCG vaccination using a different marker and further validate correlates of risk of TB in differential BCG responders defined by this new marker.

5.3.2) CXCL9 expression to define differential response to BCG vaccination

IFN-γ was one of the most differentially expressed genes between stronger and weaker BCG responders in the training set (Figure 39A). In addition, an IFN-inducible signature was one of the main pathways differentially expressed in stronger *versus* weaker responders. We therefore hypothesised that measuring IFNγ or IFNγ-induced transcripts could differentiate stronger and weaker BCG responders in the validation set. As earlier mentioned, the frequency of BCG-specific IFN-γ-producing cells is very low, making it difficult to measure the expression of this gene by qPCR. CXCL9 (MIG) is specifically induced by IFN-γ and is expressed in large amounts in myeloid cells, thereby allowing for a more sensitive analysis. This gene was also differentially expressed between stronger and weaker BCG responders (Figure 39B) and was best able to discriminate between the 2 groups with an FDR p-value <0.0005 in the training set.

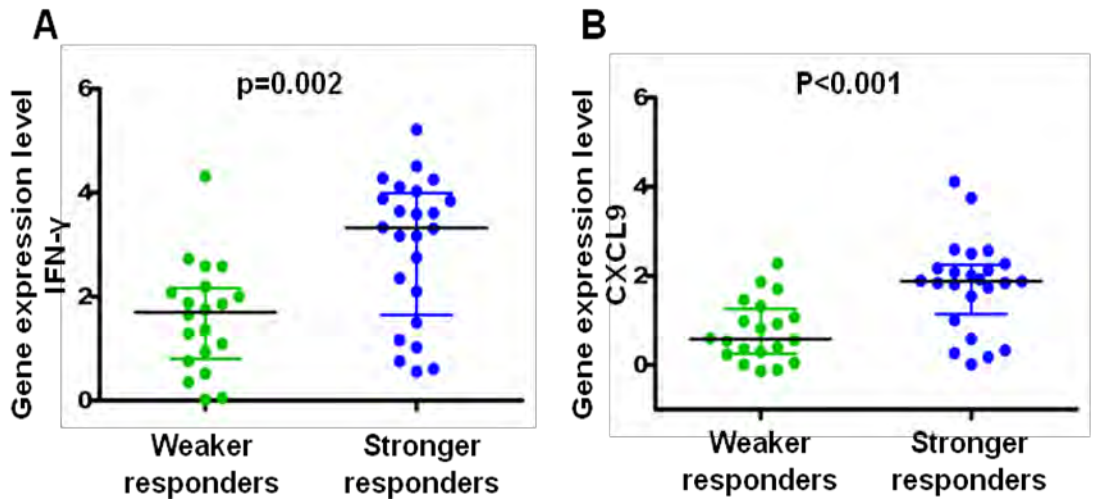

Figure 39: IFN-γ and CXCL9 gene expression between weaker and stronger responders in training set.
PBMCs were stimulated with BCG or not for 12 hours, RNA was extracted, transcribed to cDNA and microarray analysis performed as described in the method section. BCG-UNS data show difference in **A)** IFN-γ and **B)** CXCL9 gene expression between weaker (green, n=20) and stronger (blue, n=24) BCG responders. Horizontal lines and whiskers on graphs show median and interquartile range, respectively. Mann-Whitney test was used to compare differences between the two groups.

We therefore investigated the expression of CXCL9 transcript as a potential marker for differential response to BCG vaccination in the validation set. We measured the expression of this transcript by qPCR and used the Pfaffl method to quantify its expression.

To determine the efficiency of the amplification of CXCL9 and the housekeeping gene HPRT to be used for the quantification of these genes, we amplified both genes using a conventional PCR and run products on a 2% agarose gel. Figure 40A shows the expected band sizes for both CXCL9 (92bp) and HPRT (197bp). After confirmation of specific amplification, PCR bands were excised purified and six 10 fold serial dilutions made to generate a standard curve for each gene. A qPCR was performed to determine the efficiency of amplification of each transcript. Results show that the efficiencies of CXCL9 and HPRT amplification were 100% and 92% respectively (Figure 40B and C). The slopes

for both amplification curves were 3.318 and 3.526 respectively (Figure 40B and C). A linearity (r^2) ≥0.999 was obtained for both genes indicating that the final signal was proportional to input amount of cDNA (Figure 40B and C).

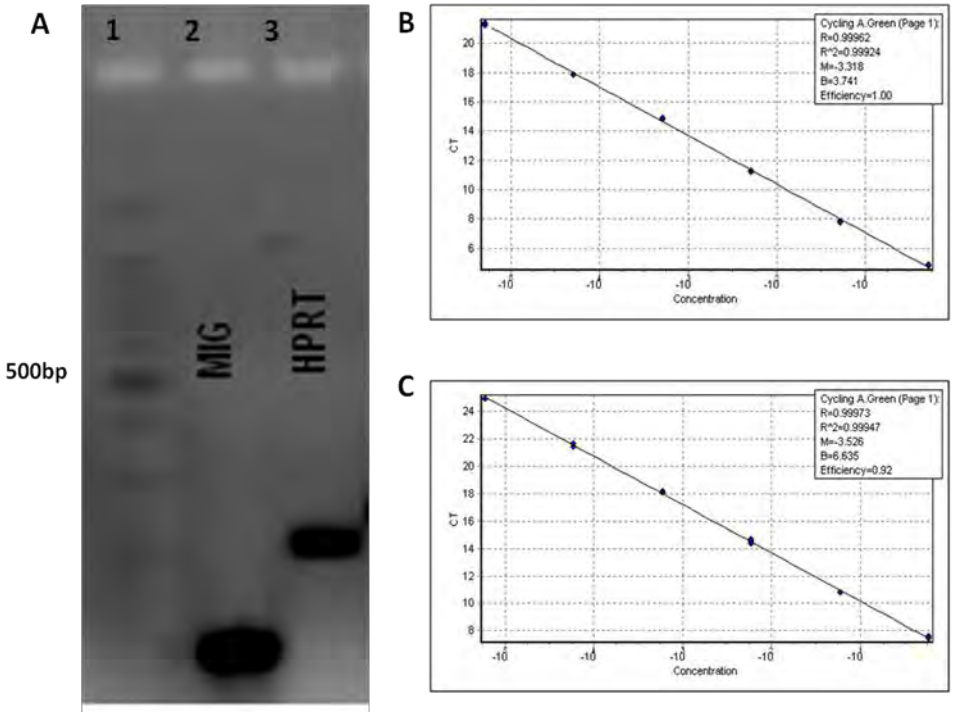

Figure 40: Efficiency of CXCL9 and HPRT amplification.
Ethidium bromide stained agarose gel (2%) showing **A)** the expected band sizes of CXCL9 (MIG) (92bp) and HPRT (197bp) amplification. Standard curve of CXCL9 **B)** and HPRT **C)** showing efficiency of amplification and linearity. Lane 1 was loaded with a 1KB DNA ladder.

The absolute quantification of gene expression using a standard reference curve requires that a good dilution curve for both the gene of interest and reference gene be included in each qPCR run. However, one of the disadvantages of using this method is that it requires extra 18 wells for each gene, significantly reducing the amount of samples that can be analysed in a single experiment. To overcome this, we ran 5 qPCR experiments on 5 different days and calculated the average of the efficiencies across the different days. Table 20 shows an average efficiency of 97.2% and 95.6% for CXCL9 and

HPRT respectively. We next calculated the coefficient of variation (CV) across the different experiments to ensure consistent results across different days. A CV of 6.1% and 3.7% was obtained for CXCL9 and HPRT respectively (Table 21). We therefore used these efficiencies for all our PCR experiments, without including all samples to generate a full standard curve in each run. Nevertheless, we included at least 2 of 6 standards in all 20 PCR runs to monitor for inter-assay variability. Variability ranged between 2.6% - 3.3% for CXCL9 and 1.8% - 2.2% for HPRT (Table 21).

Table 20: Efficiency across different qPCR amplification experiments

	Mean Efficiency	SD	CV
CXCL9	**97.2%**	**5.9**	**6.1%**
HPRT	**95.6%**	**3.5**	**3.7%**

Table 21: Variability of standards across all PCR runs

		Mean Ct value	SD	CV
CXCL9	**Standard 1**	**19.2**	**0.5**	**2.6%**
	Standard 2	**20.9**	**0.7**	**3.3%**
HPRT	**Standard 1**	**16.5**	**0.3**	**1.8%**
	Standard 2	**18.4**	**0.4**	**2.2%**

In infant samples, a strong response to BCG vaccination was defined by a CXCL9 relative expression of ≥1 (calculated according to Pfaffl method above; Figure 41), which means up-regulation of this IFN-inducible gene upon BCG stimulation. As observed in the training set, about half of the infants were classified as stronger responders, according to CXCL9 expression in the validation set.

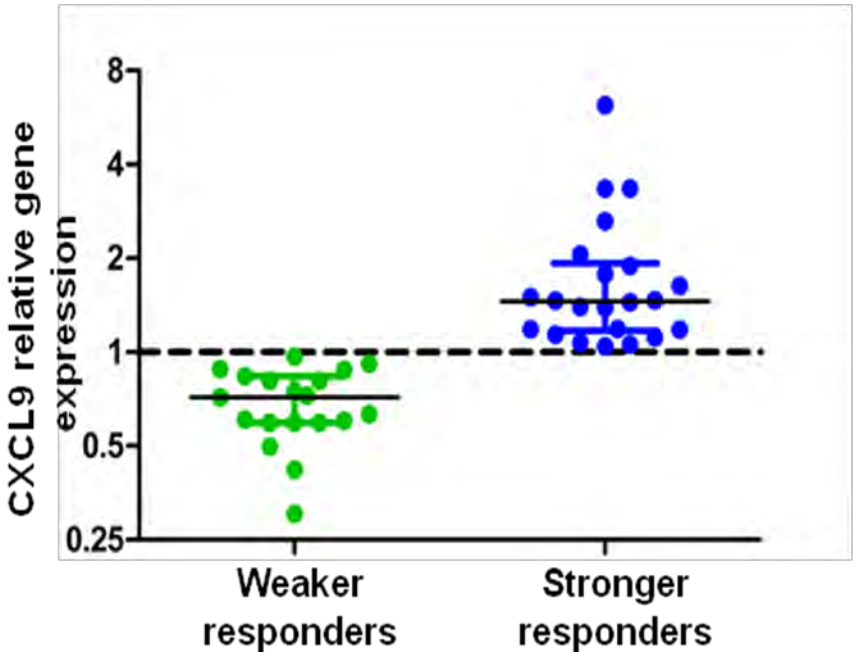

Figure 41: Differential response to BCG stimulation stratified by CXCL9 expression in the validation cohort.
PBMCs were stimulated with BCG or left unstimulated for 12 hours. RNA was extracted and transcribed to cDNA followed by qPCR on CXCL9 and HPRT (reference gene). Pfafll method was used for quantification and a CXCL9 fold change ≥1 was used as cut-off for differential response. Stronger responders (blue, n=22) and weaker responders (green, n=19)

Using this cut-off, 10/24 (sensitivity=42%) weaker responders and 8/17 (specificity=47%) stronger responders were correctly classified when benchmarked to the logistic regression model in the validation set (accuracy=43%) (Table 22). Therefore there was little agreement between these 2 biomarkers of BCG responsiveness.

Table 22: Misclassification rate based on CXCL9 gene expression

		Logistic regression		
		Weaker responders	Stronger responders	Total
CXCL9	Weaker responders	10	9	19
	Stronger responders	14	8	22
	Total	24	17	41

5.3.5) Validation of T cell correlates of risk of TB disease in differential BCG responders defined by CXCL9 gene expression

Following infant categorisation into differential BCG responders based on CXCL9 gene expression in the validation set, we sought to validate potential T cell correlates of risk of TB disease identified in the training set.

In the training set, frequencies of BCG-specific CD4+ T cells expressing IL-17 were higher in cases compared to controls in stronger BCG responders defined by clustering of gene expression profiles (Figure 20). However, there was no difference when this outcome was measured between cases and controls in stronger responders in the validation set defined by CXCL9 gene expression (Figure 42).

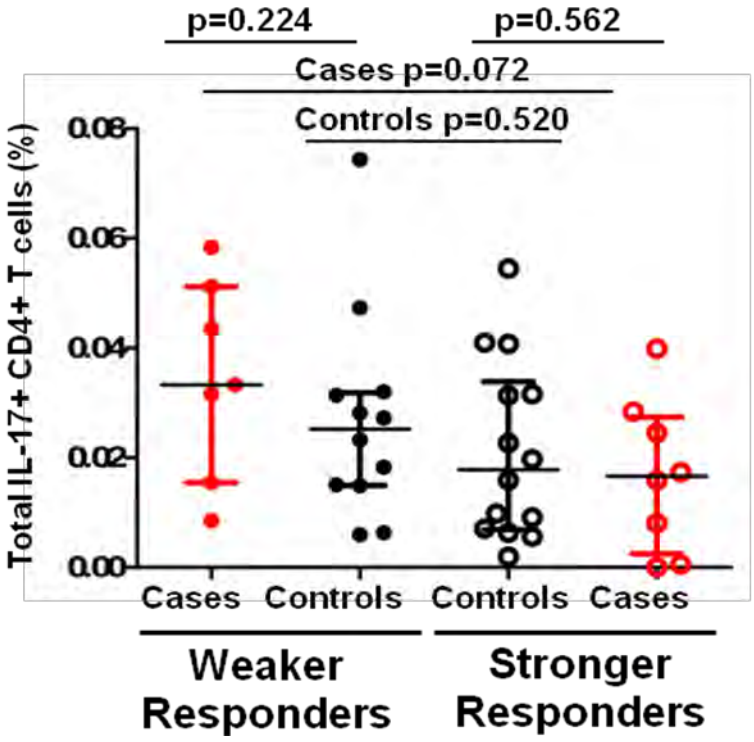

Figure 42: Frequency of BCG-specific CD4+ T cells expressing IL-17.
Whole blood was incubated with BCG for 12 hours and cytokine detected using an intracellular cytokine staining assay and flow cytometry. CXCL9 expression was used to define differential response to BCG vaccination in validation set. Frequencies of total CD4+ T cells expressing IL-17, were not different between cases (red) and controls (black) in stronger and weaker BCG responders. Mann Whitney test was used to asses differences between the two groups and all p values were >0.05. Horizontal lines and whiskers on graphs represent median and interquartile range, respectively. Weaker responders, cases n= 7 and controls n=12. Stronger responders, cases n=8 and controls n=14.

We next assessed the cytotoxic capacity of CD4+ and CD8+ T cells between cases and controls in differential BCG responders defined by CXCL9 gene expression in the validation cohort.

In weaker BCG responders defined by clustering in the training set, CD4+ T cells from cases showed higher combined expression of granulysin, granzyme B and perforin (Figure 21A), granulysin and granzyme B (Figure 21B) as well as granzyme B and perforin, compared to controls (Figure 21C). These differences were not observed in the validation set between cases and controls when

CXCL9 gene expression was used as a marker for differential response to BCG vaccination (Fig 43A-C).

In the training set, controls were associated with increased frequencies of CD4+ T cells producing perforin only (Fig 21D) compared to cases in stronger responders. Again, no difference in CD4+ T cells producing perforin only was observed between cases and controls in stronger BCG responders in the validation cohort (Fig 43D).

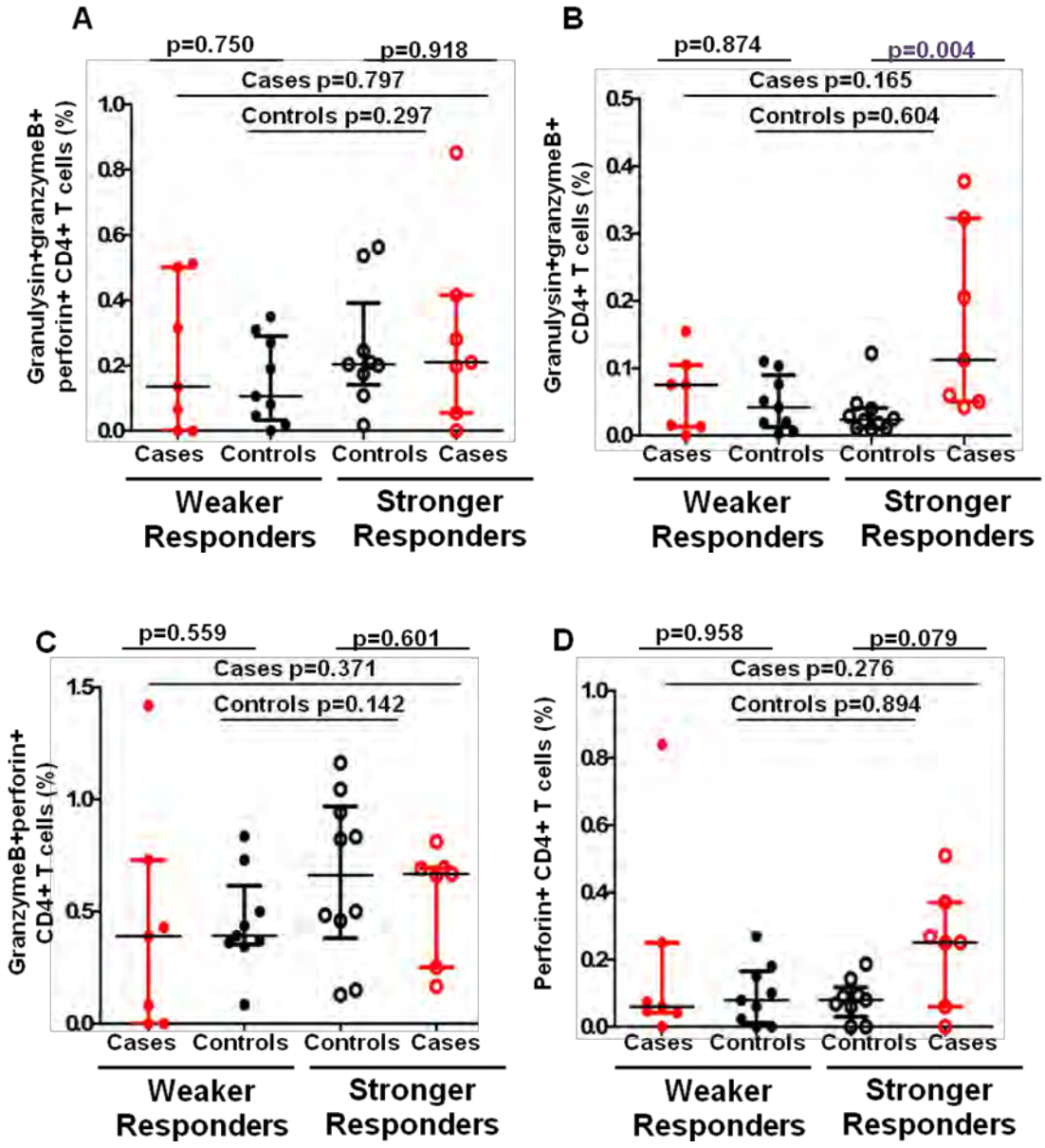

Figure 43: Cytotoxic capacity of BCG-specific CD4+ T cells.
PBMCs were stimulated with BCG or left unstimulated for 3 days and flow cytometry was used to detect BCG-specific CD4+ T cells producing granzyme B, granulysing and/or perforin. BCG-specific T cells were defined by subtracting the unstimulated value from the BCG stimulated value. CXCL9 gene expression was used to define differential response to BCG vaccination in validation set. Frequencies of CD4+ T cells producing **A)** granulysin, granzyme B and perforin together, **B)** granulysin and granzymeB together, **C)** granzyme B and perforin together and **D)** perforin between cases (red) and controls (black) in weaker and stronger BCG responders. Mann Whitney test was used to asses differences between two groups. Only p values <0.05 were considered significant (purple). Horizontal lines and whiskers on graphs denote median and interquartile range, respectively. Weaker responders, cases n= 7 and controls n=9. Stronger responders, cases n=7 and controls n=10.

Taken together, our results show that no T cell correlate of risk of TB disease could be validated when differential response to BCG vaccination was defined by CXCL9 gene expression.

5.3.6) Gene classifiers of differential response to BCG vaccination and risk of TB disease

The measurement of frequencies of BCG-specific T cells and the expression of a single transcript (CXCL9) as markers of differential response to BCG vaccination did not allow validation of correlates of risk of TB disease in BCG vaccinated infants. These two approaches were based on our interpretation of differential BCG responsiveness. We decided to implore an unbiased approach to identify a gene expression signature for differential response to BCG and risk of TB disease. K-means cluster analysis, LIMMA analysis and an empirical Bayes method were used to identify the most differentially expressed genes measured by microarray between stronger and weaker BCG responders as well as between cases and controls in stronger responders in the training set. Two gene classifiers of 89 genes (differential BCG response) and 54 genes (risk of TB disease) were then defined (Tables 23 and 24 respectively).

Table 23: Genes selected for differential responsiveness to BCG vaccination

AADACL1	CD163	EEPD1	IL12B	MPP1	SLC37A2
ACP5	CD33	ENG	IL19	NUP214	SLCO2B1
AIF1	CD36	FBP1	IL1A	PLD3	SNAI3
ALDH1A2	CD69	FCGRT	IL1F9	PLOD1	SORT1
APOC1	CD84	FCN1	IL6	PLXDC2	TLR4
APOE	CEBPA	FLJ22662	INDO	PPARG	TNF
AVPI1	CKB	FLVCR2	IRAK2	PTGER4	TNFRSF21
C12orf59	COTL1	FPR3	KCNK13	PTGS2	ZMIZ2
C1orf162	CSF2	G6PD	LIPA	RGS1	TNFAIP6
C4orf18	CTSB	GJB2	LMNA	RHOBTB3	
CAMK1	CTSC	GPNMB	LYZ	RIPK2	
CARD9	CTSD	GSN	MCOLN2	RPS6KA1	
CASP1	DDEF2	HEXB	MITF	RTN3	
CcL1	DHRS9	HK3	MMP1	SH3BGRL3	
CCL20	DUSP23	HSD3B7	MNDA	SLC25A37	
CCL4L1	EBI3	IL10	MOBKL2B	SLC29A3	

Table 24: Genes selected for risk of TB disease

ACP2	CD14	FGR	INDO	MFSD1	PVRL2
ADORA2A	CD82	FLJ11286	KCNN4	NDP	PVRL2
ALCAM	CLDN15	GCN5L2	KIAA1598	NDP	RNF19B
ALDH3B1	CTSZ	HCK	KIF1B	PCMTD2	S100A8
ASAP1	CYP27A1	HNMT	LRCH4	PILRA	SART2
BMP6	DNAJC3	HNRPH1	LRP10	PILRA	SFRS5
C17ORF56	EBF	IL12B	LTBR	PMS2L5	SLAMF7
SMG1	SPSB3	STMN3	TNFAIP6	TNIP1	UBA7
CCL1	ENO3	IL4I1	LYN	PRKDC	SLC16A3

To assess the performance of these classifiers, a 10-fold cross validation using Bioconductor's PAMR package was performed on samples from the training set. The overall error rate for the classifier of differential response to BCG was 0.03 and risk of TB disease was 0.2.

5.3.7) Assay qualification

The efficiency of TaqMan GE assays is usually tested by the manufacturer for use in qPCR reactions. However, we qualified these assays for use in our system by assessing their ability to detect difference in gene expression between different conditions using an in house qualification system, before publication of a primer qualification procedure [329]. PBMCs were stimulated with BCG, LPS, PMA and Ionomycin or left unstimulated for 12 hours. RNA was

extracted, transcribed to cDNA and a conventional qPCR performed for each transcript. For assays to qualify, the difference in the ΔCt values between unstimulated and stimulated samples had to be statistically significant ($p<0.05$) and/or the fold change of the ΔΔCt had to be ≥2 or ≤0.5. Figure 44A (CTSZ) and B (CD82) show representative assays that qualified using statistical significance. Figure 44C shows a summary of all assays that qualified using the two parameters. The left y-axis shows ΔCt p-values between the stimulation conditions. Assays that qualified had a p-value of <0.05 (below the black dotted line) (Figure 44C). The right y-axis shows the fold change between the unstimulated and any of the stimulated conditions denoted as ΔΔCt values. Assays that qualified had a ΔΔCt value of either ≥2 or ≤0.5 (above 2 or below 0.5 denoted by the green dotted lines respectively) (Figure 44C). Based on these two parameters, a total of 65 of 73 passed qualification.

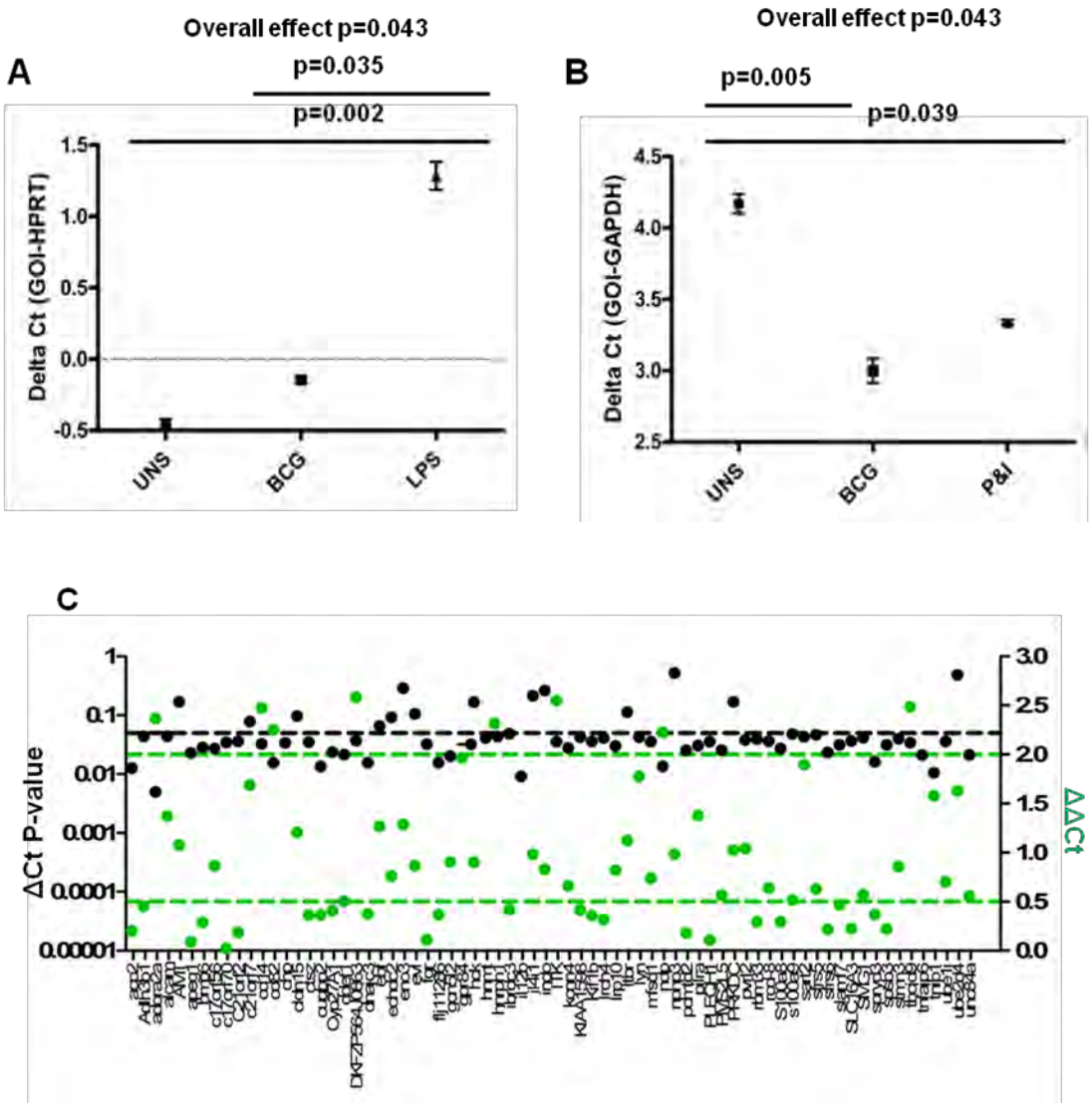

Figure 44: Qualification of TaqMan GE assays for risk of TB disease by conventional qPCR.

PBMCs were stimulated with BCG, LPS, PMA and Ionomycin (P&I) or left unstimulated (UNS) for 12hrs. RNA was extracted, transcribed to cDNA and a conventional qPCR performed. **A)** CTSZ and **B)** CD82 show examples of assays that qualified using the statistical significant method. ANOVA was used to assess differences between the three conditions and a student-t-test used to compare difference between any two conditions. Data points represent mean and SD of three replicates. **C)** Summary of all assays that qualified using any of the methods. Left y-axis denotes p values obtained from ΔCt between the unstimulated and any stimulated condition (black circles) and cut-off for qualification denoted by black dashed line ($p<0.05$). Right y-axis denotes fold change between the unstimulated and any stimulated condition as ΔΔCt (green circles) and cut-off for qualification denoted by green dashed lines (≥2 and ≤0.5). X-axis shows all genes tested.

However, the Fluidigm is significantly different from these standard qPCR reactions in that it involves the use of smaller volumes of reactions and different conditions. We therefore further qualified these assays by performing a multiplex qPCR using all transcripts on the same samples used for the conventional qPCR and assessed the same parameters. Figure 45 shows assessment of ΔCt p-value (left y-axis) and ΔΔCt (right y-axis) for all transcripts. For assays to qualify, they had to be either below the black line and/or not between the green lines (Figure 45). A total of 54 assays passed using this method. For final inclusion for analysis, priority was given to assays that qualified using this method.

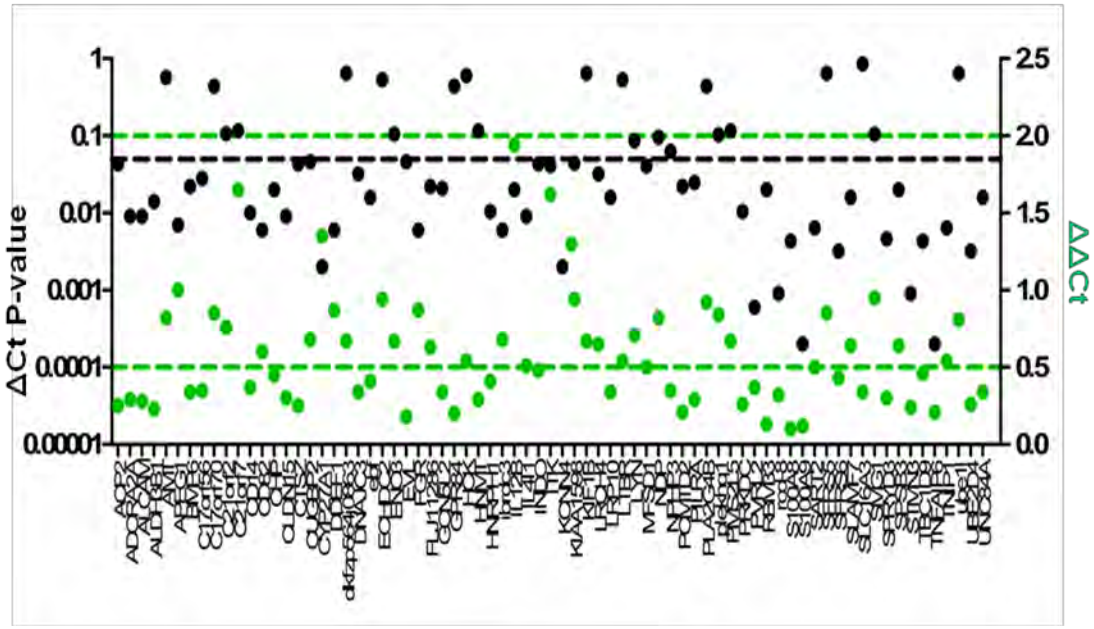

Figure 45: Qualification of TaqMan GE assays for risk of TB disease by Fluidigm.
PBMCs were stimulated with BCG, LPS, PMA and Ionomycin (P&I) or left unstimulated (UNS) for 12hrs. RNA was extracted, transcribed to cDNA and Fluidigm run performed on all transcripts. Left y-axis denotes p values obtained from ΔCt between the unstimulated and any stimulated condition (black circles) and cut-off for qualification denoted by black dashed line ($p<0.05$). Right y-axis denotes fold change between the unstimulated and any stimulated condition as ΔΔCt (green circles) and cut-off for qualification denoted by green dashed lines (≥2 and ≤0.5). X-axis shows all genes tested.

To determine optimal cDNA dilution to be used for Fluidigm, a 2 fold serial dilution of the cDNA was done eight times starting from the neat (undiluted cDNA) to 1:128 dilution. We then compared median ΔCt of all 96 genes across the different cDNA dilutions. Theoretically, the median ΔCt should not fluctuate across different cDNA dilutions. Our results showed little or no fluctuation between the median ΔCt across the different cDNA dilutions (Figure 46).

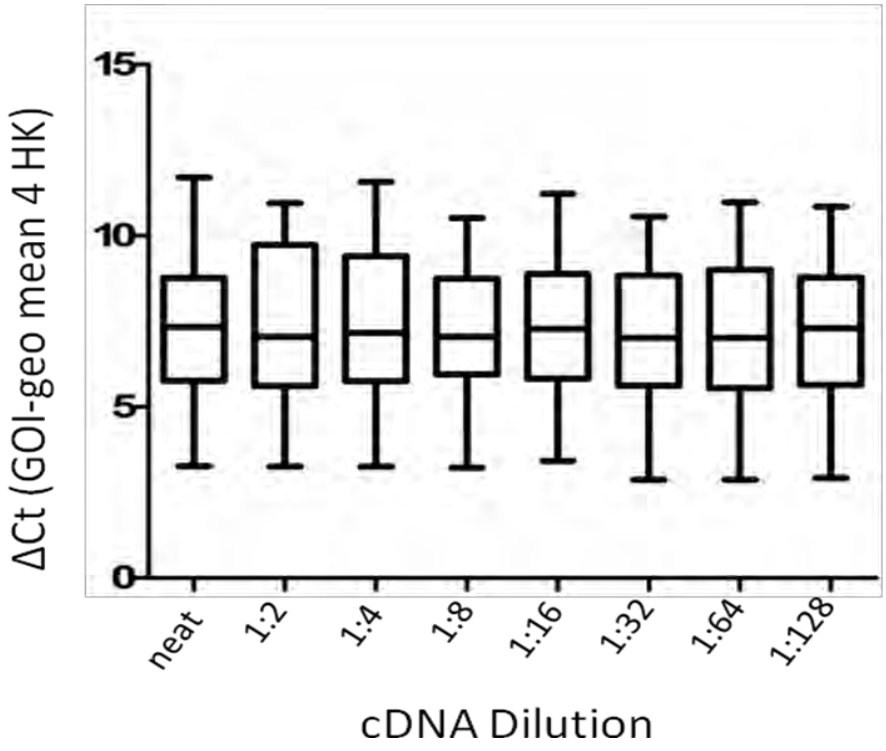

Figure 46: cDNA dilution series after preamplification.
Eight 2-fold serial dilutions of preamplified cDNA. Genes were normalized over the geometric mean of 4 housekeeping genes (B2M, HPRT, GAPDH, HBB) and ΔCt showed little fluctuation. Boxes represent the interquartile range, whiskers represent the maximum and minimum values and the horizontal lines in the boxes represent the median

In order to avoid too much or little dilution of cDNA to be able to detect specific amplification, we finally chose the 1:16 dilution. Assays that qualified using both platforms were included for analysis. We qualified 74% (54/73) of TaqMan GE assays to assess risk of TB disease.

The inhouse qualification system was used to qualify the gene signature for risk of TB disease. For the signature of differential response to BCG vaccination, a piecewise qualification method was used to assess the efficiency of these probes [329]. A wide range of RNA concentrations starting from 50ng, generated from a mixture of stimulated and unstimulated cells was used because transcript abundance and/or expression upon stimulation was not known. A total of 12 dilutions of RNA and 8 replicates of each dilution were run for assay qualification. For assays to qualify, at least 1 piecewise segment must have a linearity of ≥0.97 and efficiency between 90-110% (slope between 3.1 and 3.6). Figure 47 shows a representative example of primer qualification.

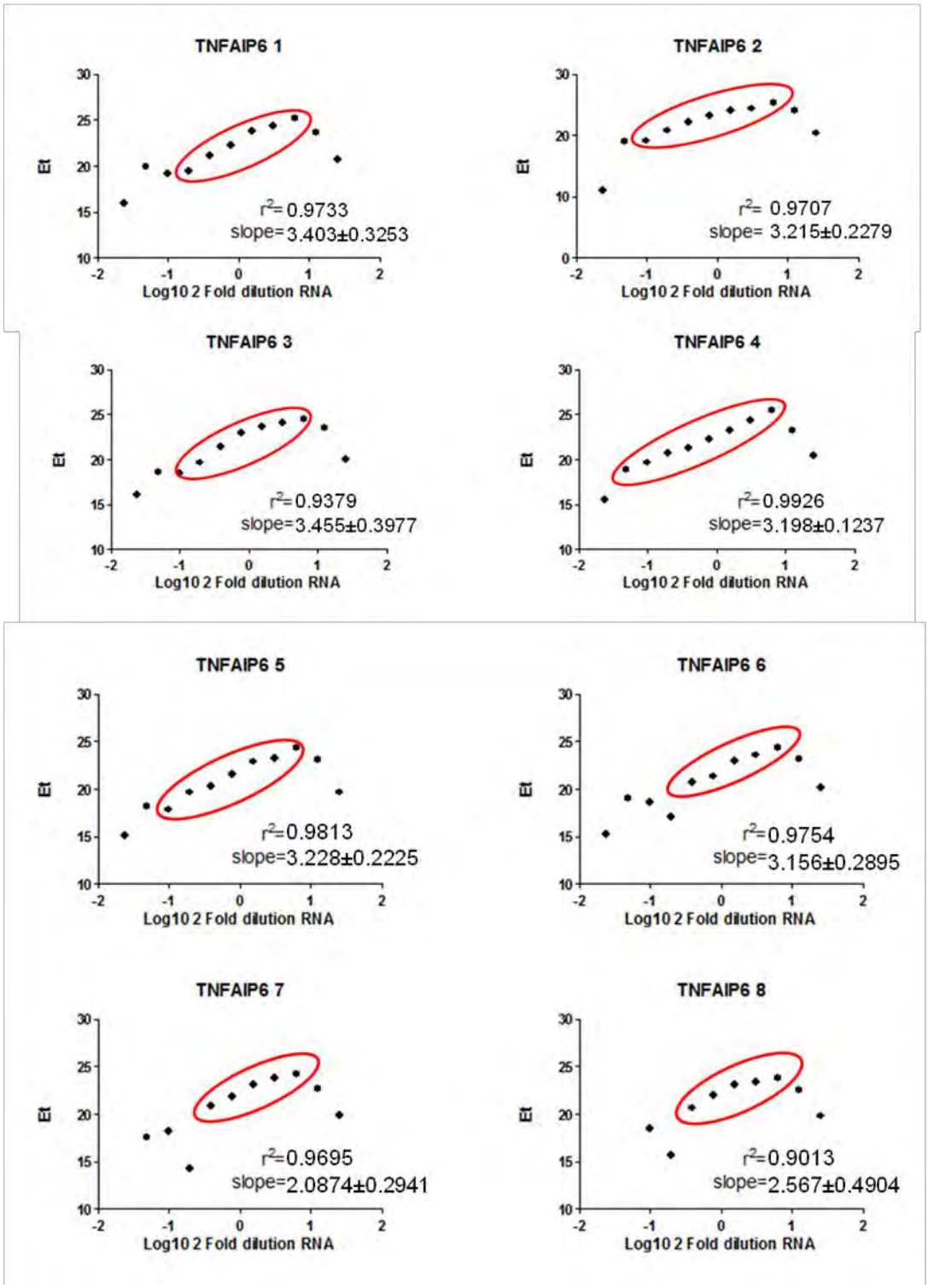

Figure 47: Piecewise method for assay qualification.
Representative primer/probe for qualification. 12 serial dilutions of bulk RNA (combined from stimulated and unstimulated cells) were run on the Fluidigm system in 8 replicates. Primer/probe with any 5 or more consecutive RNA dilutions in any of the replicates that has an r^2 =0.97 and slope=3.1-3.6 qualified for inclusion in analysis. Regions with red ring denote the best linearity for each replicate. Expression threshold (Et) =40 – Ct.

Figure 48 summarises qualification results for all primer/probe sets tested with this method. The left y-axis denotes the slope of the amplifiction curve (red closed circles) and should be between 3.1-3.6 (red dashed lines). The right y-axis denotes the linearity of the amplification R^2 (blue open circles) and the cut-off for qualification is shown by the blue dashed line ($R^2 \geq 0.97$). For assays to qualify, they must be between the red lines and on/above the blue line (Figure 48). There was no transcript amplification obserevd in any sample using 3 primer/probes. Using this method, we qualified 84% (75/89) of the primer/probes used to assess differential responsiveness to BCG vaccination

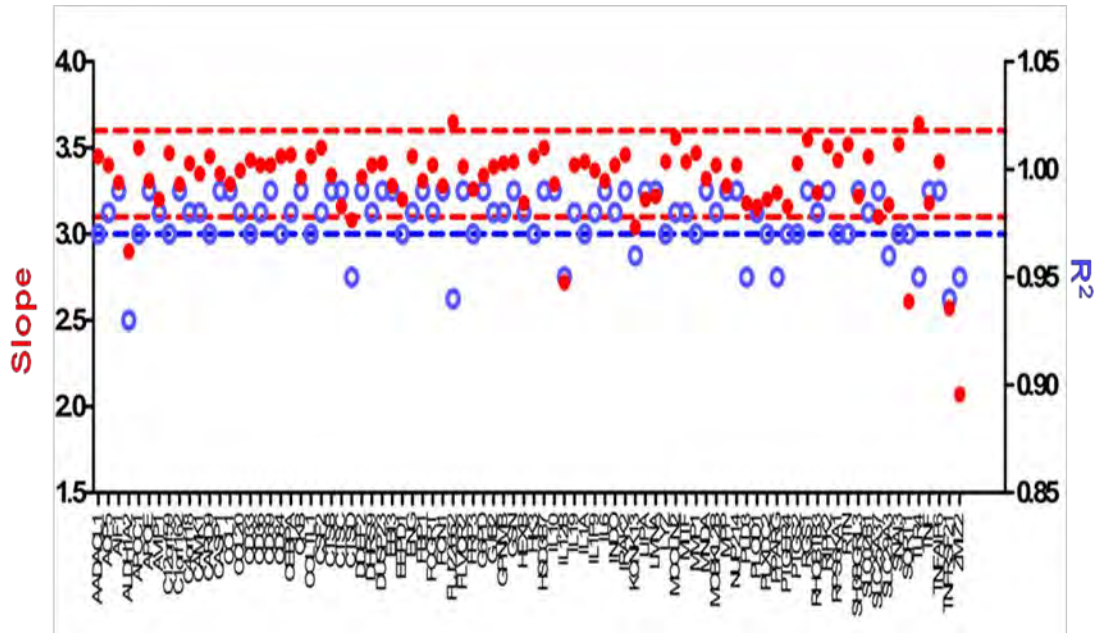

Figure 48: Qualification of TaqMan GE assays for differential response to BCG vaccination by Fluidigm.
Twelve serial dilutions of bulk RNA (combined from stimulated and unstimulated cells) were run on the Fluidigm system in 8 replicates using all primer-probe sets. The left y-axis shows the slope of the curve (red circles) and the acceptable range (3.1-3.6) denoted by red dashed lines. Right y-axis shows linearity (R^2, blue open circles) and cut-off ≥0.97 denoted by blue dashed lines. X-axis shows all genes tested.

5.3.8) Optimal pre-amplification and cDNA dilution

In the Biomark HD system each sample is split and distributed to 96 microfluidic PCR chambers. For rare transcripts to be evenly distributed across the 96

chambers, at least 4096 transcripts of each sample are needed requiring at least 12 cycles of pre-amplification if the original cDNA comprises of only 1 transcript [329]. We sought to determine how many cycles of pre-amplification and which preamplifed cDNA dilution will allow amplification of most gene transcripts (least failed assays), widest dynamic range of Ct values (clustered preferably between 20-30 Cts) and lowest variation of the ΔCt calculated using the geometric mean of the housekeeper genes.

We investigated three different numbers of amplification cycles starting with different amounts of RNA and five two-fold serial dilutions of the pre-amplified cDNA. We observed amplification of most transcripts using either of 14, 16 and 18 pre-amplification cycles with the different starting amounts of RNA (Figure 49). However, more assays failed with higher amount of RNA. Subsequent analyses were therefore performed with starting amounts of RNA between 0.195ng and 6.25ng.

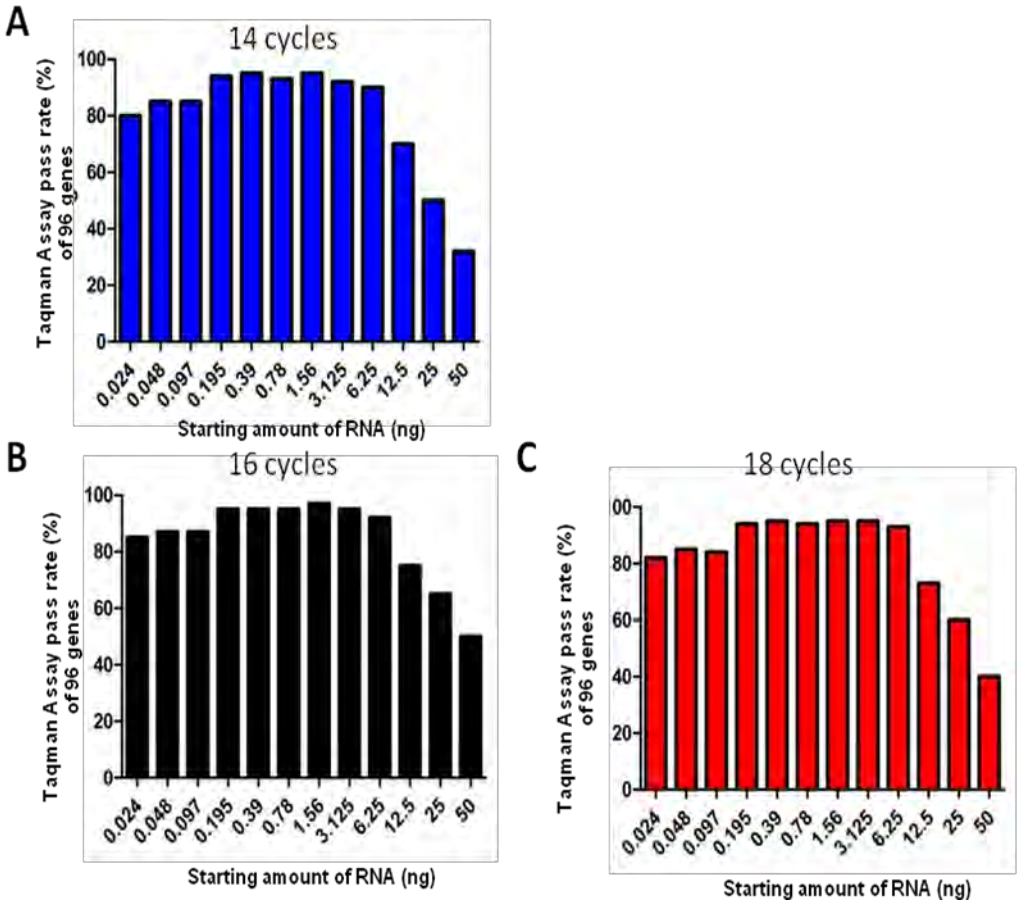

Figure 49: Percentage pass rate of TaqMan assays.
Twelve serial dilutions of bulk RNA (combined from stimulated and unstimulated cells) were transcribed to cDNA, preamplified and run on the Fluidigm system. Number of preamplification cycles shown in **A)** 14 (blue), **B)**16 (black) or **C)** 18 (red) .

We next calculated the percentage pass rate of all primer/probes for each preamplification cycle. This was done by taking the average pass rate of RNA dilutions between 0.195ng and 6.25ng for each preamplification cycle. Results show that 16 cycles of preamplification yielded the highest primer/probe pass rate (90%) compared to 14 (80%) and 18 (83%) cycles (Figure 50). We therefore chose the 16 cycles of preamplification to investigate the optimal cDNA dilutions.

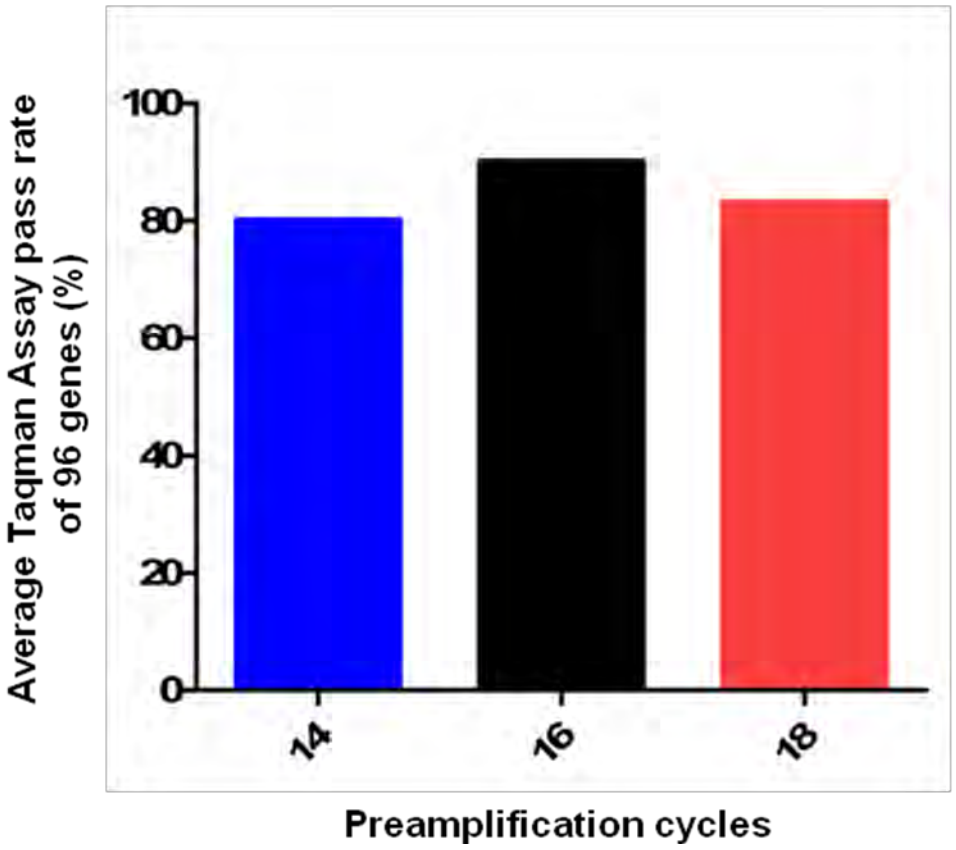

Figure 50: TaqMan GE pass rate with different preamplification cycles.
Average TaqMan GE assay pass rate with different starting amount of RNA (6.25ng-0.195ng) with different preamplification cycles. Blue (14 cycles), Black (15 cycles) and Red (18 cycles).

After 16 cycles of preamplification, a 1:5 dilution of the cDNA was made in low TE buffer. Starting from this dilution (neat cDNA), 4 other 2-fold serial dilutions were made with the highest dilution being 1:16. Calculating the ΔCt of the different cDNA dilutions showed no fluctuations in the median (Figure 51).

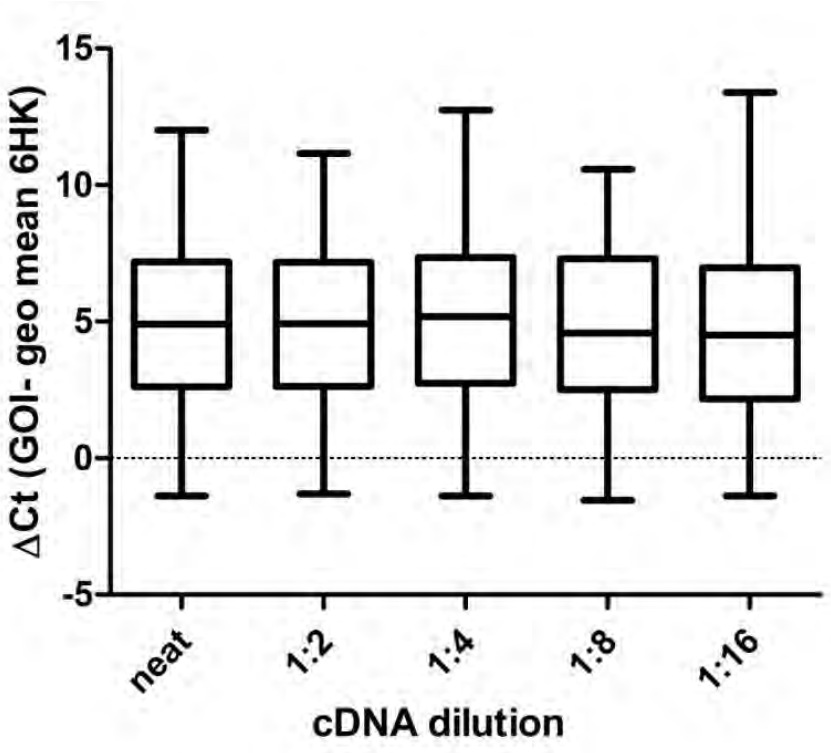

Figure 51: cDNA dilution series after 16 cycles of preamplification.
Five 2-fold dilutions of cDNA after 16 cycles of preamplification. Genes were normalized with the geometric mean of 6 housekeeping genes (B2M, HPRT, GAPDH, RPS13, RPS20 and RPL27) and ΔCt shows little fluctuation. Boxes represent the interquartile range, whiskers represent the maximum and minimum values and the horizontal lines in the boxes represent the median..

Although all dilutions showed no fluctuations in the medians, we chose the 1:16 dilution of the preamplified cDNA to ensure dilution of any residual primer/probe used for preamplification in order to detect specific amplification.

In conclusion, we chose to use 16 cycles of pre-amplification and 1:16 dilution of the preamplified cDNA for Fluidigm experiments.

5.3.9) Confirmation of same direction of gene expression profiles between microarray and the fluidigm

Following assay qualification and obtaining the optimal experimental conditions, we wanted to confirm if genes selected for differential response to BCG

vaccination as well as risk of developing TB disease have the same direction of gene expression when measured by microarray and Fluidigm in the training set. For this, we had to use RNA samples from the training set on which microarray experiments were performed. No PBMC samples were left from these participants therefore we used available RNA samples previously generated for microarray analysis. In microarray experiments, RNA is usually amplified (RNA transcribed to cDNA and back to RNA) to increase its yield. At the time of this analysis, we could include original amplified RNA for a subset of samples (n=12). For the other samples (n=15), we used non-amplified RNA. Whenever possible, we ran both amplified and non-amplified RNA from the same participant (n=11), to estimate the influence of RNA amplification on gene expression profiles. Both amplified RNA and non amplified RNA from samples in the training set were thawed, reverse transcribed to cDNA and samples run on the Fluidigm system using the experimental conditions described above.

Before running samples on the Fluidigm, we determined the RNA yield and quality generated from samples in both the training and validation sets. RNA quality is a very critical and important component in gene expression experiments. Following RNA extraction, samples were measured using an ND 2000 spectrophotometer (Nanodrop^{TM}) to determine the concentration and the purity, as a 260/280 ratio read out. Our results showed a median purity of 1.89 and 1.87 for training and validation sets respectively (Figure 52A). More than 95% of all samples in both training and validation sets were within the acceptable RNA purity range of 1.8-2.0 (Figure 52A). The median RNA yield was 27.3ng/µl and 27.9ng/µl for training and validation samples respectively (Figure 52B).

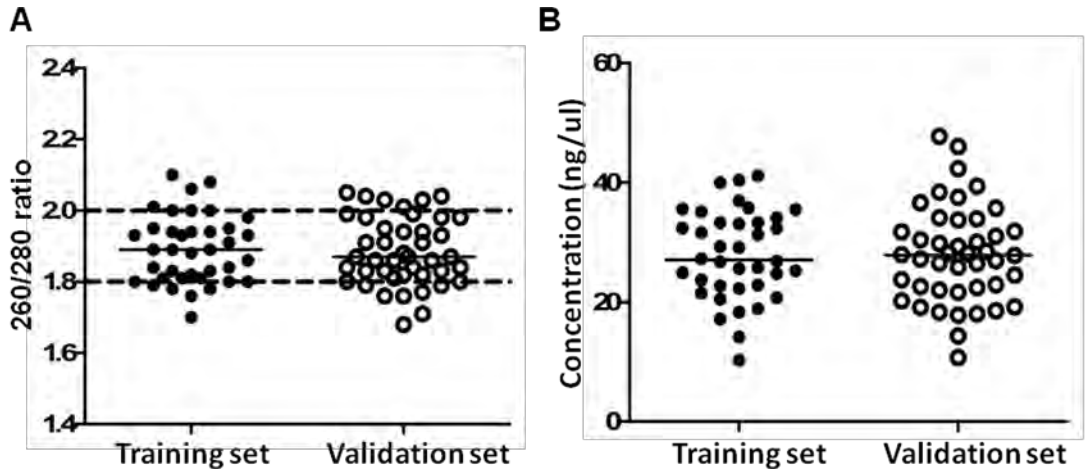

Figure 52: Quality control of RNA.
Prior to running samples on the Fluidigm, RNA quality and concentration from both training and validation samples were determined on the nanodrop. **A)** Quality denoted by 260/280 ratio with the acceptable range denoted by black dashed lines (1.8-2.0). **B)** Concentration measured in ng/µl.

5.3.9.1) Data Normalisation

Normalisation of qPCR data is the first and one of the most critical steps in data analysis. Housekeeping genes are often used to normalise qPCR data because of the assumption that their expression across different samples and conditions does not change. Quantile normalisation is another method used for data normalisation and it assumes that all samples have similar levels of transcript abundance. This method is mostly used for normalisation of microarray data and it works by transforming all the arrays to have a common distribution of intensities through averaging the quantiles across each sample. We sought to determine which of these two normalisation methods will be most appropriate for use in our data analysis.

Firstly we chose housekeeping genes based on their universal use (HPRT, GAPDH, G6PD, B2M, HBB) and from published literature [331] (OAZI, RPL27, RPS13 and RPS20). We then used a Mann Whitney test to compare the median expression of these genes between the unstimulated and BCG conditions in the training set. Genes with no differential expression between the two conditions

were retained as housekeeping genes. Results show that G6PD was differentially expressed between the two conditions ($p<0.001$) and was excluded. However, we only had space for 7 housekeeping genes and so we needed to exclude 1 more. OAZ1 was excluded because it was closest to significance of the remaining genes. Therefore of the 9 genes assessed, two were excluded (G6PD and OAZI) (Figure 53).

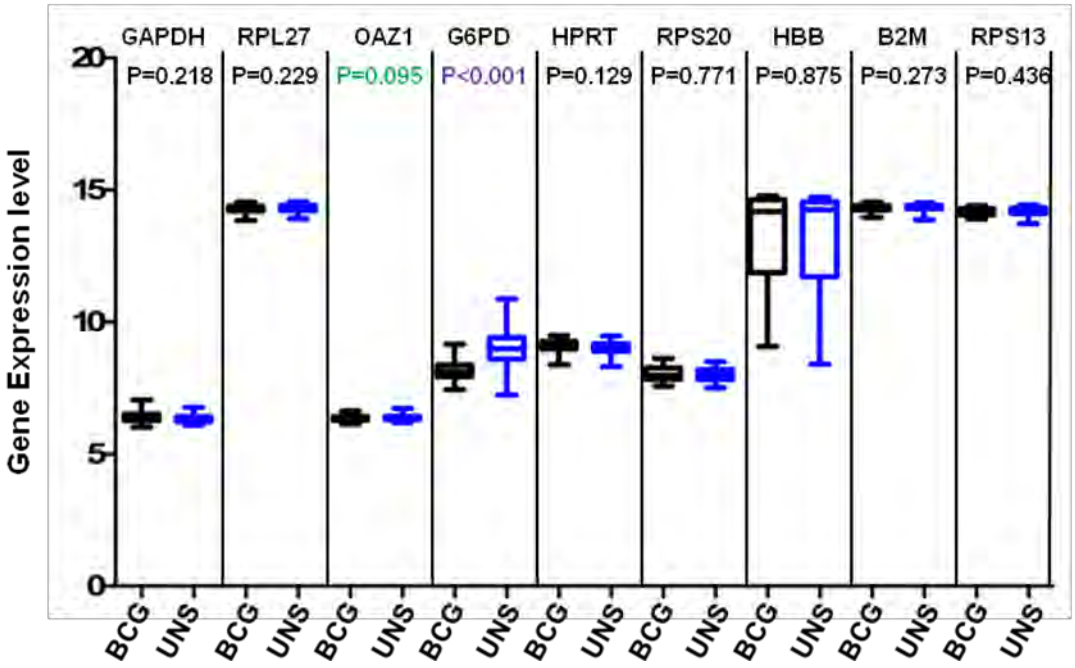

Figure 53: Selection of housekeeping genes.
Median gene expression of housekeeping genes in unstimulated (UNS) and BCG stimulated PBMCs. Mann Whitney test was used to compare the two conditions. P-values highlighted in purple and green are genes that were excluded as housekeeping genes.

We next compared different normalisation methods to use for data analysis. We observed that quantile normalisation yielded the least variability in normalisation of our data compared to using the geometric mean of several housekeeping genes for normalisation (Figure 54). The average CV with quantile normalisation was 7.35% while normalising with the geometric mean of 2, 3 or 5

housekeeping genes yielded a %CV of more than 15% (Figure 54). We also noted that normalising the data with the raw intensities of all gene expression levels also resulted in higher variability (13.65%) compared to quantile normalisation (Figure 54).

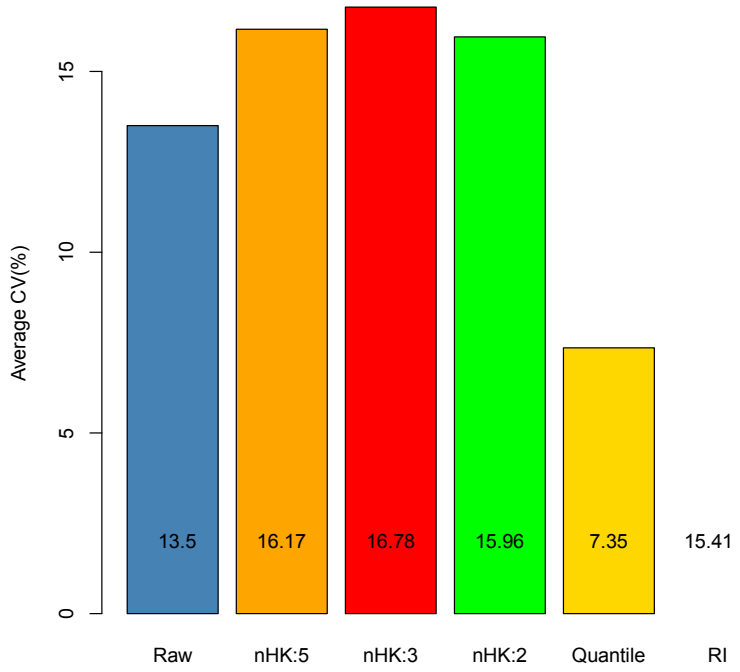

Figure 54: Normalisation of Fluidigm qRT-PCR data.
Different normalisation techniques tested for data normalisation. There was less variation with quantile normalisation (yellow bar) (7.35%) compared to the use of the geometric mean of 2 (green), 3 (red) and 5 (orange) housekeeping genes.

Based on these data, quantile normalisation was used for all subsequent analyses.

5.3.9.2) Comparison between amplified and non-amplified RNA

Because we did not know how amplification of RNA would affect gene expression profiles compared to non amplified RNA, we compared the gene

expression profiles between cDNA generated from amplified RNA and non amplified RNA to see if these samples could be analysed together. Following background subtraction (BCG-UNS), the median gene expression of all transcripts was determined for both RNA types. The medians and interquartile ranges were plotted for each RNA type and samples were excluded if the median gene expression across RNA types was different. A total of 5 samples were excluded from analysis based on this criterion (samples highlighted in red) (Figure 55).

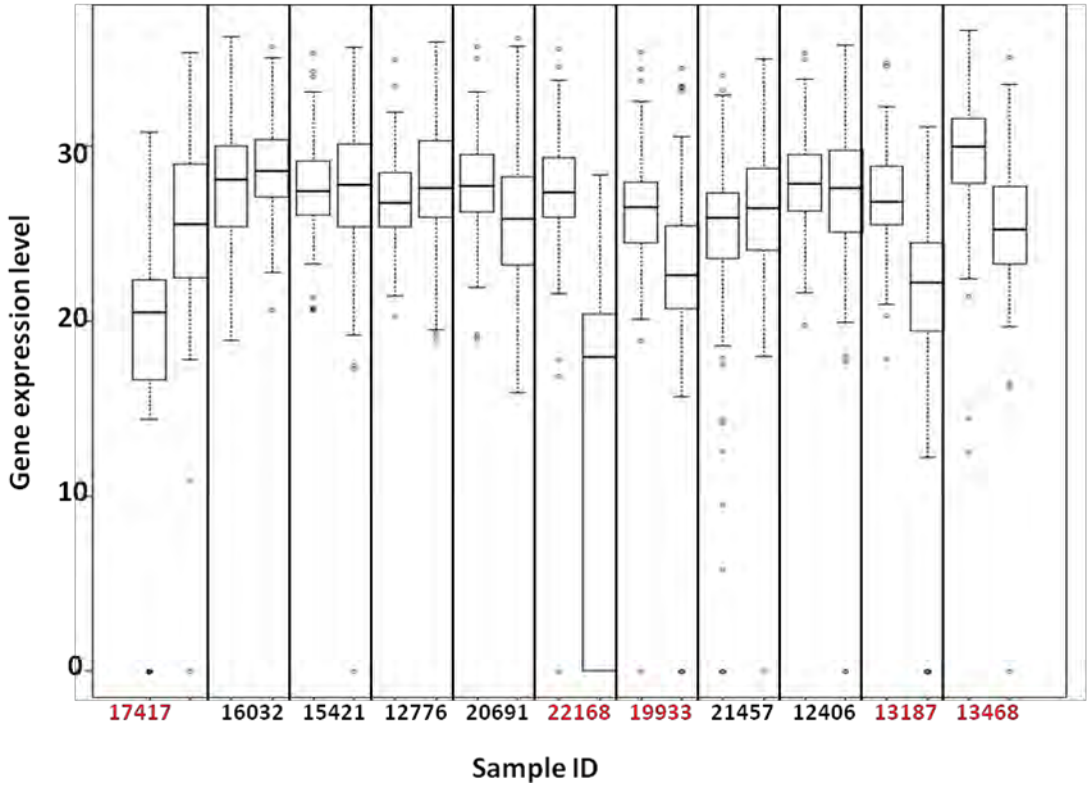

Figure 55: Comparison between amplified and non amplified RNA.
PBMCs were stimulated with BCG or not for 12 hours and RNA extracted. RNA was either amplified (amplified RNA, left boxes) or not (non amplified RNA, right boxes) and synthesised to cDNA. Samples were run on Fluidigm and median gene expression of all genes was compared between the two types of RNA. Boxes in each column show the amplified and non amplified RNA respectively and denote median and interquartile range.

Our results show that after exclusion of samples that had a significant difference in gene expression when both RNA types were analysed, it was possible to analyse samples with both RNA types together. For subsequent analyses with samples containing both RNA types, an average expression for each gene across the two available samples was used.

5.3.9.3) Correlation between Fluidigm and microarray

The Fluidigm system and microarray platform used to measure gene expression profiles operate on different principles. The detection technology of these platforms is different, implying that these two platforms might detect transcript levels differently. We therefore investigated whether differentially expressed transcripts detected by microarray were correlated with transcript levels measured by Fluidigm. Primer/probes for differential BCG responsiveness and risk of TB disease that passed qualification (75 and 54 respectively) were measured by Fluidigm using the same samples on which the microarray was performed. Spearman correlation was performed on fold change (FC) values on transcripts measured by both platforms. For differential response to BCG, the fold change was calculated by subtracting the unstimulated values from the BCG stimulated values while for risk of TB disease, the values from control samples were subtracted from case values.

Using a FC>1.3 and a p value of 0.05, 27/75 transcripts from the classifier of differential response to BCG were either up-regulated or down-regulated when measured by both microarray and Fluidigm (r=0.89) (Figure 56). Following this analysis, a 10-fold cross validation was performed using Bioconductor's PAMR package to assess the performance of these genes in the training set. A total of two samples were misclassified using these 27 genes with a misclassification rate of 0.057. The sensitivity and specificity of this classification were 0.95 and 0.93 respectively.

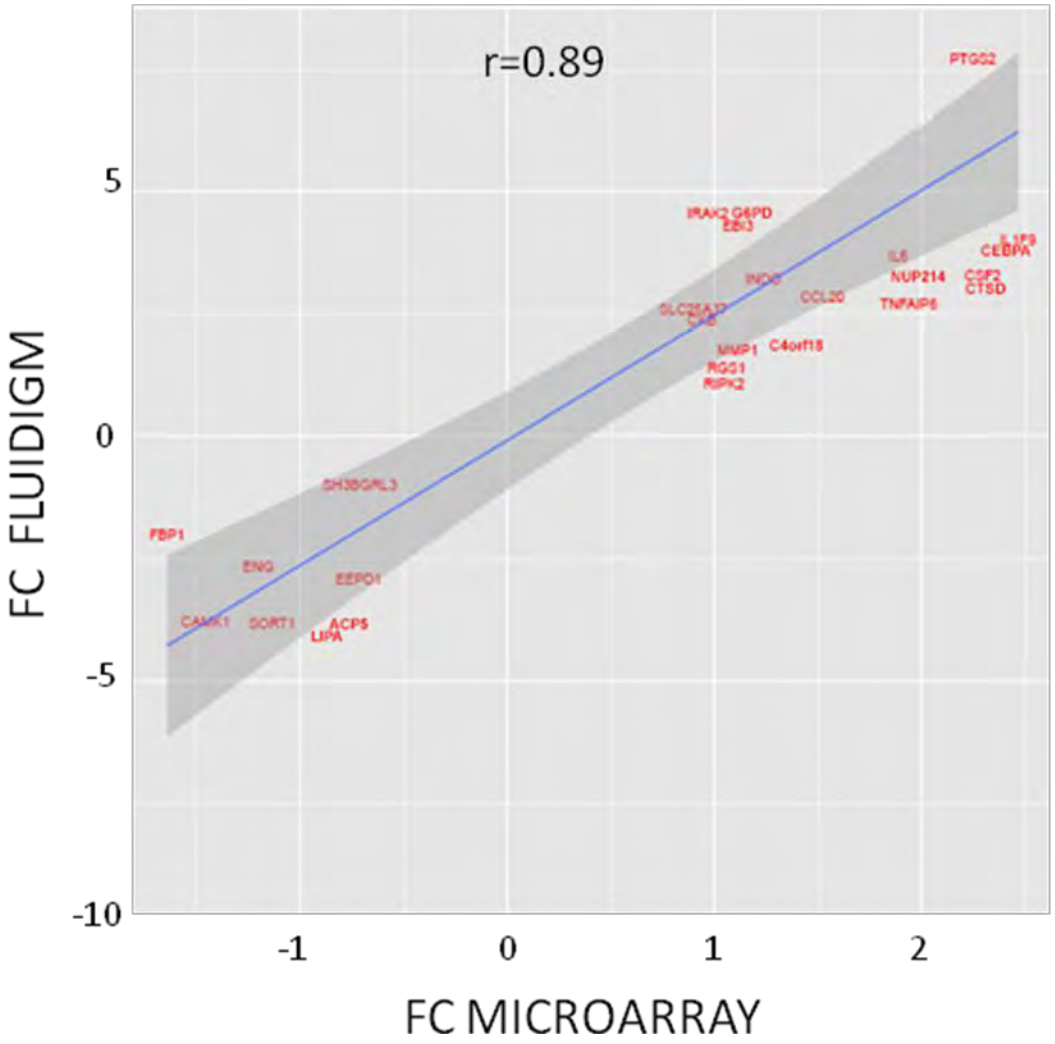

Figure 56: Correlation between mRNA transcript detection by microarray and Fluidigm to determine differential response to BCG vaccination.
RNA from training cohort on which microarray was performed were run on the Fluidigm using optimised experimental conditions and assays that passed qualification). Blue line and grey shade denote fitted values and confidence interval. Fold change (FC)= BCG-UNS.

Amongst stronger responders, only 12 of the 54 transcripts from the classifier of risk of TB disease were either up-regulated or down-regulated when measured by microarray and Fluidigm (r=0.96) (Figure 57) with a FC>1.3 and p-value of 0.05. Upon cross-validation in the training set, a total of three samples were misclassified using these 12 genes with a misclassification rate of 0.136. The sensitivity and specificity of this classification were 0.83 and 0.90 respectively.

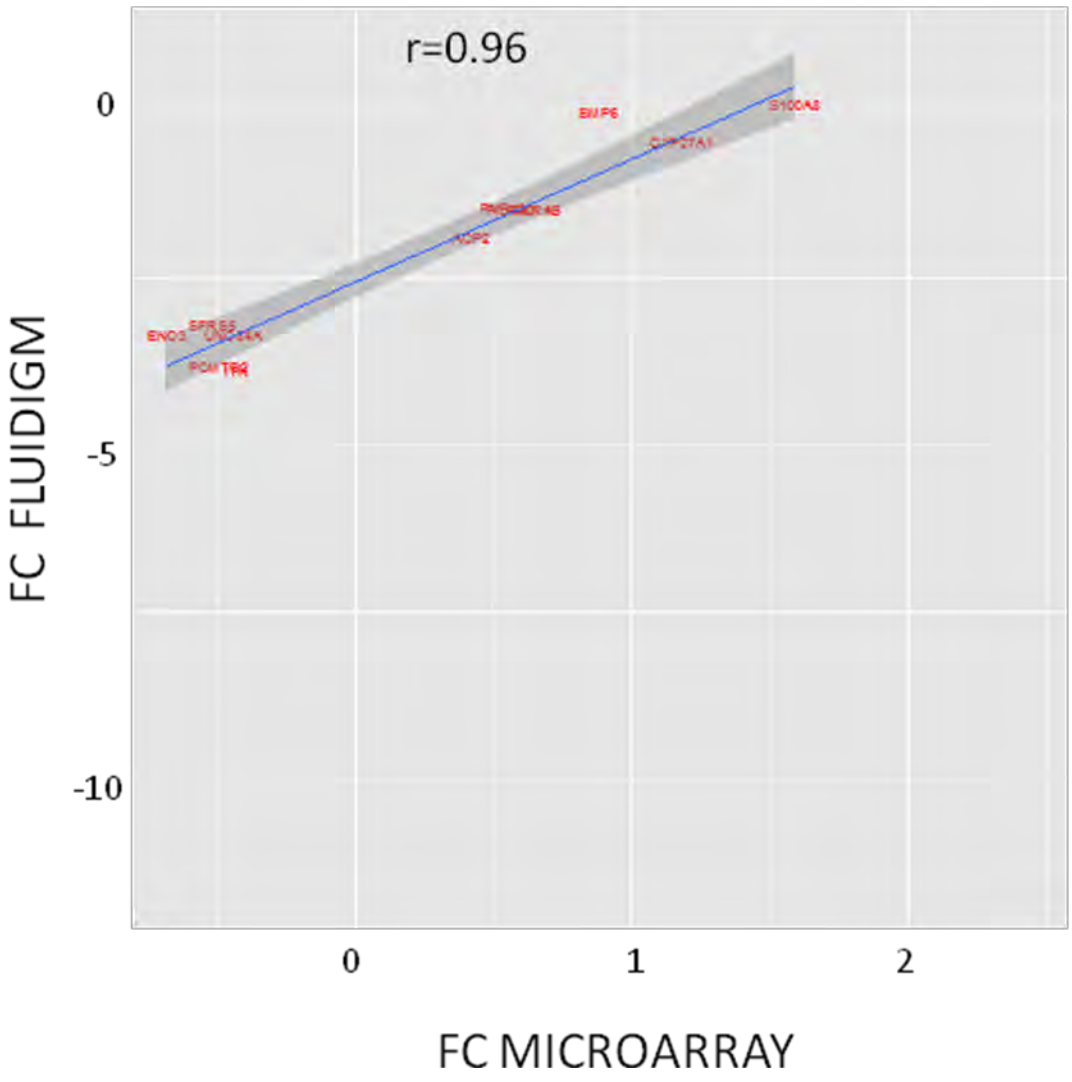

Figure 57: Correlation between mRNA transcript detection microarray and Fluidigm to determine differential response in cases and controls.
Samples from training cohort on which microarray was performed were run on the Fluidigm using optimised experimental conditions and assays that passed qualification Blue line and grey shade denote fitted values and confidence interval. Fold change (FC)= Cases-controls

We therefore locked down our classifier to 27 genes for differential response to BCG vaccination and 12 genes for risk of TB disease to be measured in the validation cohort (Table 25).

Table 25: Genes that correlated between microarray and Fluidigm

Differential response to BCG					Risk of TB disease	
ACP5	CCL20	CKB	MMP1	EEPD1	PVRL2	ACP2
RGS1	SORT1	CSF2	IRAK2	ENG	UNC84A	BMP6
INDO	TNFAIP6	NUP214	IL1F9	SLC25A37	PCMTD2	CYP27A1
LIPA	IL6	SH3BGRL3	CAMK1		KIF1B	PILRA
C4orf18	CTSD	FBP1	PTGS2		ENO3	ITK
EBI3	G6PD	CEBPA	RIPK2		SFRS5	S100A8

5.3.10) Validation of correlates of risk of TB disease in differential BCG responders defined by gene expression signature

In the validation set, differential response to BCG vaccination was defined by frequencies of BCG-specific CD4+ T cells expressing total IFN-γ, TNF-α and IL-2 identified by a logistic regression model and the expression of CXCL9 transcript. In stronger responders identified with these markers, T cell correlates of risk of TB disease identified in the training cohort could not be validated in the validation set. We now aimed to validate these correlates in infants with differential response to BCG defined by a gene signature.

Firstly, to assign infants as either a weaker or stronger BCG responder using the 27 gene classifier in the validation cohort, partial least square-discriminant analysis (PLS-DA) in Bioconductor's CMA package was used. Using this method, 32 infants were classified as stronger responders while 16 were classified as weaker responders in the validation set (Figure 58). There were 10 cases and 22 controls among the stronger responders while there were 8 cases and 8 controls among the weaker BCG responders (Figure 58).

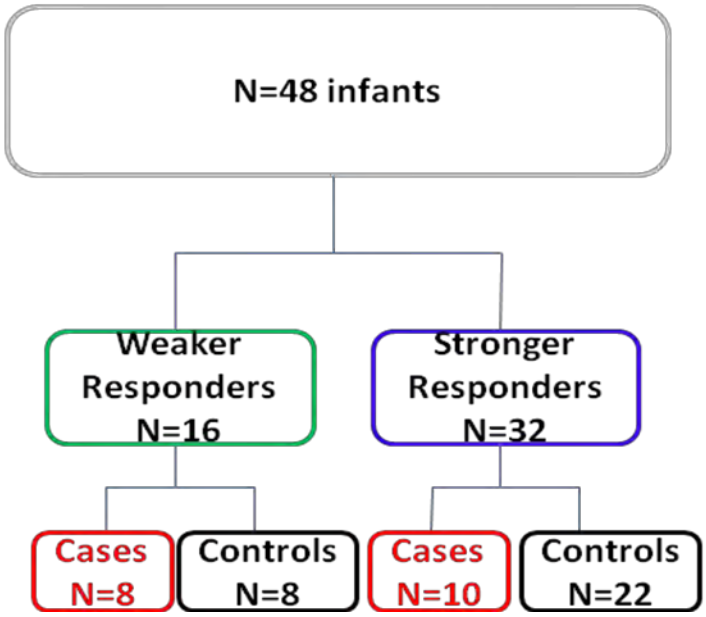

Figure 58: Distribution of cases and controls among stronger and weaker BCG responders defined by 27 gene classifier in the validation cohort measured by Fluidigm. PLS-DA was performed on 27 genes to assign infants into the two BCG response groups. Cases (red) and controls (black) within BCG weaker (green) and stronger (blue) responders.

We next assessed the performance of this 27 gene classifier in the validation cohort. Since there was no microarray analysis done in this cohort, the performance of this classifier was benchmarked to the frequencies of a combination of CD4+ T cells expressing total IFN-γ, TNF-α and IL-2 identified as markers of differential BCG response by a logistic regression model. This model had been previously shown to accurately classify 90% of infants correctly when benchmarked to microarray classification However, there were only 39 samples on which we had both gene expression and ICS data. The accuracy to correctly classify a stronger responder was 56.3% and a weaker responder was 26.1%, with the overall accuracy being 38.5% (Table 26).

Table 26: Classification rate of gene signature of BCG responsiveness

		Logistic regression		
		Weaker responders	**Stronger responders**	**Total**
Gene classifier	**Weaker responders**	**6**	**7**	**13**
	Stronger responders	**17**	**9**	**26**
	Total	**23**	**16**	**39**

We next assessed correlates of risk of TB disease identified in the training set. In the training set, cases in stronger responders showed increased frequency of CD4+ IL-17 producing cells compared to controls. Using the 27-gene classifier for BCG responsiveness, we identified stronger and weaker BCG responders in the validation cohort. In the stronger responders, there was no difference between cases and controls when we compared the frequency of BCG specific CD4+ T cells producing IL-17 (Figure 59).

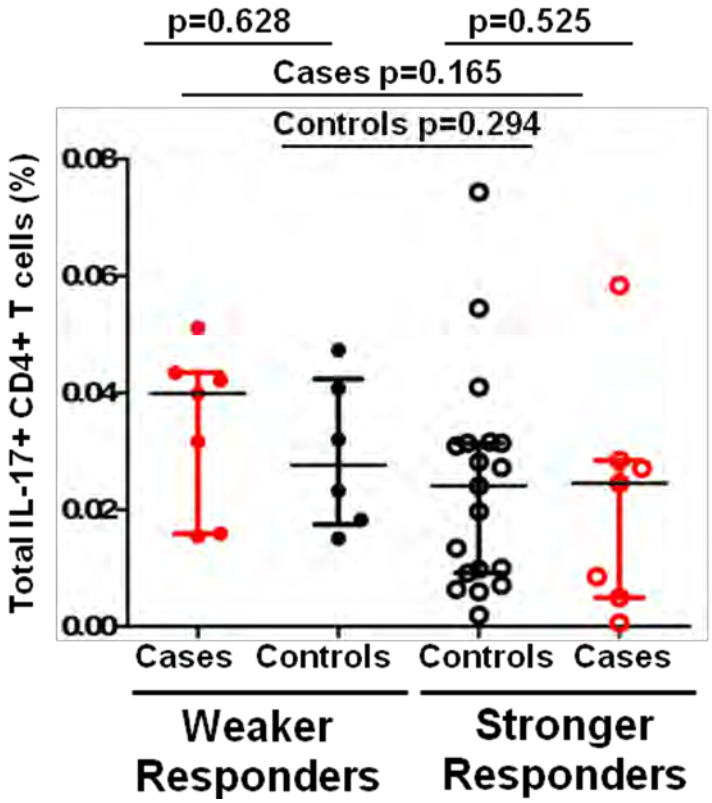

Figure 59: Frequencies of BCG-specific CD4+ T cells producing IL-17.
Whole blood was incubated with BCG for 12 hours and cytokines were detected using an intracellular cytokine staining assay and flow cytometry. A 27-gene signature was used to define differential response to BCG vaccination in the validation set. In stronger responders, frequencies of BCG-specific CD4+ cells producing IL-17 were not different between cases (red) and controls (black). The Mann Whitney test was used to compare differences between two groups. All p values were >0.05. Horizontal lines and whiskers on graph denote median and interquartile range, respectively. Weaker responders, cases n= 7 and controls n=6. Stronger responders, cases n=7 and controls n=19.

We next assessed the cytotoxic capacity of CD4+ and CD8+ T cells between cases and controls in differential BCG responders defined by the 27 gene classifier in the validation cohort.

In weaker BCG responders defined by clustering in the training set, CD4+ T cells from cases showed higher combined expression of granulysin, granzyme B and perforin (Figure 21A), granulysin and granzyme B (Figure 21B) as well as granzyme B and perforin compared to controls (Figure 21C). However, there were no differences in any of these combinations when we defined differential response to BCG using the 27 gene classifier (Figure 60A -C).

Controls in stronger responders were associated with increased frequency of CD4+ T cells producing perforin only (Figure 21D) compared to cases in the training set. Again, this difference was not observed in the validation set (Figure 60D).

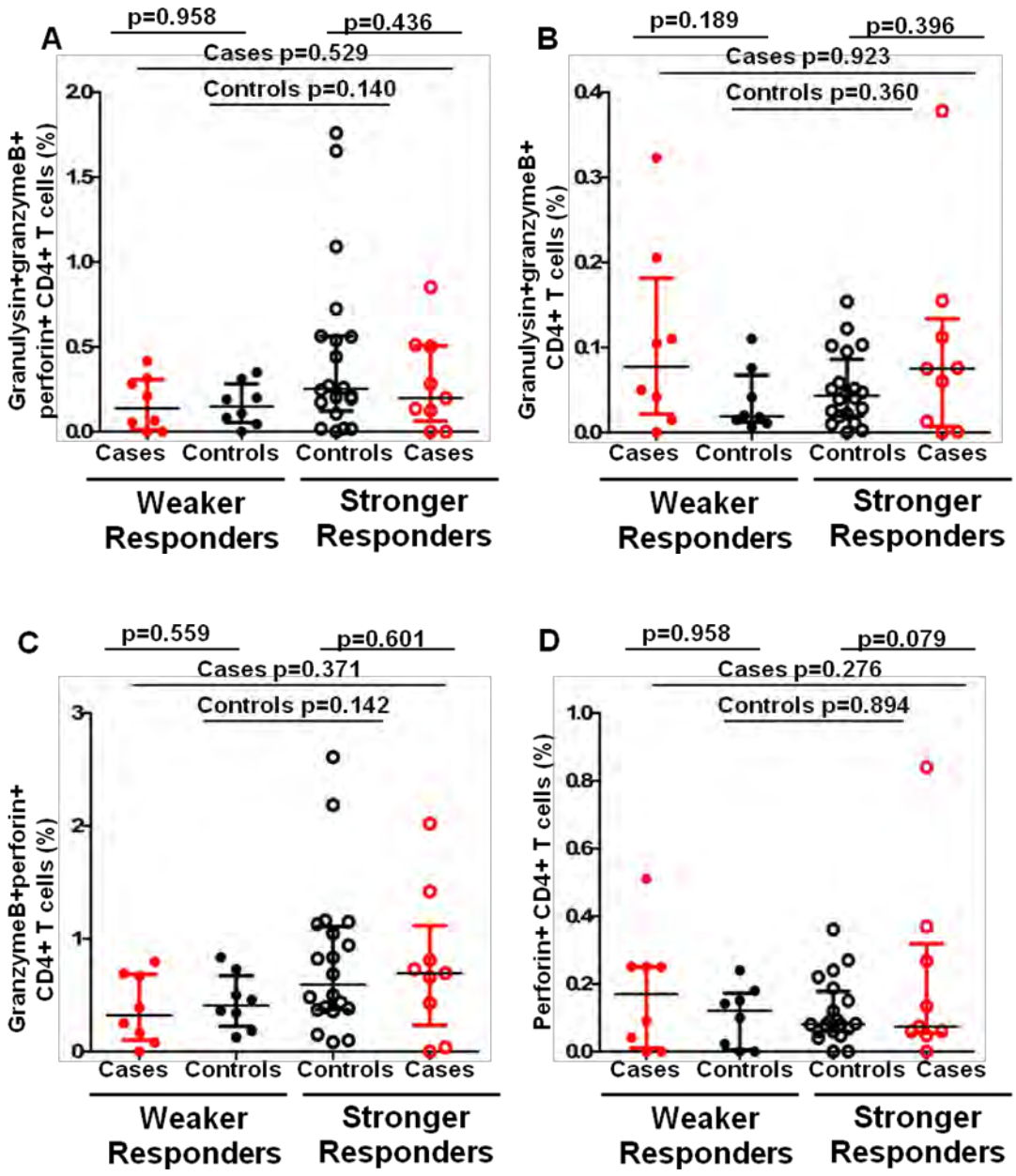

Figure 600: Cytotoxic capacity of BCG-specific CD4+ T cells.
PBMCs were stimulated with BCG or left unstimulated for 3 days and flow cytometry was used to detect BCG-specific CD4+ T cells expressing granzyme B, granulysing and/or perforin. BCG-specific T cells were defined by subtracting the unstimulated value from the BCG stimulated value. A 27 gene classifier was used to define differential response to BCG vaccination in the validation set. Frequencies of CD4+ T cells producing of **A)** granulysin, granzyme B and perforin together, **B)** granulysin and granzyme B together**, C)** granzyme B and perforin together and **D)** perforin only. Cases (red) and controls (black) in weaker and stronger BCG responders. The Mann Whitney test was used to assess differences between the two groups. All p were values> 0.05. Horizontal lines on graphs denote median while whiskers denote interquartile, range. Weaker responders, cases n= 8 and controls n=8. Stronger responders, cases n=9 and controls n=20.

Following the finding that no T cell correlate of risk of TB disease could be validated in infants with differential response to BCG as defined by the 27-gene classifier, we sought to validate the gene classifier for risk of TB disease identified in the training set. Infants were again divided into weaker and stronger BCG responders using the 27-gene classifier and in stronger responders only, we assessed the performance of the 12-gene classifier of risk of TB disease. There overall accuracy of classification was 69% with a sensitivity and specificity of 30% and 86.4% respectively (Table 27).

Table 27: Classification rate of gene signature of risk of TB disease

		Logistic regression		
		Cases	**Controls**	**Total**
Gene classifier	**Cases**	**3**	**3**	**6**
	Controls	**7**	**19**	**26**
	Total	**10**	**22**	**32**

5.4) Discussion

In the training set, correlates of risk of TB disease were identified when infants who either had strong or weak recall response to BCG vaccination were separated. These correlates were absent if response to BCG vaccination was not taken into account. Because the identification of these correlates involved in-depth analysis and data mining with the measurement of multiple outcomes, validation in an independent cohort was necessary. However, microarrays cannot be done on the scale of a clinical trial for the application of such validate correlates of risk. For this reason, we investigated the use of intracellular cytokine staining as well as quantitative real time PCR to assess the performance of three different biomarkers of differential response to BCG vaccination for the validation of correlates of risk of TB disease. Using a logistic regression model we identified a T cell classifier of differential response to BCG vaccination in the training set. This classifier involved the use of a combination of the frequencies of BCG-specific CD4+ T cells producing total IFN-γ, TNF-α and IL-2. Although there was no statistical significance in differentiating between the two groups when this classifier was used, it gave the overall best prediction and classification when compared to clustering analysis in the training set. The lack of significance is an important limitation in the study because the probability of classifying differential response to BCG could be due to chance. Nevertheless, we had a good rationale for using this marker to define differential response to BCG vaccination. As earlier mentioned, the magnitude of Th1 responses is used in most TB vaccine trials to determine immunogenicity [64, 323, 324]. Also, in a systems biology analysis of immune responses induced by a novel HIV vaccine, Zak *et al* also used the magnitude of T cell responses to identify higher and lower responders to MRKAd5/HIV vaccine [325]. However, in this study T cell responses were defined as serum cytokines and chemokines produced by CD8+ T cells [325] as opposed to Th1 cytokines produced by CD4+ T cells measured in whole blood in our study. For a vaccine to be considered immunogenic, CD4+ T cells expressing these cytokines should be higher in vaccinees compared to placebo recipients. However, we do not know if

Th1 responses will translate into vaccine-induced protection. In the training set, there was good agreement between frequencies of Th1 cells measured by flow cytometry and clustering of gene expression profiles measured by microarray. This suggests that routine measurement of Th1 responses is a good proxy for the more complex PBMC response to Th1 inducing vaccines. This is further supported by the strong correlation between IFN-γ mRNA expression measured by microarray and the frequency of IFN-γ-expressing CD4+ T cells. Soares *et al* showed that BCG responses post-vaccination in babies peaks at 6-10 weeks [191]. Since BCG responses were measured during the peak response in our study, this might account for the synchronization between inflammation and Th1 responses observed. It would be important to determine if this association between this early inflammation and the magnitude of Th1 cells also holds true when the memory response, months after vaccination is measured. Based on these data which suggest that magnitude of Th1 cells is a good classifier of BCG responsiveness, we used the frequencies of BCG-specific CD4+ T cells producing total IFN-γ, TNF-α and IL-2 in the validation set to separate infants into weaker and stronger BCG responders.

In a second analysis, we used mRNA expression of CXCL9 gene as a marker for differential response to BCG stimulation in the validation set. Based on the microarray data generated in the training set, IFN-γ itself and pathways including IFN-γ-inducible genes were among the most differentially expressed genes between weaker and stronger BCG responders. Since we were able to show that measuring the protein expression of this cytokine was also significantly higher in stronger responders compared to weaker responders, we wanted to investigate the use of this transcript in the validation set to define differential response to BCG vaccination. Validation of microarray results can be done by qPCR of the most differentially expressed genes. We used the expression of CXCL9, which is a gene specifically induced by IFN-γ, to define differential response to BCG vaccination. Brice *et al* showed that CXCL9 measurement is a more sensitive measurement of biocative IFN-γ than IFN-γ itself [332]. CXCL9 has been examined as an alternative marker for

immunogenicity [333] and has been used in several studies to define vaccine immunogenicity [332, 334, 335]. For example, in a trial of a candidate malaria vaccine, Berthoud *et al* showed that CXCL9 was a more sensitive measure than IFN-γ in detecting antigen-specific T cell responses [334]. Therefore, we defined differential response to BCG vaccination in the validation cohort using the expression of this gene. Similar to what was observed in the training set with the clustering analysis, there was a 50% split of the infants into stronger and weaker responders using CXCL9. Nevertheless, when we benchmarked the classification by CXCL9 to the logistic regression model, there was little agreement between the two markers. Also there was a poor correlation between CXCL9 mRNA expression and frequency of IFN-γ-expressing CD4+ T cells in the validation set (Appendix 1) even though there was a good correlation between the two in the training set. Technical issues such as RNA quality, viability of PBMCs, storage age of samples as well as assay used, could be the reasons for this observation. The RNA quality of most of the samples was within the acceptable range as determined by the 260/280 and the median viability of the thawed PBMCs was 84% (Appendix 2). The most probable reason for this disparity could be the different platforms used to measure CXCL9 expression in the training and validation sets. In the training set, CXCL9 mRNA expression was measured by microarray while in the validation set, qRT-PCR was used for the measurement of this transcript. These two platforms operate on slightly different technologies in mRNA detection.

Our hypothesis-driven approaches to define differential response to BCG vaccination did not allow validation of correlates of risk of TB disease. The use of a single gene might be suboptimal in defining differential response. We therefore also sought to use a gene expression signature rather than the expression of a single gene to define this differential response. Several studies have used unbiased systems biology approaches as to define vaccine immunogenicity [325, 327, 336-338]. Recently, Tan *et al* used this approach and identified a gene set to developing predictors of vaccine outcome and showed that enrichment of signatures corresponding to proliferating B cells accurately

defined antibody responses to influenza vaccine [327]. A similar approach was used by Henn *et al*, who showed that a plasma cell gene signature correlated with influenza vaccine responses [338]. In HIV, Zak *et al*, identified an innate immune signature that was up-regulated post-vaccination compared to pre-vaccination with the MRKAd5/HIV vaccine, and this signature correlated with the magnitude of CD8+ T cells [325]. We identified a gene signature of differential BCG response in the training set and used a high throughput qRT-PCR system (Fluidigm) to measure the expression of these genes in the validation set. This platform allows measurement of 96 transcripts from 96 different samples. As part of the optimisation process, we qualified each primer/probe for inclusion in analysis. Primer/probe qualification is a very important quality control step in qRT-PCR. We applied the piecewise qualification process described by Dominguez *et al* [329]. Hu *et al* had applied this qualification process to non human primates (NHP) and found cross-reactivity between NHP specific primers and human mRNA, and vice versa [339]. In our study, not all primer/probes could be qualified using this system but the overall qualification rate was similar to those reported in these two other studies. One of the possible reasons for failure in qualification could be the fact that Applied Biosystems uses a different qualification platform: these assays are tested individually using a conventional qRT-PCR. In our qualification experiments, we multiplexed these assays and ran them on the Fluidigm.

The gene expression signature of risk of TB disease in differential BCG responders did not validate in the validation set. We tried to investigate the possible reasons for this observation. Firstly, we assessed the cDNA quality in the validation set. We had shown that running samples from the training set using the Fluidigm allowed identification of a locked-down classifier of 27 genes for differential BCG response and 12 genes for risk of TB disease. Poor cDNA quality has a negative effect on downstream gene expression results [340, 341]. However, we observed no difference in cDNA quality or amplification between samples generated from the training and validation set. Possible reasons to account for the lack of correlation could be: i) Not enough transcripts from the

initial classifiers were applied in the validation set due to lack of correlation between microarray and Fluidigm, resulting in a loss of predictive power. ii) Different definitions of cases and controls in the training and validation sets. In the training set, all cases were infants with definite TB (microbiological confirmation) and controls were household controls. In the validation set, cases were identified as probable TB (no microbiological confirmation but strong clinical and epidemiological features) and controls were community controls that were never investigated for TB disease. Importantly, at the time of blood collection for analysis (10 weeks of age) all infants were healthy, and therefore the difference in TB diagnosis would not have influenced the analyses at 10 weeks of age. Regardless, our study design was suboptimal, which may have contributed to undermining successful validation.

Our results suggest that the T cell outcomes we measured do not robustly predict who is at risk of developing TB disease. Our results also suggest that frequencies of BCG-specific Th1 CD4+ T cells appear to correlate to BCG recall responsiveness (e.g. immunogenicity) [191], but not with reduced risk of developing TB disease. These observations support the previous observation that frequencies of Th1 cells do not correlate with risk of TB in infants [175]. A correlation between extent of disease measured on chest X-ray and immunological/genetic finding would have given a good insight on these correlates. However, at the time when these infants were diagnosed with TB, there was no grading system yet on disease severity on chest X-ray. In addition, the sample size for definite TB cases was too small for this analysis as there will be a lot of variation to come to a final conclusion.

Prospective biomarker studies rely on robust clinical case definition, appropriate sample size, adequate samples and technology [342]. Our study however had important limitations and therefore data should be interpreted with caution. Some of the limitations and lessons learned in this study include:

I) Sample sizes used for analysis. Not all participant samples were always available for all analyses. The microarray analysis on which clustering of gene

expression profiles was identified included 44 samples. This had to be further divided into stronger and weaker responders before evaluating differences between cases and controls in each sample. However, classical sample size calculations are challenging for such complex analyses, as these cannot rely on precise assumptions and effect of sizes are not known [343]. The sample sizes used in this study were based on availability of samples and our previous experience conducting similar immunology and systems biology studies, as well as cost and feasibility considerations.

II) The definition of participants in training and validation (test) sets. Cases and controls in both sets of the study had different clinical and epidemiological definitions. However, all analyses were performed on samples collected at 10 weeks of age, well before TB disease or exposure occurred, when all participants were healthy and there was no evidence of household exposure to TB. Moreover, if a biomarker of prospective risk of TB disease will be identified and validated, its broad applicability to the general population cannot rely on strict definitions. Regardless, an ideal study design would include identical clinical and epidemiological definitions for training and validation set with samples randomly split selected for each set.

III) Validation strategy. We applied three different strategies to validate what we observed when gene expression profiles were analysed by microarray. Different assay platforms operate on different technologies and generate data with different sensitivities, dynamic ranges as well as limit of detection. Performing a validation using the same technique would greatly reduce variability in results. However, the initial finding becomes more reliable if it can be confirmed with another technique.

IV) Analysis plan. Before starting such studies, pre-defined analysis strategies including cut offs should be locked-down. This helps in determining how feasible the study is, as well as addressing possible limitations up front, while eliminating potential bias as the analyses proceed.

5.5) Conclusions

This is the first study of its kind that has investigated prospective correlates of risk of TB disease in infants with differential response to BCG vaccination. We showed that although frequencies of BCG-specific Th1 cells did not correlate with risk of developing TB disease, they indeed correlated with a broader measurement of immune recall response to BCG, when differential responsiveness is taken into account, and therefore represent a solid tool to assess vaccine-induced immunogenicity. We also showed that inflammatory, myeloid and interferon gene pathways were associated with risk of TB disease in infants who were either stronger or weaker responders to BCG vaccination. Several studies have also shown this in TB disease patients compared to latent individuals. In our study, all infants were healthy at time of analysis and the fact that we also observe the same finding suggests that it will be interesting to further investigate this. In addition, the implication that the same immune response pattern can be both beneficial and pathological may have hindered identification of correlates of risk in other studies. Given the complex nature of the immune response to mycobacteria, we propose that other T cell functions, cross-talk between adaptive and innate immunity as well as variability in vaccine-induced responses be included in future studies of correlates of risk of TB disease. Findings from such studies will help significantly in the possible identification of these correlates and contribution in the field of TB vaccinology.

REFERENCES

1. NIAID, *http://www.niaid.nih.gov/topics/tuberculosis/understanding/whatistb/pages/tbdefinitions.aspx.* 2012 (Accessed 15th February 2013). .
2. Lawn, S.D., et al., *Impact of HIV infection on the epidemiology of tuberculosis in a peri-urban community in South Africa: the need for age-specific interventions.* Clin Infect Dis, 2006. **42**(7): p. 1040-7.
3. Lawn, S.D., et al., *Short-term and long-term risk of tuberculosis associated with CD4 cell recovery during antiretroviral therapy in South Africa.* AIDS, 2009. **23**(13): p. 1717-25.
4. Griffiths-Chu, S., et al., *Characterization of immature T cell subpopulations in neonatal blood.* Blood, 1984. **64**(1): p. 296-300.
5. Kollmann, T.R., et al., *Neonatal innate TLR-mediated responses are distinct from those of adults.* J Immunol, 2009. **183**(11): p. 7150-60.
6. Marais, B.J., et al., *The natural history of childhood intra-thoracic tuberculosis: a critical review of literature from the pre-chemotherapy era.* Int J Tuberc Lung Dis, 2004. **8**(4): p. 392-402.
7. WHO, *Global Tuberculosis Report 2013 (Accessed 15th February 2014).* http://apps.who.int/iris/bitstream/10665/75938/1/9789241564502_eng.pdf , 2013.
8. Moyo, S., et al., *Age-related tuberculosis incidence and severity in children under 5 years of age in Cape Town, South Africa.* Int J Tuberc Lung Dis, 2010. **14**(2): p. 149-54.
9. Lawn, S.D. and M.P. Nicol, *Xpert(R) MTB/RIF assay: development, evaluation and implementation of a new rapid molecular diagnostic for tuberculosis and rifampicin resistance.* Future Microbiol, 2011. **6**(9): p. 1067-82.
10. Lee, E. and R.S. Holzman, *Evolution and current use of the tuberculin test.* Clin Infect Dis, 2002. **34**(3): p. 365-70.
11. Ranganathan, S., T. Connell, and N. Curtis, *Interferon-gamma release assays in children--no better than tuberculin skin testing?* J Infect, 2007. **54**(4): p. 412-3; author reply 414-5.
12. Ewer, K., et al., *Comparison of T-cell-based assay with tuberculin skin test for diagnosis of Mycobacterium tuberculosis infection in a school tuberculosis outbreak.* Lancet, 2003. **361**(9364): p. 1168-73.
13. Connell, T.G., et al., *Enhanced ex vivo stimulation of Mycobacterium tuberculosis-specific T cells in human immunodeficiency virus-infected persons via antigen delivery by the Bordetella pertussis adenylate cyclase vector.* Clin Vaccine Immunol, 2007. **14**(7): p. 847-54.
14. Mahomed, H., et al., *Comparison of mantoux skin test with three generations of a whole blood IFN-gamma assay for tuberculosis infection.* Int J Tuberc Lung Dis, 2006. **10**(3): p. 310-6.

15. Machingaidze, S., et al., *The utility of an interferon gamma release assay for diagnosis of latent tuberculosis infection and disease in children: a systematic review and meta-analysis.* Pediatr Infect Dis J, 2011. **30**(8): p. 694-700.
16. Sadatsafavi, M., et al., *A statistical method was used for the meta-analysis of tests for latent TB in the absence of a gold standard, combining random-effect and latent-class methods to estimate test accuracy.* J Clin Epidemiol, 2010. **63**(3): p. 257-69.
17. Chegou, N.N., et al., *Tuberculosis assays: past, present and future.* Expert Rev Anti Infect Ther, 2011. **9**(4): p. 457-69.
18. Zar, H.J., *Chronic lung disease in human immunodeficiency virus (HIV) infected children.* Pediatr Pulmonol, 2008. **43**(1): p. 1-10.
19. Olivieri, D., R. D'Ippolito, and A. Chetta, *Induced sputum: diagnostic value in interstitial lung disease.* Curr Opin Pulm Med, 2000. **6**(5): p. 411-4.
20. Ruiz Jimenez, M., et al., *"Induced sputum versus gastric lavage for the diagnosis of pulmonary tuberculosis in children".* BMC Infect Dis, 2013. **13**(1): p. 222.
21. Connell, T.G., H.J. Zar, and M.P. Nicol, *Advances in the diagnosis of pulmonary tuberculosis in HIV-infected and HIV-uninfected children.* J Infect Dis, 2011. **204 Suppl 4**: p. S1151-8.
22. Zeka, A.N., S. Tasbakan, and C. Cavusoglu, *Evaluation of the GeneXpert MTB/RIF assay for rapid diagnosis of tuberculosis and detection of rifampin resistance in pulmonary and extrapulmonary specimens.* J Clin Microbiol, 2011. **49**(12): p. 4138-41.
23. Trebucq, A., et al., *Xpert(R) MTB/RIF for national tuberculosis programmes in low-income countries: when, where and how?* Int J Tuberc Lung Dis, 2011. **15**(12): p. 1567-72.
24. Van Rie, A., et al., *Xpert((R)) MTB/RIF for point-of-care diagnosis of TB in high-HIV burden, resource-limited countries: hype or hope?* Expert Rev Mol Diagn, 2010. **10**(7): p. 937-46.
25. Hatherill, M., et al., *Induced sputum or gastric lavage for community-based diagnosis of childhood pulmonary tuberculosis?* Arch Dis Child, 2009. **94**(3): p. 195-201.
26. Zar, H.J., et al., *Induced sputum versus gastric lavage for microbiological confirmation of pulmonary tuberculosis in infants and young children: a prospective study.* Lancet, 2005. **365**(9454): p. 130-4.
27. WHO, *Treatment of Tuberculosis Guidelines, 4th Edition 2011 (Accessed 2nd April 2013).* http://whqlibdoc.who.int/publications/2010/9789241547833_eng.pdf, 2011.
28. WHO, *Guidance for national tuberculosis programmes on the management of tuberculosis in children. Geneva.* 2006.
29. CDC, *(Accessed 2nd April 2013).* http://www.cdc.gov/tb/topic/treatment/ltbi.htm, 2012.
30. Tuberculosis, I.a., *(Accessed 2nd April 2013).* http://www.tbfacts.org/tb-treatment.html, 2012.

31. Yoshiyama, T., et al., *Development of acquired drug resistance in recurrent tuberculosis patients with various previous treatment outcomes.* Int J Tuberc Lung Dis, 2004. **8**(1): p. 31-8.
32. NIAID, *(Accessed 2nd April 2013).* http://www.niaid.nih.gov/topics/tuberculosis/Understanding/Pages/treatment.aspx, 2012.
33. Hatherill, M., *Prospects for elimination of childhood tuberculosis: the role of new vaccines.* Arch Dis Child, 2011. **96**(9): p. 851-6.
34. Rodrigues, L.C., V.K. Diwan, and J.G. Wheeler, *Protective effect of BCG against tuberculous meningitis and miliary tuberculosis: a meta-analysis.* Int J Epidemiol, 1993. **22**(6): p. 1154-8.
35. Rodrigues, L.C. and P.G. Smith, *Tuberculosis in developing countries and methods for its control.* Trans R Soc Trop Med Hyg, 1990. **84**(5): p. 739-44.
36. Colditz, G.A., et al., *Efficacy of BCG vaccine in the prevention of tuberculosis. Meta-analysis of the published literature.* JAMA, 1994. **271**(9): p. 698-702.
37. Ottenhoff, T.H. and S.H. Kaufmann, *Vaccines against tuberculosis: where are we and where do we need to go?* PLoS Pathog, 2012. **8**(5): p. e1002607.
38. Hesseling, A.C., et al., *The risk of disseminated Bacille Calmette-Guerin (BCG) disease in HIV-infected children.* Vaccine, 2007. **25**(1): p. 14-8.
39. Comstock, G.W., *Identification of an effective vaccine against tuberculosis.* Am Rev Respir Dis, 1988. **138**(2): p. 479-80.
40. Davids, V., et al., *The effect of bacille Calmette-Guerin vaccine strain and route of administration on induced immune responses in vaccinated infants.* J Infect Dis, 2006. **193**(4): p. 531-6.
41. Ritz, N., et al., *To TST or not to TST: is tuberculin skin testing necessary before BCG immunisation in children?* Vaccine, 2012. **30**(8): p. 1434-6.
42. Sutherland, I. and V.H. Springett, *Effectiveness of BCG vaccination in England and Wales in 1983.* Tubercle, 1987. **68**(2): p. 81-92.
43. Ponnighaus, J.M., et al., *Efficacy of BCG vaccine against leprosy and tuberculosis in northern Malawi.* Lancet, 1992. **339**(8794): p. 636-9.
44. Mangtani, P., et al., *Protection by BCG vaccine against tuberculosis: a systematic review of randomized controlled trials.* Clin Infect Dis, 2014. **58**(4): p. 470-80.
45. Brahmajothi, V., et al., *Association of pulmonary tuberculosis and HLA in south India.* Tubercle, 1991. **72**(2): p. 123-32.
46. Jouanguy, E., et al., *Interferon-gamma-receptor deficiency in an infant with fatal bacille Calmette-Guerin infection.* N Engl J Med, 1996. **335**(26): p. 1956-61.
47. Jouanguy, E., et al., *Partial interferon-gamma receptor 1 deficiency in a child with tuberculoid bacillus Calmette-Guerin infection and a sibling with clinical tuberculosis.* J Clin Invest, 1997. **100**(11): p. 2658-64.
48. Goldfeld, A.E., et al., *Association of an HLA-DQ allele with clinical tuberculosis.* JAMA, 1998. **279**(3): p. 226-8.

49. Shey, M.S., et al., *Single nucleotide polymorphisms in toll-like receptor 6 are associated with altered lipopeptide- and mycobacteria-induced interleukin-6 secretion.* Genes Immun, 2010. **11**(7): p. 561-72.
50. Randhawa, A.K., et al., *Association of human TLR1 and TLR6 deficiency with altered immune responses to BCG vaccination in South African infants.* PLoS Pathog, 2011. **7**(8): p. e1002174.
51. Young, S.L., et al., *Environmental strains of Mycobacterium avium interfere with immune responses associated with Mycobacterium bovis BCG vaccination.* Infect Immun, 2007. **75**(6): p. 2833-40.
52. Fine, P.E., *Bacille Calmette-Guerin vaccines: a rough guide.* Clin Infect Dis, 1995. **20**(1): p. 11-4.
53. Elias, D., et al., *Poor immunogenicity of BCG in helminth infected population is associated with increased in vitro TGF-beta production.* Vaccine, 2008. **26**(31): p. 3897-902.
54. Rook, G.A., K. Dheda, and A. Zumla, *Do successful tuberculosis vaccines need to be immunoregulatory rather than merely Th1-boosting?* Vaccine, 2005. **23**(17-18): p. 2115-20.
55. Hatherill, M., et al., *The potential impact of helminth infection on trials of novel tuberculosis vaccines.* Vaccine, 2009. **27**(35): p. 4743-4.
56. Hawkridge, A., et al., *Efficacy of percutaneous versus intradermal BCG in the prevention of tuberculosis in South African infants: randomised trial.* BMJ, 2008. **337**: p. a2052.
57. Frick, M., *The TB vaccine pipeline. Where are we going, Where have we been?* http://www.tbvi.eu/fileadmin/user_upload/Documenten/News/TBVaccines_pipeline_report_TAG_1July2013.pdf, 2013.
58. McShane, H., et al., *Recombinant modified vaccinia virus Ankara expressing antigen 85A boosts BCG-primed and naturally acquired antimycobacterial immunity in humans.* Nat Med, 2004. **10**(11): p. 1240-4.
59. Tameris, M.D., et al., *Safety and efficacy of MVA85A, a new tuberculosis vaccine, in infants previously vaccinated with BCG: a randomised, placebo-controlled phase 2b trial.* Lancet, 2013. **381**(9871): p. 1021-8.
60. Martin, C., *Tuberculosis vaccines: past, present and future.* Curr Opin Pulm Med, 2006. **12**(3): p. 186-91.
61. Hess, J., et al., *Mycobacterium bovis Bacille Calmette-Guerin strains secreting listeriolysin of Listeria monocytogenes.* Proc Natl Acad Sci U S A, 1998. **95**(9): p. 5299-304.
62. Grode, L., et al., *Increased vaccine efficacy against tuberculosis of recombinant Mycobacterium bovis bacille Calmette-Guerin mutants that secrete listeriolysin.* J Clin Invest, 2005. **115**(9): p. 2472-9.
63. Desel, C., et al., *Recombinant BCG DeltaureC hly+ induces superior protection over parental BCG by stimulating a balanced combination of type 1 and type 17 cytokine responses.* J Infect Dis, 2011. **204**(10): p. 1573-84.

64. Abel, B., et al., *The novel tuberculosis vaccine, AERAS-402, induces robust and polyfunctional CD4+ and CD8+ T cells in adults.* Am J Respir Crit Care Med, 2010. **181**(12): p. 1407-17.
65. Smaill, F., et al., *A human type 5 adenovirus-based tuberculosis vaccine induces robust T cell responses in humans despite preexisting anti-adenovirus immunity.* Sci Transl Med, 2013. **5**(205): p. 205ra134.
66. Vogel, F.R., *Improving vaccine performance with adjuvants.* Clin Infect Dis, 2000. **30 Suppl 3**: p. S266-70.
67. Day, C.L., et al., *Induction and regulation of T-cell immunity by the novel tuberculosis vaccine M72/AS01 in South African adults.* Am J Respir Crit Care Med, 2013. **188**(4): p. 492-502.
68. van Dissel, J.T., et al., *Ag85B-ESAT-6 adjuvanted with IC31 promotes strong and long-lived Mycobacterium tuberculosis specific T cell responses in naive human volunteers.* Vaccine, 2010. **28**(20): p. 3571-81.
69. Billeskov, R., et al., *The HyVac4 subunit vaccine efficiently boosts BCG-primed anti-mycobacterial protective immunity.* PLoS One, 2012. **7**(6): p. e39909.
70. Parida, S.K. and S.H. Kaufmann, *Novel tuberculosis vaccines on the horizon.* Curr Opin Immunol, 2010. **22**(3): p. 374-84.
71. Marais, B.J., *Childhood turberculosis: reflections from the front line.* Pediatr Ann, 2004. **33**(10): p. 695-8.
72. Wood, R., et al., *Burden of new and recurrent tuberculosis in a major South African city stratified by age and HIV-status.* PLoS One, 2011. **6**(10): p. e25098.
73. Brennan, M.J. and J. Thole, *Tuberculosis vaccines: a strategic blueprint for the next decade.* Tuberculosis (Edinb), 2012. **92 Suppl 1**: p. S6-13.
74. Hanekom, W.A., et al., *SATVI - after 10 years closing in on a new and better vaccine to prevent tuberculosis.* S Afr Med J, 2012. **102**(6): p. 438-41.
75. Poland, G.A., *Variability in immune response to pathogens: using measles vaccine to probe immunogenetic determinants of response.* Am J Hum Genet, 1998. **62**(2): p. 215-20.
76. Poland, G.A., et al., *Heterogeneity in vaccine immune response: the role of immunogenetics and the emerging field of vaccinomics.* Clin Pharmacol Ther, 2007. **82**(6): p. 653-64.
77. Sinha, P., et al., *The major histocompatibility complex haplotypes dictate and the background genes fine-tune the dominant versus the cryptic response profile of a T-cell determinant within a native antigen: relevance to disease susceptibility and vaccination.* Scand J Immunol, 2007. **65**(2): p. 158-65.
78. Ovsyannikova, I.G., et al., *HLA supertypes and immune responses to measles-mumps-rubella viral vaccine: findings and implications for vaccine design.* Vaccine, 2007. **25**(16): p. 3090-100.
79. Ovsyannikova, I.G., et al., *The contribution of HLA class I antigens in immune status following two doses of rubella vaccination.* Hum Immunol, 2004. **65**(12): p. 1506-15.

80. van Eden, W., et al., *HLA-DR3 associated genetic control of response to multiple skin tests with new tuberculins.* Clin Exp Immunol, 1983. **52**(2): p. 287-92.
81. Ottenhoff, T.H., et al., *Evidence for an HLA-DR4-associated immune-response gene for Mycobacterium tuberculosis. A clue to the pathogenesis of rheumatoid arthritis?* Lancet, 1986. **2**(8502): p. 310-3.
82. Fitzgerald, J.C., et al., *A simian replication-defective adenoviral recombinant vaccine to HIV-1 gag.* J Immunol, 2003. **170**(3): p. 1416-22.
83. Casimiro, D.R., et al., *Comparative immunogenicity in rhesus monkeys of DNA plasmid, recombinant vaccinia virus, and replication-defective adenovirus vectors expressing a human immunodeficiency virus type 1 gag gene.* J Virol, 2003. **77**(11): p. 6305-13.
84. Harro, C.D., et al., *Safety and immunogenicity of adenovirus-vectored near-consensus HIV type 1 clade B gag vaccines in healthy adults.* AIDS Res Hum Retroviruses, 2009. **25**(1): p. 103-14.
85. Buchbinder, S.P., et al., *Efficacy assessment of a cell-mediated immunity HIV-1 vaccine (the Step Study): a double-blind, randomised, placebo-controlled, test-of-concept trial.* Lancet, 2008. **372**(9653): p. 1881-93.
86. McElrath, M.J., et al., *HIV-1 vaccine-induced immunity in the test-of-concept Step Study: a case-cohort analysis.* Lancet, 2008. **372**(9653): p. 1894-905.
87. Targonski, P.V. and G.A. Poland, *Pneumococcal vaccination in adults: recommendations, trends, and prospects.* Cleve Clin J Med, 2007. **74**(6): p. 401-6, 408-10, 413-4.
88. Cook, I.F., *Sexual dimorphism of humoral immunity with human vaccines.* Vaccine, 2008. **26**(29-30): p. 3551-5.
89. Kagina, B.M., et al., *Delaying BCG vaccination from birth to 10 weeks of age may result in an enhanced memory CD4 T cell response.* Vaccine, 2009. **27**(40): p. 5488-95.
90. Burl, S., et al., *Delaying bacillus Calmette-Guerin vaccination from birth to 4 1/2 months of age reduces postvaccination Th1 and IL-17 responses but leads to comparable mycobacterial responses at 9 months of age.* J Immunol, 2010. **185**(4): p. 2620-8.
91. Lutwama, F., et al., *Distinct T-cell responses when BCG vaccination is delayed from birth to 6 weeks of age in Ugandan infants.* J Infect Dis, 2014. **209**(6): p. 887-97.
92. Landrum, M.L., et al., *Hepatitis B vaccination and risk of hepatitis B infection in HIV-infected individuals.* AIDS, 2010. **24**(4): p. 545-55.
93. Hung, C.C., et al., *A 5-year longitudinal follow-up study of serological responses to 23-valent pneumococcal polysaccharide vaccination among patients with HIV infection who received highly active antiretroviral therapy.* HIV Med, 2010. **11**(1): p. 54-63.
94. Walzl, G., et al., *Immunological biomarkers of tuberculosis.* Nat Rev Immunol, 2011. **11**(5): p. 343-54.
95. Ernst, J.D., *The immunological life cycle of tuberculosis.* Nat Rev Immunol, 2012. **12**(8): p. 581-91.

96. Wolf, A.J., et al., *Mycobacterium tuberculosis infects dendritic cells with high frequency and impairs their function in vivo.* J Immunol, 2007. **179**(4): p. 2509-19.
97. Kang, D.D., et al., *Profiling early lung immune responses in the mouse model of tuberculosis.* PLoS One, 2011. **6**(1): p. e16161.
98. Jo, E.K., *Mycobacterial interaction with innate receptors: TLRs, C-type lectins, and NLRs.* Curr Opin Infect Dis, 2008. **21**(3): p. 279-86.
99. Harding, C.V. and W.H. Boom, *Regulation of antigen presentation by Mycobacterium tuberculosis: a role for Toll-like receptors.* Nat Rev Microbiol, 2010. **8**(4): p. 296-307.
100. Chen, Y.C., et al., *Toll-like receptor 2 gene polymorphisms, pulmonary tuberculosis, and natural killer cell counts.* BMC Med Genet, 2010. **11**: p. 17.
101. Caws, M., et al., *The influence of host and bacterial genotype on the development of disseminated disease with Mycobacterium tuberculosis.* PLoS Pathog, 2008. **4**(3): p. e1000034.
102. Ferwerda, G., et al., *NOD2 and toll-like receptors are nonredundant recognition systems of Mycobacterium tuberculosis.* PLoS Pathog, 2005. **1**(3): p. 279-85.
103. Reiling, N., et al., *Cutting edge: Toll-like receptor (TLR)2- and TLR4-mediated pathogen recognition in resistance to airborne infection with Mycobacterium tuberculosis.* J Immunol, 2002. **169**(7): p. 3480-4.
104. Abel, B., et al., *Toll-like receptor 4 expression is required to control chronic Mycobacterium tuberculosis infection in mice.* J Immunol, 2002. **169**(6): p. 3155-62.
105. Branger, J., et al., *Toll-like receptor 4 plays a protective role in pulmonary tuberculosis in mice.* Int Immunol, 2004. **16**(3): p. 509-16.
106. Branger, J., et al., *Role of Toll-like receptor 4 in gram-positive and gram-negative pneumonia in mice.* Infect Immun, 2004. **72**(2): p. 788-94.
107. Drennan, M.B., et al., *Toll-like receptor 2-deficient mice succumb to Mycobacterium tuberculosis infection.* Am J Pathol, 2004. **164**(1): p. 49-57.
108. Sugawara, I., et al., *Mycobacterial infection in TLR2 and TLR6 knockout mice.* Microbiol Immunol, 2003. **47**(5): p. 327-36.
109. Holscher, C., et al., *Containment of aerogenic Mycobacterium tuberculosis infection in mice does not require MyD88 adaptor function for TLR2, -4 and -9.* Eur J Immunol, 2008. **38**(3): p. 680-94.
110. Dorhoi, A., et al., *Activation of the NLRP3 inflammasome by Mycobacterium tuberculosis is uncoupled from susceptibility to active tuberculosis.* Eur J Immunol, 2012. **42**(2): p. 374-84.
111. Flynn, J.L., *Mutual attraction: does it benefit the host or the bug?* Nat Immunol, 2004. **5**(8): p. 778-9.
112. Flynn, J.L., J. Chan, and P.L. Lin, *Macrophages and control of granulomatous inflammation in tuberculosis.* Mucosal Immunol, 2011. **4**(3): p. 271-8.

113. Barry, C.E., 3rd, et al., *The spectrum of latent tuberculosis: rethinking the biology and intervention strategies.* Nat Rev Microbiol, 2009. **7**(12): p. 845-55.
114. Rustad, T.R., et al., *Hypoxia: a window into Mycobacterium tuberculosis latency.* Cell Microbiol, 2009. **11**(8): p. 1151-9.
115. Divangahi, M., S.M. Behar, and H. Remold, *Dying to live: how the death modality of the infected macrophage affects immunity to tuberculosis.* Adv Exp Med Biol, 2013. **783**: p. 103-20.
116. Wang, T.T., et al., *Cutting edge: 1,25-dihydroxyvitamin D3 is a direct inducer of antimicrobial peptide gene expression.* J Immunol, 2004. **173**(5): p. 2909-12.
117. Martineau, A.R., et al., *Neutrophil-mediated innate immune resistance to mycobacteria.* J Clin Invest, 2007. **117**(7): p. 1988-94.
118. Liu, P.T., et al., *Toll-like receptor triggering of a vitamin D-mediated human antimicrobial response.* Science, 2006. **311**(5768): p. 1770-3.
119. Liu, P.T., et al., *Cutting edge: vitamin D-mediated human antimicrobial activity against Mycobacterium tuberculosis is dependent on the induction of cathelicidin.* J Immunol, 2007. **179**(4): p. 2060-3.
120. Krutzik, S.R., et al., *IL-15 links TLR2/1-induced macrophage differentiation to the vitamin D-dependent antimicrobial pathway.* J Immunol, 2008. **181**(10): p. 7115-20.
121. Dorhoi, A., S.T. Reece, and S.H. Kaufmann, *For better or for worse: the immune response against Mycobacterium tuberculosis balances pathology and protection.* Immunol Rev, 2011. **240**(1): p. 235-51.
122. Davis, J.M. and L. Ramakrishnan, *The role of the granuloma in expansion and dissemination of early tuberculous infection.* Cell, 2009. **136**(1): p. 37-49.
123. Cambier, C.J., et al., *Mycobacteria manipulate macrophage recruitment through coordinated use of membrane lipids.* Nature, 2014. **505**(7482): p. 218-22.
124. Chackerian, A.A., et al., *Dissemination of Mycobacterium tuberculosis is influenced by host factors and precedes the initiation of T-cell immunity.* Infect Immun, 2002. **70**(8): p. 4501-9.
125. Khader, S.A., et al., *Interleukin 12p40 is required for dendritic cell migration and T cell priming after Mycobacterium tuberculosis infection.* J Exp Med, 2006. **203**(7): p. 1805-15.
126. Blomgran, R., et al., *Mycobacterium tuberculosis inhibits neutrophil apoptosis, leading to delayed activation of naive CD4 T cells.* Cell Host Microbe, 2012. **11**(1): p. 81-90.
127. Velmurugan, K., et al., *Mycobacterium tuberculosis nuoG is a virulence gene that inhibits apoptosis of infected host cells.* PLoS Pathog, 2007. **3**(7): p. e110.
128. Miller, J.L., et al., *The type I NADH dehydrogenase of Mycobacterium tuberculosis counters phagosomal NOX2 activity to inhibit TNF-alpha-mediated host cell apoptosis.* PLoS Pathog, 2010. **6**(4): p. e1000864.
129. Wallgren, A., *BCG inoculation and BCG vaccination.* Am J Dis Child, 1948. **76**(5): p. 485-91.

130. Poulsen, A., *Some clinical features of tuberculosis. 1. Incubation period.* Acta Tuberc Scand, 1950. **24**(3-4): p. 311-46.
131. Lin, P.L., et al., *Sterilization of granulomas is common in active and latent tuberculosis despite within-host variability in bacterial killing.* Nat Med, 2014. **20**(1): p. 75-9.
132. Reiley, W.W., et al., *ESAT-6-specific CD4 T cell responses to aerosol Mycobacterium tuberculosis infection are initiated in the mediastinal lymph nodes.* Proc Natl Acad Sci U S A, 2008. **105**(31): p. 10961-6.
133. Wolf, A.J., et al., *Initiation of the adaptive immune response to Mycobacterium tuberculosis depends on antigen production in the local lymph node, not the lungs.* J Exp Med, 2008. **205**(1): p. 105-15.
134. Marino, S. and D.E. Kirschner, *The human immune response to Mycobacterium tuberculosis in lung and lymph node.* J Theor Biol, 2004. **227**(4): p. 463-86.
135. Mogues, T., et al., *The relative importance of T cell subsets in immunity and immunopathology of airborne Mycobacterium tuberculosis infection in mice.* J Exp Med, 2001. **193**(3): p. 271-80.
136. Gill, W.P., et al., *A replication clock for Mycobacterium tuberculosis.* Nat Med, 2009. **15**(2): p. 211-4.
137. Ford, C.B., et al., *Use of whole genome sequencing to estimate the mutation rate of Mycobacterium tuberculosis during latent infection.* Nat Genet, 2011. **43**(5): p. 482-6.
138. Kwan, C.K. and J.D. Ernst, *HIV and tuberculosis: a deadly human syndemic.* Clin Microbiol Rev, 2011. **24**(2): p. 351-76.
139. Diedrich, C.R., et al., *Reactivation of latent tuberculosis in cynomolgus macaques infected with SIV is associated with early peripheral T cell depletion and not virus load.* PLoS One, 2010. **5**(3): p. e9611.
140. Pancholi, P., et al., *Sequestration from immune CD4+ T cells of mycobacteria growing in human macrophages.* Science, 1993. **260**(5110): p. 984-6.
141. Cooper, A.M., *T cells in mycobacterial infection and disease.* Curr Opin Immunol, 2009. **21**(4): p. 378-84.
142. Aaron, L., et al., *Tuberculosis in HIV-infected patients: a comprehensive review.* Clin Microbiol Infect, 2004. **10**(5): p. 388-98.
143. North, R.J. and Y.J. Jung, *Immunity to tuberculosis.* Annu Rev Immunol, 2004. **22**: p. 599-623.
144. Flynn, J.L. and J. Chan, *Immunology of tuberculosis.* Annu Rev Immunol, 2001. **19**: p. 93-129.
145. Warren, R.M., et al., *Patients with active tuberculosis often have different strains in the same sputum specimen.* Am J Respir Crit Care Med, 2004. **169**(5): p. 610-4.
146. Glynn, J.R., et al., *High rates of recurrence in HIV-infected and HIV-uninfected patients with tuberculosis.* J Infect Dis, 2010. **201**(5): p. 704-11.
147. Lillebaek, T., et al., *Stability of DNA patterns and evidence of Mycobacterium tuberculosis reactivation occurring decades after the initial infection.* J Infect Dis, 2003. **188**(7): p. 1032-9.

148. Geldmacher, C., et al., *Early depletion of Mycobacterium tuberculosis-specific T helper 1 cell responses after HIV-1 infection.* J Infect Dis, 2008. **198**(11): p. 1590-8.
149. Harris, J. and J. Keane, *How tumour necrosis factor blockers interfere with tuberculosis immunity.* Clin Exp Immunol, 2010. **161**(1): p. 1-9.
150. Wallis, R.S., *Mycobacterial disease attributable to tumor necrosis factor-alpha blockers.* Clin Infect Dis, 2008. **47**(12): p. 1603-5; author reply 1605-6.
151. Clay, H., H.E. Volkman, and L. Ramakrishnan, *Tumor necrosis factor signaling mediates resistance to mycobacteria by inhibiting bacterial growth and macrophage death.* Immunity, 2008. **29**(2): p. 283-94.
152. Nadkarni, S., C. Mauri, and M.R. Ehrenstein, *Anti-TNF-alpha therapy induces a distinct regulatory T cell population in patients with rheumatoid arthritis via TGF-beta.* J Exp Med, 2007. **204**(1): p. 33-9.
153. Bruns, H., et al., *Anti-TNF immunotherapy reduces CD8+ T cell-mediated antimicrobial activity against Mycobacterium tuberculosis in humans.* J Clin Invest, 2009. **119**(5): p. 1167-77.
154. Vallerskog, T., G.W. Martens, and H. Kornfeld, *Diabetic mice display a delayed adaptive immune response to Mycobacterium tuberculosis.* J Immunol, 2010. **184**(11): p. 6275-82.
155. Jick, S.S., et al., *Glucocorticoid use, other associated factors, and the risk of tuberculosis.* Arthritis Rheum, 2006. **55**(1): p. 19-26.
156. Cattamanchi, A., et al., *Interferon-gamma release assays for the diagnosis of latent tuberculosis infection in HIV-infected individuals: a systematic review and meta-analysis.* J Acquir Immune Defic Syndr, 2011. **56**(3): p. 230-8.
157. Lewinsohn, D.A., M.C. Gold, and D.M. Lewinsohn, *Views of immunology: effector T cells.* Immunol Rev, 2011. **240**(1): p. 25-39.
158. Torrado, E. and A.M. Cooper, *IL-17 and Th17 cells in tuberculosis.* Cytokine Growth Factor Rev, 2010. **21**(6): p. 455-62.
159. Feng, C.G. and W.J. Britton, *CD4+ and CD8+ T cells mediate adoptive immunity to aerosol infection of Mycobacterium bovis bacillus Calmette-Guerin.* J Infect Dis, 2000. **181**(5): p. 1846-9.
160. Chan, S.H., C. Benoist, and D. Mathis, *In favor of the selective model of positive selection.* Semin Immunol, 1994. **6**(4): p. 241-8.
161. Cooper, A.M., et al., *Interleukin 12 (IL-12) is crucial to the development of protective immunity in mice intravenously infected with mycobacterium tuberculosis.* J Exp Med, 1997. **186**(1): p. 39-45.
162. Sahiratmadja, E., et al., *Association of polymorphisms in IL-12/IFN-gamma pathway genes with susceptibility to pulmonary tuberculosis in Indonesia.* Tuberculosis (Edinb), 2007. **87**(4): p. 303-11.
163. Gomez-Reino, J.J., et al., *Treatment of rheumatoid arthritis with tumor necrosis factor inhibitors may predispose to significant increase in tuberculosis risk: a multicenter active-surveillance report.* Arthritis Rheum, 2003. **48**(8): p. 2122-7.
164. Singh, S.B., et al., *Human IRGM induces autophagy to eliminate intracellular mycobacteria.* Science, 2006. **313**(5792): p. 1438-41.

165. Keane, J., et al., *Infection by Mycobacterium tuberculosis promotes human alveolar macrophage apoptosis.* Infect Immun, 1997. **65**(1): p. 298-304.
166. Lalvani, A. and K.A. Millington, *T Cells and Tuberculosis: Beyond Interferon-gamma.* J Infect Dis, 2008. **197**(7): p. 941-3.
167. Forbes, E.K., et al., *Multifunctional, high-level cytokine-producing Th1 cells in the lung, but not spleen, correlate with protection against Mycobacterium tuberculosis aerosol challenge in mice.* J Immunol, 2008. **181**(7): p. 4955-64.
168. Darrah, P.A., et al., *Multifunctional TH1 cells define a correlate of vaccine-mediated protection against Leishmania major.* Nat Med, 2007. **13**(7): p. 843-50.
169. Day, C.L., et al., *Functional capacity of Mycobacterium tuberculosis-specific T cell responses in humans is associated with mycobacterial load.* J Immunol, 2011. **187**(5): p. 2222-32.
170. Harari, A., et al., *Dominant TNF-alpha+ Mycobacterium tuberculosis-specific CD4+ T cell responses discriminate between latent infection and active disease.* Nat Med, 2011. **17**(3): p. 372-6.
171. Caccamo, N., et al., *Analysis of Mycobacterium tuberculosis-specific CD8 T-cells in patients with active tuberculosis and in individuals with latent infection.* PLoS One, 2009. **4**(5): p. e5528.
172. Harrington, L.E., P.R. Mangan, and C.T. Weaver, *Expanding the effector CD4 T-cell repertoire: the Th17 lineage.* Curr Opin Immunol, 2006. **18**(3): p. 349-56.
173. Liang, S.C., et al., *Interleukin (IL)-22 and IL-17 are coexpressed by Th17 cells and cooperatively enhance expression of antimicrobial peptides.* J Exp Med, 2006. **203**(10): p. 2271-9.
174. Peng, R., et al., *The IL-17F sequence variant is associated with susceptibility to tuberculosis.* Gene, 2013. **515**(1): p. 229-32.
175. Kagina, B.M., et al., *Specific T cell frequency and cytokine expression profile do not correlate with protection against tuberculosis after bacillus Calmette-Guerin vaccination of newborns.* Am J Respir Crit Care Med, 2010. **182**(8): p. 1073-9.
176. Scriba, T.J., et al., *Distinct, specific IL-17- and IL-22-producing CD4+ T cell subsets contribute to the human anti-mycobacterial immune response.* J Immunol, 2008. **180**(3): p. 1962-70.
177. Sutherland, J.S., et al., *Pattern and diversity of cytokine production differentiates between Mycobacterium tuberculosis infection and disease.* Eur J Immunol, 2009. **39**(3): p. 723-9.
178. Matthews, K., et al., *Predominance of interleukin-22 over interleukin-17 at the site of disease in human tuberculosis.* Tuberculosis (Edinb), 2011. **91**(6): p. 587-93.
179. Gopal, R., et al., *IL-23-dependent IL-17 drives Th1-cell responses following Mycobacterium bovis BCG vaccination.* Eur J Immunol, 2012. **42**(2): p. 364-73.

180. Cruz, A., et al., *Cutting edge: IFN-gamma regulates the induction and expansion of IL-17-producing CD4 T cells during mycobacterial infection.* J Immunol, 2006. **177**(3): p. 1416-20.
181. Khader, S.A., et al., *IL-23 and IL-17 in the establishment of protective pulmonary CD4+ T cell responses after vaccination and during Mycobacterium tuberculosis challenge.* Nat Immunol, 2007. **8**(4): p. 369-77.
182. Khader, S.A., et al., *IL-23 compensates for the absence of IL-12p70 and is essential for the IL-17 response during tuberculosis but is dispensable for protection and antigen-specific IFN-gamma responses if IL-12p70 is available.* J Immunol, 2005. **175**(2): p. 788-95.
183. Umemura, M., et al., *IL-17-mediated regulation of innate and acquired immune response against pulmonary Mycobacterium bovis bacille Calmette-Guerin infection.* J Immunol, 2007. **178**(6): p. 3786-96.
184. Gopal, R., et al., *Unexpected role for IL-17 in protective immunity against hypervirulent Mycobacterium tuberculosis HN878 infection.* PLoS Pathog, 2014. **10**(5): p. e1004099.
185. Ordway, D.J., et al., *Mycobacterium bovis BCG-mediated protection against W-Beijing strains of Mycobacterium tuberculosis is diminished concomitant with the emergence of regulatory T cells.* Clin Vaccine Immunol, 2011. **18**(9): p. 1527-35.
186. Jaron, B., et al., *Effect of attenuation of Treg during BCG immunization on anti-mycobacterial Th1 responses and protection against Mycobacterium tuberculosis.* PLoS One, 2008. **3**(7): p. e2833.
187. Vankayalapati, R. and P.F. Barnes, *Innate and adaptive immune responses to human Mycobacterium tuberculosis infection.* Tuberculosis (Edinb), 2009. **89 Suppl 1**: p. S77-80.
188. Guyot-Revol, V., et al., *Regulatory T cells are expanded in blood and disease sites in patients with tuberculosis.* Am J Respir Crit Care Med, 2006. **173**(7): p. 803-10.
189. Canaday, D.H., et al., *CD4(+) and CD8(+) T cells kill intracellular Mycobacterium tuberculosis by a perforin and Fas/Fas ligand-independent mechanism.* J Immunol, 2001. **167**(5): p. 2734-42.
190. Turner, J. and H.M. Dockrell, *Stimulation of human peripheral blood mononuclear cells with live Mycobacterium bovis BCG activates cytolytic CD8+ T cells in vitro.* Immunology, 1996. **87**(3): p. 339-42.
191. Soares, A.P., et al., *Longitudinal changes in CD4(+) T-cell memory responses induced by BCG vaccination of newborns.* J Infect Dis, 2013. **207**(7): p. 1084-94.
192. Thiery, J., et al., *Perforin pores in the endosomal membrane trigger the release of endocytosed granzyme B into the cytosol of target cells.* Nat Immunol, 2011. **12**(8): p. 770-7.
193. Okada, S., et al., *Intracellular mediators of granulysin-induced cell death.* J Immunol, 2003. **171**(5): p. 2556-62.
194. Kaspar, A.A., et al., *A distinct pathway of cell-mediated apoptosis initiated by granulysin.* J Immunol, 2001. **167**(1): p. 350-6.

195. Stenger, S., et al., *An antimicrobial activity of cytolytic T cells mediated by granulysin.* Science, 1998. **282**(5386): p. 121-5.
196. Goping, I.S., et al., *Granzyme B-induced apoptosis requires both direct caspase activation and relief of caspase inhibition.* Immunity, 2003. **18**(3): p. 355-65.
197. Flynn, J.L., et al., *Major histocompatibility complex class I-restricted T cells are required for resistance to Mycobacterium tuberculosis infection.* Proc Natl Acad Sci U S A, 1992. **89**(24): p. 12013-7.
198. Chen, C.Y., et al., *A critical role for CD8 T cells in a nonhuman primate model of tuberculosis.* PLoS Pathog, 2009. **5**(4): p. e1000392.
199. Caruso, A.M., et al., *Mice deficient in CD4 T cells have only transiently diminished levels of IFN-gamma, yet succumb to tuberculosis.* J Immunol, 1999. **162**(9): p. 5407-16.
200. Scanga, C.A., et al., *Depletion of CD4(+) T cells causes reactivation of murine persistent tuberculosis despite continued expression of interferon gamma and nitric oxide synthase 2.* J Exp Med, 2000. **192**(3): p. 347-58.
201. Soares, A.P., et al., *Bacillus Calmette-Guerin vaccination of human newborns induces T cells with complex cytokine and phenotypic profiles.* J Immunol, 2008. **180**(5): p. 3569-77.
202. Lancioni, C., et al., *CD8+ T cells provide an immunologic signature of tuberculosis in young children.* Am J Respir Crit Care Med, 2012. **185**(2): p. 206-12.
203. Young, D.B., H.P. Gideon, and R.J. Wilkinson, *Eliminating latent tuberculosis.* Trends Microbiol, 2009. **17**(5): p. 183-8.
204. Alcais, A., et al., *Tuberculosis in children and adults: two distinct genetic diseases.* J Exp Med, 2005. **202**(12): p. 1617-21.
205. Alcais, A., et al., *Life-threatening infectious diseases of childhood: single-gene inborn errors of immunity?* Ann N Y Acad Sci, 2010. **1214**: p. 18-33.
206. Brandli, O., *The clinical presentation of tuberculosis.* Respiration, 1998. **65**(2): p. 97-105.
207. Lin, P.L. and J.L. Flynn, *Understanding latent tuberculosis: a moving target.* J Immunol, 2010. **185**(1): p. 15-22.
208. O'Garra, A., et al., *The immune response in tuberculosis.* Annu Rev Immunol, 2013. **31**: p. 475-527.
209. Medlar, E.M., *The pathogenesis of minimal pulmonary tuberculosis; a study of 1,225 necropsies in cases of sudden and unexpected death.* Am Rev Tuberc, 1948. **58**(6): p. 583-611.
210. Capuano, S.V., 3rd, et al., *Experimental Mycobacterium tuberculosis infection of cynomolgus macaques closely resembles the various manifestations of human M. tuberculosis infection.* Infect Immun, 2003. **71**(10): p. 5831-44.
211. Mack, U., et al., *LTBI: latent tuberculosis infection or lasting immune responses to M. tuberculosis? A TBNET consensus statement.* Eur Respir J, 2009. **33**(5): p. 956-73.
212. Plotkin, S.A., *Vaccines: correlates of vaccine-induced immunity.* Clin Infect Dis, 2008. **47**(3): p. 401-9.

213. Tuaillon, E., et al., *Detection of memory B lymphocytes specific to hepatitis B virus (HBV) surface antigen (HBsAg) from HBsAg-vaccinated or HBV-immunized subjects by ELISPOT assay.* J Immunol Methods, 2006. **315**(1-2): p. 144-52.
214. Coursaget, P., et al., *Twelve-year follow-up study of hepatitis B immunization of Senegalese infants.* J Hepatol, 1994. **21**(2): p. 250-4.
215. Potsch, D.V., et al., *Vaccination against hepatitis B with 4-double doses increases response rates and antibodies titers in HIV-infected adults.* Vaccine, 2012. **30**(41): p. 5973-7.
216. Reber, A. and J. Katz, *Immunological assessment of influenza vaccines and immune correlates of protection.* Expert Rev Vaccines, 2013. **12**(5): p. 519-36.
217. Ohmit, S.E., et al., *Influenza hemagglutination-inhibition antibody titer as a correlate of vaccine-induced protection.* J Infect Dis, 2011. **204**(12): p. 1879-85.
218. Voordouw, A.C., et al., *Evaluation of serological trials submitted for annual re-licensure of influenza vaccines to regulatory authorities between 1992 and 2002.* Vaccine, 2009. **28**(2): p. 392-7.
219. CPMP, C.F.P.M.P., *NOTE FOR GUIDANCE ON HARMONISATION OF REQUIREMENTS FOR INFLUENZA VIRUS.* 1997, 2002.
220. Kaufmann, S.H., *Fact and fiction in tuberculosis vaccine research: 10 years later.* Lancet Infect Dis, 2011. **11**(8): p. 633-40.
221. Qin, L., et al., *A framework for assessing immunological correlates of protection in vaccine trials.* J Infect Dis, 2007. **196**(9): p. 1304-12.
222. Kaforou, M., et al., *Detection of tuberculosis in HIV-infected and -uninfected African adults using whole blood RNA expression signatures: a case-control study.* PLoS Med, 2013. **10**(10): p. e1001538.
223. Berry, M.P., et al., *An interferon-inducible neutrophil-driven blood transcriptional signature in human tuberculosis.* Nature, 2010. **466**(7309): p. 973-7.
224. Dawany, N., et al., *Identification of a 251 Gene Expression Signature That Can Accurately Detect M. tuberculosis in Patients with and without HIV Co-Infection.* PLoS One, 2014. **9**(2): p. e89925.
225. Maertzdorf, J., et al., *Human gene expression profiles of susceptibility and resistance in tuberculosis.* Genes Immun, 2011. **12**(1): p. 15-22.
226. Ottenhoff, T.H., et al., *Genome-wide expression profiling identifies type 1 interferon response pathways in active tuberculosis.* PLoS One, 2012. **7**(9): p. e45839.
227. Cayabyab, M.J., L. Macovei, and A. Campos-Neto, *Current and novel approaches to vaccine development against tuberculosis.* Front Cell Infect Microbiol, 2012. **2**: p. 154.
228. Cassman, M., *Barriers to progress in systems biology.* Nature, 2005. **438**(7071): p. 1079.
229. Kitano, H., *Computational systems biology.* Nature, 2002. **420**(6912): p. 206-10.
230. Ideker, T., T. Galitski, and L. Hood, *A new approach to decoding life: systems biology.* Annu Rev Genomics Hum Genet, 2001. **2**: p. 343-72.

231. Mohr, S. and C.C. Liew, *The peripheral-blood transcriptome: new insights into disease and risk assessment.* Trends Mol Med, 2007. **13**(10): p. 422-32.
232. Eisen, M.B. and P.O. Brown, *DNA arrays for analysis of gene expression.* Methods Enzymol, 1999. **303**: p. 179-205.
233. King, H.C. and A.A. Sinha, *Gene expression profile analysis by DNA microarrays: promise and pitfalls.* JAMA, 2001. **286**(18): p. 2280-8.
234. Pollock, J.D., *Gene expression profiling: methodological challenges, results, and prospects for addiction research.* Chem Phys Lipids, 2002. **121**(1-2): p. 241-56.
235. Wang, Z., M. Gerstein, and M. Snyder, *RNA-Seq: a revolutionary tool for transcriptomics.* Nat Rev Genet, 2009. **10**(1): p. 57-63.
236. Cao, H., J. Yuen, and R.A. Hegele, *Single nucleotide polymorphisms of the fukutin gene.* J Hum Genet, 2001. **46**(8): p. 487-9.
237. Greenberg, S.A., *DNA microarray gene expression analysis technology and its application to neurological disorders.* Neurology, 2001. **57**(5): p. 755-61.
238. Altman, R.B. and S. Raychaudhuri, *Whole-genome expression analysis: challenges beyond clustering.* Curr Opin Struct Biol, 2001. **11**(3): p. 340-7.
239. Wyrick, J.J., et al., *Genome-wide distribution of ORC and MCM proteins in S. cerevisiae: high-resolution mapping of replication origins.* Science, 2001. **294**(5550): p. 2357-60.
240. van 't Veer, L.J., et al., *Gene expression profiling predicts clinical outcome of breast cancer.* Nature, 2002. **415**(6871): p. 530-6.
241. Clarke, P.A., et al., *Gene expression microarray analysis in cancer biology, pharmacology, and drug development: progress and potential.* Biochem Pharmacol, 2001. **62**(10): p. 1311-36.
242. De Hertogh, B., et al., *A benchmark for statistical microarray data analysis that preserves actual biological and technical variance.* BMC Bioinformatics, 2010. **11**: p. 17.
243. Leung, Y.F. and D. Cavalieri, *Fundamentals of cDNA microarray data analysis.* Trends Genet, 2003. **19**(11): p. 649-59.
244. Quackenbush, J., *Microarray data normalization and transformation.* Nat Genet, 2002. **32 Suppl**: p. 496-501.
245. Lee, P.D., et al., *Control genes and variability: absence of ubiquitous reference transcripts in diverse mammalian expression studies.* Genome Res, 2002. **12**(2): p. 292-7.
246. Yang, Y.H., et al., *Normalization for cDNA microarray data: a robust composite method addressing single and multiple slide systematic variation.* Nucleic Acids Res, 2002. **30**(4): p. e15.
247. Qiu, X., H. Wu, and R. Hu, *The impact of quantile and rank normalization procedures on the testing power of gene differential expression analysis.* BMC Bioinformatics, 2013. **14**: p. 124.
248. Bolstad, B.M., et al., *A comparison of normalization methods for high density oligonucleotide array data based on variance and bias.* Bioinformatics, 2003. **19**(2): p. 185-93.

249. Gentleman, R.C., et al., *Bioconductor: open software development for computational biology and bioinformatics.* Genome Biol, 2004. **5**(10): p. R80.
250. Eisen, M.B., et al., *Cluster analysis and display of genome-wide expression patterns.* Proc Natl Acad Sci U S A, 1998. **95**(25): p. 14863-8.
251. Tavazoie, S., et al., *Systematic determination of genetic network architecture.* Nat Genet, 1999. **22**(3): p. 281-5.
252. Tamayo, P., et al., *Interpreting patterns of gene expression with self-organizing maps: methods and application to hematopoietic differentiation.* Proc Natl Acad Sci U S A, 1999. **96**(6): p. 2907-12.
253. Kerr, M.K., M. Martin, and G.A. Churchill, *Analysis of variance for gene expression microarray data.* J Comput Biol, 2000. **7**(6): p. 819-37.
254. Long, A.D., et al., *Improved statistical inference from DNA microarray data using analysis of variance and a Bayesian statistical framework. Analysis of global gene expression in Escherichia coli K12.* J Biol Chem, 2001. **276**(23): p. 19937-44.
255. Wu, T.D., *Analysing gene expression data from DNA microarrays to identify candidate genes.* J Pathol, 2001. **195**(1): p. 53-65.
256. Reiner, A., D. Yekutieli, and Y. Benjamini, *Identifying differentially expressed genes using false discovery rate controlling procedures.* Bioinformatics, 2003. **19**(3): p. 368-75.
257. Hakak, Y., et al., *Genome-wide expression analysis reveals dysregulation of myelination-related genes in chronic schizophrenia.* Proc Natl Acad Sci U S A, 2001. **98**(8): p. 4746-51.
258. Theilhaber, J., et al., *Bayesian estimation of fold-changes in the analysis of gene expression: the PFOLD algorithm.* J Comput Biol, 2001. **8**(6): p. 585-614.
259. Ben-Dor, A., et al., *Tissue classification with gene expression profiles.* J Comput Biol, 2000. **7**(3-4): p. 559-83.
260. Akutsu, T., S. Miyano, and S. Kuhara, *Inferring qualitative relations in genetic networks and metabolic pathways.* Bioinformatics, 2000. **16**(8): p. 727-34.
261. Liang, S., S. Fuhrman, and R. Somogyi, *Reveal, a general reverse engineering algorithm for inference of genetic network architectures.* Pac Symp Biocomput, 1998: p. 18-29.
262. Friedman, N., et al., *Using Bayesian networks to analyze expression data.* J Comput Biol, 2000. **7**(3-4): p. 601-20.
263. Hartemink, A.J., et al., *Using graphical models and genomic expression data to statistically validate models of genetic regulatory networks.* Pac Symp Biocomput, 2001: p. 422-33.
264. Firestein, G.S. and D.S. Pisetsky, *DNA microarrays: boundless technology or bound by technology? Guidelines for studies using microarray technology.* Arthritis Rheum, 2002. **46**(4): p. 859-61.
265. Benes, V. and M. Muckenthaler, *Standardization of protocols in cDNA microarray analysis.* Trends Biochem Sci, 2003. **28**(5): p. 244-9.

266. Mimmack, M.L., J. Brooking, and S. Bahn, *Quantitative polymerase chain reaction: validation of microarray results from postmortem brain studies.* Biol Psychiatry, 2004. **55**(4): p. 337-45.
267. Murphy, D., *Gene expression studies using microarrays: principles, problems, and prospects.* Adv Physiol Educ, 2002. **26**(1-4): p. 256-70.
268. Melin, J. and S.R. Quake, *Microfluidic large-scale integration: the evolution of design rules for biological automation.* Annu Rev Biophys Biomol Struct, 2007. **36**: p. 213-31.
269. Spurgeon, S.L., R.C. Jones, and R. Ramakrishnan, *High throughput gene expression measurement with real time PCR in a microfluidic dynamic array.* PLoS One, 2008. **3**(2): p. e1662.
270. Ramakrishnan, R., et al., *Integrated Fluidic Circuits (IFCs) for digital PCR.* Methods Mol Biol, 2013. **949**: p. 423-31.
271. Hanekom, W.A., et al., *Novel application of a whole blood intracellular cytokine detection assay to quantitate specific T-cell frequency in field studies.* J Immunol Methods, 2004. **291**(1-2): p. 185-95.
272. Apostolopoulos, V. and F.M. Marincola, *Methods to measure vaccine immunity.* Expert Rev Vaccines, 2010. **9**(6): p. 545-6.
273. Abu-Raddad, L.J., et al., *Epidemiological benefits of more-effective tuberculosis vaccines, drugs, and diagnostics.* Proc Natl Acad Sci U S A, 2009. **106**(33): p. 13980-5.
274. Baran, J., et al., *Three-color flow cytometry detection of intracellular cytokines in peripheral blood mononuclear cells: comparative analysis of phorbol myristate acetate-ionomycin and phytohemagglutinin stimulation.* Clin Diagn Lab Immunol, 2001. **8**(2): p. 303-13.
275. Mao, J.H., et al., *[Regulation of CD3, CD4 and CD8 expressions on PMA-activated human peripheral T cells].* Zhejiang Da Xue Xue Bao Yi Xue Ban, 2004. **33**(2): p. 155-9.
276. Fletcher, H.A., et al., *Transcriptional profiling of mycobacterial antigen-induced responses in infants vaccinated with BCG at birth.* BMC Med Genomics, 2009. **2**: p. 10.
277. Golub, T.R., et al., *Molecular classification of cancer: class discovery and class prediction by gene expression monitoring.* Science, 1999. **286**(5439): p. 531-7.
278. Bonnefoi, H., et al., *Predictive signatures for chemotherapy sensitivity in breast cancer: are they ready for use in the clinic?* Eur J Cancer, 2009. **45**(10): p. 1733-43.
279. Pascual, V., D. Chaussabel, and J. Banchereau, *A genomic approach to human autoimmune diseases.* Annu Rev Immunol, 2010. **28**: p. 535-71.
280. Bean, A.G., et al., *Structural deficiencies in granuloma formation in TNF gene-targeted mice underlie the heightened susceptibility to aerosol Mycobacterium tuberculosis infection, which is not compensated for by lymphotoxin.* J Immunol, 1999. **162**(6): p. 3504-11.
281. Flynn, J.L., et al., *Tumor necrosis factor-alpha is required in the protective immune response against Mycobacterium tuberculosis in mice.* Immunity, 1995. **2**(6): p. 561-72.

282. Flynn, J.L., et al., *IL-12 increases resistance of BALB/c mice to Mycobacterium tuberculosis infection.* J Immunol, 1995. **155**(5): p. 2515-24.
283. Flynn, J.L., et al., *An essential role for interferon gamma in resistance to Mycobacterium tuberculosis infection.* J Exp Med, 1993. **178**(6): p. 2249-54.
284. Orme, I.M., *The role of CD8+ T cells in immunity to tuberculosis infection.* Trends Microbiol, 1993. **1**(3): p. 77-8.
285. Smith, S.M., et al., *Human CD8+ CTL specific for the mycobacterial major secreted antigen 85A.* J Immunol, 2000. **165**(12): p. 7088-95.
286. Silva, C.L. and D.B. Lowrie, *Identification and characterization of murine cytotoxic T cells that kill Mycobacterium tuberculosis.* Infect Immun, 2000. **68**(6): p. 3269-74.
287. Kozakiewicz, L., et al., *B cells regulate neutrophilia during Mycobacterium tuberculosis infection and BCG vaccination by modulating the interleukin-17 response.* PLoS Pathog, 2013. **9**(7): p. e1003472.
288. Chen, R.T., et al., *Measles antibody: reevaluation of protective titers.* J Infect Dis, 1990. **162**(5): p. 1036-42.
289. Mathias, R.G., et al., *The role of secondary vaccine failures in measles outbreaks.* Am J Public Health, 1989. **79**(4): p. 475-8.
290. Casadevall, A. and L.A. Pirofski, *The damage-response framework of microbial pathogenesis.* Nat Rev Microbiol, 2003. **1**(1): p. 17-24.
291. Chen, J.J., *Key aspects of analyzing microarray gene-expression data.* Pharmacogenomics, 2007. **8**(5): p. 473-82.
292. Tavor, S., et al., *The CXCR4 antagonist AMD3100 impairs survival of human AML cells and induces their differentiation.* Leukemia, 2008. **22**(12): p. 2151-5158.
293. Pomeroy, S.L., et al., *Prediction of central nervous system embryonal tumour outcome based on gene expression.* Nature, 2002. **415**(6870): p. 436-42.
294. Shipp, M.A., et al., *Diffuse large B-cell lymphoma outcome prediction by gene-expression profiling and supervised machine learning.* Nat Med, 2002. **8**(1): p. 68-74.
295. Joosten, S.A., H.A. Fletcher, and T.H. Ottenhoff, *A helicopter perspective on TB biomarkers: pathway and process based analysis of gene expression data provides new insight into TB pathogenesis.* PLoS One, 2013. **8**(9): p. e73230.
296. Smyth, G.K., *Limma: linear models for microarray data. In: Bioinformatics and Computational Biology Solutions using R and Bioconductor, R. Gentleman, V. Carey, S. Dusoit, R. Irizarry, W.Huber (eds).* Springer, New York, 2005: p. 397-420.
297. Tibshirani, R., et al., *Diagnosis of multiple cancer types by shrunken centroids of gene expression.* Proc Natl Acad Sci U S A, 2002. **99**(10): p. 6567-72.

298. Subramanian, A., et al., *Gene set enrichment analysis: a knowledge-based approach for interpreting genome-wide expression profiles.* Proc Natl Acad Sci U S A, 2005. **102**(43): p. 15545-50.
299. Chaussabel, D., et al., *A modular analysis framework for blood genomics studies: application to systemic lupus erythematosus.* Immunity, 2008. **29**(1): p. 150-64.
300. Van Laere, S.J., et al., *Identification of cell-of-origin breast tumor subtypes in inflammatory breast cancer by gene expression profiling.* Breast Cancer Res Treat, 2006. **95**(3): p. 243-55.
301. Makretsov, N.A., et al., *Hierarchical clustering analysis of tissue microarray immunostaining data identifies prognostically significant groups of breast carcinoma.* Clin Cancer Res, 2004. **10**(18 Pt 1): p. 6143-51.
302. Grossi, F., et al., *Prognostic stratification of stage IIIA pN2 non-small cell lung cancer by hierarchical clustering analysis of tissue microarray immunostaining data: an Alpe Adria Thoracic Oncology Multidisciplinary Group study (ATOM 014).* J Thorac Oncol, 2010. **5**(9): p. 1354-60.
303. Badsha, M.B., et al., *Robust complementary hierarchical clustering for gene expression data analysis by beta-divergence.* J Biosci Bioeng, 2013. **116**(3): p. 397-407.
304. Sampson, B., et al., *Hyperzincaemia and hypercalprotectinaemia: a new disorder of zinc metabolism.* Lancet, 2002. **360**(9347): p. 1742-5.
305. Corbin, B.D., et al., *Metal chelation and inhibition of bacterial growth in tissue abscesses.* Science, 2008. **319**(5865): p. 962-5.
306. Gopal, R., et al., *S100A8/A9 proteins mediate neutrophilic inflammation and lung pathology during tuberculosis.* Am J Respir Crit Care Med, 2013. **188**(9): p. 1137-46.
307. Areeshi, M.Y., et al., *CD14 -159 C>T gene polymorphism with increased risk of tuberculosis: evidence from a meta-analysis.* PLoS One, 2013. **8**(5): p. e64747.
308. Wieland, C.W., et al., *CD14 contributes to pulmonary inflammation and mortality during murine tuberculosis.* Immunology, 2008. **125**(2): p. 272-9.
309. Homolka, J., et al., *Evaluation of soluble CD 14 and neopterin as serum parameters of the inflammatory activity of pulmonary sarcoidosis.* Clin Investig, 1992. **70**(10): p. 909-16.
310. Hoheisel, G., et al., *Increased soluble CD14 levels in BAL fluid in pulmonary tuberculosis.* Chest, 1995. **108**(6): p. 1614-6.
311. Naranbhai, V., et al., *Ratio of monocytes to lymphocytes in peripheral blood identifies adults at risk of incident tuberculosis among HIV-infected adults initiating antiretroviral therapy.* J Infect Dis, 2014. **209**(4): p. 500-9.
312. Pitabut, N., et al., *Potential function of granulysin, other related effector molecules and lymphocyte subsets in patients with TB and HIV/TB coinfection.* Int J Med Sci, 2013. **10**(8): p. 1003-14.
313. Ameixa, C. and J.S. Friedland, *Interleukin-8 secretion from Mycobacterium tuberculosis-infected monocytes is regulated by protein tyrosine kinases but not by ERK1/2 or p38 mitogen-activated protein kinases.* Infect Immun, 2002. **70**(8): p. 4743-6.

314. Casarini, M., et al., *Cytokine levels correlate with a radiologic score in active pulmonary tuberculosis.* Am J Respir Crit Care Med, 1999. **159**(1): p. 143-8.
315. Sadek, M.I., et al., *Chemokines induced by infection of mononuclear phagocytes with mycobacteria and present in lung alveoli during active pulmonary tuberculosis.* Am J Respir Cell Mol Biol, 1998. **19**(3): p. 513-21.
316. Kurashima, K., et al., *Elevated chemokine levels in bronchoalveolar lavage fluid of tuberculosis patients.* Am J Respir Crit Care Med, 1997. **155**(4): p. 1474-7.
317. Yamada, Y., et al., *Cytokines in pleural liquid for diagnosis of tuberculous pleurisy.* Respir Med, 2001. **95**(7): p. 577-81.
318. Friedland, J.S., et al., *Inhibition of ex vivo proinflammatory cytokine secretion in fatal Mycobacterium tuberculosis infection.* Clin Exp Immunol, 1995. **100**(2): p. 233-8.
319. Fallon, J., et al., *In vivo induction of massive proliferation, directed migration, and differentiation of neural cells in the adult mammalian brain.* Proc Natl Acad Sci U S A, 2000. **97**(26): p. 14686-91.
320. Cliff, J.M., et al., *Distinct phases of blood gene expression pattern through tuberculosis treatment reflect modulation of the humoral immune response.* J Infect Dis, 2013. **207**(1): p. 18-29.
321. Rand, L., et al., *Matrix metalloproteinase-1 is regulated in tuberculosis by a p38 MAPK-dependent, p-aminosalicylic acid-sensitive signaling cascade.* J Immunol, 2009. **182**(9): p. 5865-72.
322. Yang, C.S., et al., *ASK1-p38 MAPK-p47phox activation is essential for inflammatory responses during tuberculosis via TLR2-ROS signalling.* Cell Microbiol, 2008. **10**(3): p. 741-54.
323. Hanekom, W.A., et al., *Immunological outcomes of new tuberculosis vaccine trials: WHO panel recommendations.* PLoS Med, 2008. **5**(7): p. e145.
324. Aagaard, C., et al., *Protection and polyfunctional T cells induced by Ag85B-TB10.4/IC31 against Mycobacterium tuberculosis is highly dependent on the antigen dose.* PLoS One, 2009. **4**(6): p. e5930.
325. Zak, D.E., et al., *Merck Ad5/HIV induces broad innate immune activation that predicts CD8(+) T-cell responses but is attenuated by preexisting Ad5 immunity.* Proc Natl Acad Sci U S A, 2012. **109**(50): p. E3503-12.
326. Querec, T.D., et al., *Systems biology approach predicts immunogenicity of the yellow fever vaccine in humans.* Nat Immunol, 2009. **10**(1): p. 116-25.
327. Tan, Y., et al., *Gene signatures related to B-cell proliferation predict influenza vaccine-induced antibody response.* Eur J Immunol, 2014. **44**(1): p. 285-95.
328. Teles, R.M., et al., *Type I interferon suppresses type II interferon-triggered human anti-mycobacterial responses.* Science, 2013. **339**(6126): p. 1448-53.

329. Dominguez, M.H., et al., *Highly multiplexed quantitation of gene expression on single cells.* J Immunol Methods, 2013. **391**(1-2): p. 133-45.
330. Pfaffl, M.W., *A new mathematical model for relative quantification in real-time RT-PCR.* Nucleic Acids Res, 2001. **29**(9): p. e45.
331. de Jonge, H.J., et al., *Evidence based selection of housekeeping genes.* PLoS One, 2007. **2**(9): p. e898.
332. Brice, G.T., et al., *Expression of the chemokine MIG is a sensitive and predictive marker for antigen-specific, genetically restricted IFN-gamma production and IFN-gamma-secreting cells.* J Immunol Methods, 2001. **257**(1-2): p. 55-69.
333. Brahmbhatt, S., et al., *Human T cell responses to peptides of the Mycobacterium leprae 45-kD serine-rich antigen.* Clin Exp Immunol, 2002. **128**(1): p. 140-8.
334. Berthoud, T.K., et al., *MIG (CXCL9) is a more sensitive measure than IFN-gamma of vaccine induced T-cell responses in volunteers receiving investigated malaria vaccines.* J Immunol Methods, 2009. **340**(1): p. 33-41.
335. Abramo, C., et al., *Monokine induced by interferon gamma and IFN-gamma response to a fusion protein of Mycobacterium tuberculosis ESAT-6 and CFP-10 in Brazilian tuberculosis patients.* Microbes Infect, 2006. **8**(1): p. 45-51.
336. Pulendran, B., S. Li, and H.I. Nakaya, *Systems vaccinology.* Immunity, 2010. **33**(4): p. 516-29.
337. Nakaya, H.I., S. Li, and B. Pulendran, *Systems vaccinology: learning to compute the behavior of vaccine induced immunity.* Wiley Interdiscip Rev Syst Biol Med, 2012. **4**(2): p. 193-205.
338. Henn, A.D., et al., *High-resolution temporal response patterns to influenza vaccine reveal a distinct human plasma cell gene signature.* Sci Rep, 2013. **3**: p. 2327.
339. Hu, S.L., *Non-human primate models for AIDS vaccine research.* Curr Drug Targets Infect Disord, 2005. **5**(2): p. 193-201.
340. Dumur, C.I., et al., *Evaluation of quality-control criteria for microarray gene expression analysis.* Clin Chem, 2004. **50**(11): p. 1994-2002.
341. Silvy, M., et al., *Improvement of gene expression analysis by RQ-PCR technology: addition of BSA.* Leukemia, 2004. **18**(5): p. 1022-5.
342. Mayeux, R., *Biomarkers: potential uses and limitations.* NeuroRx, 2004. **1**(2): p. 182-8.
343. Bacchetti, P., S.G. Deeks, and J.M. McCune, *Breaking free of sample size dogma to perform innovative translational research.* Sci Transl Med, 2011. **3**(87): p. 87ps24.

APPENDICES

Appendix 1: Correlation between CXCL9 mRNA expression and IFN-γ-expressing CD4+ T cells in the validation cohort.

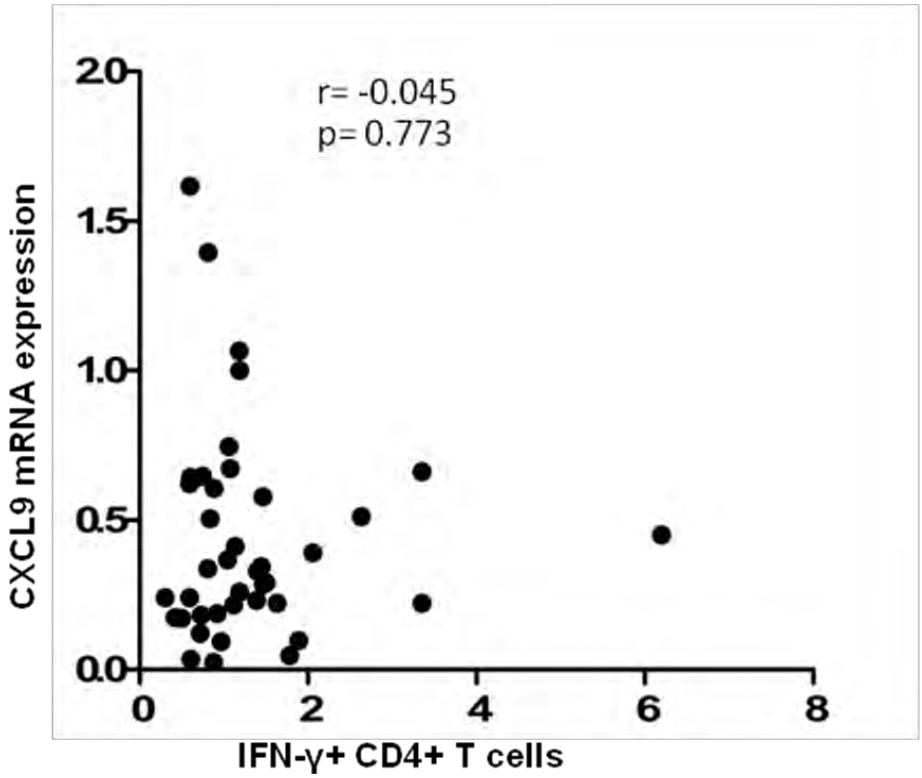

Correlation between CXCL9 mRNA expression and IFN-γ-expressing CD4+ T cells in the validation cohort.
PBMCs were stimulated with BCG or left unstimulated for 12 hrs. RNA was extracted, transcribed to cDNA and CXCL9 expression was measured by convention qRT-PCR. Whole blood was incubated with BCG or left unstimulated for 12 hours and frequencies of IFN-γ-expressing CD4+ T cells measured by intracellular cytokine staining assay and flow cytometry. Following background subtraction, correlation between CXCL9 mRNA expression and frequencies of IFN-γ+CD4+ T cells were determined using spearman rank correlation.

Appendix 2: Cell count and viability of thawed PBMCs from participants in the validation cohort.

Study Number	Total Number of cells (10^6)	Viability (%)
14365	7.2	72.22
11438	8.5	90.58
14383	7.9	69.62
14401	5.4	77.77
14423	6.3	60.31
12984	7.2	79.16
14483	6.2	79.03
14516	10.1	85.14
15224	8.5	74.11
14437	8.6	86.04
14978	14.6	82.87
15259	5.5	80.00
15594	14.2	81.54
15641	13.2	77.27
15666	6.8	80.88
16292	25.9	92.66
18508	7.4	81.08
16016	18	87.77
16098	31.2	84.93
16204	36.2	85.54
16647	28.3	88.33
19021	11.9	81.51
19391	36.4	86.78
19530	37.2	80.08
16491	12.3	74.79
16562	5.2	78.84
16663	25.1	82.02
16849	6.8	82.35
16859	10.1	79.20
19563	11.7	89.74
19636	27.6	90.94
16872	27.2	83.45
16926	35	90.00
17058	29.1	91.06

14496	8.1	93.82
20016	22.3	86.99
20096	46.7	88.86
20700	23	87.82
15137	15.6	84.61
15686	14.2	77.46
16185	13.5	93.33
16969	7.6	89.47
21580	13	90.76
21668	7.7	81.81
14637	13.8	79.71
16984	25.1	87.64
17038	35.6	89.88
14557	18.1	91.16
19210	33.2	90.36
20466	32.5	87.69
14341	25	90.00
14530	25.6	83.98
15769	8.9	88.76
15881	9	78.88
16149	18.2	84.61
17029	7	71.42
14552	22.3	82.95
16292	23.5	79.57
19061	25.3	86.95
19573	10.6	79.24